Roles for the Type 2 Diabetes-Associated Genes *C2CD4A* and *C2CD4B* in the Control of Insulin Secretion

Seyedeh Neda Mousavy Gharavy

Imperial College London

Department of Metabolism, Digestion and Reproduction

Section of Cell Biology and Functional Genomics

Thesis presented for the degree of Doctor of Philosophy and diploma of Imperial College London

Declaration of Authenticity and Copyright

I declare that the following work presented in this thesis is original, except where indicated by special reference in the text, and that no part of the dissertation has been submitted for any other degree.

Some of the results contained here have been presented at conferences and seminars.

Acknowledgements

I would like to say thanks to Professor Guy Rutter for giving me the opportunity to carry out a PhD in his lab and all his support and guidance throughout this journey. Thanks to Diabetes UK and MRC for funding this PhD.

Special thanks to Dr Aida Martinez-Sanchez for helping me to start in the lab and all her support throughout the project.

Many thanks to Dr Marie-Sophie Nguyen-Tu for her support inside and outside the lab.

Thanks to all collaborators and lab members supporting with additional experiments including Dr Aida Martinez-Sanchez and Grazia Pizza for generating RNA-seq data, Dr Steven Millership generating mass spectrometry data, Dr Bryn Owen for generating gonadectomised animals and performing beautiful hormone measurements, Dr Eleni Georgiadou and Dr Ming Hu for their support with the final experiments, and all the members of the Section of Cell Biology and Functional Genomics at Imperial College London. Also thanks a lot to people for helping me editing this thesis, Steven Parks, Joseph Harris, Dr Gaelle Carrat and Dr Ines Cebola.

And, of course, lots of thanks to the ‘Minions’ (Rebecca Callingham, Grazia Pizza, Jo Harris, Steven Parks and Rebecca Cheung) and Marie-Sophie for their everyday support and their company. This experience wouldn’t have been the same without you.

Muchisimas gracias Juanmi Sanchez por todo tu apoyo y ayuda, cada dia durante mi doctorado. Gracias por estar siempre, en todos momentos dificiles y felices. It was not possible to go through it without you.

Lots of thanks to my family for their support and belief in me.

Abstract

Genome-wide Association Studies (GWAS) have identified several SNPs in human chromosome 15 at the *C2CD4A/C2CD4B/VPS13C* locus associated with increased proinsulin levels and type 2 diabetes (T2D) risk. A recent *in vivo* study has shown that murine *Vpc13c* has a minor role in glucose homeostasis. Therefore, in this study, I sought to investigate the roles of *C2CD4A* and *C2CD4B* in glucose homeostasis and insulin secretion.

C2CD4A and *C2CD4B* have been predicted to encode nucleus-localised calcium-binding proteins in endothelial cells. To investigate the role of these genes in pancreatic β-cells, we first addressed their subcellular localisation. Our results suggested a novel role for these genes products since they showed localisation at the plasma membrane in addition to the nucleus as shown previously in endothelial cells. We also found that C2CD4A translocates from the cytoplasm to the plasma membrane in response to an elevation in intracellular free calcium. This suggests that the C2 domain of this protein binds to calcium and membrane phospholipids.

We also studied the role of *C2cd4b in vivo*. Our data showed that a lack of *C2cd4b* in female mice leads to impaired glucose tolerance, caused by a significantly decreased plasma insulin level. In these mice, we also observed a significant reduction of follicle-stimulating hormone (FSH). In contrast to the latter data, *C2cd4a* null mice did not present any glucose intolerance phenotype, suggesting a minor role for this gene in glucose homeostasis. However, in humans, deletion of this gene from human pancreas-derived β-cells caused an impairment in insulin secretion.

Taken together, our data demonstrate a novel role for these genes in the control of insulin secretion and glucose homeostasis. Further studies investigating the structures, their specific functions and interacting partners may demonstrate the mechanisms of action of the nearby T2D variants and open new avenues for the treatment of T2D.

Table of Contents

List of Figures

List of Tables

Abbreviations

ATP	Adenosine triphosphate
AgRP	Agouti-related peptide
AMP	Adenosine monophosphate
ARX	Aristaless Related Homeobox
C2CD4A and -B	C2 Calcium Dependent Domain Containing 4-A and -B
CART	Cocaine- and amphetamine-related transcript
CCK	Cholecystokinin
CLAMS	Columbus Instruments Comprehensive Lab Animal Monitoring System
DAG	Diacylglycerol
DAPI	4,6-diamidino-2-phenylindole
DMEM	Dulbecco's modified eagle media
DMSO	Dimethylsulfoxide
DTT	Dithiothreitol
E2	Estradiol
ELISA	Enzyme-linked immunosorbent assay
EM	Electron microscopy
ER	Endoplasmic reticulum
E-Syt	Extended synaptotagmin
FACS	Fluorescence-activated cell sorting
FFA	Free Fatty Acids
FGF2	Fibroblast growth factor 2
FoxO1	Forkhead Box O1
FSH	Follicle-stimulating hormone
GAPDH	Glyceraldehyde 3-phosphate dehydrogenase
GFP	Green fluorescence protein
GHIH	Growth Hormone Inhibiting Hormone
GIP	Glucose-dependent insulinotropic polypeptide
GLP1/2	Glucagon like peptide-1/2
GLUT	Glucose transporter
GRP	Gastrin-releasing peptide
GPCR	G-protein coupled receptors
GPR	G-protein–coupled receptor
GSIS	Glucose stimulated insulin secretion
GWAS	Genome wide association study
HCSP	Highly Ca^{2+}-sensitive pool of granules
HFD	High-fat and -sucrose diet
HTRF	Homogeneous Time Resolved Fluorescence
hGH	Human growth hormone
IBMX	Isobutyl methyl xanthine
IP_3	Inositol 1,4,5 -trisphosphate
IPGTT	Intraperitoneal glucose tolerance test
ITT	Insulin tolerance test

K_{ATP}	ATP-dependent K^+ channel
Kir6.2	Potassium inwardly rectifying channel
KRBH	Krebs-Ringer bicarbonate buffer
KSIS	KCl-stimulated insulin secretion
LD	Linkage disequilibrium
LH	Luteinising hormone
MafA/B	V-maf musculoaponeurotic fibrosarcoma oncogene homologue A/B
MC3r	Melanocortin 3 Receptor
MNX1	Motor Neuron and Pancreas Homeobox Protein 1
NeuroD1	Neurogenic differentiator 1
Nkx6.1	Homeobox Protein Nkx-6.1
NLF1/2	Nuclear-Localized Factor 1/2
NPY	Neurons co-express neuropeptide Y
OGTT	Oral glucose tolerance test
PACAP	Pituitary adenylate cyclase activating polypeptide peptide
PAM	Protospacer adjacent motif
Pax	Paired box protein
PBS	Phosphate buffered saline
Pdx1	Pancreatic and duodenal homeobox-1
PKC	Protein kinase C
PLC	Phospholipase C
POMC	Pro-opiomelanocortin
PP	Pancreatic polypeptide
PRM	Rotation per minute
RIP	Rat *Ins 2* promoter
RNA-seq	RNA sequencing
RC	Regular chow diet
RT-q-PCT	Reverse transcription quantitative PCR
shRNA	Small hairpin RNA
SNARE	Soluble N-ethylmaleimide-sensitive factor-attachment receptor
SNP	Single nucleotide polymorphism
Syncollin	LDCV-associated protein syncollin
T1D	Type 1 diabetes
T2D	Type 2 diabetes
TCF7L2	Transcription factor 7-like 2
TNG	Trans-Golgi networks
VIP	Vasoactive intestinal polypeptide
Wnt	Wingless-related integration site
WT	Wild type

Chapter 1: Introduction

1.1.1. Pancreatic Islets, β-Cells and Glucose Metabolism

1.1.2. Pancreas

The pancreas is an organ which specialises in nutrient metabolism. It is derived from the epithelial bud during early development and consists of two distinct cell populations; the exocrine and the endocrine cells (Slack, 1995; Gittes, 2009; Shih, Wang & Sander, 2013). The exocrine pancreas consists of acinar and ductal cells, whose main role is to aid the digestion of nutrients by the gut. The acinar cells produce pancreatic juice which is transported through the ductal system to the duodenum to catalyse the breakdown of proteins, carbohydrates, and lipids (Slack, 1995; Gittes, 2009; Shih, Wang & Sander, 2013). Most of the enzymes in the pancreatic juices are secreted as inactive precursors and become activated after they enter the duodenum (Williams, 2010). The endocrine pancreas, on the other hand, is involved in the regulation of glucose homeostasis by releasing hormones into the bloodstream. The endocrine cells are grouped into islets of Langerhans, which are compact spherical clusters embedded in the exocrine tissue (Williams, 2010).

1.1.3. Islets of Langerhans

The islets of Langerhans play a central role in the systemic regulation of metabolism. They consist of at least five distinct cell types. In humans and other mammals, β-cells are the most common, which form 50-70% of islets in humans and 60-80% in mice (Slack, 1995). These cells secrete insulin and amylin (Quianzon & Cheikh, 2012; Gittes, 2009; Merino, 2004). Amylin has a role in gastric emptying and satiety after food intake (Pillay & Govender, 2013). Insulin is a peptide hormone which regulates the metabolism of carbohydrates, fats and proteins. It promotes the absorption of carbohydrates, specifically glucose from the blood into liver, skeletal muscles and fat tissues. α-cells form around 20-40% and 10-20% of the cells in the islets in humans and mice, respectively, and secrete glucagon. Glucagon is a peptide hormone which increases the concentration of glucose and fatty acids in the blood. Other cell types in the islets include δ-cells and pancreatic polypeptide (PP) cells. Representing less than 5-10% of the cells in islets from humans and mice, PP and δ-cells produce pancreatic polypeptides and somatostatin, respectively.

Somatostatin, also known as Growth Hormone Inhibiting Hormone (GHIH), is a peptide hormone which affects neurotransmission and cell proliferation. In addition to the above, ε-cells comprise less than 1% of cells, and produce ghrelin (Dolenšek *et al.*, 2015; Shih, Wang & Sander, 2013). Ghrelin, which is also secreted by the small intestine and brain, has numerous roles including in appetite stimulation, control of food intake and storage of fat (Brissova *et al.*, 2005).

The spatial organisation of the endocrine cells within the islets differs between humans and mice. In mice, non-β-cells are positioned towards the periphery, while β-cells are positioned in the core of the islets. In humans, on the other hand, these different cells types are positioned in a more unorganised manner (Dolenšek *et al.*, 2015; Williams, 2010). It is not yet clear why this difference exists in the architecture of islets in the two species.

The hormones secreted from different cell types in the islets are released directly into the bloodstream. Therefore, islets are highly vascularised and receive approximately 10 times more blood than the exocrine pancreas per unit of weight (Dolenšek *et al.*, 2015).

1.1.4. Pancreas Development

The development of the pancreas is the result of the spatiotemporal dynamics of gene expression in the developing embryo. Expression of certain transcription factors and morphogen secretion at specific time points during the development and at a specific location determine the fate of the pancreatic progenitors as well as many other progenitors (Shih, Wang & Sander, 2013). In mouse, the first sign of a pancreas appears at embryonic day (E) 8.5 (Gittes & Rutter, 1992). It initiates from the distal part of the endodermal foregut and proximal part of the midgut, based on the initial expression of pancreas-specific genes (pancreatic and duodenal homeobox 1 and pancreas associated transcription factor 1a are among these genes). By E9, the first morphological sign of pancreatic development appears, with the emergence of epithelial buds on opposing sides of the foregut endoderm. In humans, this occurs just prior to 26 days of gestation (Kallman & Grobstein, 1964). In mouse, the two pancreatic buds subsequently elongate alongside the presumptive duodenum and stomach and, as a result of the gut rotation, eventually fuse into a single organ by E12.5. During this time cell proliferation leads to a rapid increase in the size of the pancreatic buds, and the developing gland begins to form a branched tubular

structure. From E12.5 this branching expands to form a complex and highly organised tubular network. During this period, differentiation of pancreatic progenitors leads to the appearance of endocrine, acinar, and ductal cells (Shih, Wang & Sander, 2013) (Figure 1. 1 and 1. 2).

Interestingly, it appears that the specific region in the gut where the pancreatic progenitors originate from has the multipotency to develop either into pancreas or liver based on the signals and morphogens to which it is exposed (Gilbert, 2014). While the presence of heart and the absence of notochord induces liver formation, the presence of notochord and the absence of heart causes the pancreas to form. Signals from the notochord suppress Shh protein signals from the endoderm specifically in the region in which pancreas develops (Hebrok, Kim & Melton, 1998). Three specific regions from foregut which are surrounded by notochord, and an aorta and two vitelline veins start the development towards a pancreatic endoderm fate. Interestingly, if the blood vessels are removed from these regions, the early pancreas progenitors, which are known for the expression of pancreatic and duodenal homeobox 1 (PDX1*)* and pancreas associated transcription factor 1a (PTF1A) transcription factors, will fail to form (Lammert, Cleaver & Melton, 2001).

One of the first studies using lineage-tracing to provide direct evidence to show the origins of the pancreatic cells was published in 2002 by Gu *et al.* (Gu, Dubauskaite & Melton, 2002). This study showed that both the endocrine and exocrine parts of pancreas are derived from the same progenitors. It appears that the level of *Ptf1* regulates the proportion of cells in these lineages (Dong *et al.*, 2008). While the exocrine cells have a higher level of *Ptf1*, in endocrine progenitors, PDX1 acts in

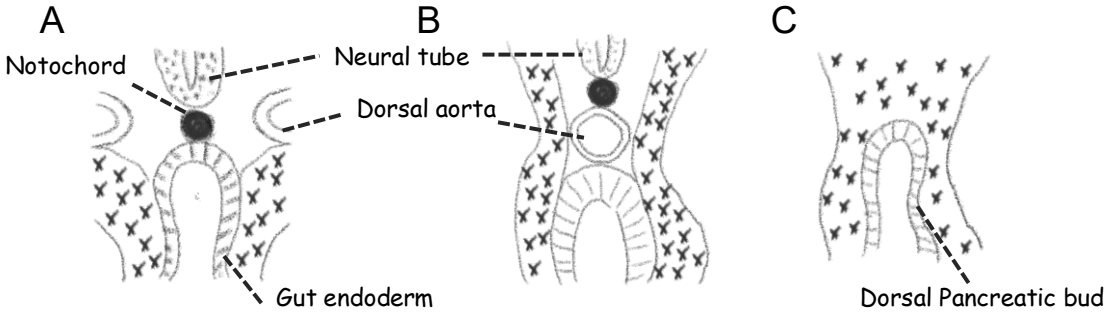

Figure 1.1. Early development of pancreas. A. At the embryonic 15 somite-stage, the notochord is adjacent to the neural tube and the gut. B. At the 20 somite-stage the dorsal aorta locates between the gut and the notochord. C. By the 28 somite-stage mesenchyme surrounds the whole gut and the dorsal pancreatic bud is formed. Image created using PowerPoint.

concert with other transcription factors to derive endocrine cells (Burlison *et al.*, 2008). The endocrine progenitors can form two populations. They can either differentiate into the progenitors of β- and δ- cells (which express Paired box protein 4, *Pax4*) or to the progenitors of α- and PP cells (which express aristaless related homeobox, *Arx*). If the progenitors that express *Pax4* also express *MafA*, they become β-cells and if they do not co-express *MafA*, they develop into δ-cells (Figure 1. 1 shows early stages of pancreatic development).

There are several differences in the development of pancreas in human and mouse. These include spatiotemporal aspects of the expression of key transcription factors as reviewed by (Jennings *et al.*, 2013). For instance, NKX2.2 is present in mouse islet multipotent progenitors before endocrine commitment, while in human islet progenitors, this transcription factor is not detected before endocrine commitment (Prado *et al.*, 2004; Sussel *et al.*, 1998; Jørgensen *et al.*, 2007). Another difference is the appearance of NEUROG3 during embryogenesis. In mouse NEUROG3 appears in two phases. The initial wave is between E8 to 11, and the second wave starts from E12 to E18, with the peak at E15.5 (Villasenor, Chong & Cleaver, 2008). In humans, however, NEUROG3 appears only in one phase which is at the end of embryogenesis and is followed by β-cell differentiation (Jennings *et al.*, 2013; Villasenor, Chong & Cleaver, 2008). These differences could potentially be the reason for the anatomical and functional differences in pancreas of these two species which were briefly mentioned in Chapter 1.1.3.

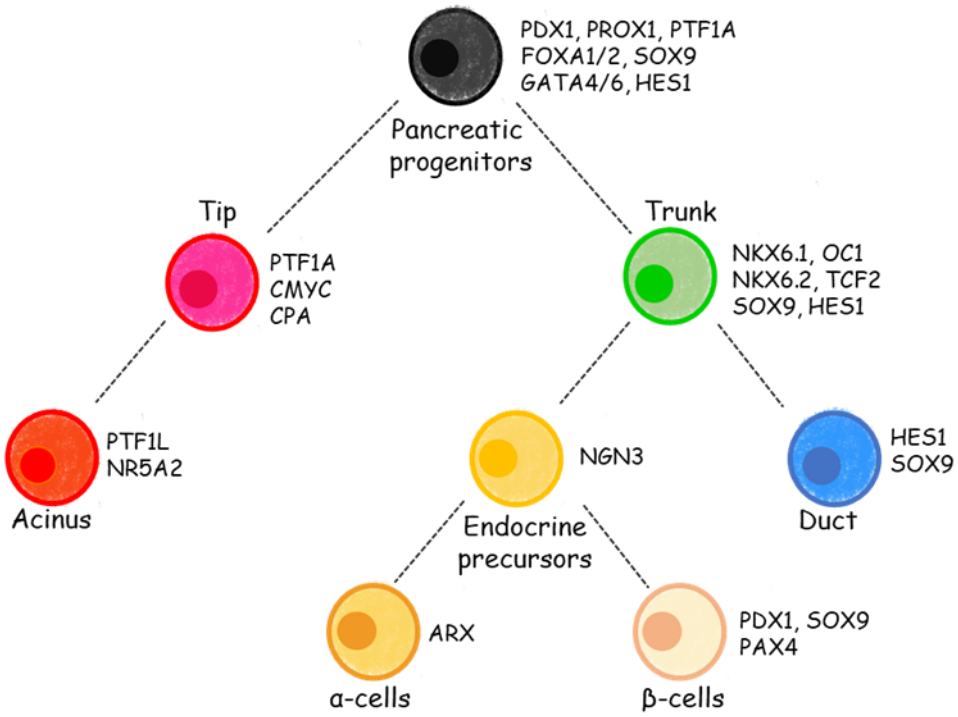

Figure 1.2. Pancreatic cell lineage differentiation during development. Different cell populations with the specific transcription factors expressed throughout the differentiation of pancreatic progenitors towards differentiated cells. Image created using PowerPoint.

1.1.5. β-cell Heterogeneity

Recent advances in single cell technologies have greatly facilitated studies of cell subpopulations (Gutierrez, Gromada & Sussel, 2017). This has created a new area in β-cell biology. Evidence from many studies has raised the possibility of the existence of different subpopulation in β-cells. It has been shown that during pancreas development, some endocrine cells express multiple combinations of the endocrine hormones, and they are termed polyhormonal (Bocian-Sobkowska *et al.*, 1999). When islets develop further, these polyhormonal cells become functionally mature and become specialised to produce only a single hormone. This raises the question of whether all β-cells are generated from a single lineage of multihormonal cells. Heterogeneity also occurs during the maturation of β-cells. It has been shown that the β-cells located at the periphery in islets, tend to mature first compared to the β-cells located in the core (Bocian-Sobkowska *et al.*, 1999). Further studies in rodent also supported the existence of a heterogeneous population of insulin-producing cells (Bocian-Sobkowska *et al.*, 1999). Deletion of the gene encoding the homeobox

protein *Nkx6.1* transcription factor from endocrine progenitor cells resulted in a reduction of insulin-positive cell number by almost half, and changes in the transcriptional identity of the remaining cells. Similar experiments, deleting different transcription factor-coding genes involved in β-cell development and function, such as *Mafb* or Motor Neuron and Pancreas Homeobox Protein 1 *(Mnx1)* led to a partial, but not complete, loss of β-cells (Schaffer *et al.*, 2013; Bocian-Sobkowska *et al.*, 1999). These, and similar experiments (reviewed in Gutierrez *et al*. (Gutierrez, Gromada & Sussel, 2017)) suggest that there are different subpopulations of β-cells that exist within islets, and they do not all share the same origin.

In addition, heterogeneity in the morphology and function of β-cells has been observed. Several studies revealed differences in the size and the composition of sub-cellular organelles as well as differences the number of Gap junctions between β-cells (Gutierrez, Gromada & Sussel, 2017).

β-cells also respond differently to physiological challenges such as those in glucose levels. While there are some β-cells that are responsive to an elevation in glucose concentration, some cells are not responsive to it (Giordano *et al.*, 1991). It has been shown that within islets not all β-cells are secreting insulin in response to an elevation in glucose levels. Interestingly, among β-cells, 75% stay within their responsive or unresponsive state with different stimulations, while 25% of cells switch between these two states (Giordano *et al.*, 1991). Further studies also confirmed differences in β-cells in response to an elevation of glucose concentration (Ling *et al.*, 1998; Van Schravendijk, Kiekens & Pipeleers, 1992).

In addition, heterogeneity in Ca^{2+} dynamics has been observed in β-cells. Thus, it has been shown that the elevation of intracellular Ca^{2+} in response to glucose stimulation starts earlier is some β-cells which are also known as ‘hub cells’ or ‘leader cells’ (Johnston *et al.*, 2016a). Thus, ‘hub cells’ were originally discovered as those hosting the majority of connections between individual β-cells (Johnston *et al.*, 2016b). This was assessed by examining the correlated activity of individual β-cells in a single plane within the islet, based on Ca^{2+} dynamics (Johnston *et al.*, 2016b). Interestingly, when these ‘hub’ cells were reversibly inactivated by optogenetic intervention, the overall intercellular Ca^{2+} dynamics of islets were massively disturbed. The existence of highly connected ‘hubs’ as well as ‘leader cells’ and ‘follower cells’ was also recently demonstrated *in vivo*, in the islets from zebrafish, mice and humans (Salem *et al.*, 2019).

Many studies have shown that β-cells are heterogeneous in many ways. The development of novel technologies has allowed us to further understand the molecular footprint of these diverse subpopulations of β-cells. Several studies investigated differences in β-cells based on mRNA or protein expression (Bader *et al.*, 2016; Johnson *et al.*, 2006; Li *et al.*, 2016; Dorrell *et al.*, 2016; Muraro *et al.*, 2016).

The above studies have led to the separation of β-cells into groups that differ in their protein expression, and the discovery of several molecular markers, from cell-surface proteins to intracellular molecules. Some of these are involved in metabolism, and their differential expression in a given β-cell subpopulation suggests a role in establishing a particular metabolic state. A study categorising β-cells based on their cell surface antigen markers CD9 and ST8SA1 identified four distinct groups (Dorrell *et al.*, 2016). Another study categorising β-cells based on the expression of factors involved in proliferation, signalling pathways, maturation, and previously-identified heterogeneity factors, has identified three subpopulations of cells (Wang *et al.*, 2016). Many more studies also categorised islet subpopulations according to other parameters such as proliferation or pathophysiology (reviewed by Gutierrez *et al*., 2017) (Gutierrez, Gromada & Sussel, 2017).

Other studies have aimed to address the differences between the β-cells in healthy individuals or people with T2D. Understanding the differences between these two groups could lead to improved therapies for people with T2D. For instance, Dorrell *et al*. (Dorrell *et al.*, 2016) identified β-cell subpopulations based on cell surface marker expression. When comparing samples from 17 healthy individuals to individuals with T2D, the proportions of the subpopulations were shifted. Although, in a later study, Wang *et al*. (Wang *et al.*, 2016) did not detect the existence of different populations in healthy and T2D donors, when individual sample populations were compared, correlations to body mass, age and diabetes were observed. Further studies using larger sample sizes are therefore warrantied to investigate in-depth the differences in β-cell identities between healthy and T2D populations.

1.1.6. β-Cells and Insulin Secretion

The main role of β-cells is the secretion of an appropriate amount of insulin in response to an increase of nutrients in the bloodstream. Insulin reduces blood glucose levels and leads to the storage of the sugar as glycogen or after more

extensive metabolism, triglyceride in peripheral tissues, liver, muscles and adipose tissue. Located on the membrane of β-cells, high capacity glucose transporters are responsible for the rapid transport of glucose into the cell. As discussed in more detail below (section 1.1.6), intracellular glucose metabolism activates several signalling pathways which ultimately lead to insulin secretion (Rutter, 2001; Maechler & Wollheim, 2000; Henquin, 2000).

1.1.7. Insulin

Purification and utilisation of insulin as a treatment for diabetes was a joint effort of J.B Collip, F. Banting, C. Best and R. Macleod at the University of Toronto. In 1923, Banting and Macleod were awarded the Nobel Prize for this discovery (Quianzon & Cheikh, 2012). The human insulin gene consists of two intronic and three exonic regions. Exon 2 encodes a signal peptide, a portion of connecting (C)-peptide and B-chain. Exon 3 encodes the A-chain and the remaining amino acids of the C-peptide (Steiner & Oyer, 1967). Pre-proinsulin mRNA is transcribed from the insulin gene and contains a signal peptide, C-peptide, chain A and chain B peptides (Chance, Ellis & Bromer, 1968). In the endoplasmic reticulum (ER) the N-terminal signal is removed, and proinsulin is produced. Proinsulin is then transferred to the Golgi apparatus and is packaged into dense core secretory granules. In the maturing granules, proinsulin is digested to C-peptide and insulin (Goodge & Hutton, 2000) (Figure 1. 3). Interestingly, while insulin in humans is encoded from a single gene, in mouse and rats two insulin genes (*Ins1* and Ins2) encode this hormone (Lomedico *et al.*, 1979). Several transcription factors bind to the regulatory region in enhancer regions of these and the human orthologue to control gene expression. These transcription factors include pancreatic duodenal homeobox-1 (Pdx1), neurogenic differentiator 1 (NeuroD1) and V-maf musculoaponeurotic fibrosarcoma oncogene homologue A (MafA) (Hay & Docherty, 2006; Sharma & Stein, 1994).

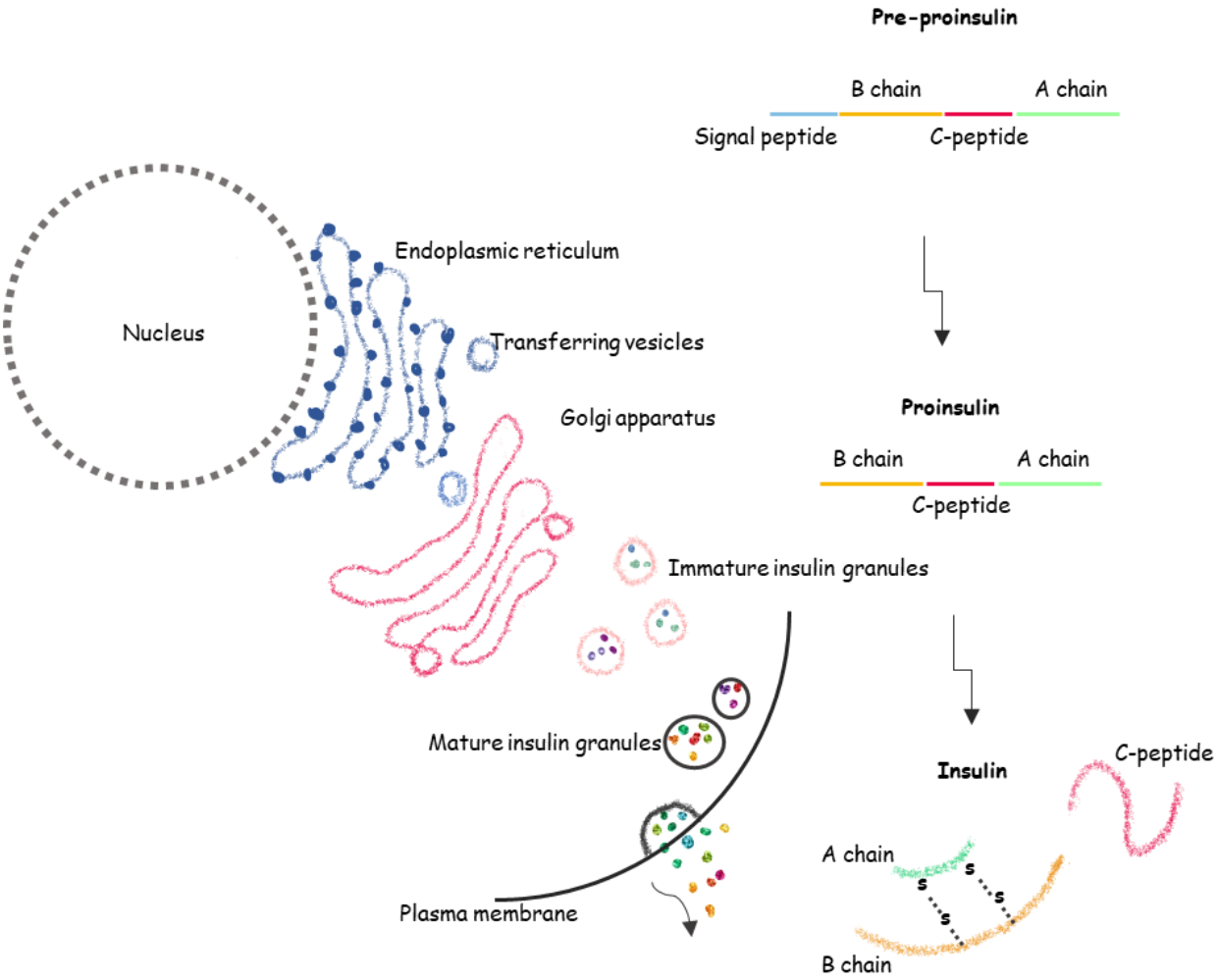

Figure 1.3. Insulin biosynthesis. Pre-proinsulin is transcribed from the insulin gene which consists of a signal peptide, B chain, C-peptide and A chain. In the endoplasmic reticulum, proinsulin is generated by removing the signal peptide. Proinsulin is then transferred to the Golgi apparatus and packaged into immature secretory granules. Before insulin release, the C-peptide is also removed and, upon secretion, both C-peptide and insulin are released from the cell. Image created using PowerPoint.

1.1.8. Glucose-Stimulated Insulin Secretion

Insulin secretion from β-cells is under the control of blood glucose concentrations, several hormones and neurotransmitters. The consensus model of glucose-stimulated insulin secretion (GSIS) consists of a sequence of events. Initially, glucose enters the β-cells by facilitated diffusion, and is metabolised by oxidative glycolysis which leads to increased ATP production. The increase in cytosolic ATP/ADP ratio leads to a decrease of K^+ conductance by closing ATP-sensitive K^+ (K_{ATP}) channels. This is followed by membrane depolarisation and intracellular Ca^{2+} influx via voltage-gated Ca^{2+} channels, triggering insulin secretion (Rutter, 2001; Maechler & Wollheim, 2000; Henquin, 2000) (Figure 1. 4).

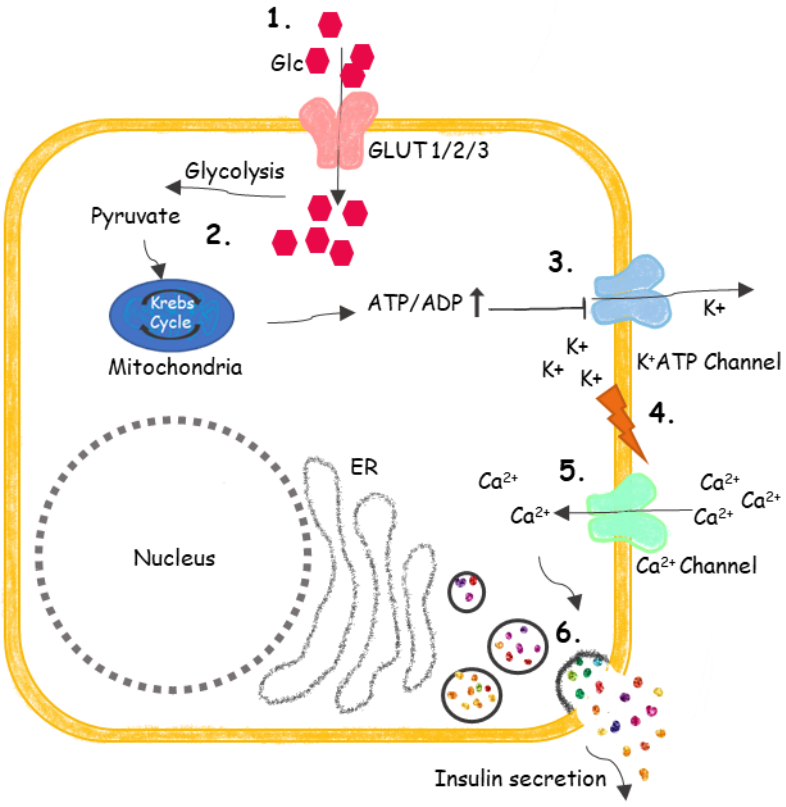

Figure 1.4. Glucose-stimulated insulin secretion (GSIS): triggering mechanisms. 1. GSIS is initiated by the entrance of glucose into β-cells by facilitated diffusion. 2. Metabolism of glucose by oxidative glycolysis subsequently leads to a rise in the cytosolic ATP/ADP ratio. 3. Increased ATP/ADP levels leads to the closure of K_{ATP} channels which then leads to membrane depolarisation (4) and an elevation in intracellular Ca^{2+} levels (5) to trigger insulin secretion (6). Image created using PowerPoint.

1.1.9. Glucose Transport into β-Cells

As introduced above, glucose entry into β-cells is catalysed by a family of facilitated diffusion glucose transporters (GLUTs, encoded by the *SLC2A* genes). The GLUT family includes 14 members. These have distinct amino acid sequences, substrate specificities, kinetic properties, tissue and subcellular localisations (Mueckler & Thorens, 2013). In rodents, GLUT2 transports glucose into β-cells (Cells, Thorens & Sarkar, 1988). In humans, on the other hand, GLUT1 (Mueckler & Thorens, 2013) (*SLC2A1*) and GLUT3 (*SLC2A3)* (McCulloch *et al.*, 2011) also plays an important role alongside GLUT2 (Schuit, 1997). Confirming a role for the latter in man, mutations in the *SLC2A2* gene in humans cause transient neonatal diabetes (Sansbury *et al.*, 2012). In human islets, however, the expression of GLUT2 has been shown to be minimal when compared to GLUT1, and when compared with rodent, GLUT2 expression is ~100 lower in human islets. Therefore, it is suggested that the *SLC2A2* variants exert their effect on fasting glucose levels through defects in other tissues rather than islets (McCulloch *et al.*, 2011).

GLUT2 has a high Michaelis constant (K_M>10mM) and high capacity for glucose which allows fast equilibration of extra- and intra-cellular glucose across the β-cell plasma membrane (Thorens, 2015). This also means that glucose transport through the membrane does not usually have a high control strength for glucose metabolism. Instead, the rate-controlling step in GSIS is the activity of glucokinase, the enzyme that catalyses the phosphorylation of glucose to glucose-6-phosphate in these cells (Thorens, 2015).

1.1.10. Signal Generation

Once glucose enters the cell it is metabolised to a variety of different molecules which may play roles, in addition to ATP, in the control of insulin release. Both cytosolic and mitochondrial molecules resulting from glucose metabolism have been suggested to be involved in the control of hormone secretion. Early studies suggested that increased concentrations of pyridine nucleotides, an elevated NAD(P)H to NAD(P)+ ratio (Panten *et al.*, 1973), as well as triose phosphates, such as phosphoenolpyruvate (Infirmary, 1977), may all have a role. Products of mitochondrial metabolism such as malonyl-CoA (Prentkisg *et al.*, 1992), citrate and glutamate (Wollheim & Maechler, 2002) have also been implicated.

1.1.11. ATP-Sensitive K^+ Channels and Insulin Secretion

ATP-sensitive K^+ (K_{ATP}) channels are tetramers consisting of two main sub-units, SUR1, a sulphonylurea receptor, and Kir6.2, a pore-forming inward rectifier potassium channel. These channels are spontaneously active in β-cells at low (fasting) glucose concentrations and, therefore, they play a key role in maintaining the resting plasma membrane potential (-70 mV or lower), by transferring K^+ to the outside of the cells. The predominant characteristic of these channels is inhibition by ATP. Thus, the presence of high glucose concentrations, and in consequence increased ATP/ADP levels, lead to K_{ATP} channel closure. In mice, at the fasting glycaemia level of 5 mmol/L, the activity of K_{ATP} channels is reduced by 90%, but even the 10% remaining activity of the channels is enough to maintain the resting potential (Rorsman & Braun, 2013; Rorsman *et al.*, 2011). At the fed glycaemia level of between 8-10 mmol/L, the activity of these channels is almost completely suppressed. This closure leads to membrane depolarisation to the threshold for action potential firing (between -60 and -50 mV) [27,] (Rorsman & Braun, n.d.).

K_{ATP} channels function in insulin secretion as a transducer of metabolic changes induced by glucose into biophysical changes at the plasma membrane. Their involvement in insulin secretion has been demonstrated by using inhibitors and activators which do not interfere with glucose metabolism. Thus, the use of diazoxide to open K_{ATP} channels in mouse islets leads to a reduction of intracellular [Ca^{2+}] and inhibition of insulin secretion. In addition, performing the opposite experiment using K_{ATP} channel inhibitors of the sulphonylurea class such as tolbutamide, leads to increases in intracellular [Ca^{2+}] and triggers insulin secretion (Gilontj, 1992). Also, in humans, it has been shown that heterozygous activating mutations in *KCNJ11* gene, encoding Kir6.2, lead to permanent neonatal diabetes (Gloyn *et al.*, 2004). Also, gain-of-function mutations in the gene encoding the SUR1 channel (*ABCC8)* cause neonatal diabetes, and loss-of-function mutations in *KCNJ11* result in congenital hyperinsulinism (Flanagan *et al.*, 2017).

Although many experiments have confirmed the key role of K_{ATP} channels in controlling insulin secretion, glucose can still induce insulin secretion when K_{ATP} channels are held partly open (Henquin, 2000), and intracellular Ca^{2+} concentrations are not affected by the sugar (i.e. they are 'clamped'). Thus, several studies in rodent (Meredith, Rabaglia & Metz, 1995; Jijakli & Malaisse, 1997) and human islets (Straub *et al.*, 1998), as well as perfused rat pancreas (Abdel-halim *et al.*, 1996), and insulin-

secreting cell lines (Hohmeier *et al.*, 2000b) have shown K^+ induced depolarisation in the presence of diazoxide. These experiments led to the identification of a K_{ATP} channel independent pathway, and a possible dual control of insulin secretion (Eliasson *et al.*, 2008).

1.1.12. Signal amplification

As mentioned above, the identification of a K_{ATP} channel-independent pathway, led to the proposal of a dual control of insulin secretion prompted by glucose and other stimuli (Eliasson *et al.*, 2008). These pathways are known as triggering and amplifying pathways (Eliasson *et al.*, 2008), (Rorsman & Renström, 2003). These two interact to control both the temporal nature and amplitude of this bi-phasic process. The first phase of insulin secretion is triggered by glucose and leads to an increase of intracellular Ca^{2+} concentration and then to insulin secretion. Amplifying mechanisms seem to drive the second phase of insulin secretion (Henquin, 2009). More recent studies have also provided evidence for the involvement of the amplifying pathway under physiological conditions (Heart *et al.*, 2006; Henquin *et al.*, 2006). One example is a study comparing the increase in intracellular Ca^{2+} concentrations and insulin secretion in the presence of various glucose concentrations (Henquin *et al.*, 2006). The poor correlation between the Ca^{2+} concentration profile and the secreted insulin triggered by glucose suggested that an additional signal (i.e. an amplifying signal), in addition to the increase in Ca^{2+} concentrations, is produced in response to glucose stimulation to drive insulin secretion. At present, a molecular understanding of these amplifying signals remains to be achieved.

1.1.13. Ca^{2+} Channels

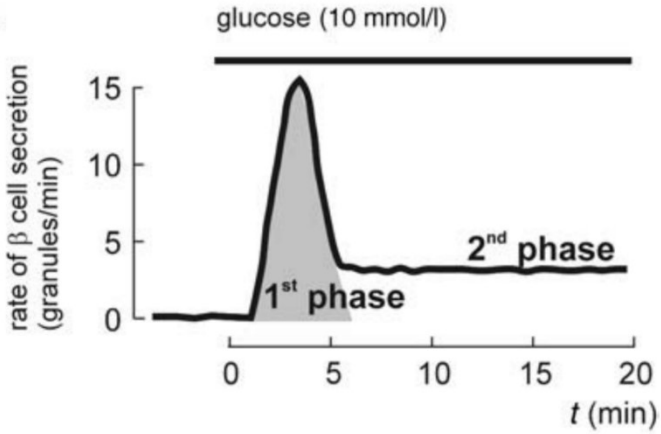

Figure 1.5. Schematic of insulin secretion. This graph shows the bi-phasic insulin secretion upon stimulation with 10 mmol/L of glucose. Image adopted from (Rorsman & Renström, 2003).

Elevated intracellular Ca^{2+} concentrations trigger a broad range of responses in excitable cells. These include promoting exocytosis in endocrine cell and neurons, and muscle contraction in myocytes (Catterall, 2000). Ca^{2+} can enter the cells through voltage-gated Ca^{2+} channels. Different types of such Ca^{2+} channels include L-, N-, P-, Q-, R-, and T-type channels. They consist of α_1 subunit, a pore-forming subunit, of α_2 and δ subunits, a transmembrane, disulphide-linked complex, intracellular β subunits and, in some cases, transmembrane γ subunits (Catterall, 2000). In mouse β-cells, L-type Ca^{2+} channels (which control 50% of total calcium currents) (Safayhi *et al.*, 2014), R-type Ca^{2+} channels (25% of total), and P/Q-type Ca^{2+} (10-15%) channels are responsible for the Ca^{2+} current (Schulla *et al.*, 2003). In β-cells, the drop in voltage caused by the closure of K_{ATP} channels (Section 1.1.10) leads to the opening of voltage-sensitive L-type Ca^{2+} channels and the associated Ca^{2+} entry leads, via elevation of the sub-membrane [Ca^{2+}] (Mitchell, Lai & Rutter, 2003), to the stimulation of Ca^{2+}-dependent exocytosis of insulin-containing secretory granules (Safayhi *et al.*, 2014).

At low glucose concentrations (below 5 mM*, in vitro*), the β-cell membrane potential is stable, and the cell is electrically inactivated. Cells start firing action potentials when a threshold potential is exceeded, -55 mV to -50 mV and at above ~6 mM glucose, membrane depolarisation occurs. Electrical activity increases progressively as glucose concentrations rise further from 6 to 17 mM. This activity is usually oscillatory and is formed of groups of action potentials separated by repolarised,

electrically silent intervals. Glucose, therefore, induces concentration-dependent increases in insulin secretion by forcing the cell to cycle between these electronically-active and -silent phases. When the glucose concentration exceed 20 mM electrical activity is essentially continuous (Rorsman, Braun & Zhang, 2012).

1.1.14. Insulin Granule Dynamics and Insulin Secretion

As mentioned previously (Section 1.1.6), insulin and free C-peptide are packaged in the Golgi into dense core secretory granules which accumulate in the cytoplasm (Goodge & Hutton, 2000). Within secretory granules, insulin can be stored for several days before being released or degraded (Schnell, Swenne & Borg, 1988). There are at least two distinct pools of secretory granules in β-cells. The larger pool is known as the 'reserve pool', consisting of granules which are distant from the cell membrane. A smaller pool, known as the readily-releasable pool, is comprised of granules docked beneath the cell membrane and comprises ~7% of all insulin-containing granules (Olofsson *et al.*, 2002).

Glucose-stimulated insulin secretion has a characteristic biphasic time course with an initial peak which initiates rapidly but lasts a few seconds, followed by a slowly developing but sustained second phase (see Section 1.1.11) (Curry, Bennet & Grodsky, 1968). Although it is still a matter of debate, several studies have suggested that the readily-releasable pool of vesicles is responsible for insulin secretion during the first-phase of GSIS, and the second-phase is associated with movement of the reserve pool to the plasma membrane (reviewed in (Eliasson *et al.*, 2008)).

L-type Ca^{2+} channels, and changes in intracellular free Ca^{2+}, have a critical role in the spatial control of the exocytosis of secretory vesicles. Thus, it has been shown that secretory granules form a tight complex with above-mentioned Ca^{2+} channels to ensure exposure to high intracellular [Ca^{2+}] (Wiser *et al.*, 2002). In addition, β-cells contain a highly Ca^{2+}-sensitive pool of granules (HCSP) (Barg & Rorsman, 2004). However, it has also been demonstrated that exocytosis can occur in the presence of low intracellular [Ca^{2+}] -close to the resting level- in the presence of protein kinase A (PKA) and protein kinase C (PKC) activators (Eliasson *et al.*, 2008). Therefore, a wide range of intracellular Ca^{2+} concentrations can trigger exocytosis, and the identity of the relevant Ca^{2+} sensor molecules is still the subject of further research (Eliasson *et al.*, 2008). Nonetheless, roles for soluble N-ethylmaleimide-sensitive factor-attachment receptor (SNARE) proteins including synaptotagmin-7 (Syt7) have been provided by several studies (Wollheim & Maechler, 2002), (Fukui *et al.*, 2005) .

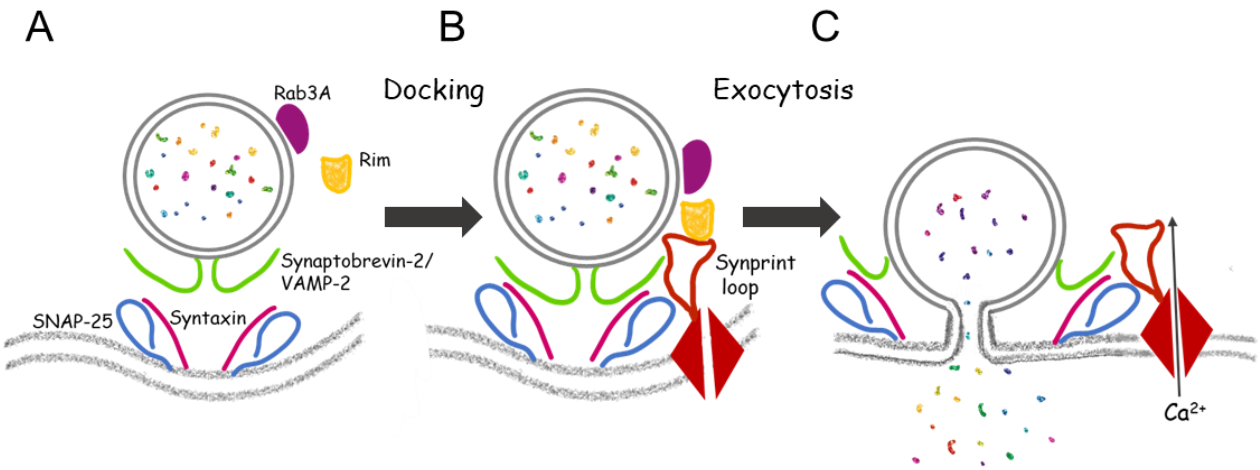

Figure 1.6. SNARE proteins involved in granule dockings and exocytosis. A-B. During docking, the vesicle protein VAMP-2 binds to its partner, SNAP-25 and syntaxin, at the plasma membrane. This process tethers the vesicle to the plasma membrane and to the Ca^{2+} channels. C. Opening of the Ca^{2+} channels leads to a localised increase of Ca^{2+} concentration which is then followed by to the fusion of the two membranes, and exocytosis. The GTP-binding protein Rab3A and its interaction partner Rim, are also indicated in A and B. Image created using Microsoft PowerPoint.

SNARE proteins play a critical role in membrane fusion and exocytosis (Rorsman & Renström, 2003). The SNARE family consists of a group of proteins which form complexes that will fuse with the plasma membrane proteins such as syntaxin and SNAP-25, and vesicular proteins synaptobrevin. It has been suggested (Bruns & Jahn, 2002) that during exocytosis SNARE proteins facilitate this process by bringing the vesicle membrane in close contact with the plasma membrane similar to a zipper. The energy required for this process is provided by the conformational changes that occur. The SNARE proteins are insufficient to account for the rapid Ca^{2+}-dependent exocytosis that represents a hallmark of secretory cells (Shin, Rizo & Südhof, 2002). Synaptotagmin has been suggested to act as a Ca^{2+}-sensor in synaptic vesicle fusion (Shin, Rizo & Südhof, 2002) (Figure 1. 6 shows in summary the process of docking and exocytosis). It has also been suggested that SNARE proteins, in addition to exocytosis, play a role in the entrance of Ca^{2+} specifically to the areas to the plasma membrane which are in close contact with the secretory granules (Barg *et al.*, 2002).

1.2. Other Factors Influencing Insulin Secretion

1.2.1. Incretins

The gastrointestinal tract has a crucial role in postprandial glucose homeostasis. Hormone release from the gut regulates the digestion and absorption of nutrients. The released hormones regulate gastric emptying and the release of insulin independently from the direct effect of glucose (Holst *et al.*, 2016). Interestingly, increased insulin response is observed after oral ingestion of glucose, compared to that observed when the same glucose load is administered parenterally (Perley & Kipnis, 1967). This phenomenon is known as the incretin effect (Perley & Kipnis, 1967). The incretin effect is, in fact, the amplification of insulin secretion by gastrointestinal factors (note that this is different to the 'amplification' process discussed on p25, Section 1.1.11). The incretin effect is due to the hormones secreted from the entero-endocrine cells located in the epithelium of the stomach, small bowel, and large bowel that are secreted at low, basal levels in the fasting state. Circulating levels of most gut hormones rise highly within minutes after nutrient intake and fall rapidly since they are enzymatically inactivated by the kidney. Glucose-dependent insulinotropic polypeptide (GIP) and glucagon-like peptide 1 (GLP-1) are among incretins which are secreted from the gut. Incretins have also been suggested to facilitate the uptake of glucose by muscle tissue and the liver while simultaneously suppressing glucagon secretion by the α-cells of the islets (Perley & Kipnis, 1967). The mechanisms involved in these actions are, however, unclear, given the absence of canonical incretin receptors on these tissues (Holst *et al.*, 2016).

GIP is secreted from the stomach and intestinal K-cells that are localised within duodenum and jejunum of the small intestine (Theodorakis *et al.*, 2006). In rodents, it has been shown that the GIP promotor region has binding sites for the transcription factors GATA-4, ISL-1 and PDX-1 (Drucker *et al.*, 1987) which mediate cell-specific promoter activity. GIP release from K-cells is stimulated by a variety of nutrients including glucose and fats (Besterman *et al.*, 1979). Interestingly, the triggering signal is rather the rate of nutrient absorption than the mere presence of nutrients. Therefore, the secretion of this hormone is reduced in individuals presenting with intestinal malabsorption or after the administration of pharmacologic agents that reduce nutrient absorption (Besterman *et al.*, 1979). GIP acts in a glucose-dependent

manner to increase insulin secretion from pancreatic β-cells. It mediates its effect by increasing the intracellular cAMP levels and by inhibition of K_{ATP} channels, which together act to increase insulin output (Gromada *et al.*, 1998). GIP levels in people with T2D are similar or increased compared to healthy individuals (Ross, Brown & Dupré, 1977; Vilsbøll *et al.*, 2001). However, the GIP receptor is thought to be downregulated in T2D which makes the therapies that modulate GIP levels and/or activity ineffective (Lynn *et al.*, 2001).

Another crucial incretin is GLP-1, which is a post-translational product of the proglucagon gene that is released by intestinal enteroendocrine L-cells located mainly at the distal ileum and colon (Theodorakis *et al.*, 2006). Enzymatic cleavage of full length precursors leads to the generation of both biologically active forms of GLP-1, GLP1(7-37) and GLP1(7-36)NH2 (Dhanvantari, Seidah & Brubaker, 1996). Secretion of this hormone is stimulated by a variety of nutrient, particularly foods rich in fat, neural, and endocrine factors (Baggio & Drucker, 2007). The release of GLP-1 can be stimulated by oral consumption of several nutrients including glucose and other sugars, fatty acids, essential amino acids and dietary fibre (Herrmann *et al.*, 1995). Interestingly, it has been shown that a variety of other factors such as the autonomic nervous system, neurotransmitters such as gastrin-releasing peptide (GRP) and acetylcholine, and the peptide hormone GIP can all also contribute to the rapid release of GLP-1 after nutrient ingestion (Baggio & Drucker, 2007). The GLP1 receptor (GLP1R) belongs to a family of 7-transmembrane G-protein coupled receptors (GPCRs) (Cho, Merchant & Kieffer, 2012). They are expressed in α-, β- and δ-cells of pancreatic islets, as well as other tissues such as the stomach, heart, hypothalamus and hindbrain (Richards *et al.*, 2014). In β-cells, upon binding of GLP-1, a conformational change occurs at the ligand binding site of the GLP1R facilitating the interaction of its intracellular residues with signalling proteins. GLP1R interacts with a specific subpopulation of guanine nucleotide binding proteins (G proteins) and other interactors such as the β-arrestins among others. In various GLP-1-responsive tissues, activation of the cAMP signalling pathway has been demonstrated (Dalvi *et al.*, 2012; Drucker *et al.*, 1987). In GLP-1 responsive tissues cAMP production is activated by guanine nucleotide exchange and heterotrimeric G protein activation/dissociation to release the stimulatory G protein subunit Gαs, which in turn activates adenylate cyclase (Roger *et al.*, 2010). The increase in intracellular levels of cAMP have been suggested to acts at multiple stages in the secretory pathway

including K_{ATP} channel closure, Ca^{2+} entry and vesicle trafficking in β-cells (Koole *et al.*, 2013).

1.2.2. Free Fatty Acids

Free fatty acids (FFAs) also stimulate insulin secretion in a glucose-dependent manner. In other words, they do not stimulate insulin secretion directly, but rather amplify the effect of GSIS (Crespin, Greenough III & Steinberg, 1969). FFAs trigger GSIS by at least two distinct mechanisms. FFAs are transported into cells, activated into long-chain acyl-CoA, and metabolised to generate lipid signalling molecules that promote insulin exocytosis (Nolan *et al.*, 2006). Furthermore, acting externally at the cell surface, FFAs can also bind to and activate the G-protein–coupled receptor Firstly FFAR1 (GPR40), which is mainly coupled to $G\alpha_{g/11}$. (Ferdaoussi *et al.*, 2012). Binding to GPR40 leads to activation of phospholipase C (PLC) which leads to activation of both diacylglycerol (DAG) and inositol 1,4,5 -trisphosphate (IP_3) production. The increased IP_3 leads to increased intracellular Ca^{2+} levels, via the modification of ER-associated Ca^{2+} stores, seen upon GPR40 activation and, therefore, amplification of insulin secretion (Ferdaoussi *et al.*, 2012).

1.2.3. Neural Factors

An observation that lesions of specific nuclei in the hypothalamus produce profound increases or decreases in food intake and body weight led to the discovery that brain plays a role in controlling energy balance (Seeley & Woods, 2003). In the hypothalamus, an intricate neuronal circuit involving the arcuate nucleus, which is located adjacent to the floor of the third ventricle, play roles in controlling the food intake, energy expenditure and glucose homeostasis. This circuit of neurons consists of neurons co-expressing pro-opiomelanocortin (POMC) and cocaine- and amphetamine-related transcript (CART) (Schwartz *et al.*, 2003). These neurons regulate the actions of an anabolic pathway, comprising neuropeptide Y (NPY)/agouti-related protein neurons (AgRP) (Schwartz *et al.*, 2000; Seeley & Woods, 2003). Insulin stimulates the activity of POMC neurons while it inhibits neuronal NPY release. POMC neurons are stimulated by input from insulin and leptin (Cowley *et al.*, 2001). Binding of melanocortins to melanocortin 3 Receptor (MC3r) and MC4r inhibits food intake and promotes weight loss (Cowley *et al.*, 2001).

It is essential for the brain to be exposed to sufficient levels of glucose as its main source of energy. Therefore, maintaining glycaemia at around 5 mM is crucial. It has been shown that a still poorly understood brain-islet axis plays a role in controlling insulin secretion (Chan & Sherwin, 2012). Activation of neurons in the hypothalamus in response to hyper- or hypoglycaemia and other areas in brain is critical to regulate the secretion of insulin and other islet hormones. Therefore, insulin action in the hypothalamus influences both energy balance and glucose metabolism. It has been suggested that hypothalamic glucose sensing may also provide an additional input to β-cells to regulate the first-phase insulin response to an elevation of glucose levels (Osundiji *et al.*, 2012). It has been shown that the chronic suppression of insulin receptors in the ventromedial hypothalamus leads to glucose intolerance and β-cell dysfunction (Paranjape *et al.*, 2011). Other studies also demonstrated that deletion of the insulin-responsive glucose transporter, GLUT4, in the brain causes impairments in glucose sensing and glucose intolerance in mice (Lin *et al.*, 2011; Reno *et al.*, 2017). GLUT4 is expressed in the brain in the hippocampus, cortex, cerebellum and in the hypothalamus (McEwen & Reagan, 2004).

It has been shown that glucose-sensing neurons exist in the brain which activate sympathetic or parasympathetic branches of the autonomic nervous system. These branches not only control insulin and glucagon secretion from pancreatic islets, but also regulate α- and β-cell number (Thorens, 2011). This neural control of insulin and glucagon secretion is the result of both the presence of nerve endings in pancreatic islets and of specific neurotransmitter receptors present in *α*-and *β*-cells (Ahrén, 2000). Therefore, both total *β*-cell number and secretion activity can be regulated by vagal control. These effects are mediated, at least in part, by acetylcholine acting on the *β*-cell and also neuropeptides such as vasoactive intestinal polypeptide (VIP), pituitary adenylate cyclase activating polypeptide peptide (PACAP), or gastrin-releasing peptide (GRP) (Thorens, 2011)·(Henquin & Nenquin, 1988; Woods & Seeley, 2006; Gautam *et al.*, 2010).

1.3. Diabetes Mellitus

Diabetes mellitus is a chronic disease which occurs when the body cannot make enough insulin (i.e. β-cell dysfunction) and/or there is insulin resistance in peripheral tissues. This condition currently affects 1 in 11 adults worldwide (Anon, n.d.). There are three main types of diabetes which include, type 1, type 2 and gestational diabetes (Anon, n.d.). Whilst these are complex polygenic diseases, monogenic form of T2D with Mendelian inheritance, termed maturity onset of diabetes (MODY) also exists (Tattersall & Mansell, 1991).

1.3.1. Type 1 Diabetes

Type 1 diabetes (T1D) was formerly known as insulin-dependent diabetes. Around 10% of people with diabetes live with this condition (Anon, n.d.). T1D is usually diagnosed in children and adolescents. This condition arises following the autoimmune destruction of β-cells (Atkinson, 2012). Due to destruction of β-cells, not enough insulin is synthesised to counter the increase in blood glucose. This leads to high levels of glucose in blood and urine. Therefore, administration of insulin is usually essential for people with T1D. Despite being influenced to some extent by genetic factors, T1D does not fit any simple pattern of inheritance and is considered a complex, multifactorial disease. It has been shown that both environmental and genetic factors are the underlying cause of this condition with 30-70% disease discordance in monozygotic twins (Redondo *et al.*, 2008). Therefore, to study this condition multiple factors such as genetics and the role of environmental factors need to be considered.

1.3.2. Type 2 Diabetes

Type 2 diabetes (T2D) is the most common form of diabetes (>90% of all cases (Anon, n.d.)). Different factors, including genetic susceptibility, over-nutrition and limited physical inactivity (leading to obesity) are among the risk factors for this disease. Genetic factors play a more important role in T2D than T1D with concordance between monozygotic twins approximately 100% in the former disease (Medici *et al.*, 1999). In Europe in 2017, 58 million people have been diagnosed with diabetes and this number is predicted to increase to 67 million by 2045. Currently, 12% of global health expenditure is spent on diabetes and its complications (Anon, n.d.). The only therapeutic options currently available improve glycaemia but do not

address the decline in β-cell dysfunction over time. The latter is the most important driver of disease development and progression (Srimanunthiphol, Beddow & Arakaki, 2000). Therefore, to prevent and/or control this condition more effectively, it is crucial to further understand the genetics and the molecular pathways involved in the disease.

1.3.3. Maturity Onset Diabetes of the Young

MODY is a group of hereditary disorders caused by mutations in autosomal genes (Thomas & Philipson, 2015). MODY usually presents in adolescence or in young adulthood. This condition affects 1-2% of the population. Due to its low frequency, it is often misdiagnosed as type 1 or type 2 diabetes (Thomas & Philipson, 2015). Up to now, up to 11 genes have been linked with this type of diabetes (Table 1) (Naylor *et al.*, 2018). The most common form of MODY is caused by mutations in *HNF1A* (MODY 3) in populations with European ancestry (Frayling *et al.*, 2001). The latter gene encodes a transcription factor essential for β-cell function and maintenance (Fajans, Bell & Polonsky, 2001). Mutations in *HNF1A* account for more than 50% of monogenic diabetes (Pihoker *et al.*, 2013). Several other genes have also been associated with MODY and are listed in Table 1 (reviewed in Naylor *et al.*, 2018 (Naylor *et al.*, 2018)).

Gene name	**% of all MODY**
HNF4A	5%-10%
GCK	30%-50%
HNF1A	36%-65%
PDX1	1%
HNF1B	<5%
NEUROD1	<1%
CEL	<1%
PAX4	<1%
INS	<1%
ABCC8	<1%
KCNJ11	<1%

Table 1. Associated genes with MODY. Up to now at least 11 genes have been associated with MODY (Naylor *et al.*, 2018).

1.4. Sexual Dimorphism and Glucose Homeostasis

Although sexual differences represent one of the best conserved features of biology, they have until recently been underappreciated in biomedical research. It was not until the early 1990s that the National Institutes of Health (NIH) Revitalisation Act mandated the inclusion of women in clinical trials, so that the outcome of all NIH-funded clinical research would generate data that is relevant to both males and females (Mauvais-Jarvis, 2015).

Unfortunately, many animal studies have also ignored gender differences. Even today, many research studies have been only focused on male subjects; based on these being smaller variations over time and between individuals, many drugs have been tested using only male animals to avoid extra costs in the projects. It has been shown that pharmacology and neuroscience studies are more male sex biased, while female sex bias is more apparent in immunology (Beery & Zucker, 2011).

Since there are fundamental gender-specific differences in metabolic homeostasis, half of the population might not benefit from treatments if only one gender is considered in basic and clinical research (Mauvais-Jarvis, 2015). Therefore, it is critical to understand, and further investigate, these gender dimorphic differences.

It has been shown in several studies that some aspects of glucose homeostasis and energy balance are regulated in a sexual dimorphic manner (Mauvais-Jarvis, 2017). These gender-specific differences are thereby likely to be driven by multiple factors that need to be studied to develop gender-based therapeutic approached for metabolic conditions such as T2D.

There are gender-specific differences in human metabolism and adipose storage. Not only there are differences in the percentage of adipose tissue between males and females, their distribution pattern is gender-specific (Karastergiou *et al.*, 2012). It has been shown while women predominantly store adipose tissue in subcutaneous areas, men have a higher tendency towards storing fat at intra-abdominal sites (visceral and mesenteric adipose tissue). These differences in body fat storage could highlight the gender-specific differences in the function of adipose tissue. Subcutaneous adipocytes are more adopted to long-term storage, while visceral adipocytes are more metabolically active and prone to lipolysis (Karastergiou *et al.*, 2012). Also, the function of the adipocyte seems to be gender-specific. Circulating

concentrations of both leptin and adiponectin, the two major adipokines, are higher in women compared to men (Nishizawa *et al.*, 2002). Some of these differences could be related to the actions of sex hormones. However, in females the circulating leptin level is higher before puberty and after menopause. This suggests its increased level in females compared to males is independent of sex hormones (Nagy *et al.*, 1997; Rosenbaum *et al.*, 1996).

In relation to glycaemic traits, while women have better glucose homeostasis, men are more predisposed to T2D (Mauvais-Jarvis, 2015). Interestingly, while women show the traits that are predicted to promote insulin resistance such as more adipose tissues mass, more circulating free fatty acids and higher intramyocellular lipid content, they are less prone to insulin resistance compared to males (Frias *et al.*, 2001). The beneficial glucose homeostasis observed in women has been linked to circulating estrogen levels between puberty and menopause. It has been shown that circulating estrogen levels elevate beyond the physiological level (Mauvais-Jarvis, Clegg & Hevener, 2013), or when strong synthetic estrogens are used (Perseghin *et al.*, 2001) insulin resistance phenotypes appear. There are also differences between males and females in glycaemic traits. While women are more likely to show impairments in glucose tolerance, males are more prone to elevated fasting glucose, regardless of their ethnicity (Williams *et al.*, 2003; Sicree *et al.*, 2008). Although the possible reasons behind the latter differences in glycaemic traits are unknown, they could be associated with lower muscle mass or physical fitness in women (Mauvais-Jarvis, 2015). A survey of the global diabetic population revealed that there are more diabetic men before puberty while there are more diabetic women after menopause (Rathmann & Giani, 2004). This further emphasises the role of sex hormones, among other factors such as different body fat distribution and related biomarkers, such as higher adiponectin, in glucose homeostasis. Estrogen has been shown to have direct effects on β-cells. It has been demonstrated that estrogen has a protective effect against apoptosis in β-cells (Le May *et al.*, 2006), stimulates secretion from these cells (Wong *et al.*, 2010) and improves insulin sensitivity (Ribas *et al.*, 2010).

There is not much known about the role of incretins in sexual dimorphism. However, in women with T2D, it has been shown that GLP-1 levels are 25% lower in response to an oral challenge compared to males. It is known that GLP-1 stimulates insulin secretion (Section 1.2.1) and it is related to a better insulin secretion in response to

food intake. Therefore, these decreased GLP-1 levels in women with T2D could potentially contribute to relatively lower β-cell function (Færch *et al.*, 2013).

1.5. Genome-Wide Association Studies

Genome-wide association studies (GWAS) are designed to identify associations between specific genetic variants at specific *loci* and phenotypic traits. One of the ultimate objectives of these studies is thus to reveal the genetic basis of human diseases and to discover more efficient and personalised therapeutic options and/or disease prevention (Visscher *et al.*, 2017). In practice, however, it is challenging to associate DNA variants with specific traits since such studies are dependent upon different factors including experimental sample size, the distribution of effect sizes of (unknown) causal genetic variants that are segregating in the population, the frequency of those variants, and the linkage disequilibrium (LD) between observed genotyped DNA variants and the unknown causal variants (Visscher *et al.*, 2017). Other crucial factors that need to be considered include the effect size, allele frequency and disease heterogeneity (Visscher *et al.*, 2017).

Considering these challenges, GWAS have nevertheless made several significant advances. For example, the GWAS identified gene *SLC30A8,* encoding the insulin granule zinc transporter ZnT8 and its association with T2D has led to the concept of ZnT8 antagonists as therapies. Similarly, *PAD14/IL6R* association with rheumatoid arthritis has led to BB-CI-amidine candidate drug development (Nelson *et al.*, 2015). Many more examples of these drug candidates have been mentioned in the literature (Nelson *et al.*, 2015).

1.5.1. Type 2 Diabetes and GWAS

Since 2007, several genetic variants have been associated with T2D (Rutter, 2014) as a result of GWAS studies (Sladek *et al.*, 2007; Ng *et al.*, 2014; Watson *et al.*, 2019; Pascoe *et al.*, 2007; Unoki *et al.*, 2008; Ng *et al.*, 2008; Wu *et al.*, 2008). Thanks to these studies, more than 400 independent signals at 243 *loci* have now been associated with T2D risk (Mahajan *et al.*, 2018a).

The first GWAS for T2D analysed normal-weight T2D individuals of European-ancestry, comparing them to non-diabetic individuals, and identified variants at five novel *loci* in increasing disease risk (Sladek *et al.*, 2007). In the later study, transcription factor 7-like 2 (*TCF7L2)* was one of the candidates which was associated with T2D. TCF7L2 is a transcription factor downstream of wingless-

related integration site (Wnt)/β-catenin pathway and plays a role in embryonic development and cell differentiation and division (Peifer & Polakis, 2000). The role of this gene in T2D was shown in previous GWAS studies (Grant *et al.*, 2006). Several studies, using functional studies, have shown the role of this gene in the liver and β-cells in the regulation of glucose homeostasis (Savic *et al.*, 2011; da Silva Xavier *et al.*, 2012; Shu *et al.*, 2009). *SLC30A8* (a β-cell specific Zn^{2+} transporter) was another gene associated with T2D risk and discovered by Salek *et al*. The three other gene variants (*IDE-KIF11*, *HHEX* and *EXT2-ALX4*) were found in regions of DNA that are involved in β-cell development/function. This initial GWAS was followed by several other studies which confirmed the previous genes and added several more candidate genes to the previous list (Burton *et al.*, 2007; Zeggini *et al.*, 2007; Steinthorsdottir *et al.*, 2007).

After the initial identification of the above *loci* by GWAS, subsequent meta-GWAS, involving multiple cohorts to increase statistical power, led to the identification of new variants, chiefly single nucleotide polymorphism (SNPs) (Mahajan *et al.*, 2018b).

1.5.1. Causal genes at T2D risk *loci*

Following a decade of GWAS locus discovery, 'post-GWAS methodologies' have been implemented to functionally characterise the underlying genes and identify the disease pathways (Grotz, Gloyn & Thomsen, 2017). Identifying the causal variants can provide a direct association between the observed phenotype and the observed disease phenotype. Methodologies that can be employed to explore these causal variants are the interrogation of coding variants, establishing variant-gene links for non-coding variants, and using high-throughput screens to prioritise candidate genes.

Missense variants at the coding regions could lead to change in protein structure. Therefore, harnessing coding variation can offer powerful insights into causal mechanism. This approach, however, is fundamentally limited by the occurrence of natural variation (in outbred and isolated populations) which requires larger association studies to detect rare, coding variation (Mahajan *et al.*, 2018b). In addition, identification of a coding variant per se does not guarantee causality and, therefore, it is crucial to identify the causal coding variants by additional fine-mapping of non-coding regions to exclude the contribution of non-coding variants as drivers of the association signal. An interesting example are variants located on coding

region at the *SLC30A8* locus which demonstrates the importance of these variants for ascertaining causal mechanisms (Rutter & Chimienti, 2015). This gene encodes a zinc transporter (ZnT8) that is located on the membrane of the secretory vesicles of β-cells. A common missense variant in this gene was first discovered by GWAS as a T2D susceptibility gene (Sladek *et al.*, 2007). However, a more recent study (Flannick *et al.*, 2014) has discovered several rare protein-truncating variants in this gene. Interestingly, the later study discovered that these independent loss-of-function coding variants in *SLC30A8* were associated with *reduced* risk of T2D. A more recent study (Dwivedi *et al.*, 2019) also confirmed the previous studies and showed that the loss-of-function mutation in *SLC30A8* mediates reduced T2D risk by enhancing insulin secretion due to enhanced glucose responsiveness and proinsulin conversion. Studies on this locus highlight the importance of discovering an extended allelic series to understand functional mechanisms.

Another challenge facing GWAS is the identification of the relevant effector transcripts, given that most variants map to non-coding (intergenic or intronic) sequences (Schaub *et al.*, 2012). Thus, important variants are likely to be located in regions which control the expression of nearby genes. The identification of both the causal variant(s), and the gene(s) through which these mediate their effects on cell physiology, are thus crucial objectives if the potential of GWAS is to be fully realised.

The first of these – the identification of causal variants – is usually achieved by genetic fine mapping, followed by reweighting of posterior probabilities based on epigenomic annotations of disease-relevant tissues (so-called functional GWAS or fGWAS (Pickrell, 2014)). Identification of effector transcripts then involves expression quantitative trait locus (eQTL) analysis. Thus, by assessing expression in disease-relevant tissues – often pancreatic islets or β-cells the majority of GWAS-identified T2D variants affect insulin secretion rather than action (Rutter, 2014) – it may be possible to determine whether the expression of nearby genes is affected by the possession of the most likely causal variants (cis-eQTL) (Rutter, 2014). However, if the identified variant does not regulate the expression of a nearby gene, eQTL studies are not guaranteed to identify the causal transcript. In this case a search maybe necessary for a trans-eQTL wherein the regulated gene may be located a substantial distance from the genomic locus. To study such long-range effects, call-based approaches such as chromatin conformational capture (3C) (Hagège *et al.*, 2007) may be useful to detect a physical interaction in three dimensions between a

given variant and an effector gene in disease-relevant tissues (Rutter, 2014). Going through these filters can lead to the identification of better candidates for future functional studies.

In addition to the above methodologies, experimental prioritisation, and *in silico* prediction tools could also be utilised to identify the causal variants. These approaches have been deployed to search for causal variants at several GWAS *loci* for instance at the *JAZF1* and *CDC123/CAMK1D loci* (Fogarty *et al.*, 2014, 2013; Zeggini *et al.*, 2008). Variants located at these *loci* and in high LD ($r^2 > 0.8$) with the lead GWAS SNP were selected for functional analysis based on maps of open chromatin. The causal variant at these *loci* mediates its effect in each case, by affecting the transcription factor binding sites of the downstream genes. However, these types of experiments also have their practical limitations and to overcome this and to identify causal variants, *in silico* prediction tools offer an alternative method. For instance, a computational approach, termed phylogenetic module complexity analysis (PMCA), can be used to identify a clustering of homeobox transcription factor binding sites at T2D risk *loci*. This model was used to propose a potential causal variant at the *PPARG* locus, which allowed for a subsequent functional interpretation (Claussnitzer *et al.*, 2014).

1.5.2. The *VPS13C/C2CD4A*/*C2CD4B* T2D locus

Several studies have shown that single nucleotide polymorphisms (SNPs) on human chromosome 15 near *C2CD4A, C2CD4B* and *VPS13C* are associated with T2D and glycaemic traits [43–50]. As such, these studies have identified potential roles for these genes in the regulation of insulin secretion and glucose homeostasis.

In 2010 GWAS studies (Saxena *et al.*, 2010; Ingelsson *et al.*, 2010) involving individuals of European descent, showed an association between SNP rs17271305 (in the coding region of *VPS13C*) and higher 2-hour glucose and lower fasting pro-insulin levels. In the Japanese population, however, SNPs at this position were reported to be causal for T2D (Yamauchi *et al.*, 2010a). Other studies from individuals of white European and American descent, as well as middle-aged Danish subjects, showed an association between the risk allele rs11071657 (in the intergenic region between *C2CD4A* and *C2CD4B*), and higher proinsulin to insulin ratio, a trend towards increased fasting glucose (Ingelsson *et al.*, 2010), a significantly elevated fasting glucose but not T2D (Dupuis *et al.*, 2010) and a

significant decrease in GSIS (Boesgaard *et al.*, 2010). A meta-analysis in Japanese and Asian populations (Yamauchi *et al.*, 2010a), in addition to the previous European descent data (Dupuis *et al.*, 2010)' (Ingelsson *et al.*, 2010), have added two other SNPs at rs7172432 and rs1436953, that are associated with increased risk of T2D (Yamauchi *et al.*, 2010a). The latter study also showed that risk alleles at rs7172432, rs1436953 and rs1370176 are in high LD with each other (Yamauchi *et al.*, 2010a) (Figure 1. 7). SNPs at rs7172432 in Danish (Grarup *et al.*, 2011) and Chinese populations (Cui *et al.*, 2011) also have been shown to be associated with decreased glucose-stimulated insulin release and increased T2D risks, respectively. Table 2 summarises crucial GWAS SNPs in the *C2CD4A/C2CD4B/VPS13C* locus that are associated with glycaemic traits.

Although the above GWAS-identified SNPs in the *C2CD4A* and C2CD4*B* locus were associated with glycaemic traits and disease risk, it was only in 2012 that Schaub and colleagues (Schaub *et al.*, 2012) identified the 'lead' and the 'functional' SNPs in this region. The latter study thus identified variants that are the most likely to play a crucial biological role. It should be emphasised that a SNP that overlaps an experimentally detected transcription factor binding site, and is in strong linkage disequilibrium with a SNP associated with a phenotype, is more likely to play a biological role than other SNPs in the associated region. Taking this into account, the above authors (Schaub *et al.*, 2012) identified a novel 'functional SNP', rs7163757, in this region. They demonstrated that the latter SNP (Schaub *et al.*, 2012) is in a strong LD with rs7172432, a SNP in several populations with a strong association with decreased glucose-stimulated insulin release and increased T2D risk (Grarup *et al.*, 2011; Cui *et al.*, 2011) (Figure 1. 8). Interestingly, more recent studies have demonstrated that rs7163757 is located in an islet 'stretch enhancer' region (Miguel-Escalada *et al.*, 2018)' (Kycia *et al.*, 2018). Stretch enhancers are large chromatin regulatory elements which are at least 3 kb long (Quang *et al.*, 2015). More importantly stretch enhancers, also referred to as super enhancers or clusters of enhancers, are associated with the regulation of tissue-specific functions (i.e. insulin secretion in β-cells) (Pasquali *et al.*, 2014). In addition, a Meta-analysis using 898,130 individuals associated variant at rs8037894 in the *C2CD4A/C2CD4B/VPS13C* locus with increased risk of T2D (Mahajan *et al.*, 2018a).

Risk allele	Glycaemic trait	Effect allele	Number of individuals analysed	Population	Study
rs17271305	Lower fasting proinsulin levels	G	29,084	White adults from Europe or the U.S.	Ingelsson 2010 (Ingelsson *et al.*, 2010), Diabetes
rs11071657	Higher proinsulin to ins levels, A trend towards increase fasting glucose	A	29,084	White adults from Europe or the U.S.	Ingelsson 2010 (Ingelsson *et al.*, 2010), Diabetes
rs17271305	Higher 2-h glucose	G	15,234 plus 30,620	European descent	Saxena 2010 (Saxena *et al.*, 2010), Nature Genetics
rs11071657	Higher fasting glucose, found less significant T2D associations	G/A	40,655 T2D cases and 87,022 nondiabetic control	Meta-analysis on glycaemic trait, European descent	Dupuis 2010 (Dupuis *et al.*, 2010), Nature Genetics
rs7172432, rs1436953	T2D risk	A, N/A	stage 1, 4,470 cases and 3,071 controls; stage 2, 2,886 cases and 3,087 controls; stage 3, 3,622 cases and 2,356 controls	Stage 3 results in the meta-analyses of the Japanese populations	Yamauchi 2010 (Yamauchi *et al.*, 2010b), Nature Genetics
rs7172432	T2D risk	A	T2D: 21,731 Control: 20,377	Japanese, East Asians and European	Yamauchi 2010(Yamauchi *et al.*, 2010b), Nature Genetics
rs1436953	T2D risk	N/A	T2D: 20,335 Control: 18,933	Japanese, East Asians and European	Yamauchi 2010(Yamauchi *et al.*, 2010b), Nature Genetics
rs11071657	Lower insulin release as assessed by the CIR index BIGTT-AIR index and higher fasting plasma glucose	A	6,784	Danish-Middle age	Boesgaard, 2010 (Boesgaard *et al.*, 2010), Diabetologia
rs7172432	Higher waist circumference, higher fasting glycaemia, higher glycaemia during OGTT	A	5,722	Danish	Grarup 2011 (Grarup *et al.*, 2011), Diabetologia
rs4502156	Higher fasting proinsulin, 2-h post load glucose Lower insulinogenic index, fasting glucose, decreased HOMA-B	T	16,378	European descent	Strawbridge 2011 (Strawbridge *et al.*, 2011a), Diabetes
rs7172432, rs1370176	Higher risk of T2D	A, C	T2D: 4,445 Controls: 4,458	Chinese	Cui 2011 (Cui *et al.*, 2011), PLOS One
rs7172432	Higher proinsulin levels	A	8,229	Nondiabetic Finnish males	Huyghe 2013 (Huyghe *et al.*, 2013), Nature Genetics
rs4502156	Higher 2-h Glu, FP/CIR and FG	T	26,037	Nondiabetic individuals	Prokopenko 2014 (Prokopenko *et al.*, 2014), PLOS Genetics
rs7163757	Lower first-phase insulin secretion IVGTT	C	5,567	Variant background	Wood 2017 (Wood *et al.*, 2017), Diabetes
rs8037894	Increased risk of T2D	G	898,130	European descent	(Mahajan *et al.*, 2018a)

Table 2. Associations between risk alleles at the *C2CD4A/C2CD4B/VPS13C* locus and glycaemic traits in GWA studies. Phenotypes: *FG* fasting glucose, *FI* fasting insulin, *FP* fasting proinsulin, *2hGlu* two-hour post-prandial glucose, *1hGlu* one-hour post-prandial glucose, *CIR* corrected insulin response to glucose.

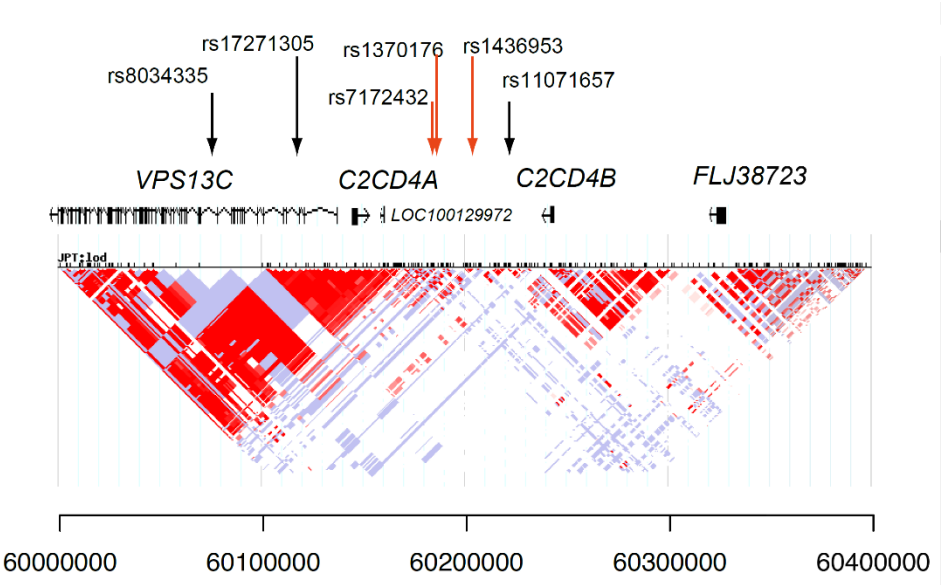

Figure 1.7. Map of SNPs and linkage disequilibrium identified in human chromosome 15 near *C2CD4A*, *C2CD4B* and *VPS13C*. Figure adopted from Yamauchi *et al.* 2010 (Yamauchi *et al.*, 2010b).

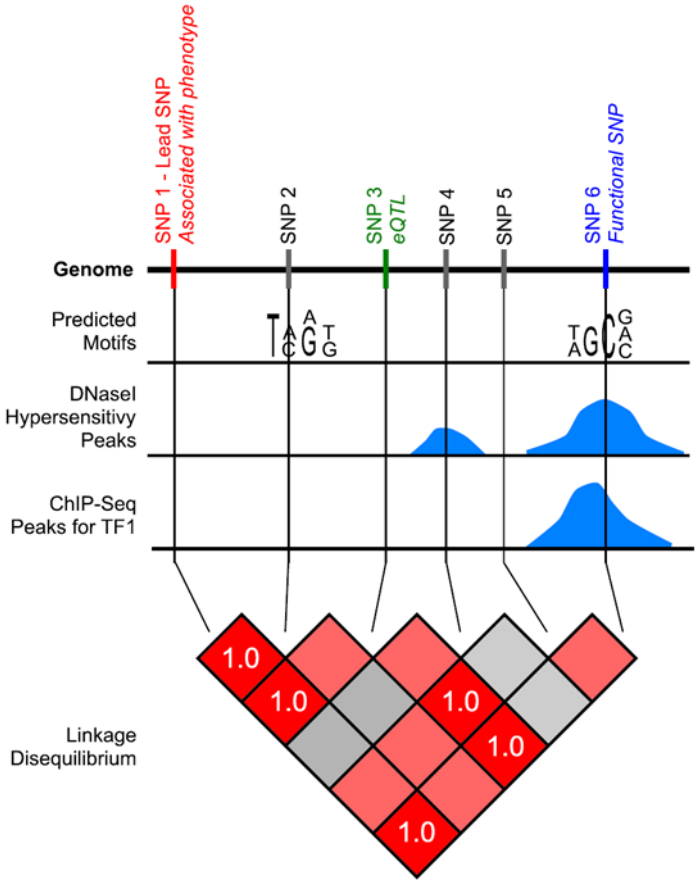

Figure 1.8. Schematic overview of the 'functional SNP' approach. Different SNPs from previous studies were identified (SNP1 to 6); SNP1 is associated with the phenotype; also, multiple sources confirm that SNP6 is in the regulatory region. SNP1 and SNP6 are in perfect LD (r^2=1.0). Therefore, SNP6 is identified as the most likely 'functional' SNP in the region. Figure adopted from (Schaub *et al.*, 2012).

1.5.3. The Effect of Variants at the *VPS13C/C2CD4A*/*C2CD4B* Locus on Gene Expression

Since several SNPs in the *C2CD4A* and *C2CD4B* locus have been identified, it is crucial to determine how these variants mediate their effect on the expression of the nearby genes, and in this way ascribe putative functional roles for these genes in the control of glucose homeostasis.

With this in mind, expression quantitative loci (eQTL) analysis was recently used to study the impact of causal variants on the expression of nearby genes. Thus, using islets samples from 53 human donors, Mehta *et al.* (Mehta *et al.*, 2016) tested the association between genotype at one of the previously identified SNPs rs4502156, as well as the likely causal SNP rs7163757, and the expression of *C2CD4A, C2CD4B* and *VPS13C.* Although upon initial analysis the risk variants did not show any association, when the data were stratified by sex, with males and females analysed separately, a significant association was apparent in female subjects between the risk allele (C) at rs7163757 and *C2CD4A* and *VPS13C* mRNA levels (Mehta *et al.*, 2016). Decreased expression of *VPS13C* and *C2CD4A* in islets were thus associated with increased risk of T2D and with other glycaemic traits.

The above data, however, have been challenged by a more recent study (Kycia *et al.*, 2018). In the latter report, islet data from the FUSION (n=32) and GROOP (n=81) cohort of subjects with European background were used to examine the association between the causal SNP rs7163757 and the expression of the nearby genes. The obtained data showed that the risk allele (C) at rs7163757 is significantly associated with *increased C2CD4B* expression in both islet cohorts. However, only a trend towards an increase was observed for *C2CD4A* expression, and no effect on *VPS13C* expression was apparent (Kycia *et al.*, 2018). This study, however, did not stratify by sex.

A possible explanation for the difference in the results from these two studies may be in the number of samples analysed. In any case, further replication will be required to resolve this question.

1.5.4. Enhancer Regions in the *C2CD4A* and *C2CD4B* Locus

Identifying the possible enhancer regions and transcription binding sites in the *C2CD4A, C2CD4B* and *VPS13C* locus as above may provide a means to identify the SNPs that are most likely to regulate the expression levels of these genes.

Using high-throughput sequencing coupled with chromatin immunoprecipitation sequencing (ChIP-seq) and RNA-sequencing (RNA-seq), in human pancreatic islet samples and T2D-relevant cell types, the GWAS SNPs rs11071657 and rs7172432, located at the non-coding region in between *C2CD4A* and *C2CD4B* and previously correlated with T2D traits, have been shown to overlap with islet stretch enhancers (Parker *et al.*, 2013). Other studies (Miguel-Escalada *et al.*, 2018)·(Kycia *et al.*, 2018) showed that rs7163757 resides in an islet active enhancer region.

Studying the genes that are specifically and significantly enriched for the presence of islet stretch enhancers, Varshney *et al.* (Varshney *et al.*, 2017) identified the enhancer regions and chromatin states of the previously documented islet-specific T2D SNPs. mRNA sequencing of 112 human islet tissue samples, and cis-eQTL analysis of these, provided dense cis-expression quantitative trait loci (cis-eQTL) maps. An additional integration with chromatin-state maps for islets and 30 other cell- and tissue-types revealed cis-eQTLs for islet-specific genes that are specifically and significantly enriched for the presence of islet stretch enhancers. Also, assay for transposase-accessible chromatin sequencing (ATAC-seq) was used in the islet samples to identify specific transcription factor footprints embedded in active regulatory elements, which are highly enriched for islet cis-eQTL. Using this approach, 28 T2D and related quantitative trait GWAS SNPs were identified as islet cis-eQTL signals (Varshney *et al.*, 2017). As shown in Figure 1. 9, *VPS13C* and *C2CD4B* were among the genes with significant islet cis-eQTLs for the T2D-implicated SNPs. However, in this study, no significant association was discovered with the previous lead SNP rs7163757 (Parker *et al.*, 2013)·(Mehta *et al.*, 2016). In contrast to the above study, Kycia *et al.* (Kycia *et al.*, 2018) have recently shown that SNP rs7163757 is the most likely causal variant in this locus. The data from the latter authors also confirmed that rs7163757 is the only variant in this locus overlapping an islet open chromatin region (Mehta *et al.*, 2016). In further agreement with the latter study, a recent paper from the Ferrer laboratory (Miguel-Escalada *et al.*, 2018) used CRISPRa and CRISPRi to target three proposed enhancer regions in the

intronic region between *C2CD4A* and *C2CD4B* in the human pancreatic β-cell line EndoC βH3 (Miguel-Escalada *et al.*, 2018). The results showed that, among these three enhancer regions, targeting the enhancer region which containing rs7163757, mediated the strongest effect on the expression of the genes located at this locus (Miguel-Escalada *et al.*, 2018).

The latter authors have also shown that this enhancer region contains binding sites for transcription factors involved in the development and function of islets, such as FOXA2, NKX2.2, NKX6.1 and PDX1 (Miguel-Escalada *et al.*, 2019). Figure 1. 10 shows the most recent SNPs (from DIAMANTE analysis) associated with T2D at the *C2CD4A/C2CD4B/VPS13C* locus and the presence of several enhancer regions at the non-coding region between *C2CD4A* and *C2CD4B*. The presence of SNPs at the enhancer regions at this locus could affect the expression levels of these nearby genes.

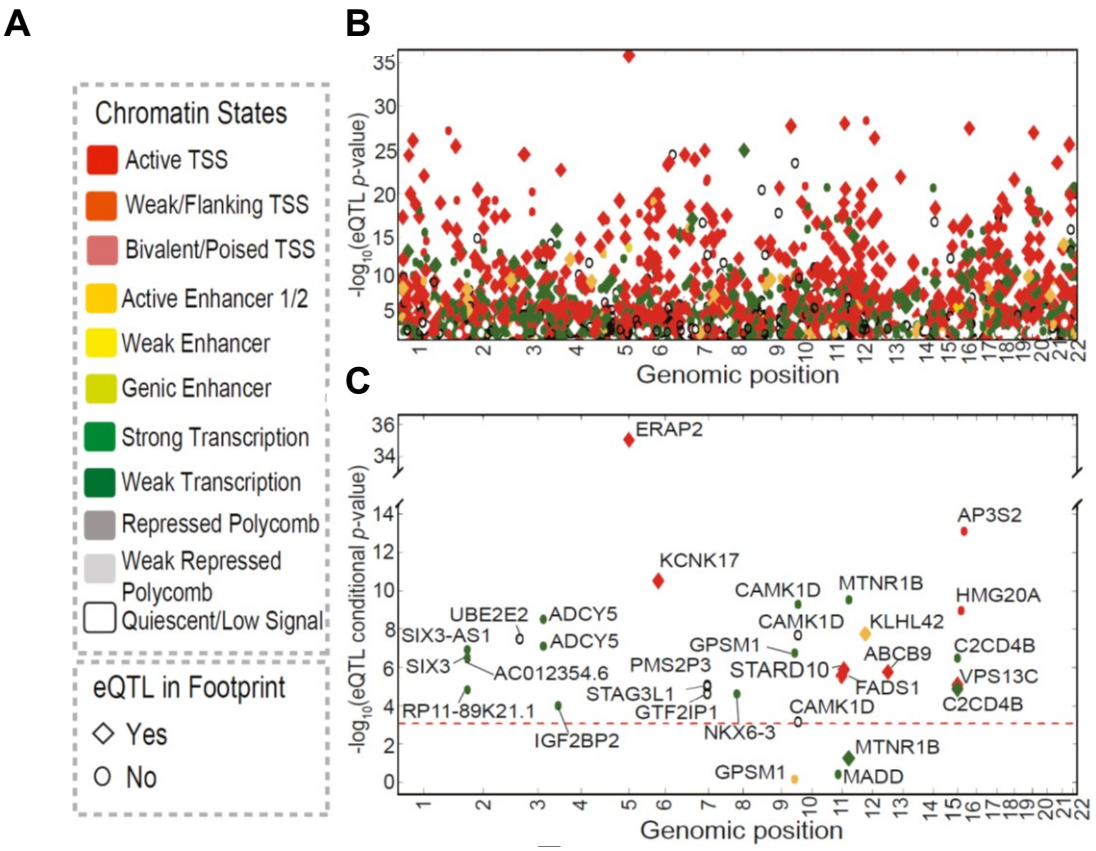

Figure 1.9. Integrated genomic, and transcriptomic analysis of human pancreatic islets. A. Chromatin state annotation, colour coded from strongly active to less active chromatin state. B. Y axis indicates plot of strength of association for all T2D GWAS SNPs with significant islets cis-eQTLs. X axis indicates genome position, and the colours correspond to the chromatin state in A. C. 28 islet-specific SNPs selected from plot B. based on the strength of islet cis-eQTLS association for T2D and after conditional analysis. Figure adopted from Varshney *et al*., 2017 (Varshney *et al.*, 2017).

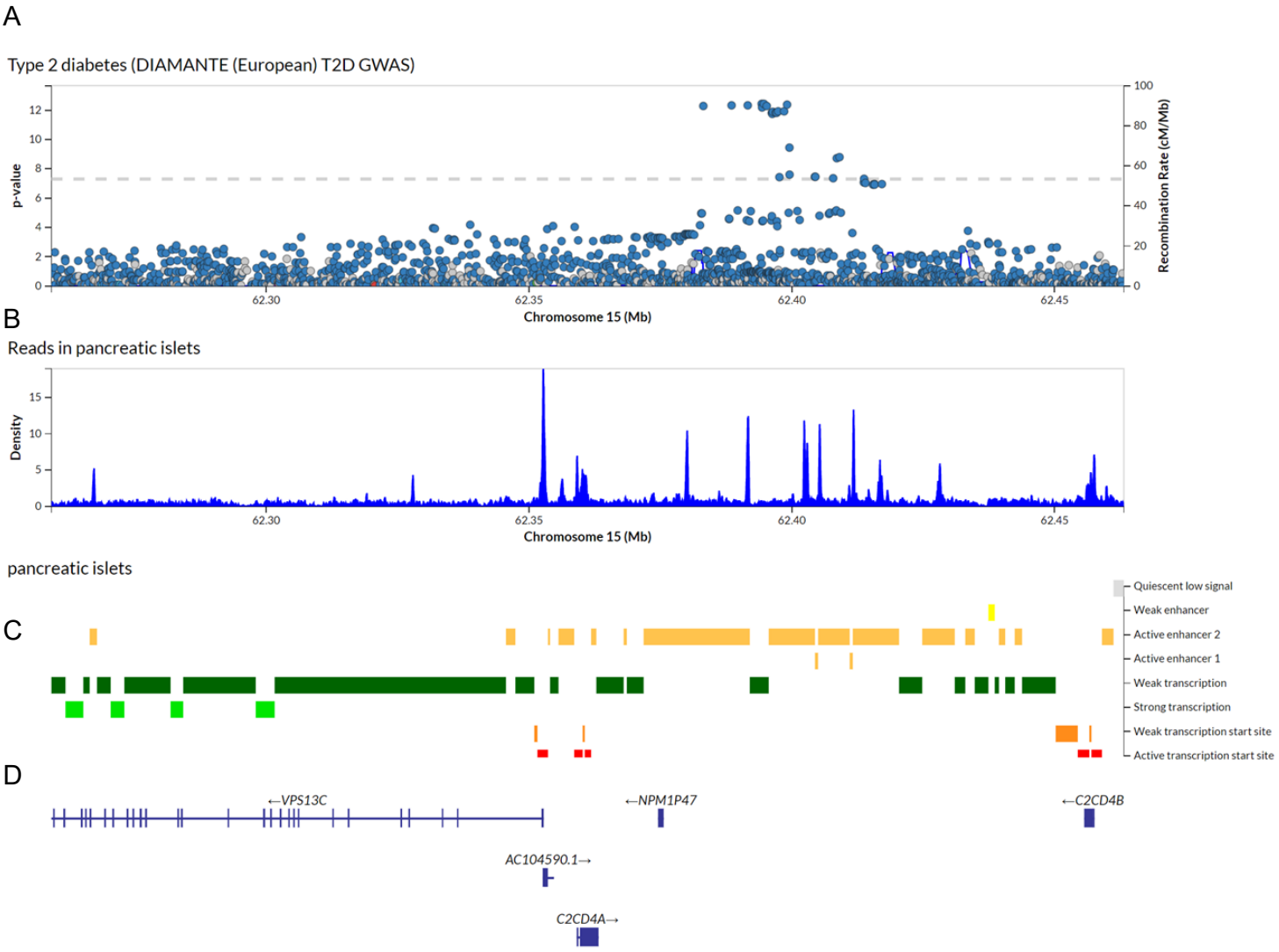

Figure 1.10. SNPs associated with T2D in the *C2CD4A* and *C2CD4B* locus. A. Several SNPs at the non-coding region at the *C2CD4A/C2CD4B/VPS13C* locus have been associated with T2D risk. B. ATAC-seq data from pancreatic islets show several open chromatin regions at the *C2CD4A/C2CD4B/VPS13C* locus. C. Chromatin states of the *C2CD4A/C2CD4B/VPS13C* locus shows active enhancer regions at the non-coding region between *C2CD4A* and *C2CD4B.* D. Human chromosome 15, *C2CD4A/C2CD4B/VPS13C* locus. (adopted from http://www.type2diabetesgenetics.org/gene/geneInfo/C2CD4A# on 4/02/2020).

1.6. C2CD4A and C2CD4B

The genes encoding C2 Calcium Dependent Domain Containing 4-A and -B (*C2CD4A* and -*B*), also known as Nuclear-Localized Factor 1 and 2 (*NLF1* and *NLF2*), are located on human chromosome 15 at close proximity to one another (90 kb apart). These genes were first discovered as highly up-regulated in response to inflammatory cytokines (interleukin 1β and tumour necrosis factor α) in endothelial cells (Warton *et al.*, 2004). In addition, it was shown that, again in endothelial cells, the encoded proteins play roles in cell adhesion and in acute inflammatory responses. It was also shown that they possessed C2-like domains (Nalefski & Falke, 1996) at their C-terminus which are predicted to bind to Ca^{2+} and phospholipids (Warton *et al.*, 2004).

In addition to endothelial cells, *C2CD4A* and *C2CD4B* expression levels are increased in response to inflammatory cytokines in human pancreatic islets (Eizirik *et al.*, 2012) , the INS1 (832/13) (Hohmeier *et al.*, 2000a) cell line (Kycia *et al.*, 2018) and MIN6 cells (Kuo *et al.*, 2019). Also, in human islets, it has been shown that the expression of *C2CD4A* is increased in response to the saturated fatty acid, palmitate(Cnop *et al.*, 2014).

1.6.1. C2CD4 family

The C2CD4 family consists of C2CD4A, C2CD4B, C2CD4C and C2CD4D. These proteins have similarities in their sequences and possess a C2 domain which is predicted to bind to Ca^{2+} and phospholipids. The phylogenetic tree of this family indicates that human *C2CD4A* and *C2CD4B* arise from a common ancestor (Figure 1. 11). In addition to human, murine *C2cd4a* and *C2cd4b* also evolved from one ancestor. This suggests that murine *C2cd4b* could have similar roles as (i.e. to be the orthologues of) human *C2CD4A* and/or *C2CD4B*.

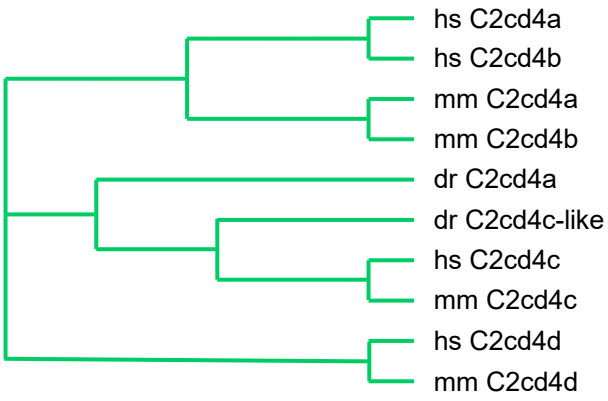

Figure 1.11. Phylogenetic tree of C2CD4 family. *C2CD4A* and *C2CD4B* in human and mice rise from the same ancestors. The Phylogenetic tree was reproduced based on AlignX program of Vector NTI, using the full-length amino acid sequences of vertebrate members of the C2CD4 family.

1.6.2. The C2 Domain

C2 domains are Ca^{2+}-dependent membrane-targeting elements that consist of about 130 amino acids (Islam, Md. Shahidul, n.d.). C2 domains were first discovered in the Ca^{2+}-dependent protein kinase C (PKC) protein family (Nalefski & Falke, 1996). In conventional PKCs, C2 domains mediate calcium-dependent binding to membrane lipid phosphatidylserine (PS) and to phosphoinositide - 4,5-bisphosphate [PIP2]. However, in C2CD4A and C2Cd4B the function of the C2 domain is not fully understood. A previous study suggested that the C2 domains in C2CD4A and C2CD4B do not contain fully canonical C2 sequences and, therefore, are not able to bind Ca^{2+} (Nalefski & Falke, 1996). In contrast to this finding, amino acid (aa) sequence alignments of C2 domains from C2CD4A and C2CD4B with PKCα suggest that one predicted Ca^{2+} binding site in C2CD4A and two in C2CD4B are conserved (Nalefski & Falke, 1996) (Figure 1. 12).

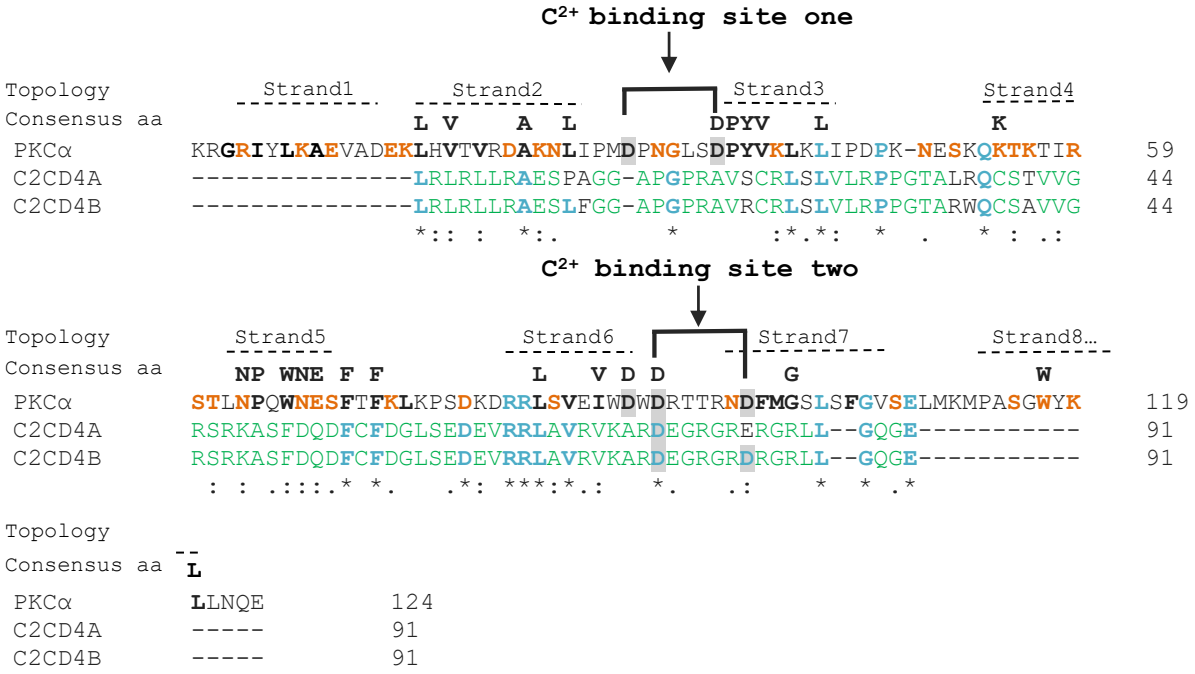

Figure 1.12. Amino acid sequence alignment of the C2 domains of hPKCα, hC2CD4A and hC2CD4B. The secondary structure is schematically indicated above the sequence as hashed lines, which indicate β-strands in synaptotagmin, a Ca^{2+} sensor protein. The consensus sequence present in >50% of the C2 domains from 65 previously published C2 domains are indicated in bold on top (PKC structure and topology adopted from Nalefski *et al,* 1996 (Nalefski & Falke, 1996)). Amino acids shown in bold and black are non-polar or aromatic while if shown in orange they are polar or charged amino acids in consensus C2 domains. Highlighted in grey are side chains which are predicted to coordinate Ca^{2+} in synaptotagmin and PKCα. The amino acids shown in blue are conserved in PKCα; shown in green are identical aa sequences between C2CD4A and C2CD4B. (Figure generated using sequence alignment on NCBI).

1.6.3. Sub-cellular localisation

It was previously reported *in vitro*, by over-expressing GFP-tagged *C2CD4A* and *C2CD4B* constructs in the Cos-7 cell line, that the sub-cellular localisation of these proteins is limited to the nucleus (Warton *et al.*, 2004). A recent publication investigating the role of *FoxO1* and *C2cd4a* in insulin secretion also showed that GFP-tagged *C2cd4a* is localised only in the nucleus in MIN6 cells and in mouse islets (Holst *et al.*, 2016). The above authors concluded from this observation, together with RNA-seq data, that murine *C2cd4a* acts as a gene expression co-regulator which is located downstream of the transcription factor FOXO1.

1.6.4. Tissue distribution

C2CD4A and *C2CD4B* are expressed in a range of human tissues. In descending order of expression level, *C2CD4A* is found in the pituitary gland, pancreas, kidney, stomach and liver among others; *C2CD4B* is expressed in pancreas, stomach, breast, adipose tissue, lung and pituitary gland (Figure 1. 13, data from GTEx portal). The mouse *C2cd4b* gene is highly expressed in similar tissues including pancreas, pituitary gland, stomach and intestine (Figure 1. 14). In human islets, the expression of *C2CD4A* and *C2CD4B* is similar, while in mouse islets, *C2cd4b* is much more abundantly expressed than *C2cd4a* (Table 3) (Blodgett *et al.*, 2015), (Kone *et al.*, 2014; Benner *et al.*, 2014).

Gene name	Expression	Tissue	Publication	Expression	Tissue	Publication
Murine *C2cd4a*	6.98 (RPKM)	β	Benner *et al.* (Benner *et al.*, 2014)	5.5 (RPKM)	Mouse pancreatic islets	Kone *et al.* (Kone *et al.*, 2014)
Murine *C2cd4b*	71.6 (RPKM)			40.7 (RPKM)		
Human *C2CD4A*	57.9 (RPKM)	β	Benner *et al.* (Benner *et al.*, 2014)	18.5 (TPM)	β	Blodgett *et al.* (Blodgett *et al.*, 2015)
Human *C2CD4B*	52.8 (RPKM)			15.7 (TPM)		

Table 3. Expression of *C2CD4A* and *C2CD4B* in human and mouse islets and β-cells. While both *C2CD4A* and *C2CD4B* are expressed at the same level in human β-cells, in mouse *C2cd4b* is more predominantly expressed compared to *C2cd4a*. β=FACS purified β-cells.

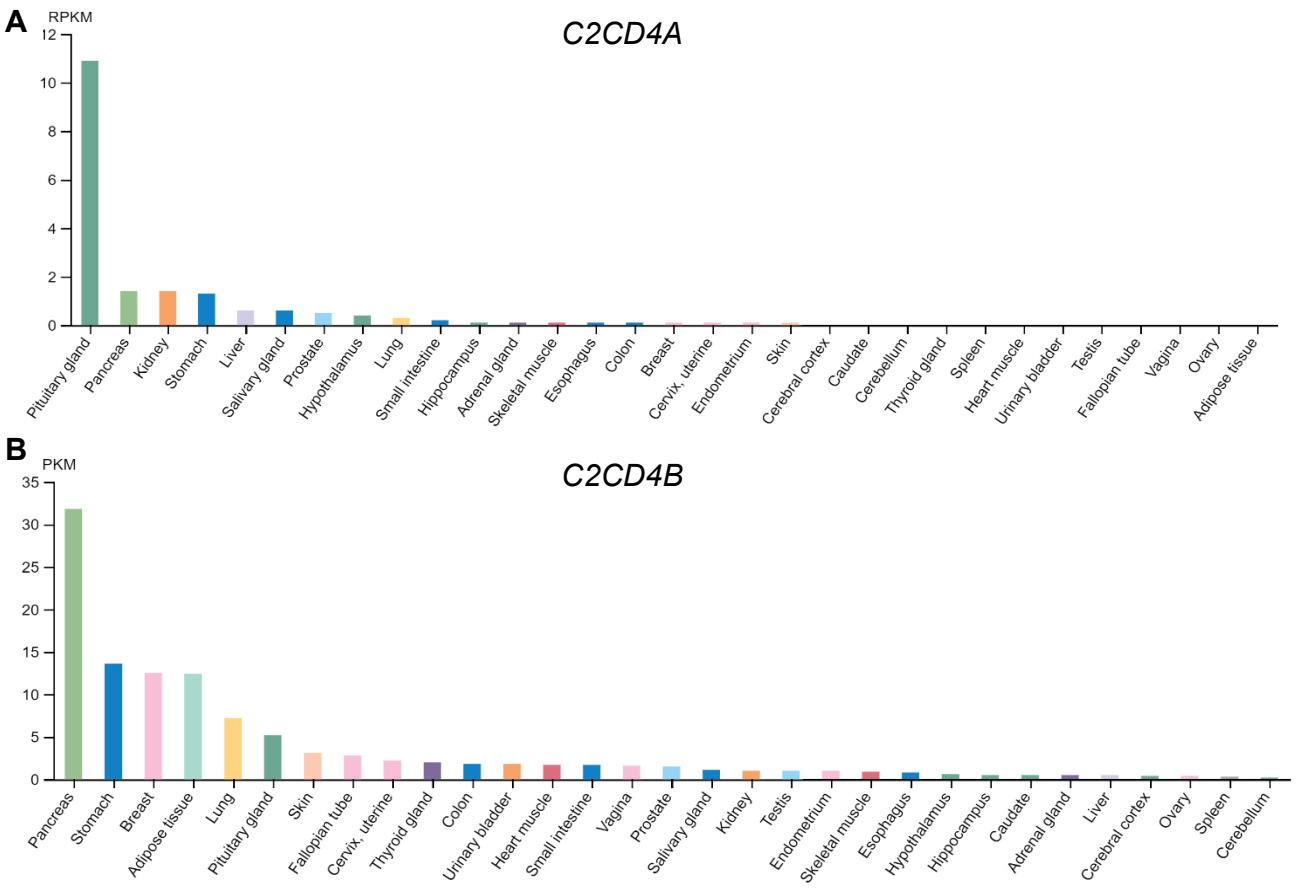

Figure 1.13. *C2CD4A* and *C2CD4B* expression levels in human tissues.

A. *C2CD4A* is expressed, from high to low levels, in the pituitary gland, pancreas, kidney, stomach, liver, salivary gland, prostate, lung and small intestine; and B. *C2CD4B* is expressed in pancreas, stomach, breast, adipose tissue, lung, pituitary gland, skin, thyroid, small intestine and etc. (Data Source: GTEx data, analysed in The Human Protein Atlas, URL: https://www.proteinatlas.org/ENSG00000198535-C2CD4A/tissue, https://www.proteinatlas.org/ENSG00000205502-C2CD4B/tissue).

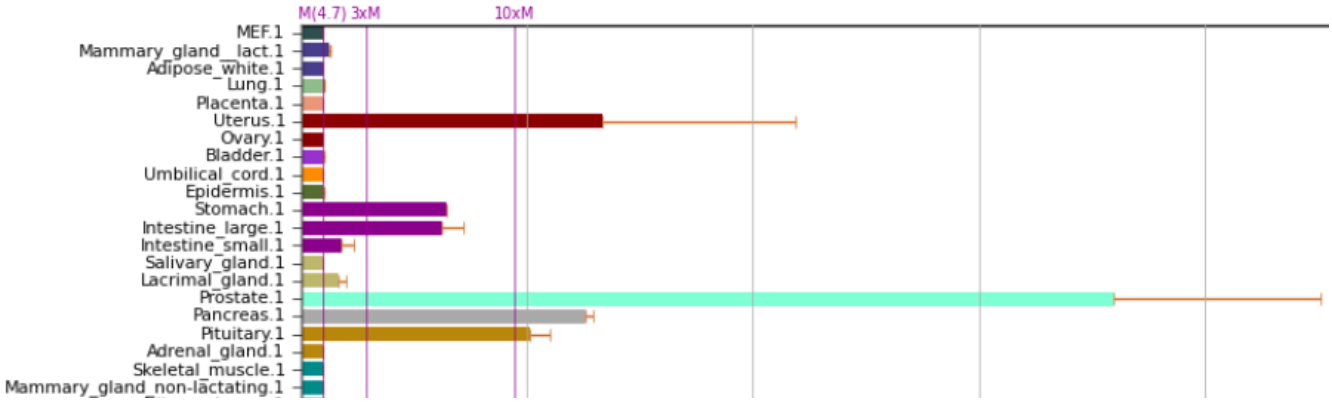

Figure 1.14. *C2cd4b* expression levels in mouse tissues.

Murine *C2cd4b* is highly expressed in prostate, pancreas, pituitary gland, uterus, intestine among other tissues. Data Source; GeneAtlas MOE430, http://biogps.org/#goto=genereport&id=75697.

1.7. Aims of Thesis

The studies detailed in this project aim to investigate the role of the type 2 diabetes-associated GWAS genes *C2CD4A* and *C2CD4B* in pancreatic β-cells and how they regulate glucose homeostasis. To address these questions, the chapters of this thesis will aim to:

1. Study the sub-cellular localisation of C2CD4A and C2CD4B and their possible interacting partners in β-cells.
2. Study the effect of deletion of *C2cd4b* or *C2cd4a in vivo* on glucose homeostasis.
3. Determine the effect of deletion of *C2CD4A in vitro* in human β-cells, on insulin secretion.

Chapter 2: Materials and Methods

2.1. Cell and tissue culture

2.1.1. Mammalian cell culture

The MIN6 cell line (mouse insulinoma) (Miyazaki *et al.*, 1990) was cultured in Dulbecco's modified Eagle's medium (DMEM; Sigma Aldrich, Dorset, UK) containing 15% [vol./vol.] foetal bovine serum (FBS), 100 U/mL penicillin and 100 U/mL streptomycin and supplemented with 50 µM 2-mercaptoethanol (Sigma-Aldrich) at 37°C with 5% CO_2.

The INS1 (832/13) rat insulinoma derived β-cell line (Hohmeier *et al.*, 2000b) was cultured in RPMI-1640 medium (Sigma), supplemented with 10% [vol./vol.] FBS, 100 U/ml penicillin and 100 mg/l streptomycin, 2 mM L-glutamine (Sigma), 1 mM Sodium-Pyruvate and 50 µM 2-mercaptoethanol (Sigma-Aldrich) at 37°C with 5% CO_2.

The human EndoC βH1 cell line (Ravassard *et al.*, 2011) was cultured in DMEM 1g/L (Sigma) medium, supplemented with 2% [wt/vol.] Albumin from Bovine Serum Fraction V, Fatty Acids Free (Roche), 50 µM 2-mercaptoethanol (Sigma-Aldrich), 10 mM Nicotinamide (Sigma), 5.5 µg/ml transferrin, 6.7 ng/ml sodium selenite, 100 units/ml Penicillin-Streptomycin and 100 µg/ml Streptomycin (Invitrogen) at 37°C with 5% CO_2.

2.1.2. Mouse islet isolation

Mice were euthanised using CO_2 chambers. To isolate pancreatic islets, 1 mg/ml Collagenase NB 8 Broad Range (Nordmark Biochemicals) in RPMI-1640 medium (Sigma) was directly injected into the bile duct and the pancreas was fully inflated with this solution. The inflated pancreas was removed from the animal. The isolated *pancreata* were incubated for 12 min. at 37°C water bath to induce digestion and separation of the islets from the remaining pancreatic tissue. Digested pancreas was washed 3 times with RPMI-1640 before the separation of endocrine and exocrine tissue by centrifugation through a histopaque gradient at densities 1.119 and 1.087 g/mL and RPMI-1640 medium (Sigma Aldrich) at 2500 rpm for 20 min. Islets were washed with RPMI and transferred to RPMI supplemented with 10% [vol./vol.] FBS, 100 U/mL penicillin and 100 U/mL streptomycin and incubated at 37°C with 5% CO_2, 24 h before further experimentation.

2.1.3. Insulin secretion assay on isolated islets

To measure insulin secretion from isolated islets, 10 size-matched islets in triplicate were picked and incubated for one h at 37°C in Krebs-HEPES-bicarbonate (KREBH) solution (KREBH buffer: 140 mM NaCl, 3.6 mM KCl, 2 mM $NaHCO_3$,0.5 mM NaH_2PO_4, 0.5 mM $MgSO_4$, 1.5 mM $CaCl_2$,, 10 mM HEPES and 0.1% [wt/vol.] BSA; all Sigma-Aldrich, pH 7.4) containing 3 mM glucose with gentle shaking. Afterwards, GSIS was carried out by incubating the islets for 30 min. in KREBH solution containing either: 3 mM glucose, 17 mM glucose or 20 mM KCl at 37°C in a water bath with gentle shaking. The supernatants were collected, and the 10 islets were picked up and lysed to measure total insulin content in acidic ethanol solution (1.5% [vol./vol.] HCl, 75% [vol./vol.] ethanol, 0.1% [vol./vol.] Triton X-100 (Sigma). The samples were kept frozen at -20 for further measurements.

2.1.4. Homogeneous Time Resolved Fluorescence (HTRF) Assay

Insulin Ultra-Sensitive Kit (Cisbio, ref. 62IN2PEH) was used according to the manufacturer's instructions to measure released or total insulin. In order to assess the final dilutions for samples, a tested with several dilutions was carried out before measuring all samples collected. Each sample was measured in duplicate and incubated with europium cryptate and the other with XL665 antibodies overnight before measuring the Förester resonance energy transfer (FRET) efficiency.

2.2. Molecular biology

2.2.1. Western (immuno)blotting

Cell or tissue samples were lysed and protein samples containing equal amounts of protein were blotted onto a Polyvinylidene Difluoride (PVDF) transfer membrane (Millipore). After membrane blocking with 0.1% [vol./vol.] Tween in Phosphate-buffered saline (PBS) + 5% milk, the membrane was incubated with anti-FLAG antibody (see the list of antibodies) diluted in 5% milk plus 0.1% [vol./vol] Tween in PBS, overnight at 4°C. After three washes with PBS-Tween, membranes were incubated in horseradish peroxidase (HRP)-conjugated secondary antibody for 1 h at room temperature. Bands were detected using chemiluminescence with ECL plus (GE Healthcare) onto photographic film.

2.2.2. RNA extraction and RT-q-PCR

Samples were incubated in TRIzol™ Reagent (Invitrogen) for 10 min. to dissolve the cells and tissues (samples were kept frozen or directly used for RNA extraction). Next, chloroform (Sigma) was added to TRIzol mix in a 1:5 ratio respectively. Samples were mixed and centrifuged for 15 min. at 4°C. After centrifugation, the RNA containing upper phase was aspirated and placed into new tubes. RNA was precipitated by adding an equal volume of isopropanol, after incubating for 1 h at -80 or overnight at -20°C to elevate the yield. This was continued by centrifugation of samples at 4°C for 15 min. and two washes in 75% [vol./vol.] ethanol. Afterwards, the pellet was airdried and dissolved in RNase- free water (Qiagen).

Total RNA (400 ng to 2 µg) was then reverse transcribed using a high capacity cDNA RT kit (Applied Biosystems) according to the manufacturers' instructions. Briefly, 10 µL of RT reaction (10X RT buffer, 4 mM dNTPs, 10X random primers and 1 µL multi-scribe reverse transcriptase) was added to an equal amount of RNA per sample and the final solution was incubated at 25°C for 10 min., at 37°C for 120 min. and 85°C for 5 min.

To measure mRNA levels SYBR green reagent (Applied Biosystems) was used. 2 µL of cDNA diluted in 1:4 was added to 6 µL of SYBR green reagent and 0.35 µL of primers (from 10 mM stock), RNase-free water was added to reach to a total volume of 12 µL.

Amplification curves for each gene, derived from fluorescent signals, were generated using the equipment software (7500 v2.06, Applied Biosystems). A threshold was manually set to determine the number of cycles (Ct) required to reach the set level of fluorescence. The relative expression was determined by normalising to either of the housekeeping genes β-actin or RPLP0 when mRNA samples from mouse and human samples were quantified, respectively. Relative expression was calculated as such: Relative gene expression = $2^{Ct(Cyclophilin)-Ct(target\ gene)}$

2.2.3. Sample preparation for RNA sequencing

Isolated islets from 5 male mice/genotype were used for RNA purification. DNase treatment was performed using TURBO DNase (Invitrogen) according to the manufacturer's instructions. RNA quantity and integrity were assessed using an RNA 6000 Nano Kit (Agilent) and an Agilent 2100 Bioanalyzer. mRNA enrichment was

achieved from 0.8-1 µg of total RNA using a NEBNext Poly(A) mRNA Magnetic Isolation Kit (NEB). Generation of double stranded cDNA and library construction were performed using NEBNext Ultra II Directional RNA Library Prep Kit for Illumina (NEB). NeBNext Multiplex Adapters (NEB) was used to perform ligation of the adapters. Each library was subsequently size selected with SPRIselect Beads (Beckman Coulter). The Adaptor ligated DNA was PCR amplified using NEBNext Ultra II Q5 Master Mix and Universal i5 and i7 primers provided in the NEBNext Kits.

Sequencing was performed by the Imperial BRC Genomics Facility as 75bp paired end reads on a HiSeq4000 according to Illumina specifications. FASTQ files were generated for each sample (5 WT and 4 null mice) and initial data quality checks of the raw sequence data were performed. Reads were then mapped to the mouse transcriptome (GRCm38, cDNA and ncRNA) using Salmon (Patro *et al.*, 2017). Total RNA profiles were consistent and generated ~20-40 million reads mapping to Ensembl genes per sample. DESeq2 (v1.20.0) (Love, Huber & Anders, 2014) with DESeq2-default normalization method and adjusted p-value threshold <0.1 was used for differential expression analysis in R using relevant BioConductor packages (Anders *et al.*, 2013).

2.2.4. Immunoprecipitation and mass spectrometry

Immunoprecipitation and mass spectrometry experiments were performed in collaboration with Dr Millership from Professor Dominic Withers laboratory in the MRC London Institute of Medical Sciences. MIN6 cells were transfected in duplicate with FLAG-tagged C2CD4A or C2CD4B constructs and with FLAG tag only construct as a negative control. 48 h post-transfection cells were homogenized in protein lysis buffer (50 mM Tris-HCl, pH 7.5, 150 mM NaCl, 1% [vol./vol.] Triton X-100, 1 mM EDTA with protease inhibitor [Complete Mini, Roche]). After centrifugation at 16,000 x *g*, supernatants were incubated with protein A-agarose beads coated with anti-FLAG antibody (M2 clone, Sigma, A2220) according to the manufacturer's instructions and washed four times with protein lysis buffer. Proteins were collected from the beads were then sent to Imperial College MRC-LMS Mass-spectrometry facility.

Proteins were selected for those containing at least two unique peptides, identified in both replicates and with a minimum of a 2-fold increase in abundance compared with FLAG-tag only control immunoprecipitates. Intensity normalisation was

performed by Progenesis and proteins were ranked by average intensity across replicates (Millership *et al.*, 2018).

The final table was generated from the highest possible interacting proteins to the lowest interacting proteins with C2CD4A or C2CD4B.

2.2.5. ELISA for insulin and proinsulin

To measure insulin levels in mouse plasma, an Ultra-Sensitive Mouse Insulin ELISA Kit (Crystal Chem, 90080) was used according to the manufacturer's instructions. Plasma samples were centrifuged and kept on ice before being loaded on the plates.

To measure proinsulin levels, a Rat/Mouse Proinsulin ELISA (Mercodia, 10-1232-01) kit was used according to the manufacturer's instructions. However, instead of 25 µL of plasma as suggested, 35 µL of plasma was added to 50 µL of Enzyme Conjugate, to promote a higher signal to noise ratio.

2.3. *In vitro* functional imaging and analysis

2.3.1. Intracellular free [Ca^{2+}] measurements

24 h after islet isolation, for each acquisition 20 islets were incubated for 45 min. in fluo2-AM (10 µM; Teflabs) diluted in a KREBS buffer solution containing 3 mM glucose.

A Nipkow spinning disk head microscope was used to capture changes in the fluorescent signals in response to intracellular free [Ca^{2+}] changes (Hodson *et al.*, 2014). Islets were maintained at 35°C to 36°C and continuously irrigated with KREBS buffer solution aerated with 95% O_2, 5% CO_2 during recordings in the presence of either 3 mM or 17 mM glucose or 20 mM KCl. On average 8-10 islets were imaged in each field of view. Two acquisitions were performed per animal.

Images were analysed using ImageJ software (URL: https://imagej.nih.gov/ij/index.html) by measuring the fluorescence over time from each individual islet. Fluorescence intensity was normalised to that at 3 mM condition where islets were unstimulated (F/Fmin). The Pearson product moment correlation analysis was performed for every possible cell pair to assess inter-cellular connectivity (Salem *et al.*, 2019).

2.3.2. Immunofluorescence on pancreatic slices

Pancreata were fixed in 4% [wt/vol.] Paraformaldehyde (PFA, Sigma-Aldrich) diluted in Phosphate-buffered saline (PBS), after dissection overnight at 4°C. Animals were dissected at 24 or 25 weeks of age. Afterwards, islets were washed with PBS and incubation through serial ethanol dilutions (25%, 50%, 70% and 100% [vol./vol.]) to dehydrate. Next, they were placed in 100% ethanol and maintained at -20°C until they were ready for the histology process. Samples sent to the histology facility at Imperial College London were embedded in paraffin and sectioned at 5 µm thickness. Each section was 150 µm apart from the previous section.

To prepare the samples for immunohistochemistry, slides were treated with Antigen Unmasking Solution (Vector Laboratories) according to the manufacturer's instructions. Antigen retrieval was performed in a microwave oven (Matsui, M 180TC) at medium power for 15 min. Afterwards, slides were left to cool down to room temperature, washed with PBS and incubated in blocking buffer (PBS containing: 0.1%Triton X-100, 2% BSA, 2% donkey serum). Primary antibodies (guineapPig anti-insulin ready to use (Dako): not diluted, mouse anti-glucagon (Sigma): 1:1000), diluted in PBS (containing: 0.25% BSA, 0.25% Triton X-100), were applied overnight at 4 °C in a humidified chamber. After overnight incubation, slides were washed in PBS-Triton X-100 and incubated with secondary antibodies (Alexa Fluor 488 goat anti-guinea-pig, Invitrogen, 1:1000, Alexa Fluor 532 goat anti-rabbit, Invitrogen,1:1000, DAPI Roche 1:5000) for 2 h at room temperature (RT). Slides were washed before mounting. To mount, a drop of mounting reagent (ProLong Dimond Antifade Mountant, Life Technologies) was added and a coverslip was placed on to each slide to cover the tissue. Slides were dried overnight and kept in 4°C until they were ready for microscopy.

An Inverted Widefield Microscope with LED illumination microscope (Zeiss Axio Observer Z1), from the Imperial College FILM facility, was used to collect images. To measure total pancreas area, a x10 objective was used and the images were tiled using Zeiss software. A x40 oil immersion objective was used to take images from individual islets present in the pancreas.

2.3.3. Immunofluorescence and imaging for sub-cellular localisations

Cells were cultured on coverslips and 12 or 24 h post transfection were fixed in 4% [wt/vol.] PFA (Sigma-Aldrich) dissolved in PBS, followed by washes in 0.1% [vol./vo.] Triton X-100 dissolved in PBS and incubated with primary antibody (mouse anti-FLAG (Sigma)1:1000) overnight at 4°C. Afterwards, the cells were washed with PBS-Triton and incubated with the secondary antibody (Alexa Fluor 488 anti-mouse, Invitrogen, 1:1000) for 2 h at room temperature. The coverslips were washed and mounted on to slides using Vectorshield (Vectorlabs) mounting reagent.

A Nikon ECLIPSE Ti spinning disk microscope was used to collect images. A x60 oil immersion objective was used for localisation and co-localisation experiments. For cells co-transfected with *C2CD4A* and *C2CD4B* FLAG-tagged constructs and KDEL: Red construct, a confocal inverted Zeiss LSM-780 microscope was used to capture images.

Quantification of sub-cellular localisation patterns was carried out manually using three independent experiment in duplicate. Between 70-150 cells were counted in each field of view.

2.3.4. Plasmid maps used for sub-cellular localisations

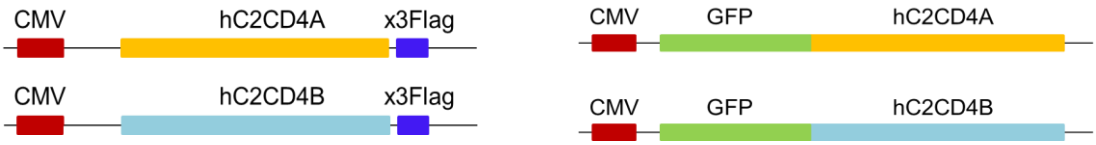

Figure 2.1. Constructs used to visualise the sub-cellular localisation of C2CD4A and C2CD4B in β-cells. A. Schematics of hC2CD4A and hC2CD4B constructs which were tagged with x3 FLAG isotopes at their C-terminus or tagged with GFP at the N terminus.

2.3.5. Time-lapse imaging from *C2CD4A* and *C2CD4B* transfected cells

Cells were grown on coverslips and transfected with either GFP-tagged C2CD4A, C2CD4B or Syt1 (Idevall-hagren *et al.*, 2015) containing constructs. 24 h post-transfection, cells were incubated for 1 h at 37°C with KREBH buffer solution aerated with 95% O_2, 5% CO_2 and containing 3 mM glucose.

After several pilot experiments, ionomycin was chosen to trigger robust increases in intracellular free [Ca^{2+}] in the cells since our positive control construct (Syt1-GFP) responded most strongly to this stimulation compared to stimulating cells with KCl.

2.4. *In vitro* over-expression of *C2CD4A* and *C2CD4B*

2.4.1. Generation of *C2CD4A* and *C2CD4B* -FLAG and -GFP tagged constructs

Human *C2CD4A* and *C2CD4B* cDNA sequences were cloned into plasmid P3XFLAG-CMV-14 (available on Addgene) in-frame at the C-terminal 3xFLAG epitope tag. GFP-tagged proteins were generated by using a GFP construct and adding the human *C2CD4A* and *-B* cDNA sequences into the C-terminus of GFP using plasmid pEGPP-C1 (available at Addgene and Clontech) as the backbone.

Constructs were sent for sequencing (Genewiz) to ensure accurate sequence alignment. In addition, Western (immuno)blotting using cells transfected with *C2CD4A* or *C2CD4B* FLAG-tagged constructs was performed to confirm the addition of FLAG epitopes. A mouse anti-FLAG antibody (Sigma) was deployed.

2.4.2. Secretion measurements upon over-expression of C2CD4A and *C2CD4B*

INS1 (832/13) cells (Hohmeier *et al.*, 2000b) were co-transfected with human growth hormone (hGH) and *C2CD4A* and *C2CD4B* FLAG-tagged constructs or FLAG constructs without any insertion as a control. This technique (Varadi *et al.*, 2004) was used instead of direct measurement of insulin secretion in order to measure the secretion only from transfected cells. 48 h post-transfection, cells were starved in 3 mM glucose medium for 4 h. Afterwards, they were incubated in Krebs-Ringer Bicarbonate Hepes buffer (KRBH) supplemented with 3 mM glucose and 0.1% BSA (fatty acids free, Sigma) for 1 h at 37°C. Afterwards, cells were incubated for 30 min. with KREBH buffer containing 3 mM glucose, 17 mM glucose, and 20 mM KCl, at 37°C in a water bath. Next, the supernatant was collected and cells in each well were lysed (KRBH buffer plus 1% Triton X-100) and used to measure total cell insulin content. Supernatants from secretion experiments and the total cellular secretion content from each well were collected and an hGH ELISA kit (Roche) was used according to the manufacturer's instructions to measure hGH content.

2.5. *In vivo* characterisation of *C2cd4b* and *C2cd4a* null mouse strains

C2cd4a (C2cd4a-Del1724-EM1-B6N) and *C2cd4b* (*C2cd4b*^{em2Wtsi}) mouse strains were generated by the International Mouse Phenotyping Consortium (IMPC) (Cacheiro *et al.*, 2019), using Clustered Regularly Interspaced Short Palindromic Repeats and CRISPR-associated 9 (CRISPR/Cas9) method (Barrangou *et al.*, 2007). Both strains were maintained on a C57BL/6N background at the IMPC. In the *C2cd4a* strain, 1742 bp were deleted from exon 2 and in *C2cd4b* strain, exon 2 was deleted entirely.

Heterozygous animals were used as breeding pairs.

2.5.1. PCR genotyping

Primers used to genotype the ***C2cd4a*** strain:

Primer Name	Primer Sequence (5'> 3')
C2cd4a_geno_F3	AAAAGCCCGGACCAGCTATC
C2cd4a_geno_R4	GCCTCATGGCCATAATTGGAA
C2cd4a-WT-F2	AGCCAGGGCTTTGTTTCAGT
C2cd4a-WT-R3	AAGGTGTCTGCCCACACAAA

C2cd4a_geno_F3 and C2cd4a_geno_R4 primer sets were used to detect the mutant band and C2cd4a-WT-F2 and C2cd4a-WT-R3 were used to detect the WT band

Expected bands: WT:93bp; mutant: 473bp

Reaction and PCR set up:

Reagent	µl
DNA	1.5
X10 Phire buffer	4
dNTP (100mM)	0.4
Primers (10mM)	1
Polymerase	0.4
ddH2O	Up to 20

Time	Temp.°C	Cycle
30 sec	98	1
10 sec	98	30
5 sec	58 WT/ 61 mutant	
30 sec	72	
5 min	72	1
O/N	4	1

Primers used to genotype the ***C2cd4b*** strain:

Primer Name	Primer Sequence (5' > 3')
C2cd4b_DF1	GCGTGACTTCCACTAAGGTATAAGT
C2cd4b_ER1	AGAGAAAAACTGTTGAATTTGGGCT
C2cd4b_DR1	TGGAGAGTTATCAAACACCAAGGAT

C2cd4b-DF1 and C2cd4b-ER1 primer sets were used to detect the WT band and C2cd4b-DF1 and C2cd4b-DR1 were used to detect the mutant band.

Expected size: WT: ~297Kb; Mutant: 868bp

Reaction and PCR set up:

Reagent	µl
DNA	1.5
X10 Phire buffer	4
dNTP (100mM)	0.4
Primers (10mM)	1
Polymerase	0.4
DMSO	Only for mutant reaction 0.6
ddH2O	Up to 20

Time	Temp.°C	Cycle
30 sec	98	1
5 sec	98	30
5 sec	58 WT/ 62 mutant	
15 sec	72	
1 min	72	1
O/N	4	1

2.5.2. Mouse maintenance and diet

Mice were housed in a pathogen-free facility with a 12-h light/dark cycle and had free access to standard mouse chow diet and water.
Animals fed with high-fat and -sucrose diet contained 58% fat and 25% carbohydrate, provided from Research Diets, Cat. No. D12331. Animals had free access to the diet. Animals were on High-fat and sucrose diet from 6 weeks of age

2.5.3. Intraperitoneal/oral glucose tolerance test (IPGTT/OGTT)

Animals were fasted overnight prior to the experiments. For IPGTTs, glucose (1 g/kg body weight) was injected into the abdomen. For OGTTs, glucose (2 g/kg body weight) was administered directly to the stomach using oral gavage. Blood glucose levels were recorded at time points 0, 15, 30, 60, 90 and 120 min. from the tail vein, using an automatic glucometer (Accucheck).

2.5.4. Insulin Tolerance Tests (ITT)

Animals were fasted for 5 h prior to experiments. Insulin (animals on RC were injected with 1.0 for males and 0.75 U/Kg body weight for females, and animals maintained on HFD were injected with 1.5 for males and 0.75 U/Kg body weight for females) was injected into the abdomen. Blood glucose levels were measured at 0, 15, 30 and 60 min. post-injection from the tail vein, using an automatic glucometer (Accucheck).

2.5.5. Plasma insulin secretion release (IT)

Animals were fasted overnight prior to experiments. Glucose (3 g/Kg body weight) was injected into the abdomen of mice. Blood glucose levels were measured at 0, 5 and 15 min. after injection from the tail vein, using an automatic glucometer (Accucheck).

2.6. Generation of Lentiviral CRISPR/Cas9 Cell lines

2.6.1. gRNA design

Guide RNAs (gRNA) were designed using the primer design tool from the Zhang lab (Ran *et al.*, 2013). gRNAs were designed to target the first 100 bp after the start codon of *hC2CD4A.* For this, 19 nucleotides upstream of the protospacer adjacent motif (PAM) sites with minimum off-targets were selected as gRNAs to target the *C2CD4A* gene with the Cas9. PAM in the bacterial genome is an essential part of DNA which is recognised by Cas9 (Mali, Esvelt & Church, 2013). Primarily, two sets of gRNAs (gRNA1 and gRNA2) were designed to select the most efficient clones.

2.6.2. Validation of *C2CD4A* deletion in EndoC βH1 cells

DNA was extracted from the different pools of cells containing either gRNA1 or the empty backbone. PCR amplification around the C2CD4A region was performed and the results sent for sequencing to detect any change in the DNA sequence (Figure 5. 2). By visualising the sequencing results several point mutations were apparent in two independent pools of cells with gRNA1 (gRNA1-a and gRNA1-b). No mutations were observed in the negative control cell population (Figure 5. 2).

Since there were no antibodies available to assess the reduction at the protein level, RT-q-PCR was used to assess any changes in C2CD4A mRNA levels. In order to

gauge the efficiency of Cas9 cutting, different sets of primers were designed, with one primer designed within the expected cutting site of Cas9. The pools of cells containing gRNA1 showed more efficient cutting at this region and were therefore used for GSIS (relative expressions: 47.1% ± 4.6 and 43.6% ± 2 at gRNA1 pool-a and pool-b respectively, $p<0.001$, data were assessed for significance using an Ordinary one-way ANOVA, Tukey's multiple comparison test).

In addition, total mRNA levels were also reduced in the transfected cells compared to control cells (*C2CD4A* total mRNA relative expression: 78.2% ± 13.8 and 94.1% ± 24 in gRNA pool-a and pool-b respectively, p=ns) (Figure 5. 3).

To measure C2CD4A at the protein level we attempted to produce a custom-made polyclonal antibody with Eurogentec. However, the antibody did not work in Western (immuno)blotting and failed to recognise C2CD4A protein (results shown in Appendix 2).

2.6.3. Sub-cloning

gRNA1 and gRNA2 were cloned into a modified LentiCRISPR v2 sequence (Addgene). LentiCRISPR v2 was modified at Dr Paul Gadue's laboratory at the Children's Hospital of Philadelphia by replacing the CMV promoter with the rat insulin 2 promotor (RIP) at the 5' end of the Cas9 sequence, to achieve high expression of Cas9 in β-cells (Figure 2. 2). LentiCRISPR v2 constructs contains Cas9 and puromycin resistance genes. After placing the gRNA into the backbone, the constructs were cloned into lentiviral vectors. EndoC βH1 (Ravassard *et al.*, 2011) cells were infected with lentivirus containing either gRNA1, gRNA2 or a construct with CRISPR/Cas9 sequence but without any gRNA as a negative control. 24 h post-infection, cells which received the vector containing Cas9 and the gRNA were selected using puromycin (4μg/mL) for one week. Subsequently, regular EndoC medium (mentioned at Cell Culture, Section 2. 1) was replaced to feed and expand the colonies. Using this method, we selected pools of cells containing the lentiviral CRISPR/Cas9 vector. This generated mixed pools of cells, each potentially carrying a different disruptive mutation, but all based on the same gRNA sequence.

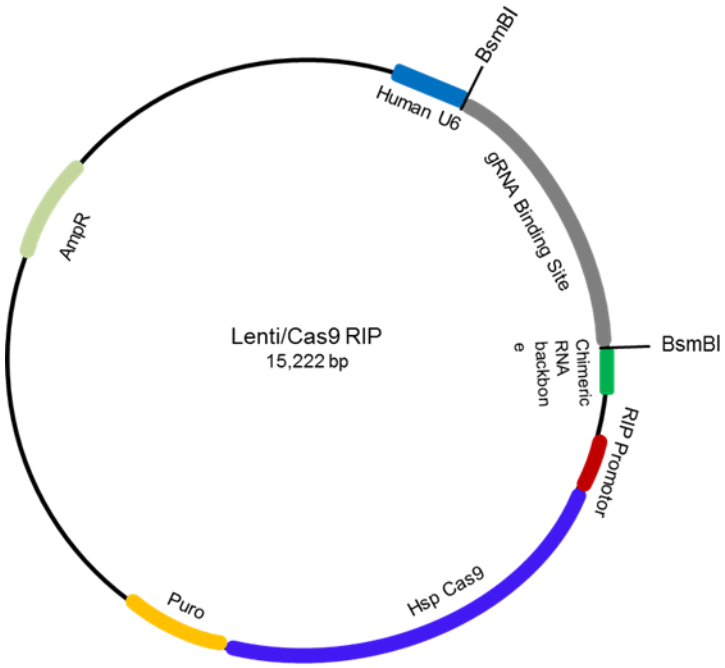

Figure 2.2. Schematic image of Lenti/Cas9 vector. Lenti/Cas9 vector (modified from Addgene) was digested by *BsmBI* restriction enzyme to remove gRNA Binding Site sequence. Afterwards, a gRNA sequence was ligated into the linearised vector.

2.6.4. Characterisation of the cell lines

DNA was extracted from the different pools of cells into which either gRNA1, gRNA2 or the empty backbone had been introduced. PCR amplification around the *C2CD4A* region was performed and the results sent for sequencing to detect any changes, by visualising the sequencing results. Several point mutations were apparent in two independent pools of cells with gRNA 1. No mutations were observed in the negative control cell population (Figure 5. 2).

RT-q-PCR was used to assess any changes in *C2CD4A* mRNA levels. In order to gauge the efficiency of Cas9 cutting, different sets of primers were designed, with one primer designed within the expected cutting site of Cas9. The pools of cells containing gRNA1 showed more efficient cutting at this region and were, therefore, used for GSIS. Two independent pools of cells infected with gRNA-1 (gRNA1 pool-a, gRNA1 pool-b) were used for GSIS measurement.

2.7. Statistical Analysis

Data are expressed as means ± SEM. Significance was tested by two tails unpaired or paired Student's t-test, or by ANOVA using Graphpad Prism 8.2.1. A value of $p<0.05$ was considered significant.

Sample sizes have been calculated using G*Power or PWR package (R), assuming normally distributed data and, when specified, Scotty (Busby *et al.*, 2013). For example:

Insulin secretion: σ=0.14μ (Martinez-Sanchez *et al.*, 2016), so for a t-test assuming independent means; to detect a 1.2 fold difference in the mean between two groups (80% power; $p<0.05$, , α=0.05), sample size is 9 replicates/group.

Ca^{2+} dynamics: previous analysis of areas under the curve for fluo2 traces indicate a value for σ of 0.3μ, requiring a sample size of 37 individual cells to detect a 1.2-fold difference; For ATP/ADP ratios, σ = 0.6μ, so we require 143 cells.

Intraperitoneal glucose tolerance tests (IPGTT): Eight mice per genotype are sufficient to provide 80 % power to detect a difference of 3 mmol/L (assuming σ=2 mmol/L, α=0.05).

Chapter 3: C2CD4A and C2CD4B in β-cells

3.1. Introduction

Multiple GWAS since 2010 have reported an association between variants at the *C2CD4A/C2CD4B/VPS13C* locus and glycaemic traits or T2D [66,72,97,98]. Further functional studies from the Rutter laboratory showed that loss of *VPS13C*, a transporter of lipids between the ER and TGN (Brickner & Fuller, 1997), selectively in pancreatic β-cells, has a minor effect on glucose homeostasis and insulin secretion (Mehta *et al.*, 2016). The latter result argues for a minimal, if any, role for this gene in glucose homeostasis and insulin secretion and suggests that the two other genes present in this locus, *C2CD4A* and *C2CD4B*, might have a more significant role in determining disease risk.

C2CD4A and *C2CD4B,* also known as *NLF1* and *NLF2,* were first described in human endothelial cells treated with inflammatory cytokines (Warton *et al.*, 2004). The same study reported that, in the Cos-7 cells, these proteins were localised to the nucleus (Introduction, Chapter 1.6). Transfecting the recombinant proteins into endothelial cells resulted in upregulation of the Rho kinases Rnd1 and Gem GTPase in this cell line. Based on these observations, Warton *et al.* (Warton *et al.*, 2004) proposed that *C2CD4A* and *C2CD4B* belong to a novel gene family encoding nuclear factors with a role in regulating cellular architecture. In addition, a recent study has shown that murine C2CD4A, in MIN6 cells and in human pancreatic islets, is also localised to the nucleus and acts as a gene co-regulator downstream of *FoxO1* (Holst *et al.*, 2016). However, the function of human C2CD4A in β-cells was not assessed in the latter paper.

In humans, C2CD4A and C2CD4B protein sequences are 83% homologous (sequences were compared on http://www.uniprot.org). Both proteins contain a C2 domain at their C-terminus, which is predicted to bind to Ca^{2+} and phospholipids (Nalefski & Falke, 1996). Unlike *C2CD4C,* another homologue of these genes (see Introduction, Chapter 1.6.2), it has been suggested that C2CD4A and C2CD4B have (partially) lost the canonical Ca^{2+} binding sites in their C2 domains (Omori *et al.*, 2016). However, it is not clear whether in β-cells they conserve their ability to bind, or respond to, intracellular Ca^{2+} and/or phospholipids. In addition, their possible roles in the β-cell, and the interacting proteins which might mediate them, remain to be discovered. The focus of this chapter is to answer these questions.

3.2. Results

3.2.1. Sub-cellular localisation of C2CD4A and C2CD4B in β-cells

To test whether C2CD4A and C2CD4B are localised to the nucleus in pancreatic β-cells, and to dissect the possible function of these proteins in these cells, we studied their sub-cellular localisation in different β-cell models (MIN6 cells, a murine β-cell line (Miyazaki *et al.*, 1990); INS1 (832-13) a rat β-cell line (Hohmeier *et al.*, 2000b); EndoC βH1 cells, a human β-cell line (Ravassard *et al.*, 2011)), using immunohistochemistry and confocal microscopy. Since antibodies against the endogenous proteins were not available commercially, to address this question we tagged cDNAs encoding *C2CD4A* or *C2CD4B* with FLAG or GFP epitopes and introduced these constructs into the cells of interest using Lipofectamine (Invitrogen) based transfection (Figure 3. 1). This induced a transient expression of our genes of interest in the target cells.

We attempted to make antibodies against murine C2CD4B with New England Peptide. Two different antibodies against murine C2CD4B were generated. Unfortunately, no specific bands were detected after performing several Western (immuno)blotting with these antibodies. Protein samples from different cell lines and tissues were used at different Western (immuno)blotting blocking buffers. Also, different protein denaturing protocols were used to attempt to optimise this protocol. We also used protein samples from isolated pancreatic islets from null and WT *C2cd4*b mice. No bands of the expected size (37.1 kDa), which is specific in WT samples, were found.

By visualising the localisation of each protein in the above β-cell systems through immunofluorescence with anti-FLAG antibody (or using intrinsic fluorescence for GFP-tagged constructs) our data showed that, in contrast to the Cos-7 cells (Warton *et al.*, 2004) and over-expression of murine *C2cd4a* (Holst *et al.*, 2016), the localisation of human C2CD4A (A) and C2CD4B (B) was not limited to the nucleus (Figure 3. 2). In fact, we observed three main localisation patterns in different cells from the same culture (Figure 3. 3). In the majority of the cells (MIN6, A: 67.2% ±10.4, B: 46.4% ±20.5; INS1 (832/13), A: 77.6% ±8.7, B: 71% ±9.5; EndoC βH1 A: 75.3% ±10.9, B: 69.3% ±7.2), C2CD4A and C2CD4B were localised in the cytoplasm and nucleus. In some cells (MIN6, A: 30.9% ±11.7, B: 43.1% ±15.5; INS1 (832/13), A: 22.1% ±8.8, B: 22.6% ±10.9; EndoC βH1, A: 23.6% ±10.71.4, B:13.7% ± 3.8),

membrane localisation in addition to cytoplasm and nucleus was observed. And finally, only in the minority of cells (MIN6, A: 1.77% ±1.4, B: 10.4% ±8.1; INS1, (832/13) A: 0.2% ±0.2, B: 6.4% ±6.4; EndoC βH1, A:1.1% ±0.2, B: 17% ±6.5) the localisation was limited to the nucleus (Figure 3. 4. A). We observed similar patterns of localisation between C2CD4A and C2CD4B, for all cell types examined (Figure 3. 4. A).

In order to determine if there was any effect on sub-cellular localisation of adding a large molecule such as GFP (27 kDa) to either protein, we quantified the localisation patterns of these GFP-tagged proteins after transfection into the cell lines above. In this case, the localisation of the GFP-tagged proteins was indistinguishable from that of the FLAG-tagged constructs (Figure 3. 4. B).

To study the possibility of involvement of these genes in insulin synthesis and processing, we explored the co-localisation between C2CD4A and C2CD4B and different cellular organelles involved in these processes, including endoplasmic reticulum (ER), trans-Golgi network (TGN) and lysosomes. Immunofluorescence was performed after transfecting β-cells with FLAG -tagged-*C2CD4A* or -*C2CD4B* constructs, using antibodies against insulin, rabbit anti-TGN46 (Abcam) and rat anti-LAMP1 (Santa Cruz), to target lysosomes. To demonstrate the possible co-localisation with ER, immunofluorescence using an antibody against the FLAG epitope was performed after co-transfecting with the *C2CD4A*: FLAG - or *C2CD4B*: FLAG-tagged constructs with the ER targeting KDEL: Red construct. The results showed that C2CD4A and C2CD4B do not co-localise with any of the above organelles (Figure 3. 5).

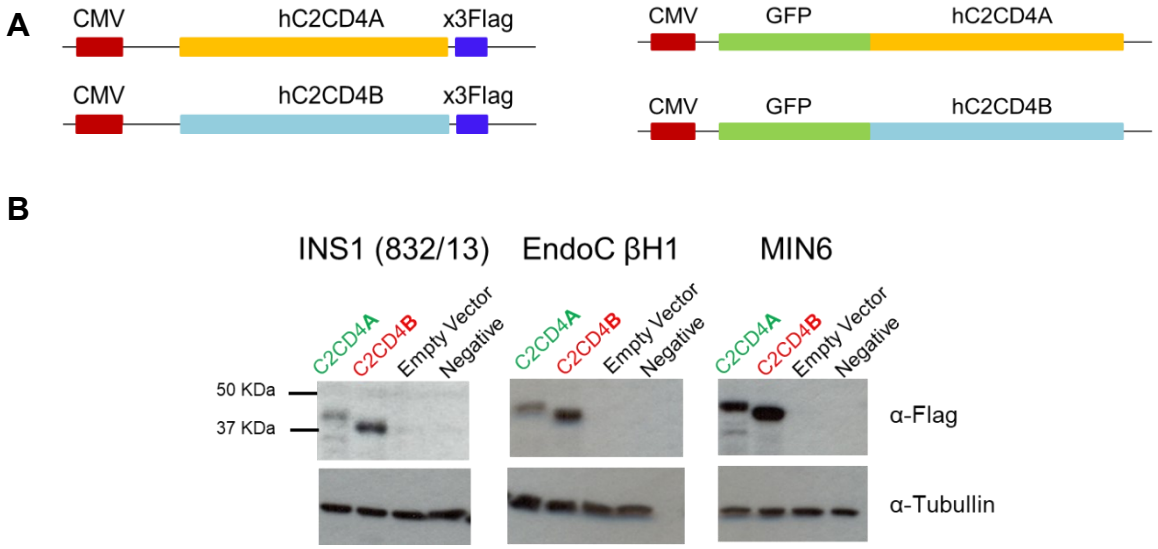

Figure 3.1. Constructs used to visualise the sub-cellular localisation of C2CD4A and C2CD4B in β-cells. A. Schematics of hC2CD4A and hC2CD4B constructs which were tagged with x3 FLAG isotopes at their C-terminus or tagged with GFP at the N terminus. B. Protein samples were collected 48 hr after the transfection of the cells with *C2CD4A*- and *C2CD4B*- FLAG confirmed the over-expression of *C2CD4A*- and *C2CD4B*- FLAG tagged constructs in the transfected cells. See Material and Methods Chapter 2.

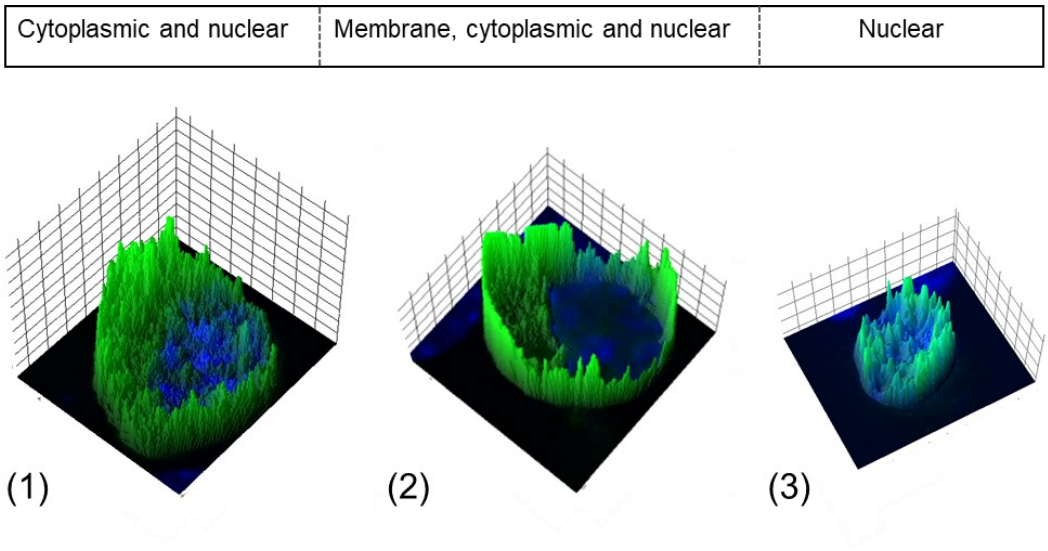

Figure 3.2. 3D intensity plots showing three different sub-cellular localisation patterns of human C2CD4A and C2CD4B in MIN6 β-Cells. Images show examples of the sub-cellular localisation patterns in MIN6 cells transfected with FLAG-tagged *C2CD4A* construct. Z axis represents the intensity of the fluorescent signal after staining. Cells were grown in regular MIN6 media containing 4500mg/L glucose and fixed in 4% [vol./vol.] PFA dissolved in PBS, 24 h post-transfection. Immunohistochemistry using an anti-FLAG antibody in green (Sigma, 1:1000) and DAPI in blue was performed to visualise the localisation of each protein. Three main localisation patterns were observed. (1) Cytoplasm and nucleus, (2) the plasma membrane in addition to cytoplasm and nucleus and (3) nucleus alone. The sub-cellular localisation patterns were similar for C2CD4A and C2CD4B. Sub-cellular localisation patterns were consistent between MIN6, INS1 (832/13), and EndoC βH1 cell lines. Anti-FLAG staining shown in green and DAPI staining shown in blue.

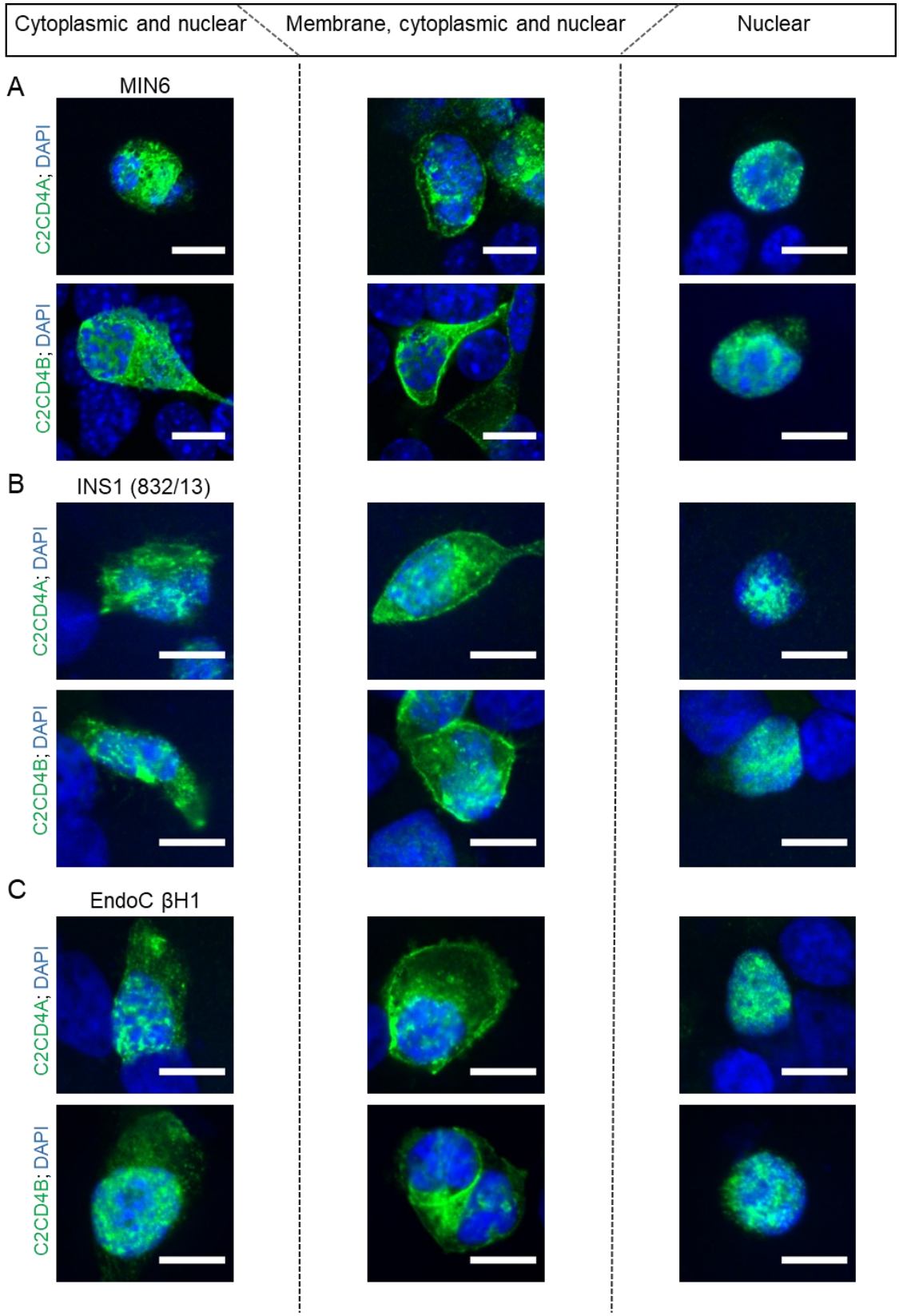

Figure 3.3. Sub-cellular localisation of C2CD4A and C2CD4B in β-cells. Three main localisation patterns were observed by visualising C2CD4A and C2CD4B proteins (in green, anti-FLAG antibody used) in (A) MIN6, (B) INS1 (832/13) and (C) EndoC βH1 cells. DAPI staining shown in blue. Scale bars=10 μm.

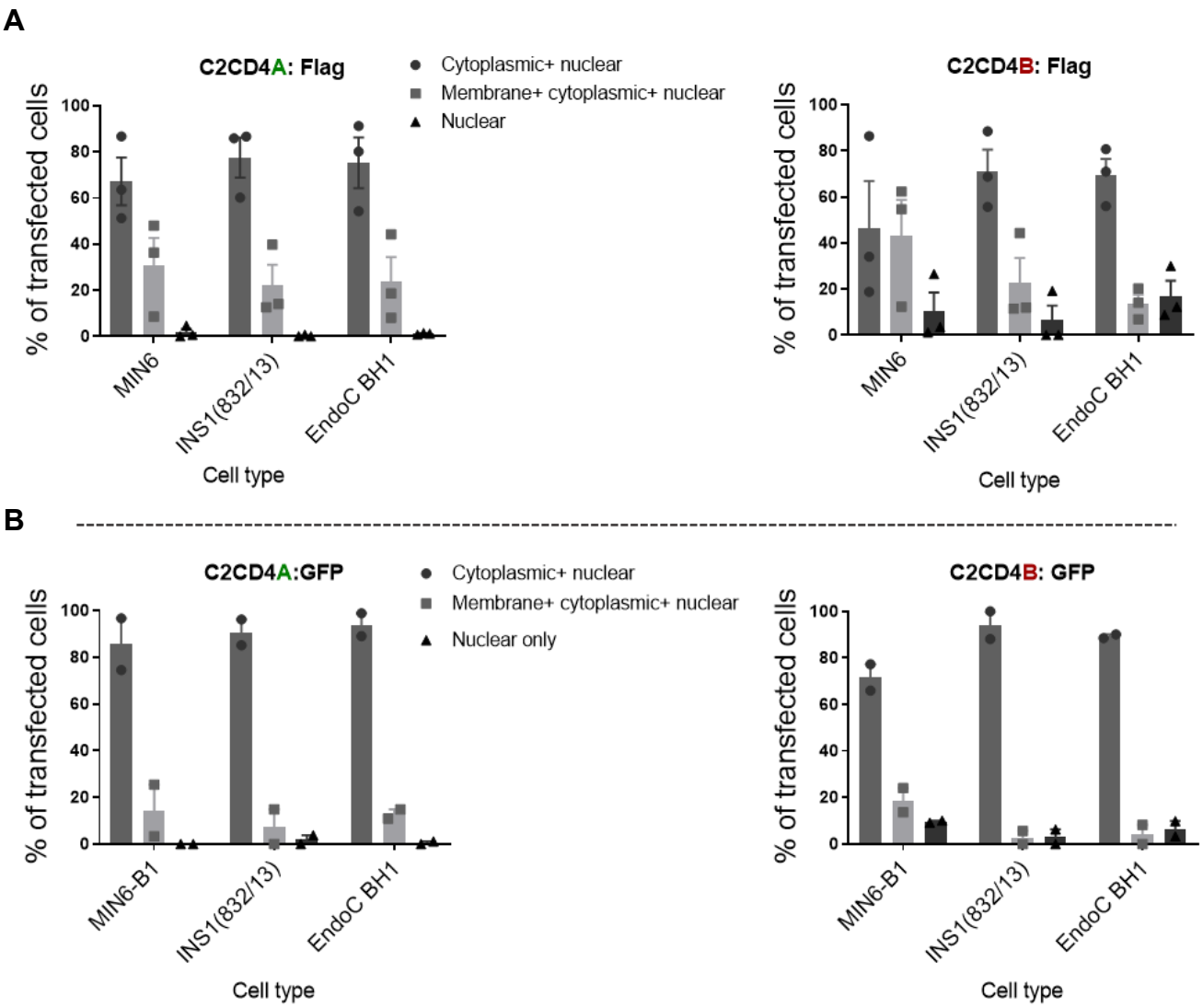

Figure 3.4. Quantification of different localisation patterns of C2CD4A and C2CD4B in β-cells. A. Quantification of different localisation patterns in different β-cell types using C2CD4A: FLAG and C2CD4B: FLAG-tagged constructs (see Chapter 2.3.3. for quantification details). B. Quantifications of different localisation patterns in different β-cell lines using GFP-tagged-C2CD4A and -C2CD4B constructs (see Chapter 2.3.3. for quantification details). The quantifications have been performed in three independent experiments. In each experiment, two separate cultures have been analysed. Around 150 cells from two seperate cultures were analysed in each experiment. No changes were detected in the localisation patterns between different cell types nor between C2CD4A and C2CD4B localisation patterns. Data were assessed for significance using a 2-way ANOVA with Bonferroni's multiple comparison test. Values represent means ± SEM.

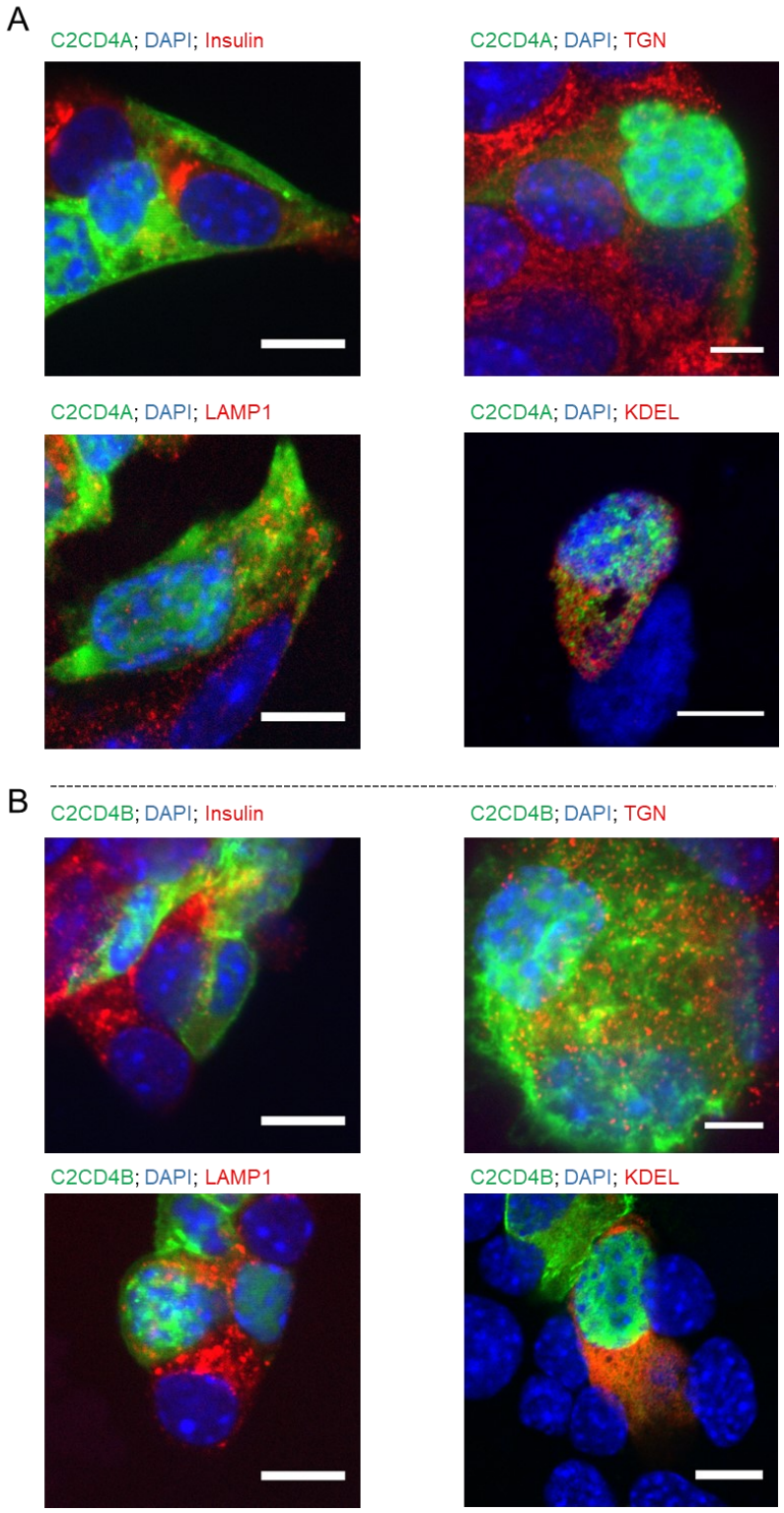

Figure 3.5. Sub-cellular co-localisation of C2CD4A and C2CD4B in MIN6 cells. A. Sub-cellular co-localisation of C2CD4A (in green) with insulin, TGN (TGN46), lysosomes (LAMP1) and ER (KDEL) (all in red). B. Sub-cellular co-localisation of C2CD4B (in green) with insulin, TGN, lysosomes (LAMP1) and ER (KDEL) (all in red). DAPI staining shown in blue. Scale bars= 10 μm.

3.2.2. C2CD4A translocation in response to increased intracellular free Ca^{2+} levels

Based on sequence analysis alone, it has been suggested by Omori *et al.* (Omori *et al.*, 2016) that the C2 domains of C2CD4A and C2CD4B do not contain functional Ca^{2+} binding domains. However, amino acid alignments suggest that these proteins might partially conserve their ability to bind to Ca^{2+} (Figure 1. 7). To test this hypothesis directly, we explored whether imposed changes in intracellular [Ca^{2+}] may elicit C2CD4A and C2CD4B translocation to the plasma membrane in β-cells, as expected for proteins bearing *bona fide* C2 domains (Nalefski & Falke, 1996),[111]. To this end, we used the proteins tagged with GFP (N-terminal) to allow live cell imaging. As a positive control, a construct in which Synaptotagmin-1 (Syt1), containing five C2 domains and fused to the reporter GFP was used (Idevall-hagren *et al.*, 2015). The latter plasmid has been shown to translocate from the ER to the plasma membrane in response to increased intracellular [Ca^{2+}]. Simultaneous confocal and total internal reflection (TIRF)-based live cell imaging was performed to monitor changes in the localisation of these proteins in response to an increase in [Ca^{2+}] induced by exposure to the ionophore ionomycin (in collaboration with Dr Pauline Chabosseau) (Figure 3. 6, A-D).

Although the changes in the localisation of C2CD4A were not as marked as those of Syt1 (Fluorescent intensity fold change: 19.7% ±4.86, n=5 acquisitions), we did observe a small but significant (Fluorescent intensity fold change: 8.02% ±1.97, n=5 acquisitions) increase in C2CD4A florescence at the plasma membrane in response to increased [Ca^{2+}]. By contrast, C2CD4B did not show any significant change in localisation (Fluorescent intensity fold change: 1.2% ±0.71, n=6 acquisitions) (Figure 3. 6, C-E).

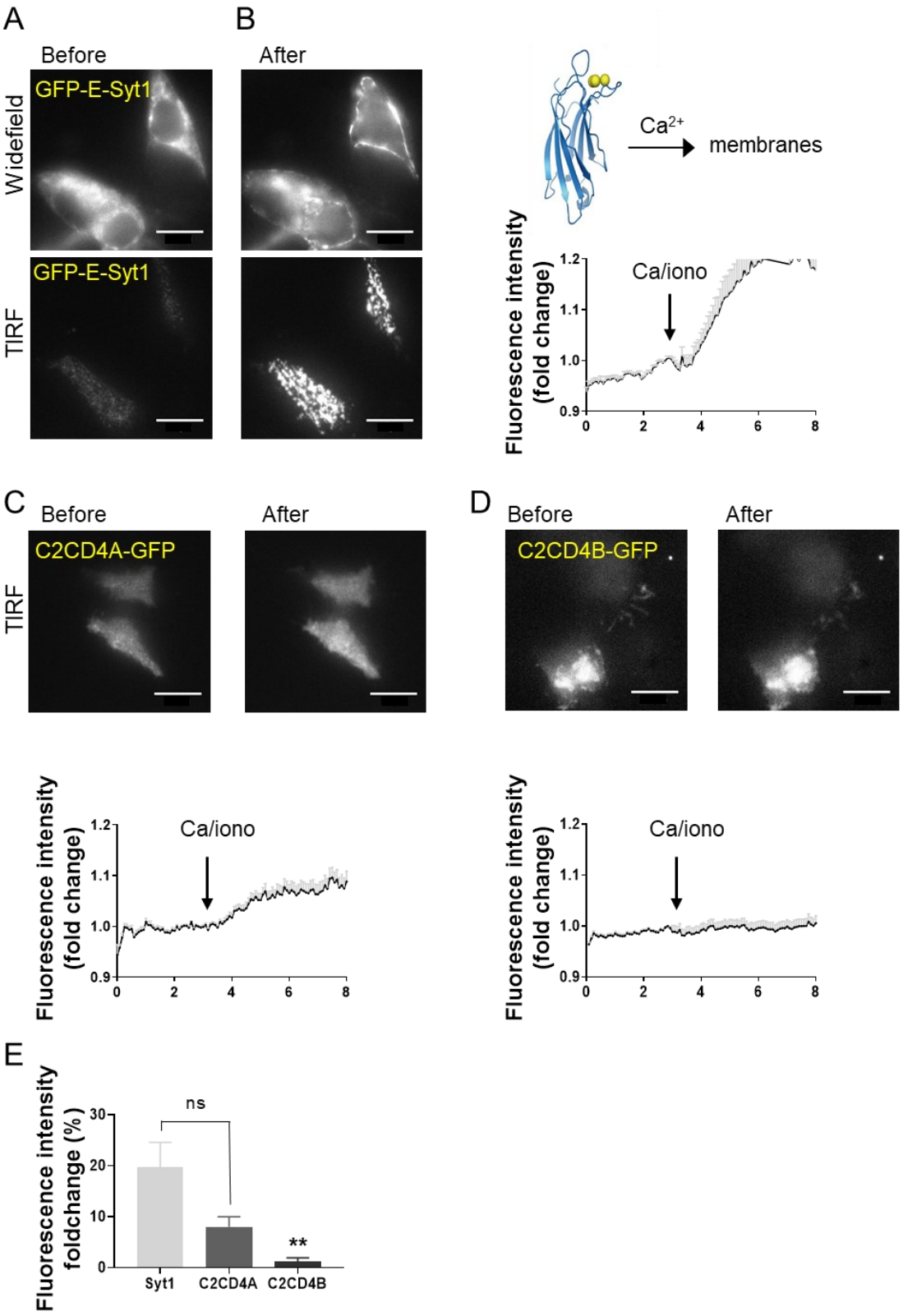
A
B
Before
After
Widefield
TIRF
GFP-E-Syt1
GFP-E-Syt1
Ca2+
membranes
Fluorescence intensity (fold change)
Ca/iono
C
D
Before
After
TIRF
C2CD4A-GFP
C2CD4B-GFP
Fluorescence intensity (fold change)
Ca/iono
Fluorescence intensity (fold change)
Ca/iono
E
Fluorescence intensity foldchange (%)
ns
**
Syt1
C2CD4A
C2CD4B

Figure 3. 6. Changes in C2CD4A and C2CD4B localisation in response to increased intracellular [Ca^{2+}]. A-B. As a positive control an expressed GFP-tagged Synaptotagmin (Syt1), which moves from the ER to the plasma membrane in response to elevated Ca^{2+}, was used. A. Localisation of the control protein, GFP-Syt1, in 5 mM glucose and added 50 µM extracellular Ca^{2+}. B. Images show localisation of the control plasmid in response to high intracellular Ca^{2+}, achieved by addition of 50 ng/ml ionomycin, during simultaneous wide-field and TIRF image acquisitions (Material and Methods, Chapter 2). C-D. Show localisation of GFP-tagged-C2CD4A and -C2CD4B before and after addition of ionomycin to the medium. E. Fluorescence intensity fold-change (%) graph shows a significant increase in C2CD4A intensity at the plasma membrane, after addition of ionomycin and an increase in intracellular Ca^{2+} levels. Inset graphs indicate fluorescence traces of GFP-tagged proteins in TIRF imaging before and after addition of ionomycin. *p<0.05, **p<0.01, data were assessed for significance using an ordinary one-way ANOVA. Solid lines represent mean ± SEM; SEM shown by grey bars. Scale bars= 10 µm.

3.2.3. C2CD4A and C2CD4B interacting proteins

To gain more insight into the possible roles and mechanism of action of these proteins, we performed a proteomic screen based on Immunoprecipitation and Mass spectrometry (MS), in collaboration with Dr Steven Millership, London Institute of Medical Sciences (LMS). For this, two independent pools of MIN6 cells, in duplicate, were transfected with C2CD4A: FLAG or C2CD4B: FLAG tagged constructs. As a negative control, a pool of MIN6 cells transfected with FLAG construct with no gene inserted was used. C2CD4A and C2CD4B were immuno-precipitated from the cytoplasm using anti-FLAG antibody. MIN6 cells were selected in this experiment as this results in high transfection efficiency in these cells (~60%) compared to EndoC βH1 (~10%).

Normalising to the negative control and placing in order from the most significant interacting protein to the least significant, Dr Millership generated a list of possible interacting proteins for C2CD4A or C2CD4B (Table 4-6 show top 15 proteins for C2CD4A and C2CD4B, and top 12 proteins interacting with both C2CD4A and C2CD4B).

Among these proteins, ten interact with both C2CD4A and C2CD4B. These proteins are Clusterin (Clu), Procollagen-lysin,2-oxoglutarate 5-dioxygenase 3 (Plod3), Glucagon (Gcg), Hyaluronan and proteoglycan line protein 4 (Hapln4), Receptor-

type tyrosine-protein phosphatase N2 (Ptprn2), Importin-5 (Ipo5), E3 ubiquitin-protein ligase UBR5, Heat shock 70 kDa protein 13 (Hspa13), Protein convertase subtilisin/Kexin type9 (Pcsk9) and Receptor-type tyrosine-protein phosphatase-like N (Ptprn). Considering the structure and function of C2CD4A and C2CD4B and their proposed roles in inflammation and glucose homeostasis, the proteins which are more likely to mediate their action in these functions are highlighted in yellow.

For instance, considering the tissue distribution and the glucose intolerance phenotype observed in both *C2cd4a* and *C2cd4b* null animals (Chapter1, 1.4.4) and FSH deficiency in *C2cd4b* animals (Chapter 4, 4.2.9), PTPRN2 and PTPRN are strong candidates to interact with and play a role in the function of C2CD4A and C2CD4B. PTPRN (PTP IA-2) and PTPRN2, also known respectively as PTP IA-2 and R-PTP-N2, are involved in the accumulation of secretory vesicles in the hippocampus, pituitary gland and pancreatic islets (Marullo, El-Sayed Moustafa & Prokopenko, 2014; Kubosaki *et al.*, 2006; Saeki *et al.*, 2002). More studies to address the possible roles of these proteins in exocytosis are essential to confirm these results.

Name	Unique peptides	Average intensity	FC over control	Function
60S ribosomal protein L36 (Rpl36)	7	408547500	2.31651774	Ribosomal protein
Bone morphogenetic protein 1 (Bmp1)	14	323217500	4.528805647	Formation of cartilage in vivo
Clusterin beta/alpha chain (Clu)	6	242922500	infinity	Basic biological events such as cell death, tumour progression, and neurodegenerative disorders
Sequestosome-1 (Sqstm1)	4	238032500	4.041972241	Scaffolding/adaptor protein in concert with TNF receptor-associated factor 6 to mediate activation of NF-kB
Glucagon;Glicentin (Gcg)	2	149391750	infinity	Glucagon, glucose homeostasis
Ttc13	9	142825000	2.147951497	A protein coding gene, unknown function
Procollagen-lysine,2-oxoglutarate 5-dioxygenase 3 (Plod3)	8	137387500	infinity	Catalyses the hydroxylation of lysyl residues in collagen-like peptides
Hyaluronan and proteoglycan link protein 4 (Hapln4)	4	129820000	infinity	Extracellular matrix structural constituent and hyaluronic acid binding
Torsin-2A;Prosalusin;Salusin-beta (Tor2a)	3	107971000	infinity	Increases intracellular [Ca^{2+}], induces cell mitogenesis
U5 small nuclear ribonucleoprotein (Snrnp40)	4	103415000	infinity	Component of the U5 small nuclear ribonucleoprotein (snRNP) particle
MAP7 domain-containing protein 1 (Map7d1)	3	102242500	infinity	Structural molecule activity
Nucleolar protein 14 (Nop14)	4	91338750	infinity	Pre-18s rRNA processing and small ribosomal subunit assembly
DNA topoisomerase 2-beta (Top2b)	4	88047000	infinity	Chromosome condensation, chromatid separation, and the relief of torsional stress
Proprotein convertase subtilisin/kexin type 9 (Pcsk9)	6	86949000	infinity	Processes protein and peptide precursors trafficking
Receptor-type tyrosine-protein phosphatase N2 (Ptprn2)	4	82972000	infinity	Required for normal accumulation of secretory vesicles in hippocampus, pituitary and pancreatic islets

Table 4. C2CD4A interacting proteins detected by mass-spectrometry. Top 15 predicted interacting proteins for C2CD4A in MIN6 cells. The given function(s) of the identified protein was adopted from GeneCards.org.

Name	Unique peptides	Average intensity	FC over control	Function
Neuroendocrine convertase 2 (Pcsk2)	18	2188050000	2.365537387	Is a protease that processes protein and peptide precursors trafficking through the secretory pathway
Renin receptor (Atp6ap2)	8	1197847500	4.624034467	Associated with the transmembrane sector of the V-type ATPases
Carboxypeptidase E (Cpe)	12	852947500	2.488765327	Involved in the biosynthesis of peptide hormones and neurotransmitters, including insulin
C2cd4a; C2cd4b	4	852000000	infinity	
Clusterin beta chain;Clusterin alpha chain (Clu)	6	364380000	infinity	Basic biological events such as cell death, tumour progression, and neurodegenerative disorders
N-acetylglucosamine-1-phosphotransferase subunit gamma (Tce7;Gnptg)	8	361852500	3.757036085	Sub-unit of an enzyme that catalyses the formation of mannose 6-phosphate (M6P) in the Golgi apparatus
Importin-5 (Ipo5)	5	274114500	infinity	Nucleoplasmic transport of proteins containing NLS
Carbohydrate sulfotransferase 11 (Chst11)	4	238460000	2.402356026	Catalyses the transfer of sulphate to position 4 of the N-acetylgalactosamine (GalNAc) residue of chondroitin
Glucagon (Gcg)	2	217025000	infinity	Glucagon, glucose homeostasis
Sequestosome-1 (Sqstm1)	4	211023500	3.868217344	Regulates activation of the nuclear factor kappa-B (NF-kB) signalling pathway
Bone morphogenetic protein 1 (Bmp1)	14	200115000	3.837129646	Formation of cartilage in vivo
Procollagen-lysine,2-oxoglutarate 5-dioxygenase 3 (Plod3)	8	195605000	infinity	Autophagy receptor required for selective macro-autophagy (aggrephagy).
Hyaluronan and proteoglycan link protein 4 (Hapln4)	4	144687500	infinity	A protein involved in Integrin Pathway and ERK Signalling
Receptor-type tyrosine-protein phosphatase N2 (Ptprn2)	4	107998500	infinity	Required for normal accumulation of secretory vesicles in hippocampus, pituitary and pancreatic islets (Marullo, El-Sayed Moustafa & Prokopenko, 2014; Kubosaki *et al.*, 2006; Saeki *et al.*, 2002)

Table 5. C2CD4B interacting proteins detected by mass-spectrometry. Top 15 predicted interacting proteins for C2CD4B in MIN6 cells. The given function(s) of the identified protein was adopted from GeneCards.org.

Name	Unique peptides	FC over count	Function
C2 calcium dependent domain containing 4	**4**	inf	
Clusterin; (Clu)	6	inf	Basic biological events such as cell death, tumour progression, and neurodegenerative disorders
Procollagen-lysine,2-oxoglutarate 5-dioxygenase 3 (Plod3)	8	inf	Autophagy receptor required for selective macroautophagy (aggrephagy).
Glucagon (Gcg)	2	inf	Glucagon, glucose homeostasis
Hyaluronan and proteoglycan link protein 4 (Hapln4)	4	inf	A protein involved in Integrin Pathway and ERK Signalling
Receptor-type tyrosine-protein phosphatase N2;Protein-tyrosine-phosphatase (Ptprn2)	4	inf	Required for normal accumulation of secretory vesicles in hippocampus, pituitary and pancreatic islets (Marullo, El-Sayed Moustafa & Prokopenko, 2014; Kubosaki *et al.*, 2006; Saeki *et al.*, 2002)
Importin-5 (Ipo5)	5	inf	Nucleoplasmic transport of proteins containing NLS
EF-hand calcium-binding domain-containing protein 5 (Efcab5)	2	inf	Calcium-binding protein
E3 ubiquitin-protein ligase UBR5 (Ubr5)	8	inf	E3 ubiquitin-protein ligases, targeting specific proteins for ubiquitin-mediated proteolysis
Heat shock 70 kDa protein 13 (Hspa13)	5	inf	A member of the heat shock protein 70 family and is found associated with microsomes
Proprotein convertase subtilisin/kexin type 9 (Pcsk9)	6	inf	Regulation of cell proliferation or differentiation.
Alpha-internexin (Ina)	2	inf	Neurofilaments comprise the exoskeleton and they functionally maintain the neuronal calibre
Receptor-type tyrosine-protein phosphatase-like N (Ptprn)	6	inf	Normal accumulation of secretory vesicles in hippocampus, pituitary and pancreatic islets (Marullo, El-Sayed Moustafa & Prokopenko, 2014; Kubosaki *et al.*, 2006; Saeki *et al.*, 2002)

Table 6. C2CD4A and C2CD4B interacting proteins detected by mass-spectrometry. Top 12 predicted interacting proteins with both C2CD4A and C2CD4B in MIN6 cells. The given function of the identified protein was adopted from GeneCards.org.

3.3. Discussion

This chapter aimed to explore the function(s) of *C2CD4A* and *C2CD4B* in β-cells. To address this question, we first studied the subcellular localisation of C2CD4A and C2CD4B in β-cells originating from humans and rodents. Our localisation data suggest novel roles for human *C2CD4A* and *C2CC4B* in the β-cell compared to those previously described (Warton *et al.*, 2004)' (Kuo *et al.*, 2019). Notably, we observed cytoplasmic and membrane localisation patterns rather than a chiefly nuclear localisation, which may suggest possible roles in cell signalling through their C2 domains. For PKCs it has been shown that in response to elevated intracellular Ca^{2+}, the C2 domain acts as a bridge with the phosphatidylserine located in the inner layer of the plasma membrane (Corbalán-García & Gómez-Fernández, 2010).

We also aimed to determine whether the C2 domains in C2CD4A and C2CD4B, contain functional Ca^{2+} binding sites. Using live cell imaging, we showed C2CD4A translocation to the plasma membrane in response to an increase in free intracellular Ca^{2+} concentrations. This suggests that although C2CD4A does not contain a canonical C2 domain, as observed in conventional PKCs, it could also bind to Ca^{2+}.

Finally, we also aimed to detect possible interacting partners for these proteins. We showed that several proteins that bind to Ca^{2+}, or have roles in NF-kB signalling, are among the possible interacting partners. In addition, proteins involved in the transport of secretory vesicles were identified, suggesting that C2CD4A and C2CD4B could have roles in Ca^{2+} mediated secretion from β-cells.

3.3.1. Novel roles of *C2CD4A* and *C2CD4B* in β-cells

Previously examined in Cos-7 cells, transfected with GFP-tagged-*C2CD4A* and -*C2CD4B* constructs, it was shown that the localisation of each protein was solely limited to the nucleus (Warton *et al.*, 2004). Likewise, it has also been recently shown that GFP-tagged murine *C2cd4a* is localised solely in the nucleus in MIN6 cells and in mouse islets (Kuo *et al.*, 2019).

Due to a lack of antibodies to detect the endogenous proteins and our inability to generate new antibodies, we also used a similar method and tagged human *C2CD4A* and *C2CD4B* with either FLAG or with GFP and examined their distribution in β-cell lines from human, mouse and rat. Surprisingly, our data showed that the sub-cellular localisation of these proteins in these cell lines is *not* limited to the nucleus. We

observed three main localisation patterns: in the cytoplasm and nucleus, in the membrane in addition to the cytoplasm and nucleus and, in the minority of the cells, the localisation was solely limited to the nucleus. These differences in the localisation patterns *versus* earlier studies may suggest novel roles for these proteins in β-cells compared to previous findings in the Cos-7 cell line (Warton *et al.*, 2004). Also, different localisation patterns observed in human C2CD4A compared to the murine orthologue, could suggest different functionality between murine and human C2CD4A proteins.

Another possible explanation for these different localisation patterns could be differences in cell cycle stages between different cells. To test this possibility, agents such as Nocodazole (Beswick, Ambrose & Wagner, 2006) which binds to β-tubulin and affects polymerisation of microtubules, stopping the cell cycle at G2/M phase, could be used to stop/synchronise the cell cycle and examine the localisation patterns at specific cell cycle stages. Another complementary method could be co-staining these cells for cell cycle markers such as cyclin E and/or cyclin B1 (Gookin *et al.*, 2017). However, one might suggest this is an unlikely explanation since cell cycle stages from the three different cell lines we studied show dramatic differences in their cell cycle speed (for instance MIN6 cells divide every 24-48 h while EndoC βH1 cells divide every 5-6 days), and no differences in localisation patterns were observed between these cell lines.

We used Lipofectamine-based transfection to deliver our GFP/FLAG-tagged constructs into the cells. This induces transient expression of the genes in cells. Another way to deliver DNA into cells is using virus-based infection methods. This method could have advantages compared to Lipofectamine-based transfection. Cells can be infected more efficiently and by quantifying the virus, we can calculate and control the amount of DNA enters the cells. On the other hand, this method is more time consuming compared to Lipofectamine transfection. In addition, considering a very low transfection efficiency with Lipofectamine in EndoC βH1 cells (around 10-20%), might also add extra limitations to our studies since we were only study 10% of the cells, which might not be representative of the majority of the cells in culture. Another limitation of our study, using a highly expressed promotor such as CMV could be additional artefacts caused by overexpression of the proteins. There may include ectopic sub-cellular localisations or erroneous formation of protein complexes among others. Also, using the transcriptional machinery of cells at such

exaggerated levels could cause stress and deficiency of the expression of other essential cell factors which needs to be added to considerations.

Another question arising from our studies is whether these genes have roles in the synthesis and/or secretion of insulin. However, and perhaps contradicting this possibility, they did not seem to co-localise at the ER, TGN or insulin vesicles. To further understand the role of these genes in insulin secretion and processing, several more studies could be performed.

For instance, electron microscopy (EM) or super-resolution microscopy could be performed to visualise the localisation of these proteins more precisely in β-cells. EM can be also used to study the effect of over-expression or deletion of these genes on secretory granules or docked granules into the plasma membrane. Since there are no antibodies available to detect these endogenous proteins, a more sophisticated way to detect these proteins compared to over-expressing with a tagged molecule, could be making a reporter β-cell line with an epitope expressed after these genes. By using this method, the possible artefacts caused by over-expression of these genes could be eliminated. This would give us more possibilities to study the dynamic of these genes *in vitro* under different glucose concentrations or stressing cells with palmitate or inflammatory cytokines.

In addition to the above studies and, to unravel the reason behind the different localisation patterns observed between murine and human C2CD4A or C2CD4B, localisation studies should be carried out using expression constructs for C2CD4A or C2CD4B from both these species. This would allow the opportunity to directly compare these proteins between the two species. We would emphasise that different degrees of over-expression are unlikely to explain the differences between the localisations reported here and in earlier works (Warton *et al.*, 2004)'(Kuo *et al.*, 2019). Thus, we did not notice any alteration in distribution when examining cells with different levels of over-expression (data not shown).

3.3.2. C2CD4A translocation in response to elevated intracellular Ca^{2+}

The C2 domains of PKC family members have been shown to have a crucial role in signal transduction by allowing the translocation of these enzymes to the plasma membrane and/or other sub-cellular organelles in response to cell stimulations (Corbalán-García & Gómez-Fernández, 2010). For PKCs, it is documented that the

C2 domain acts as a bridge with the phosphatidylserine, located at the inner layer of the plasma membrane, in response to an elevation of intracellular Ca^{2+}. The translocation between the plasma membrane and other membrane compartments has also been observed in other proteins containing C2 domains (Idevall-hagren *et al.*, 2015). For instance, in mammalian cells, e-Syt1 can translocate from the ER to the plasma membrane in response to increased intracellular Ca^{2+}. The latter protein contains five C2 domains and functions as a lipid translocator between the ER and the plasma membrane (Idevall-hagren *et al.*, 2015). Whether the C2 domains of C2CD4A and C2CD4B could also bind to Ca^{2+} is not known.

It has been suggested, solely on the basis of sequence analysis, that the C2 domains of C2CD4A and C2CD4B do not contain Ca^{2+} binding sites (Omori *et al.*, 2016). We showed in Chapter 1, by amino acid alignments, that these proteins might partially retain their ability to bind to Ca^{2+}. The plasma membrane localisation of these proteins in β-cells suggests that these proteins can potentially bind to Ca^{2+} and/or phospholipids in the membrane.

In order to test if an increase in intracellular [Ca^{2+}] induces translocation of these proteins from the nucleus or cytoplasm to the plasma membrane, live cell imaging, using wide-field and TIRF microscopy systems, was used. Interestingly, our data showed increased plasma membrane localisation of C2CD4A upon intracellular [Ca^{2+}] increase, but no change in the localisation of C2CD4B. This observation suggests that C2CD4A and C2CD4B might have different functions in β-cells in response to an elevation of intracellular [Ca^{2+}]. This could potentially suggest that C2CD4A has a more direct effect on GSIS from β-cells compared to C2CD4B.

This is an interesting question. In our view if a shift in localisation can be detected (i.e. significant statistically) then a detector MAY exist in the cell which can ‘’read out’’ is the observed translocation to the plasma membrane. However, since at the moment we are only just beginning to identify the downstream interactors, it is difficult to speculate how large a change would be sufficient to have meaningful biological impact. The way to address this, would obviously be to produce a form of either protein which is not able to move, but retains other biological activity and domains (for example by inserting mutations in the C2 domains. This would indeed be interesting for the future.

Further investigations are needed to understand the roles of different domains in these proteins. Protein truncation studies could be one way to reveal this. Furthermore, to have a more robust understanding of the 3D structure and, therefore, the function of these gene products, X-ray diffraction (Parker, 2003) could be used on the crystallised form of these proteins. The 3D structure of the proteins and the localisation of the possible hydrophobic and hydrophilic domains may be useful in predicting their possible interacting partners and function.

The possible interaction of C2CD4A and C2CD4B with secretory vesicles could also be studied further. For this, insulin granules in pancreatic β-cells could be labelled with RFP fused with LDCV-associated protein syncollin (syncollin–RFP) (Hodel & Edwardson, 2000). Co-transfecting this protein with either GFP-tagged -*C2CD4A* or -*C2CD4B* constructs would enable us to visualise the possible interaction of these proteins with secretory granules. This method can be used in different glucose concentrations or at different intracellular Ca^{2+} levels, to detect any change in the interactions between these proteins after stimulating with glucose or other secretagogues.

3.3.3. C2CD4A and C2CD4B interacting proteins

Not much is known about the structure and function of C2CD4A and C2CD4B and the proteins that interact with them. It has been shown that both proteins contain a C2 domain in their C-terminus, which is predicted to bind to Ca^{2+} and/or phospholipids. However, prior to the present studies it was not known if the C2 domain contains functional Ca^{2+} binding sites (Warton *et al.*, 2004)'(Omori *et al.*, 2016). In addition, our work to determine whether intracellular Ca^{2+} levels trigger translocation of these proteins (Figure 3. 6), suggested that C2CD4A might have a role in Ca^{2+}-dependent signal transduction, while C2CD4B is unlikely to participate in such a pathway. The nature of these patterns and the agonists whose signal may be affected remain to be identified.

It has also been shown in endothelial cells, pancreatic islets and β-cells that these genes are up-regulated in response to inflammatory cytokines including, interleukin 1β (IL 1β) (Eizirik *et al.*, 2012) and by activation of nuclear factor κB (NF-κB) (Kycia *et al.*, 2018). In pancreatic β-cells it has also been shown that murine *C2cd4a* lies downstream of transcription factor FoxO1. In MIN6 cells, over-expression of *C2cd4a*

induces glycolysis, AMPK signalling, and PKA signalling (Warton *et al.*, 2004). Concerns must be raised however, as to whether these changes would be seen in our own over-expression systems, given the distinct localisation observed.

To gain further insights into the potential role(s) of these proteins in β-cells, we performed mass spectrometry on immunoprecipitations from MIN6 cells transfected with FLAG-tagged -*C2CD4A* or -*C2CD4B* constructs. As a negative control, cells were transfected with the FLAG construct without any inserts. Lists of possible proteins interacting with C2CD4A and C2CD4B were generated by Dr Millership and were sorted from the most strongly associated with C2CD4A or C2CD4B and the protein candidates from the negative control pool were eliminated. Having done this, a list with 80 proteins interacting with C2CD4A and 19 proteins interacting with C2CD4B were generated (Tables 4-6). Among these proteins, ten were interacting with both C2CD4A and C2CD4B.

Considering the tissue distribution and functions of PTPRN2 and PTPRN, the latter are strong candidates to interact with our proteins of interest in a functionally relevant manner. PTPRN2 and PTPRN are members of the protein tyrosine kinase family and are involved in the accumulation of secretory vesicles in the hippocampus, pituitary gland and pancreatic islets (Marullo, El-Sayed Moustafa & Prokopenko, 2014; Kubosaki *et al.*, 2006; Saeki *et al.*, 2002), similar tissues to those in which C2CD4A and C2CD4B are expressed. A mouse model lacking members of this family has been shown to present with mildly impaired glucose tolerance and insulin secretion deficiency (Saeki *et al.*, 2002) (in both sexes), as well as a reduction in FSH and LH secretion in females (Kubosaki *et al.*, 2006). Strikingly, similar phenotypes were also apparent in *C2cd4b* null animals.

To assess whether C2CD4A and C2CD4B interact with the latter proteins, immunoprecipitation of PTPRN2 and PTPRN with available antibodies and performing Western (immuno)blots could be performed. Furthermore, immunostaining with these antibodies in the cells transfected with FLAG-tagged *C2CD4A* and *C2CD4B* could also be performed to detect possible co-localisation of these proteins. Another possible experiment to assess whether these proteins interact is to rescue the insulin secretion deficiency caused by deletion of C2CD4A or C2CD4B by over-expression of PTPRN2 and/or PTPRN. Direct interactions might also be explored by utilising proximity ligation assays (Fredriksson *et al.*, 2002) or by

Förster resonance energy transfer (FRET) analysis (Cheng, 2006), by the generation of compatible fluorescently labelled proteins and a variety of microscopy techniques.

To assess if the deletion of C2CD4A or C2CD4B affect secretory vesicle behaviour, quantification of the vesicles in isolated islets from *C2cd4b* or *C2cd4a* null or WT animals could be performed. This could be done by using live cell imaging and following vesicles docking in different stimulated conditions. Also, EM could be used in the islets from these animals to quantify the total number of vesicles, and the number of vesicles docked at the plasma membrane in null animals compared to WTs.

Other proteins that might interact with C2CD4A are SQSTM1 and PDCD11 since they interact with NF-κB, TOR2A and EFCAB5, which bind to Ca^{2+}, and also PCSK9, NEDD4, RAP1 and GAP2, which are involved in peptide trafficking or are bound to vesicles in cells. Proteins that are likely to bind to C2CD4B include PCSK2 and CPE, which are involved in peptide trafficking and hormone secretion, and SQSTM1 which regulates the activation of NF-κB (Table 4-6).

Further functional studies are needed to prove any interaction between these suggested proteins and C2CD4A and C2CD4B.

Chapter 4: Characterisation of a *C2cd4b* null mouse

4.1. Introduction

Many GWA studies have shown that risk alleles in *VPS13C/C2CD4A/C2CD4B* locus are associated with glycaemic traits and an increased risk of T2D [65,68,71,77], (Dupuis *et al.*, 2010) . In addition, associations between the causal SNP rs7163757 at this locus and the expression of these genes at the mRNA level have been shown by Mehta *et al.* and Kycia *et al.* (Mehta *et al.*, 2016), (Kycia *et al.*, 2018).

In addition to pancreatic islets, *C2cd4b* is expressed in the pituitary gland, adipose tissue, uterus, testis, stomach and intestine (GTEx data, from The Human Protein Atlas, URL: www.proteinatlas.org/ENSG00000198535-C2CD4A/tissue, www.proteinatlas.org/ENSG00000205502-C2CD4B/tissue). Interestingly, *C2CD4A* and *C2CD4B* are expressed at different levels in different β-cell models as well as in mouse and human islets. In human islets, both genes have similar expression levels while in mouse islets comparing to *C2cd4a*, *C2cd4b* is more predominantly (by 10 fold) expressed (Table 3) (Blodgett *et al.*, 2015), (Kone *et al.*, 2014; Benner *et al.*, 2014). For this reason, we first aimed to address the role of *C2cd4b* in glucose homeostasis and insulin secretion.

In this chapter, I study the effect of the global deletion of *C2cd4b* on glucose homeostasis by characterising *C2cd4b* global null mice from IMPC. Phenotyping experiments performed by the IMPC (URL: https://www.mousephenotype.org/data/genes/MGI:1922947), showed several significantly affected characteristics in the *C2cd4b* null mouse. These include, decreased circulating triglyceride levels ($p=1.72x10^{-06}$), total body fat ($p=7.92x10^{-05}$), circulating cholesterol level ($p=6.08x10^{-07}$) as well as increased lean body mass ($p=6.57x10^{-05}$) in *C2cd4b* null males. Furthermore, decreased circulating free fatty acid level ($p=5.71x10^{-08}$) and decreased circulating low-density lipoproteins (LDL) cholesterol level ($p=9.42x10^{-05}$) were observed in either sex (Data presented from IMPC website, URL: https://www.mousephenotype.org/data/genes/MGI:1922947). However, no glucose impairment phenotype was observed performing IPGTTs on the *C2cd4b* null mice.

It should be highlighted that experiments performed by the IMPC compared the results obtained from *C2cd4b* null animals to a large data set from all WT animals

tested. For instance, to assess circulating triglyceride, 7 female, 7 male mutants were compared to 1917 female, 1956 male controls. Here, littermate controls, usually the 'gold standard' of assay, were not performed.

Here, by comparing *C2cd4b* null animals to their littermates, we study the possible impacts of deletion of this gene on glucose homeostasis. Since *C2cd4b* expression is not limited to pancreatic islets (it is also expressed in other tissues which are involved in glucose homeostasis such as adipose tissue, stomach and intestine) it was felt essential to design specific experiments to address the function of this gene in each of these tissues.

GWAS have revealed several β-cell specific phenotypes associated with variants at this locus. For instance, risk alleles at in rs17271305 and rs4502156 were associated with lower fasting proinsulin levels and at rs11071657 were associated with higher proinsulin/insulin levels (Ingelsson *et al.*, 2010), (Strawbridge *et al.*, 2011a). Furthermore, an association between variants at rs7172432 and impaired glucose-stimulated insulin release was observed by Grarup *et al.* (Grarup *et al.*, 2011). Taking into account the latter studies, in addition to a high expression of *C2cd4b* in pancreatic islets and the predicted interaction of this protein with Ca^{2+}, the focus of this chapter is in understanding the role of this gene in insulin secretion and islet biology.

4.2. Results

4.2.1. Generation of *C2cd4b* null mice

Given the substantially more abundant expression of *C2cd4b* than *C2cd4a* in mouse islets and β-cells, we first studied the possible effects of deletion of *C2cd4b* on glucose homeostasis. *C2cd4b* global knockout animals (*C2cd4b*^{em2Wtsi}), generated by the International Mouse Phenotyping Consortium (IMPC) using CRISPR/Cas9 systems, were utilised in our studies (Figure 4. 1. A). Inter-crossing of heterozygous animals resulted in wild type (WT, *C2cd4b*$^{+/+}$), heterozygous (*C2cd4b*$^{+/-}$) and null (*C2cd4b*$^{-/-}$) littermates, which were used for characterisations (Figure 4. 1. B).

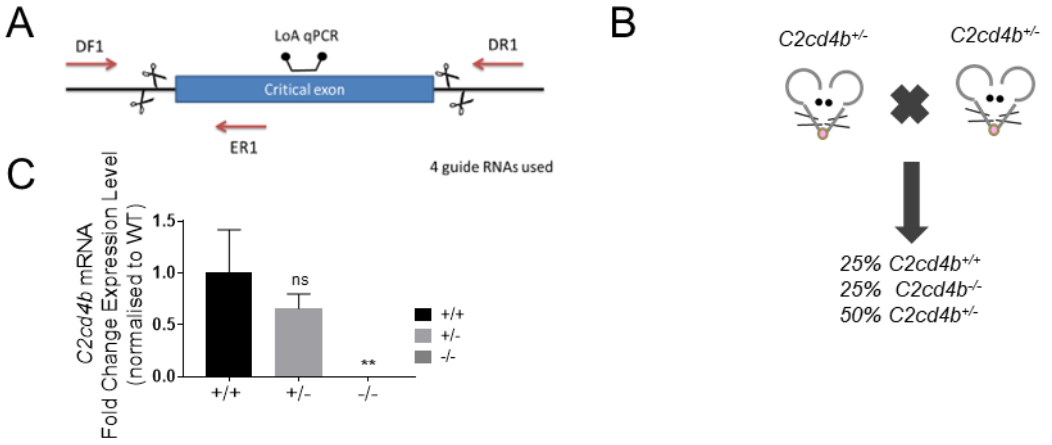

Figure 4.1. Generation of *C2cd4b* null mice. *C2cd4b* global null mice (*C2cd4b*^{em2Wtsi}) were generated by the International Mouse Phenotyping Consortium (IMPC). A. Using CRISPR/Cas9, the encoding exon from murine *C2cd4b* (exon 2) was deleted (image adopted from the IMPC website, URL: https://www.mousephenotype.org/data/genes/MGI:1922947). B. *C2cd4b*$^{+/-}$ (heterozygous) animals were setup as breeding pairs and the wild type (*C2cd4b*$^{+/+}$), heterozygous (*C2cd4b*$^{+/-}$), and homozygous (*C2cd4b*$^{-/-}$) littermates were used for characterisation. C. RT-q-PCR from isolated islets from these animals showed a significant decrease in *C2cd4b* mRNA levels in homozygous animals (p=0.0092), (*C2cd4b*$^{+/+}$ n=4, *C2cd4b*$^{+/-}$ n=3, *C2cd4b*$^{-/-}$ n=7). **p<0.01, data were assessed for significance using an unpaired Student's t-test. Values represent mean ± SEM.

4.2.2. *C2cd4b*$^{-/-}$ male mice gain more weight than WT controls on a high-fat and -sucrose diet

Both male and female *C2cd4b* null mice maintained on a regular chow diet (RC) gained weight at the same rate as their WT littermates (at 22 weeks of age, female (F), $F^{+/+}$= 24.9 ± 1.1 g *vs.* $F^{-/-}$= 24.9 ± 0.69 g, p=0.99; Male (M): $M^{+/+}$= 32.3 ± 0.90g *vs.* $M^{-/-}$= 33.12 ± 0.80g, p>0.99, mixed-effect analysis, Bonferroni's multiple comparison test) (Figure 4. 2). On the other hand, maintained on a high-fat and -sucrose diet (HFD), *C2cd4b* null male mice showed a significantly higher increase in weight gain compared to their WT littermates from 14 weeks of age (Figure 4. 2: at 21 weeks of age: $F^{+/+}$= 28.96 ± 1.38 *vs.* $F^{-/-}$= 29.11 ± 1.61 g; $M^{+/+}$= 35.10 ± 2.4 *vs*. $M^{-/-}$= 41.24 ± 1.22 g, p<0.001, mixed-effect analysis, Tukey's multiple comparison test). In addition to null animals, heterozygous *C2cd4b* male mice also showed a significant increase in weight gain from 14 weeks of age and this weight difference increased with age up to 21 weeks of age (Figure 4. 2: at 14 weeks: $M^{+/+}$= 30.56 ± 1.15 *vs*. $M^{+/-}$ = 34.2 ± 1.28, p=0.03; at 22 weeks: $M^{+/+}$= 35.06 ± 2.41 *vs.* $M^{+/-}$= 42.4 ± 1.77, p<0.0001, mixed-effect analysis, Tukey's multiple comparison test). The weight gain range from both heterozygous and homozygous *C2cd4b* male mice on HFD was comparable.

4.2.3. Male *C2cd4b*$^{-/-}$ exhibit higher fasting glycaemia than WT controls on a high-fat and -sucrose diet

No differences in fed or fasting glycaemia were apparent at 18 and 20 weeks of age respectively, between the null and WT littermates on RC (Figure 4. 3, A, B). Interestingly, on high-fat and -sucrose diet (HFD), there was a significant increase in fasting glycaemia in null male animals compared to WT littermates (Figure 4. 3, C, G): (fasting glycaemia: $M^{+/+}$=5.22 ± 0.34 *vs.* $M^{-/-}$=7.74 ± 0.48, p=0.003, unpaired Student's t-test).

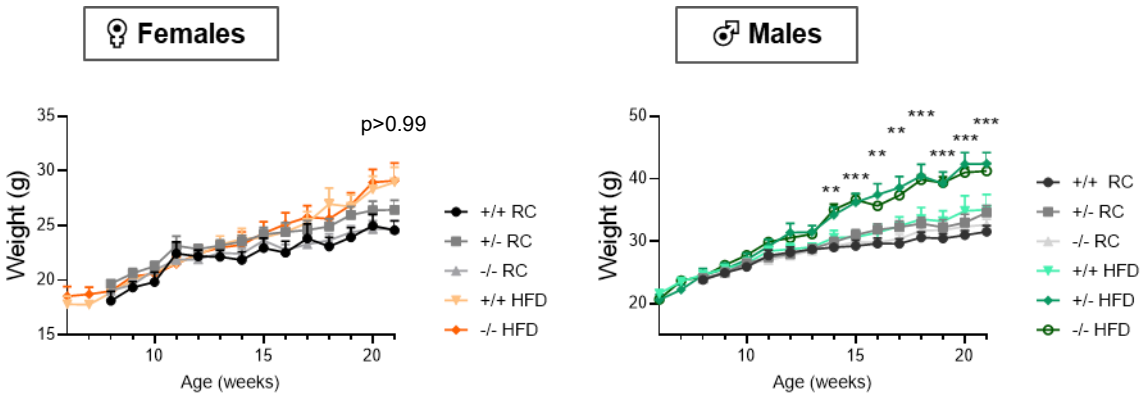

Figure 4.2. Effect of deletion of *C2cd4b* on weight gain. Changes in weight of *C2cd4b*$^{+/+}$ and *C2cd4b*$^{-/-}$ mice over time on regular chow diet (RC) or high-fat and -sucrose diet (HFD), (number of animals assessed on RC: $F^{+/+}$ n=5-6 and $F^{-/-}$ n=7-13; $M^{+/+}$ n=7-12 and $M^{-/-}$ n=10-12. HFD: $F^{+/+}$ n=10-12 and $M^{-/-}$ n=7-10; $M^{+/+}$ n=8-12 and $M^{-/-}$ n=10-12). *p<0.05, **p<0.01, ***p<0.001, the results were assessed for significance using a mixed-effect analysis, Tukey's multiple comparison test. Values represent mean ± SEM.

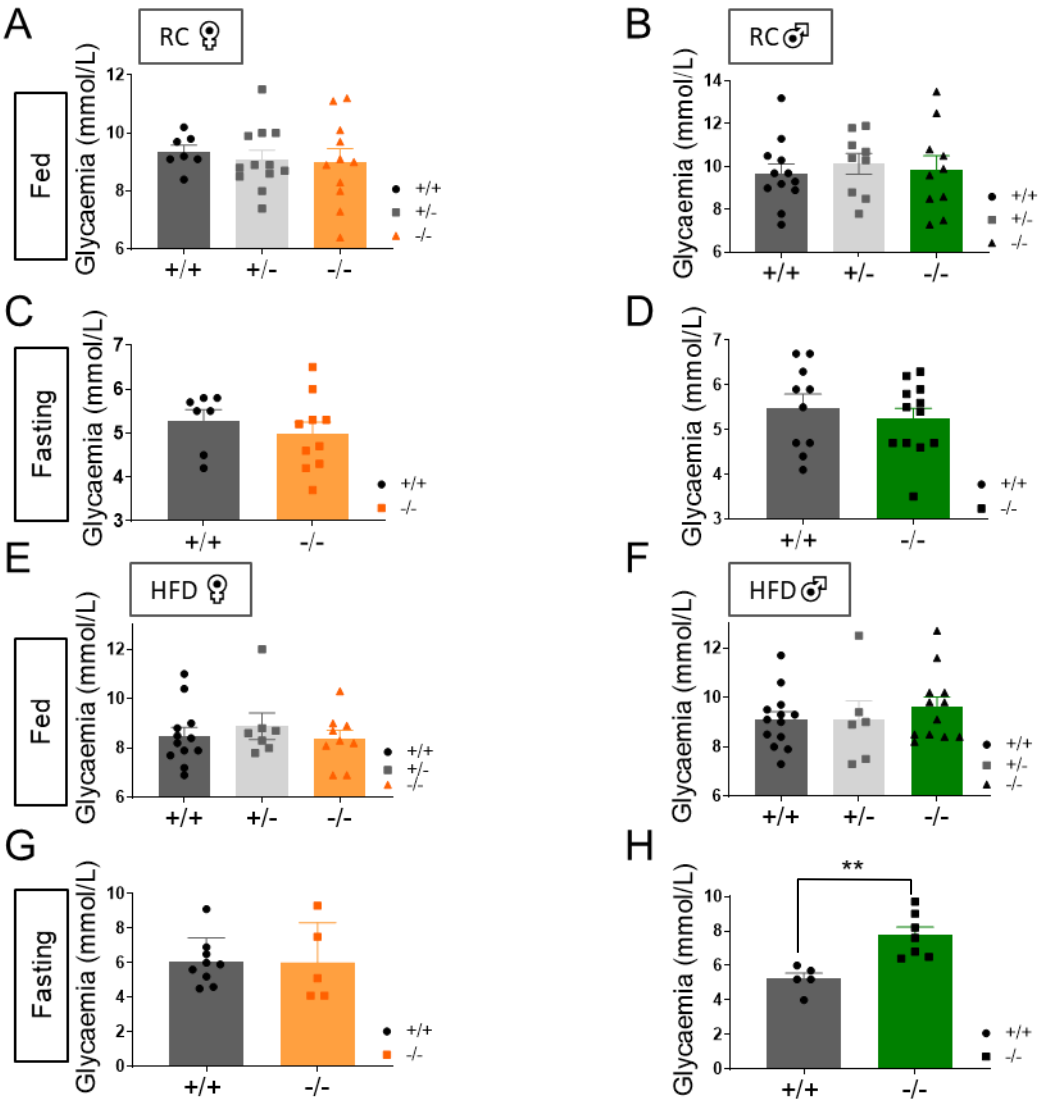

Figure 4.3. Effect of *C2cd4b* deletion on glycaemia. A-D. Fed and fasting glycaemia in *C2cd4b*$^{+/+}$ and *C2cd4b*$^{-/-}$ mice on RC, at 18 and 20 weeks of age respectively, (number of animals used for fed glycaemia, $F^{+/+}$ n=7, $F^{+/-}$ n=12, $F^{-/-}$ n=11; $M^{+/+}$ n=12, $M^{+/-}$ n=9, $M^{-/-}$ n=10; fasting glycaemia: $F^{+/+}$ n=7, $F^{-/-}$ n=10, $M^{+/+}$ n=10, $F^{-/-}$ n=12). E-H. Fed and fasting glycaemia in animals on HFD were measured at 21 and 23 weeks of age respectively (number of animals used for fed glycaemia: $F^{+/+}$ n=12, $F^{+/-}$ n=7, $F^{-/-}$ n=9; $M^{+/+}$ n=13, $M^{+/-}$ n=6, $M^{-/-}$ n=12; Fasting: $F^{+/+}$ n=9, $F^{-/-}$ n=5; $M^{+/+}$ n=5, $M^{-/-}$ n=7). Data were assessed for significance using an unpaired Student's t-test, or 2-way ANOVA where three genotypes were compared. Values represent means ± SEM.

4.2.4. Female *C2cd4b*$^{-/-}$ mice exhibit impaired glucose tolerance

To investigate the possible effects of *C2cd4b* deletion on *in vivo* glucose homeostasis, intraperitoneal glucose tolerance tests (IPGTTs) were performed on male and female *C2cd4b* mice on RC and HFD at 8, 12, 16, 20 and 22 weeks of age. After an overnight fast, a single dose of 1g of glucose per kg of body weight was injected and glycaemia was monitored over a 2-hour period.

Interestingly, on RC, female *C2cd4b*$^{-/-}$ showed a significant impairment in glucose tolerance compared to WT littermates from 12 weeks of age (Figure 4. 4; 11.2 ± 0.6 *vs.* 13.2 ± 0.8 mmol/L for WT *vs.* null mice respectively at 12-weeks of age; p= 0.003, 15 min. time point). An impairment in glucose tolerance was also apparent in female *C2cd4b*$^{-/-}$ mice at 20 and 22 weeks of age (12.9 ± 0.3 *vs*. 15.2 ± 0.9 mmol/L for WT *vs*. null mice respectively at 20 weeks of age; p=0.048, 30 min. time point; and 11.6 ± 0.9 *vs.* 15.4 ± 0.6 mmol/L for WT *vs*. null mice respectively at 22 weeks of age; p<0.001, 30 min. time point). No significant differences were observed between the WT and heterozygous null mice of either sex at any of the ages examined (Fig 4. 4). Strikingly, the glucose intolerance phenotype was sex specific and *C2cd4b*$^{-/-}$ male mice, maintained on RC diet, did not show any glucose intolerance phenotype at any measured age (from 8 to 22 weeks of age).

When homozygous null animals were challenged with HFD from 6 weeks of age, both male and female *C2cd4b*$^{-/-}$ mice exhibited glucose intolerance during IPGTTs compared to their WT littermates (Figure 4. 5). Female *C2cd4b*$^{-/-}$ mice exhibited glucose intolerance from 8 weeks of age (12.7 ± 0.6 *vs.* 15.7 ± 0.8 mmol/L for WT *vs.* null respectively; p<0.0001, 15 min. time point; 11.4 ± 0.3 *vs.* 14.4 ± 0.7 mmol/L WT *vs.* null respectively; p<0.0001, 30 min. time point). *C2cd4b*$^{-/-}$ male mice only showed glucose intolerance at 23 weeks of age (12.3 ± 0.5 *vs.* 16.8 ± 1.3 mmol/L WT *vs.* null respectively; p=0.0124, 60 min. time point; 9.3 ± 0.5 *vs*. 13.4 ± 1.8 mmol/L WT *vs.* null respectively; p=0.025, 90 min. time point).

Since male mice on HFD only exhibited glucose intolerance after the age at which null animals were significantly heavier than their WT littermates (Figure 4. 2), IPGTTs were also performed based on injecting glucose according to their lean body weight. In this way, we sought to eliminate a possible confounding effect of injecting extra glucose, based only on the presence of a metabolically less active tissue (adipose) *versus* skeletal muscle. Strikingly, when IPGTTs were performed in male *C2cd4b*$^{-/-}$

mice based on their lean body weight, there were no differences in glucose tolerance compared to their WT littermates (Figure 4. 6).

Considering *C2cd4b* is deleted globally in *C2cd4b*$^{-/-}$ animals, and gut hormones also play roles in glucose homeostasis (Holst *et al.*, 2016), oral glucose tolerance tests (OGTTs) were performed on these animals. On RC diet, no differences were observed between null animals and their WT littermates for either sex. However, both female and male null animals exhibited glucose intolerance compared to their WT littermates after maintenance on HFD (Figure 4. 7; females: 15.9 ± 0.6 *vs.* 18.7 ± 0.7 mmol/L WT *vs.* null respectively; p<0.0001, 30 min. time point; males: 15.1 ± 0.9 *vs.* 20.1 ± 0.9 mmol/L WT *vs.* null respectively; p<0.0001, 30 min. time point).

4.2.5. Unchanged insulin sensitivity in *C2cd4b*$^{-/-}$ mice

The impaired glucose tolerance observed in *C2cd4b*$^{-/-}$ mice could potentially be explained by reduced glucose clearance triggered by defective insulin signalling in insulin sensitive tissues (liver, muscle and adipose tissue) in the absence of *C2cd4b*. To investigate this possibility, insulin tolerance was examined in *C2cd4b*$^{-/-}$ *vs.* their WT littermates. For this, intraperitoneal insulin tolerance tests were performed on these mice on RC and HFD at 22 and 23 weeks of age, respectively. After 6 h of fasting, the animals were injected with insulin, and glycaemia was monitored over a one-hour period. No changes in glycaemia were observed comparing the *C2cd4b*$^{-/-}$ to their WT littermates, irrespective of sex or diet (Figure 4. 8).

4.2.6. Female *C2cd4b*$^{-/-}$ display defective insulin secretion *in vivo*

Maintained on RC, female *C2cd4b*$^{-/-}$ mice showed a significant impairment in insulin secretion *in vivo*, after injection of 3g/kg body weight of glucose (Figure 4. 9, A: plasma insulin: 0.433 ± 0.044 *vs.* 0.26 ± 0.017 ng/ml in WT *vs.* null mice respectively, at 5 min. post-injection; p=0.02; 0.557 ± 0.052 vs. 0.37 ± 0.02 ng/ml plasma insulin in WT *vs*. null mice respectively, at 15 min. post-injection; p=0.01). However, this difference was not observed in male mice (Figure 4.9, B).

In addition, on HFD, female *C2cd4b*$^{-/-}$ mice displayed unchanged insulin levels compared to their WT littermates. However, a significant elevation in glycaemia, measured at the same time points, was observed at 15 min after glucose injection (Figure 4. 9, C: glycaemia: 21.3 ± 0.39 *vs.* 28.9 ± 1.8 mmol/L WT *vs.* null mice respectively, p<0.0001). In male mouse maintained on HFD, no genotype dependent

differences were observed in plasma insulin levels or the corresponding glycaemia (Figure 4. 9, D).

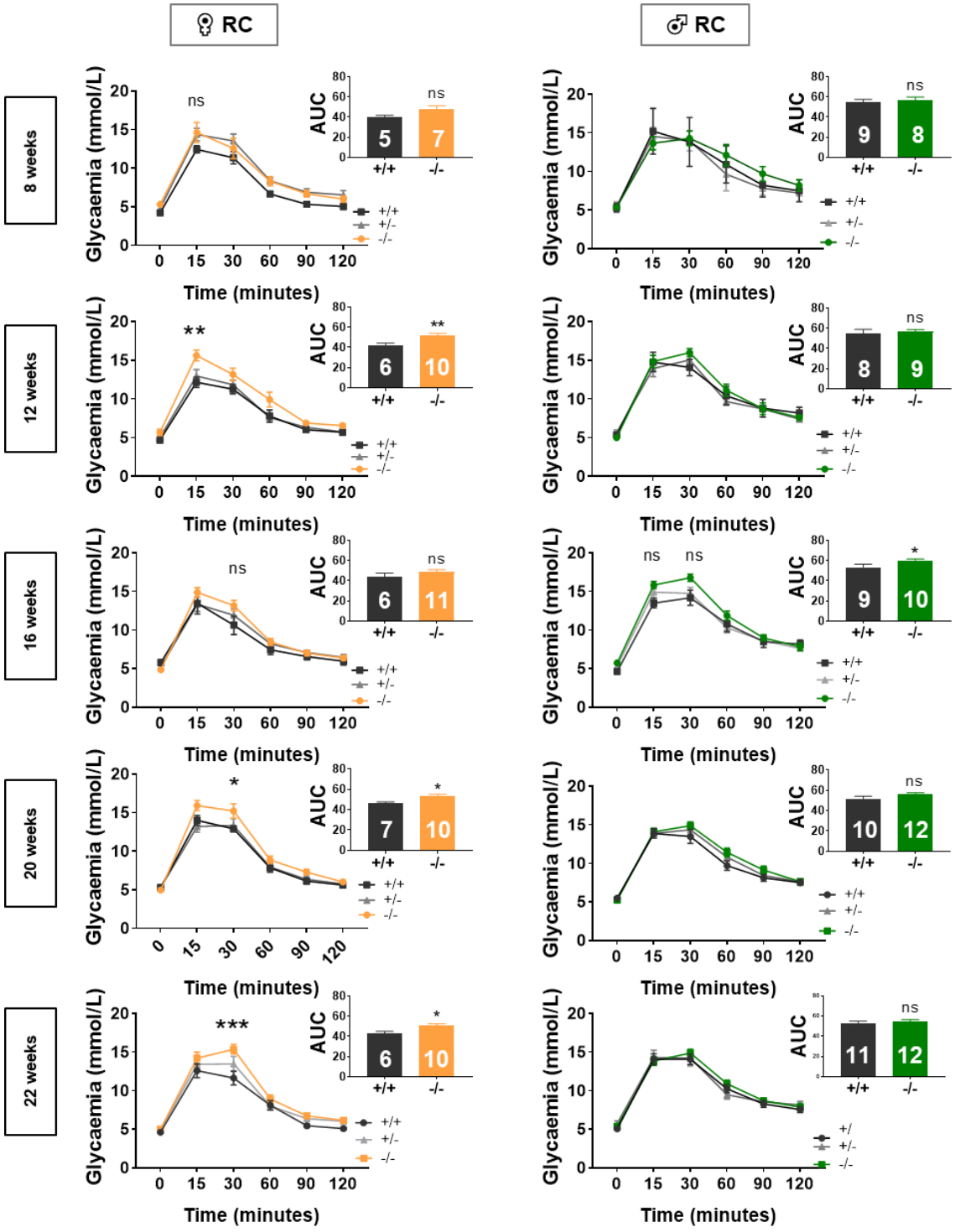

Figure 4.4. Effect of deletion of *C2cd4b* on intraperitoneal glucose tolerance in animals maintained on regular chow diet (RC). Intraperitoneal glucose tolerance tests (IPGTTs) were performed on *C2cd4b* null male and female animals on RC at 8, 12, 16, 20 and 22 weeks of age. *p<0.05, **p<0.01, ***p<0.001, data were assessed for significance using a 2-way ANOVA with Bonferroni's multiple comparison test. Inset: area under the curve (AUC) analysis; assessed for significance using an unpaired Student's t-test. Numbers in bar graphs represent the number of animals used (same number of samples used for Glycaemia and AUC graphs). Values represent means ± SEM.

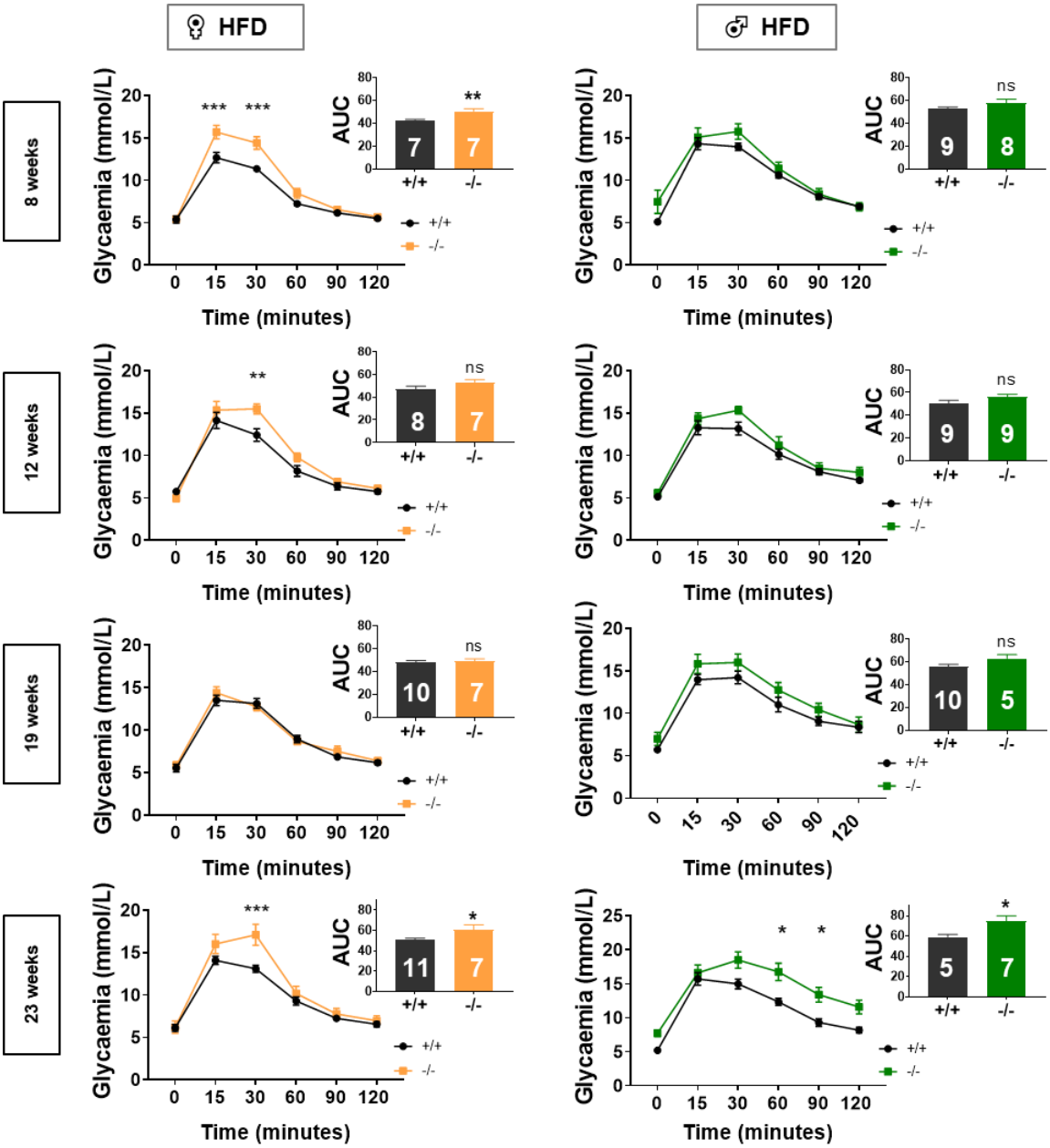

Figure 4.5. Effect of deletion of *C2cd4b* on intraperitoneal glucose tolerance in animals maintained on high-fat and -sucrose diet (HFD). Intraperitoneal glucose tolerance tests (IPGTTs) were performed on *C2cd4b* null male and female animals on HFD at 8, 12, 19 and 23 weeks of age. *p<0.05, **p<0.01, ***p<0.001, 2-way ANOVA with Bonferroni's multiple comparison test. Inset: area under the curve (AUC) analysis; data were assessed for significance using an unpaired Student's t-test. Numbers in bar graphs represent the number of animals used (same number of samples used for Glycaemia and AUC graphs). Values represent means ± SEM.

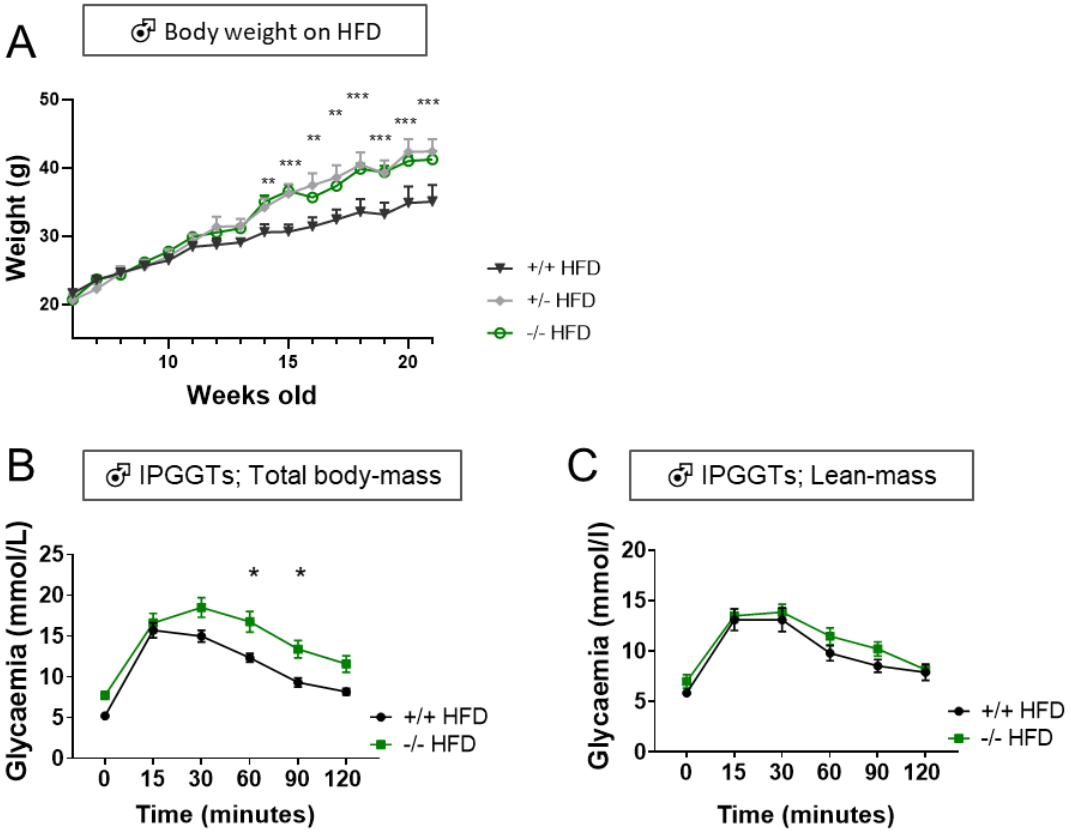

Figure 4.6. IPGTTs on *C2cd4b* male mice based on lean body weight. A. *C2cd4b* male mice weight gain on HFD. B. IPGTTs of *C2cd4b* male mice on HFD at 23 weeks of age. A-B from Figures 4.2 and 4.5. C. Intraperitoneal glucose tolerance tests (IPGTTs) were performed on *C2cd4b* male mice at 23 weeks of age based on glucose injection according to their lean body weight (n=8/genotype). *p<0.05, **p<0.01, ***p<0.001, data were assessed for significance using a 2-way ANOVA with Bonferroni's multiple comparison test. Values represent means ± SEM.

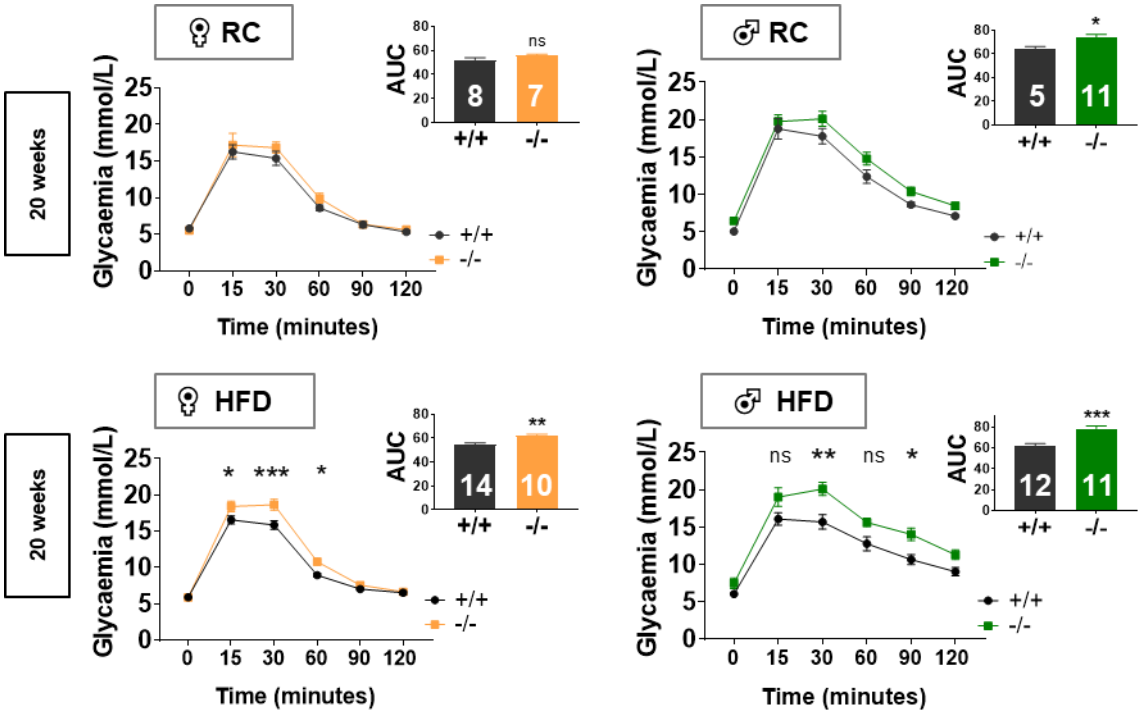

Figure 4.7. Effect of deletion of *C2cd4b* on oral glucose tolerance. Oral glucose tolerance tests (OGTTs) were performed on *C2cd4b* male and female animals maintained on RC and HFD at 20 weeks of age. *p<0.05, **p<0.01, ***p<0.001, data were assessed by 2-way ANOVA with Bonferroni's multiple comparison test. Inset: area under the curve (AUC) analysis; data assessed for significance using an unpaired Student's t-test. Numbers in bar graphs represent the number of animals used (same number of samples used for each Glycaemia and AUC graphs). Values represent means ± SEM.

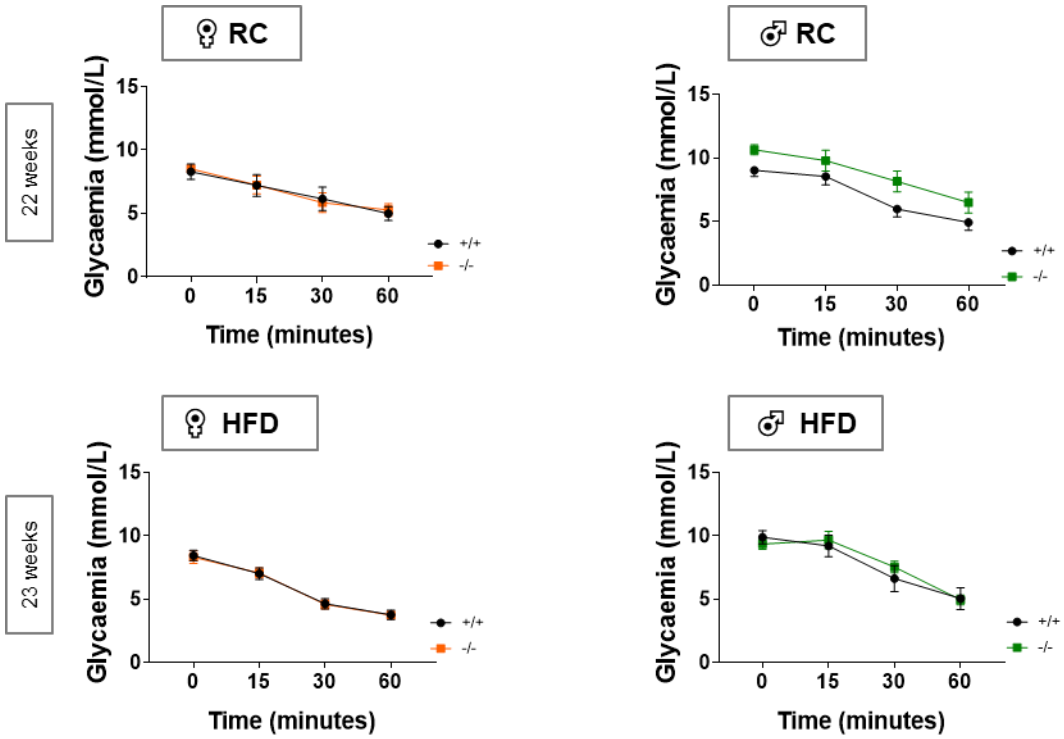

Figure 4.8. Effect of deletion of *C2cd4b* on insulin sensitivity. *C2cd4b* null and WT male ($M^{+/+}$ n=9, $M^{-/-}$ n=13) and female ($F^{+/+}$ n=6, $F^{-/-}$ n=9) mice on RC were injected with a 1 and 0.75 Unit/kg body weight dose of insulin respectively. On HFD, *C2cd4b* null and WT male (n= 8/genotype) and female ($F^{+/+}$ n=11, $F^{-/-}$ n=7) mice were injected with 1.5 and 0.75 Unit/kg body weight dose of insulin. Glycaemia was monitored over a one-hour period. Deletion of *C2cd4b* had no effect on insulin sensitivity in either sex or on either RC or HFD. Data were assessed for significance using a 2-way ANOVA with Bonferroni's multiple comparison test. Values represent mean ± SEM.

4.2.7. Unchanged proinsulin levels in *C2cd4b*$^{-/-}$ mice

We next assessed if the reduction in plasma insulin levels may be due to impaired proinsulin processing or metabolism. Blood samples were collected from *C2cd4b* mice after 5 h of fasting and insulin and proinsulin levels were measured (Figure 4. 11). The results revealed no significant differences in insulin/proinsulin levels comparing *C2cd4b* null mice to their WT littermates of either sex on RC or HFD.

4.2.8. Unchanged secretory dynamics in isolated islets from *C2cd4b*$^{-/-}$ mice

To investigate if the impairment in plasma insulin levels observed in *C2cd4b*$^{-/-}$ female mice was directly caused by defective insulin secretion from pancreatic islets, GSIS was assessed *in vitro*. For this, isolated islets from these animals of both sexes

maintained on either RC or HFD, at 24 weeks of age, were studied. Islets isolated from *C2cd4b*$^{-/-}$ mice maintained on RC demonstrated no differences in insulin secretion in response to 17 mM glucose or 20 mM KCl *vs.* WT littermates (Figure 4. 12). However, *C2cd4b*$^{-/-}$ female mice maintained on HFD, showed a significant potentiation of secretion stimulated by 17 mM glucose. On the other hand, stimulated Ca^{2+} dynamics and intercellular connectivity were unchanged in islets from female null *versus* WT mice (Figure 4. 10).

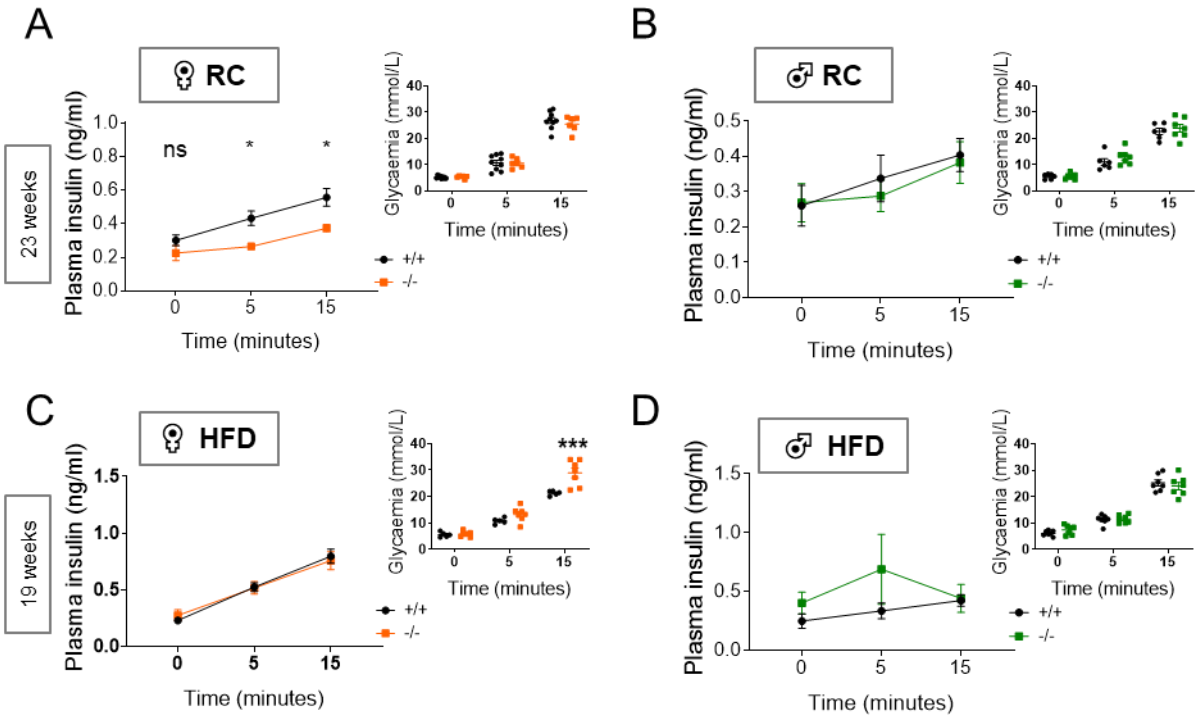

Figure 4.9. Effect of deletion of *C2cd4b* on plasma insulin levels. *In vivo* insulin levels during IPGTT in *C2cd4b* mice on RC (A-B) and HFD (C-D). (RC: $F^{+/+}$ n=9, $F^{-/-}$ n=6, $M^{+/+}$ n=7, $M^{-/-}$ n=8; HFD: $F^{+/+}$ n=5 $F^{-/-}$ n=7, M n= 6). * p<0.05, **p<0.01, ***p<0.001, data were assessed for significance using a 2-way ANOVA with Bonferroni's multiple comparison test. Values represent mean ± SEM.

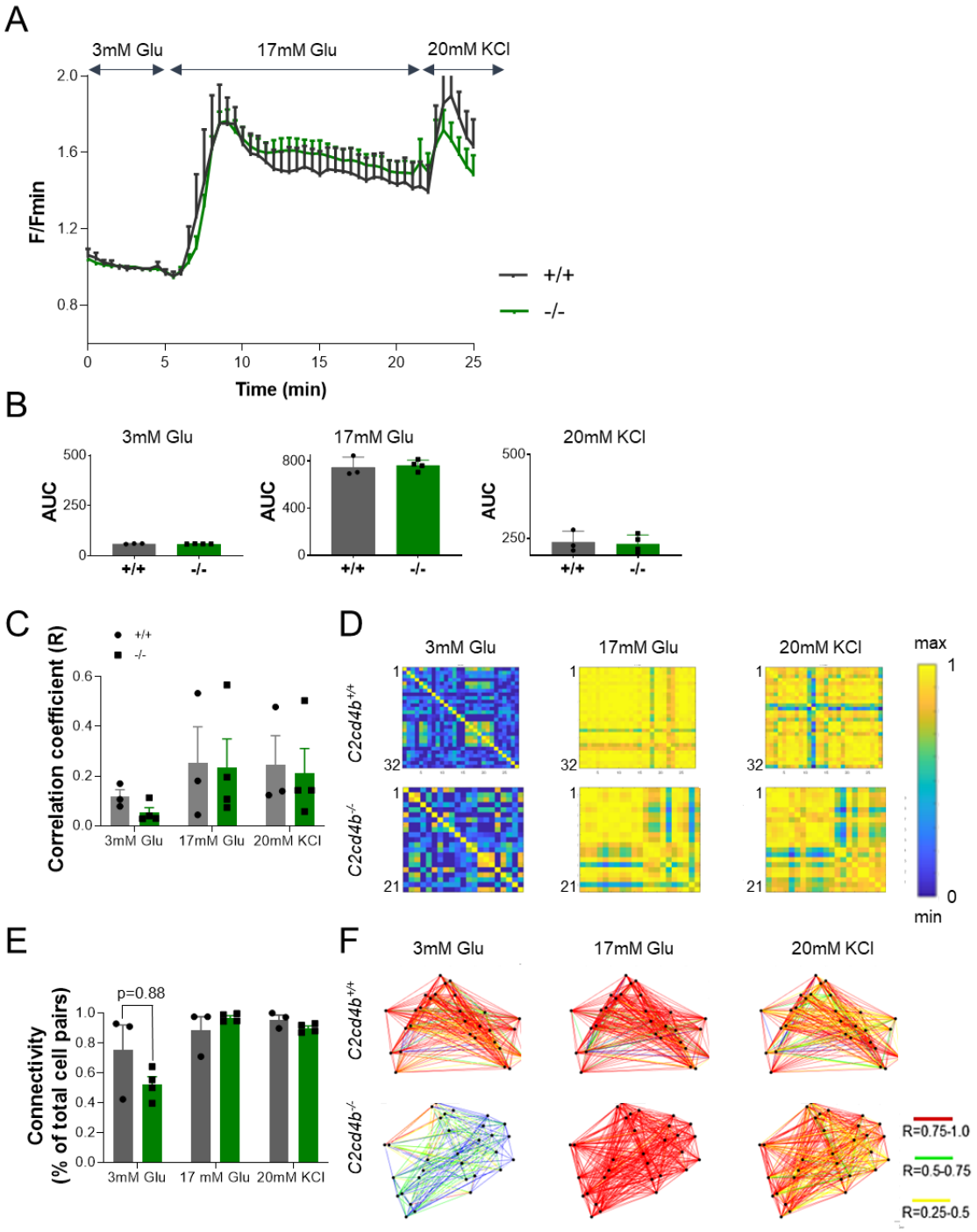

Figure 4. 10. Effect of deletion of *C2cd4b* on Ca^{2+} dynamics in isolated islets. Intracellular Ca^{2+} dynamics were assessed in isolated islets from females at 24 weeks of age maintained on RC, using spinning disk microscopy. A-B. No changes were observed in 17 mM glucose- or 20mM KCl-stimulated Ca^{2+} dynamics between *C2cd4b* null and WT ($F^{+/+}$ n=3 and $F^{-/-}$ n=4 per experiments, two acquisitions were performed in each experiment and between 8-12 islets were assessed in each acquisition; assessed for significance using an unpaired Student's t-test). C-F. No significant changes in β-cell connectivity and in the correlation coefficient was observed between the null and WT islets (three islets assessed in duplicate for each genotype; data were assessed for significance using a 2-way ANOVA with Bonferroni's multiple comparison test. Values represent mean ± SEM.

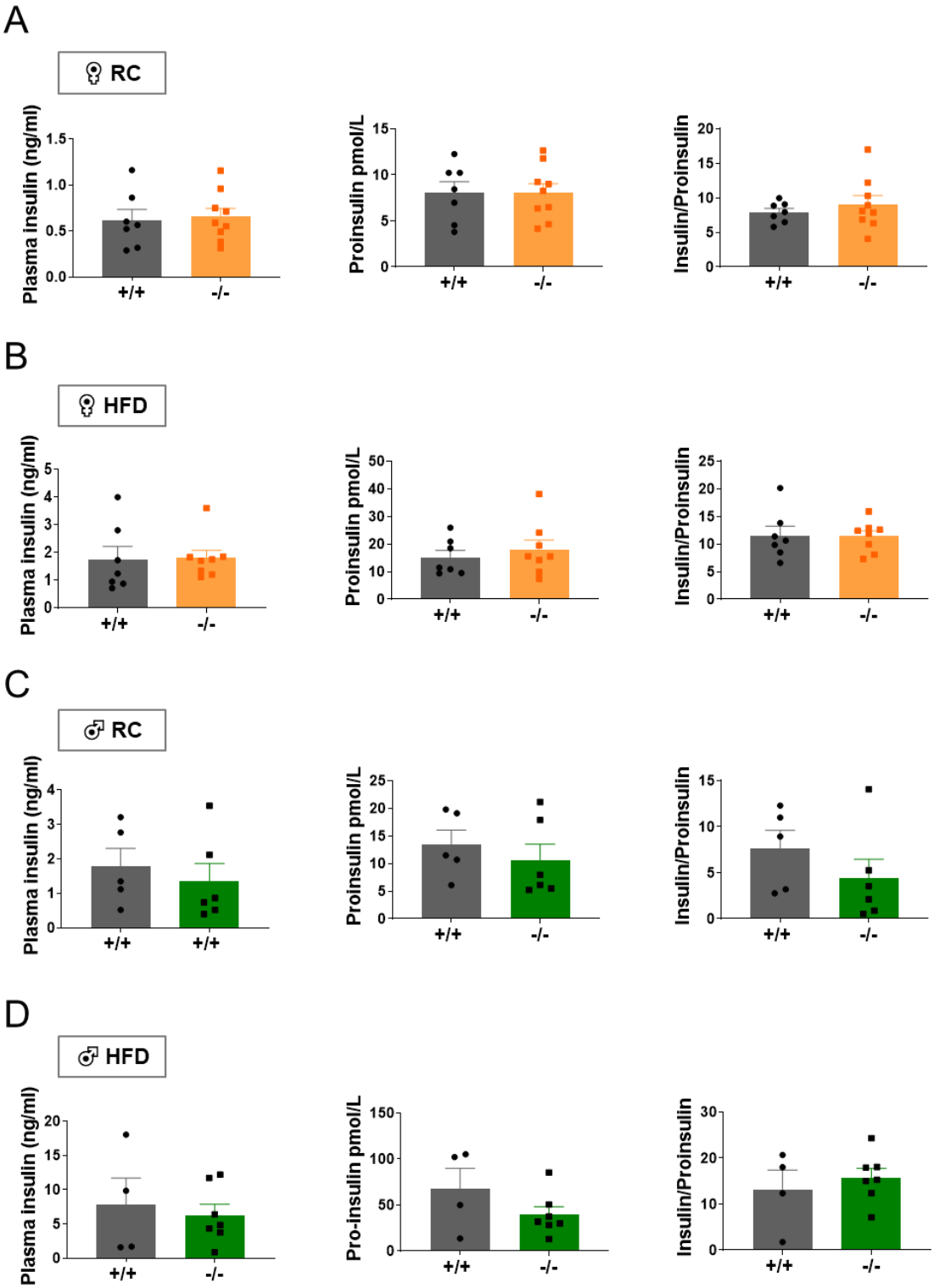

Figure 4.11. Effect of deletion of *C2cd4b* on fasting proinsulin levels. Plasma insulin and proinsulin levels were measured in *C2cd4b* null and their WT littermates on RC (A, C) and on HFD (B-D), in females (A-B) and males (C-D). (RC: $F^{+/+}$ n=7, -/- n=9; $M^{+/+}$ n=5, $M^{-/-}$ n=6; HFD: $F^{+/+}$ n=7, $F^{-/-}$ n=8, $M^{+/+}$ n=4, $M^{-/-}$ n=7). Data were assessed for significance using an unpaired Student's t-test. Values represent mean ± SEM.

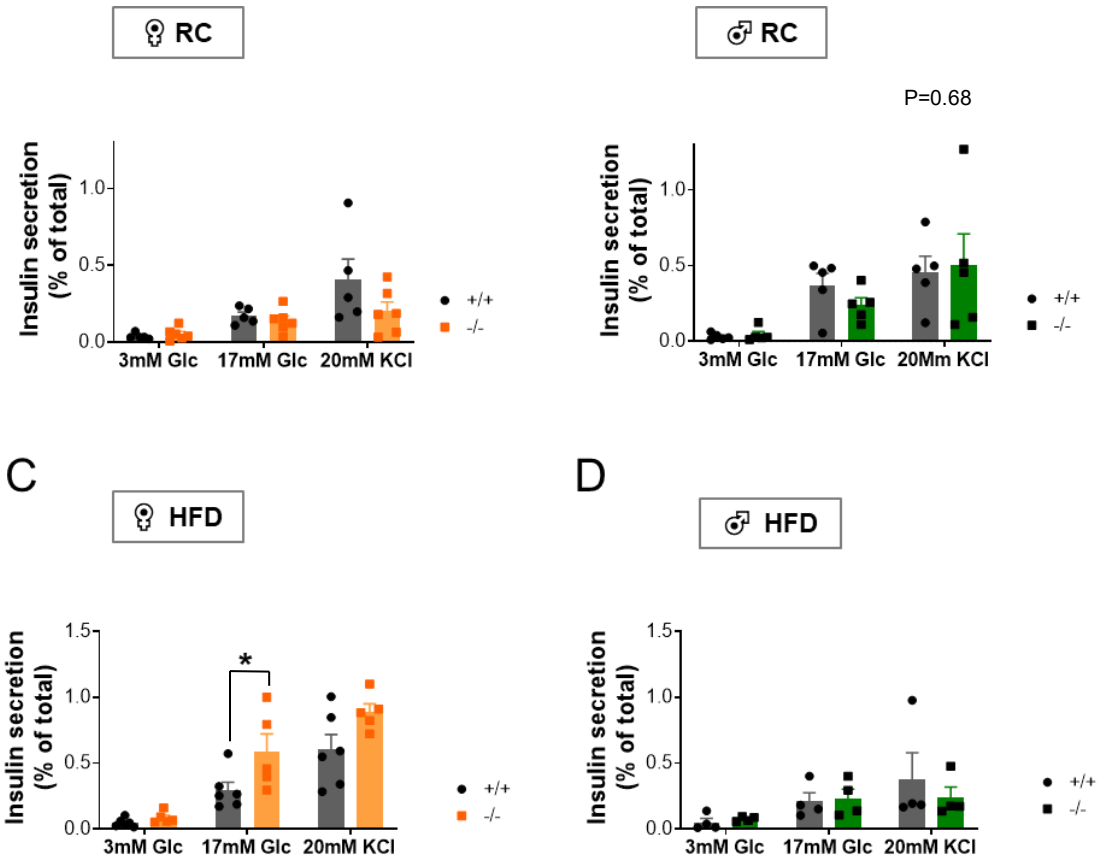

Figure 4.12. Effect of deletion of *C2cd4b* on glucose or KCl-stimulated insulin secretion from isolated islets. Insulin secretion was measured in isolated islets from *C2cd4b* mice maintained on RC (A-B) or HFD (C-D) at 24 weeks of age. (RC: $F^{+/+}$ n=5, $F^{-/-}$ n=6, M n=5/genotype; HFD: $F^{+/+}$ n=6 $F^{-/-}$ n=5, M n=4/genotype). * p<0.05, **p<0.01, ***p<0.001, 2-way ANOVA with Bonferroni's multiple comparison test. Values represent mean ± SEM.

4.2.9. Female *C2cd4b*$^{-/-}$ display impaired follicle-stimulating hormone secretion

Given the high expression levels of both *C2cd4b* and *C2cd4a* in the pituitary gland (Figure 1. 8), and the sexual dimorphism in glucose tolerance impairment observed in *C2cd4b*$^{-/-}$ mice, we assessed if deletion of *C2cd4b* might affect the secretion of pituitary sex hormones causing this gender-specific differences in glucose tolerance. The anterior pituitary gland secretes different hormones including follicle-stimulating hormone (FSH) and luteinizing hormone (LH) from gonadotropin cells, which then affect the gonads (Richards JS and Pangas SA, 2010; Whirledge & Cidlowski, 2010). These hormones are essential for reproduction. In the testis, luteinizing hormone (LH) induces testosterone production. In females, follicle-stimulating hormone (FSH) controls oestradiol hormone (E2) production and LH controls oocyte maturation, ovulation, and follicular luteinisation. Both testosterone and oestradiol levels can control the secretion of FSH and LH as well (Richards JS and Pangas SA, 2010; Whirledge & Cidlowski, 2010).

To measure FSH and LH production levels directly in the pituitary gland, and to remove the feedback loops from the ovary and testis which may affect FSH and LH secretion, *C2cd4b* mice were gonadectomised at 12 weeks of age (collaboration with Dr Bryn Owen). Blood samples were taken from these animals after injections of saline solution (Vehicle) and E2 in females, or saline (Vehicle) and testosterone in males. This was followed by measurement of circulating FSH and LH levels in the blood. Interestingly, the results indicated that FSH production from the pituitary gland is impaired in *C2cd4b*$^{-/-}$ female mice (Figure 4. 13). In contrast, FSH and LH levels in male mice remained unchanged.

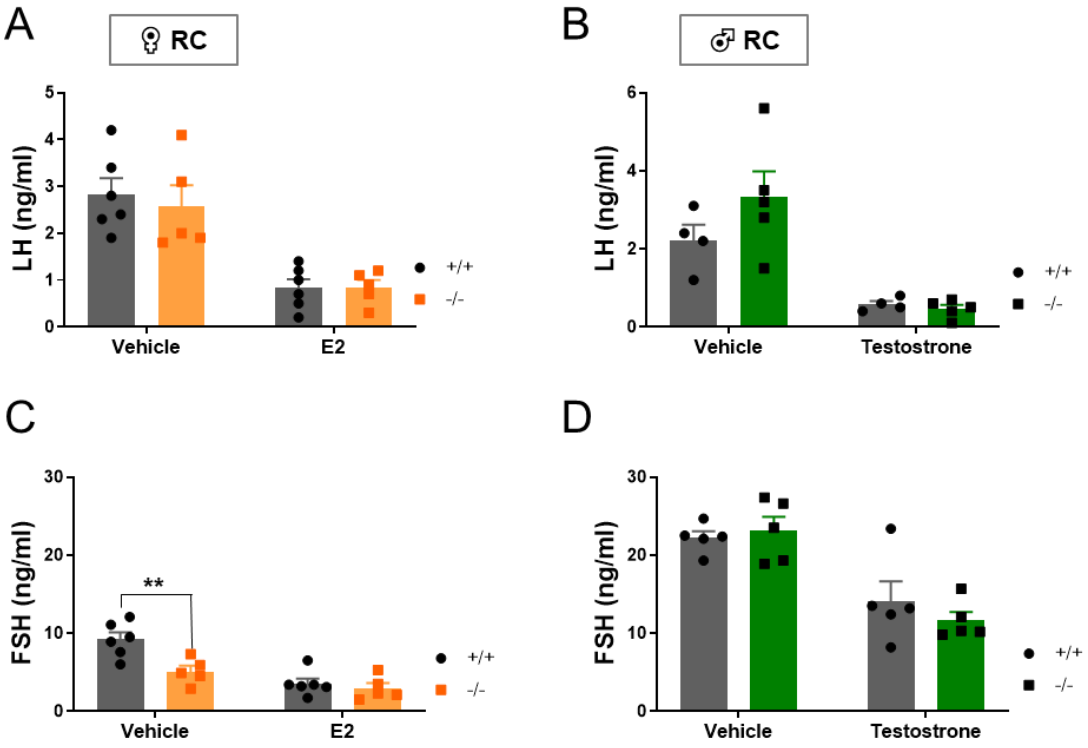

Figure 4.13. Effect of deletion of *C2cd4b* on FSH and LH release from the pituitary gland. A-B. LH levels in *C2cd4b* female and male mice after injections with saline (vehicle), E2 or testosterone respectively. C-D. FSH levels in *C2cd4b* female and male mice after injections with saline (vehicle) and E2 and testosterone respectively. Assessed for significance using an unpaired Student's t-test. n=5 mice/genotype. Values represent mean ± SEM.

4.2.10. Unchanged β-cell mass after deletion of *C2cd4b*

To assess if the reduction in plasma insulin levels in *C2cd4b* null mice was the result of a reduction in β-cell mass, β- and α-cell mass were measured in pancreatic sections from the isolated organ from *C2cd4b* null and WT mice of both sexes maintained on RC. Immunohistochemistry was performed with anti-insulin and anti-glucagon antibodies to detect β-cells and α-cells, respectively. The area stained with these antibodies was quantified to provide an assessment of the volume of these cells. No significant differences were observed in β-cell and α-cell mass comparing *C2cd4b* null mice to their WT littermates (Figures 4. 14 and 4. 15).

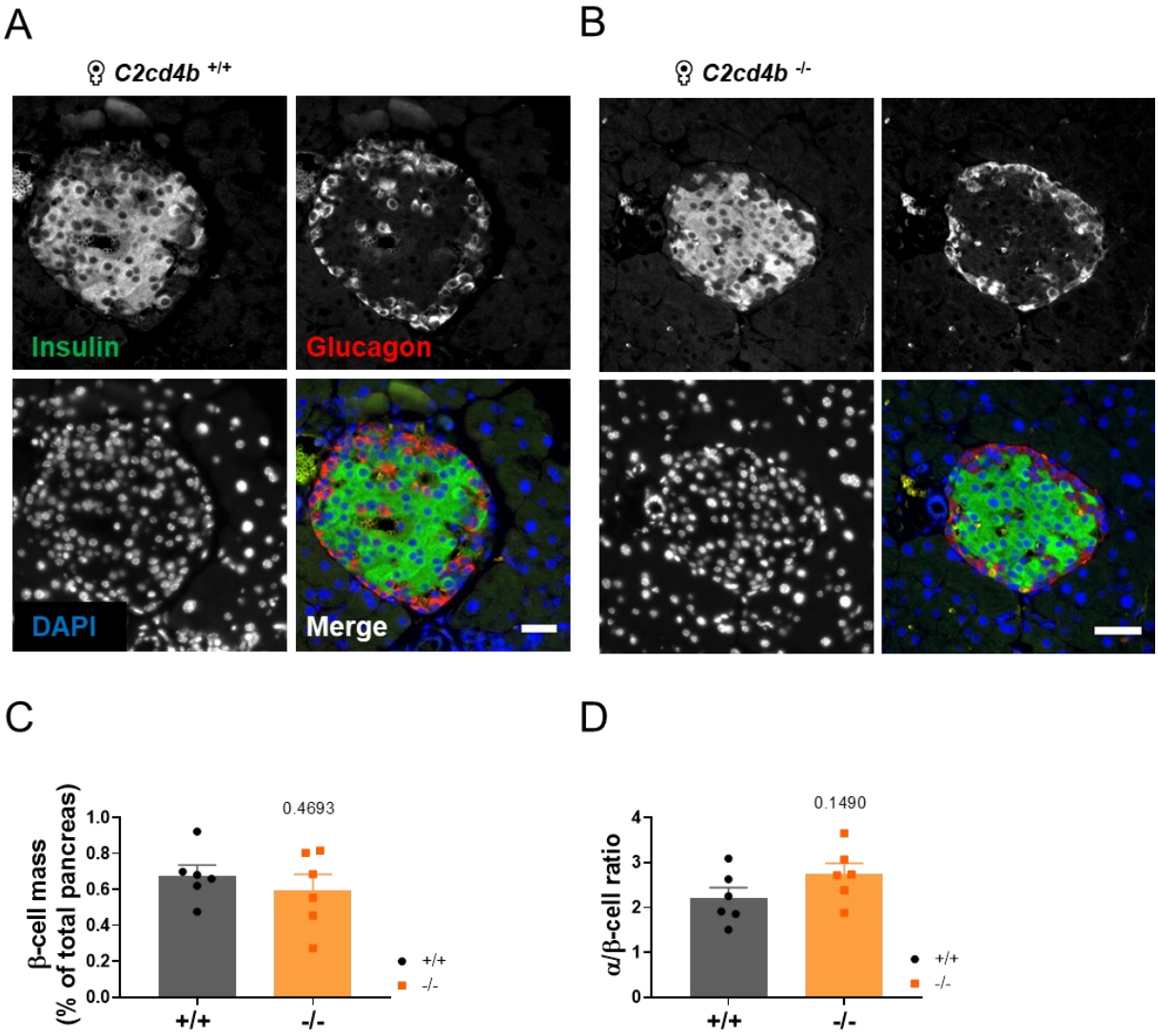

Figure 4. 14. β-cell mass in *C2cd4b* null female mice. Data were collected from dissected pancreas from six female mice per genotype at 24 weeks of age. For quantifications, three slides per animals were used. A-B. Immunohistochemistry was performed on slide sections with anti-insulin (shown in green), anti-glucagon (shown in red) antibodies, and DAPI (shown in blue). Scale bars= 30 µm. C-D. Area stained with insulin or glucagon antibodies were quantified to represent β-cell and α-cell mass, respectively, using ImageJ software. Assessed for significance using an unpaired Student's t-test. Values represent mean ± SEM.

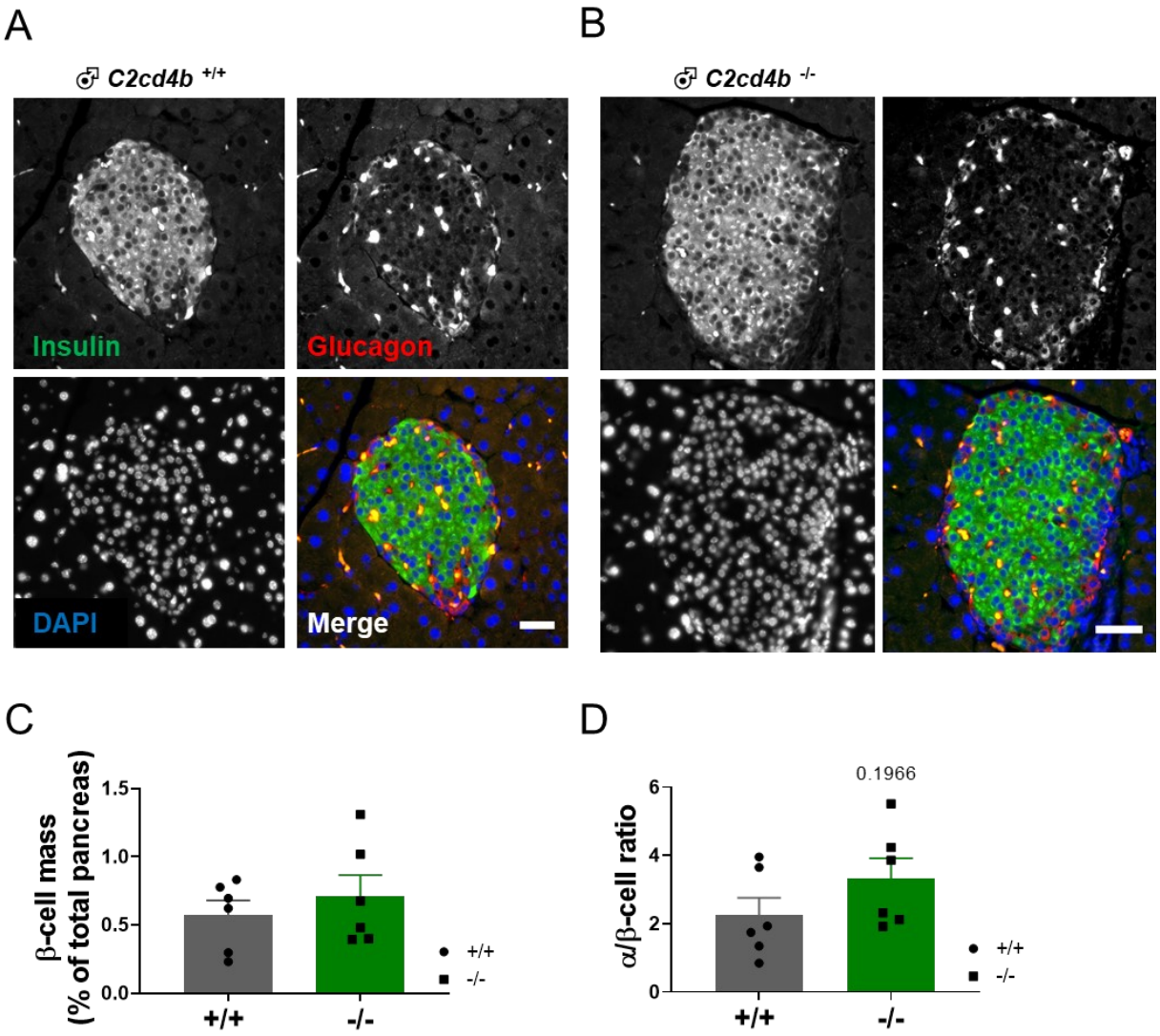

Figure 4. 15. β-cell mass in *C2cd4b* null male mice. Data were collected from dissected pancreas from six male mice per genotype at 24 weeks of age. For quantifications, two slides per animals were used. A-B. Immunohistochemistry was performed on slide sections with anti-insulin (shown in green), anti-glucagon (shown in red) antibodies, and DAPI (shown in blue). Scale bars= 30 µm. C-D. Area stained with insulin or glucagon antibodies were quantified to represent β-cell and α-cell mass, respectively, using ImageJ software. Cells appears in yellow show auto-fluorescence in blood vessels. Assessed for significance using an unpaired Student's t-test. Values represent mean ± SEM.

4.2.11. Changes in islet gene expression after deletion of *C2cd4b*

To study the possible effect of deletion of *C2cd4b* on gene regulation, we performed massive parallel sequencing (RNA-seq; Table 7) on isolated islets from *C2cd4b* null and WT male mice at 22 weeks of age (in collaboration with Dr Aida Martinez-Sanchez and Grazia Pizza). As expected, our results confirmed a significant reduction in *C2cd4b* expression (fold change=0.187, p<0.0001, adjusted p-value: p<0.0001, n=4 animals/genotype). Interestingly, our data also indicated a significant and large increase in *C2cd4a* expression levels (fold change 1.76, p<0.0001, adjusted p-value=0.04). Strikingly, the adjusted p-value was not significant for any other gene. However, a tendency towards decreased *Cpsf1, C3* and *RppL1* levels was observed, adjusted p-values= 0.06, 0.2, and 0.32, respectively. To assess if the changes in mRNA levels of these genes did not reach significance as a result of small sample sizes, RT-q-PCRs were performed on isolated islets from 10 WT and 8 *C2cd4b* null mice. The results revealed no significant differences in the expression levels of *Cpsf1 or RppL1* in the isolated islets from *C2cd4b* null mice compared to their WT littermates (Figure 4. 16).

Gene.name	baseMean	log2FoldChange	FoldChange	p value	Adjusted p value
C2cd4b	1139.51706	-2.415152232	0.187485089	1.36E-44	3.81E-40
C2cd4a	118.027192	0.814689614	1.758919692	2.86E-06	0.040127223
Cpsf1	1904.77052	-0.578923095	0.669463314	7.06E-06	0.066105298
C3	152.141699	0.741957418	1.672443436	3.45E-05	0.241943108
Rpph1	140.612162	-0.703996659	0.613869264	5.77E-05	0.323789867
Gm45322	417.49085	0.620112657	1.536995197	0.00011	0.504901364
mt-Nd4l	3597.92578	0.680785322	1.603012107	0.000126	0.504901364
Emid1	454.688167	-0.607583874	0.656294899	0.000149	0.524402308
Crb1	108.03916	-0.647844838	0.638233023	0.000268	0.766730644
Gm10076	52.4812133	-0.547066149	0.684410525	0.000273	0.766730644

Table 7. Effect of *C2cd4b* deletion on islet gene expression. The gene expression levels from isolated islets of four male mice per genotype were assessed by RNA-seq. Table presents gene expressions from high to low adjusted p values. The top ten genes with the highest adjusted p-values were selected in the above table. The top two genes are those with significant adjusted p-values. The fold change compares the expression levels in KO animals compared to the WT controls. A significant reduction in *C2cd4b* expression levels was observed comparing islets from *C2cd4b* WT to null mice. *C2cd4a* expression was increased in *C2cd4b* null mice. Highlighted in green are the genes selected for further RNA level measurements using RT-q-PCR (Figure 4. 16).

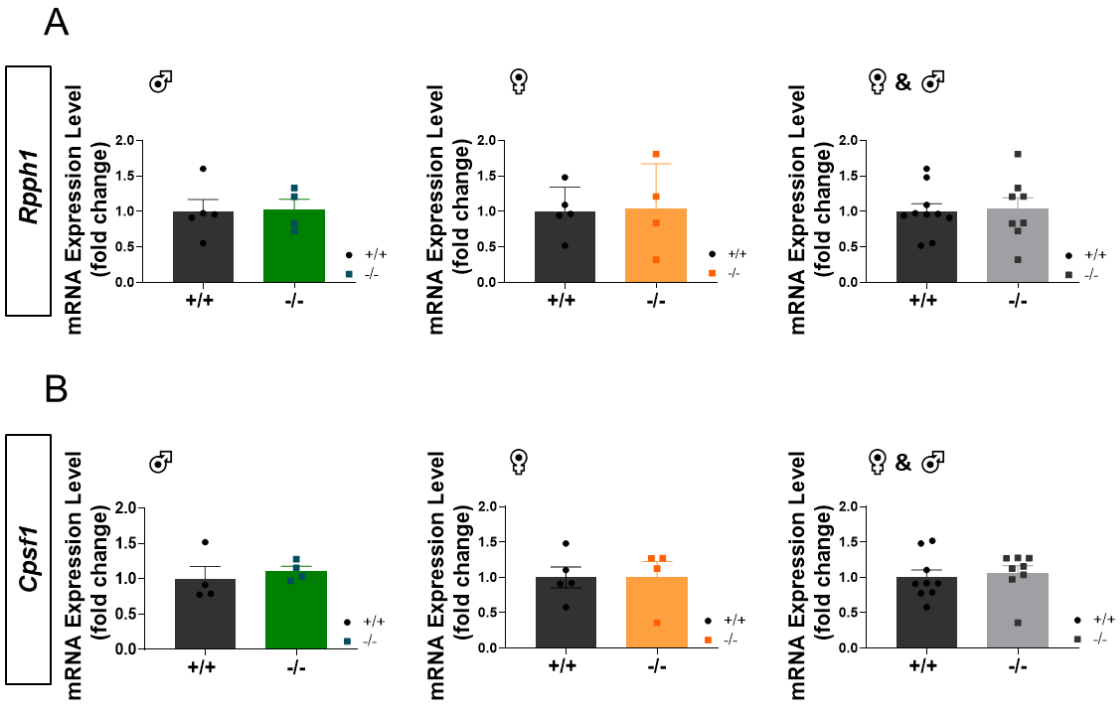

Figure 4.16. *Rpph1* and *Cpsf1* mRNA levels in *C2cd4b* null and WT mice. A. RT-q-PCR shows *Rpph1* mRNA levels in the isolated islets from *C2cd4b* null and WT mice ($F^{+/+}$ n=5, $F^{-/-}$ n=4, $M^{+/+}$ n=5, $M^{-/-}$ n=4). B. RT-q-PCR shows *Cpsf1* mRNA levels in the isolated islets from *C2cd4b* null and WT mice ($F^{+/+}$ n=5, $F^{-/-}$ n=4, $M^{+/+}$ n=5, $M^{-/-}$ n=4). Data were assessed for significance using an unpaired Student's t-test. Values represent mean ± SEM.

4.3. Discussion

It is crucial to understand the role of GWAS-discovered genes associated with T2D to uncover the identity of the key players involved in insulin secretion and in glucose homeostasis. Discovering the mechanism of action of these genes may provide more insight into molecular aspects of T2D, which will result in improvements in targeting this condition in individual patients (personalised medicine). Although knowing the molecular mechanism is not essential to produce drug for a specific disease, it can significantly narrow down the targets and increase the efficiency of the disease targeting. *C2CD4B,* as a T2D-associated gene, could potentially open new possibilities in targeting T2D more effectively.

The aim of this chapter was to characterise the effect of deletion of *C2cd4b in vivo* on glucose homeostasis and insulin secretion. For this reason, we used a total body null *C2cd4b* mouse line, generated by the IMPC. Although the IMPC has performed several studies on this line, including IPGTTs and measuring plasma insulin, a more in-depth characterisation of the *C2cd4b* null mice, studying glycaemic traits in these animals and comparing the result directly to their WT littermates remained to be performed.

4.3.1. *Male C2cd4b* null mice show increased weight gain *versus* WT

It has been shown that, along with other factors, being overweight and consuming a diet with low fibre and high *trans* fatty acid intake increases the risk of T2D (Parillo & Riccardi, 2004). To assess if Western diet compositions (high-fat and -sugar) might affect glucose homeostasis in *C2cd4b* mice, we challenged the animals with a high-fat and -sucrose diet (HFD) from 6 weeks of age. Previous studies have shown that WT C57BL/6J mice are susceptible to high-fat diets (Montgomery *et al.*, 2013). Maintained on such diets, the WT C57BL/6J mice display elevated body weight, increased adipose tissue mass, liver lipid infiltration and other alterations. Interestingly, however, HFD affects the weight gain in a sexually dimorphic manner (Montgomery *et al.*, 2013; Ingvorsen, Karp & Lelliott, 2017). It has been shown that the weight gain caused by HFD is more apparent in males (Montgomery *et al.*, 2013; Ingvorsen, Karp & Lelliott, 2017).

As expected, the weight gain of female mice maintained on HFD was not as apparent as males. In the present study we revealed that *C2cd4b* null males gain significantly

more weight compared to their WT littermates. Interestingly, also in humans, in a non-diabetic Danish population (Boesgaard *et al.*, 2010), GWAS have shown a correlation between risk allele at rs7172432 in this locus and increased (0.6 cm) waist circumference in both males and females. This shows that the effect of the risk allele of this locus in humans is comparable with the phenotype observed in *C2cd4b* null mice, suggesting further investigations, exploring the reason behind this phenotype in mice, could give us a better perspective to understand the reason behind the phenotype observed in humans. It needs to be considered, however, that association between the SNPs in *C2CD4A/C2CD4B/VPS13C* locus and BMI has not been observed in other GWAS studies while it is a strong phenotype in mice. This could be the result of the complete deletion of this gene in mice while in humans, the GWAS studies are based of SNPs in enhancer/promoter regions. This fact might indicate that the SNPs in human are not located in the open chromatin region in pituitary or adipose tissues, while in islets, they are located on the enhancer/promotor region of *C2CD4B*. The same concept could be true for observed changes in FSH levels in female mice compared to no phenotype in human.

Increases in body weight occur when energy intake is higher than energy expenditure (Morton *et al.*, 2006). This balance is affected by food intake or changes in basal metabolism, physical activity or thermogenesis (Rosen & Spiegelman, 2006). *C2cd4b*, at least in humans, is expressed in the hypothalamus and adipose tissues. It is known that the cross-talk between these tissues can significantly affect food intake. For example, the secretion of leptin from adipose tissue has a powerful anorectic effect, mainly mediated by the hypothalamus (Zhang, Cline & Gilbert, 2014). Furthermore, an interesting reason behind the observed elevated weight gain in male mice comparing to females, could be the fact that male mice have less POMC neurons in the hypothalamus compared to females (Mauvais-Jarvis, 2015). This causes the males to be less prone to the appetite-controlling signals emerging from adipose tissue and, therefore, they have less appetite control upon an increase in adipose tissue mass. However, the same effect has not yet been studied in humans.

In addition, bearing in mind that *C2cd4b* is expressed in the hypothalamus, our result may suggest that *C2cd4b* has a role in appetite control. However, whether the increased body weight in *C2cd4b* null males is due to an increase in food intake, slower body metabolism, or to less physical activity in these animals is unclear and will need to be investigated further. To investigate the reason behind this weight gain,

a Columbus Instruments Comprehensive Lab Animal Monitoring System (CLAMS), a system with metabolic cages, could be used for this purpose. In this method, animals are individually caged and numerous metabolic factors including food consumption and locomotor activity levels are measured. These cages can also provide an accurate measurement of food intake in male mice maintained on HFD.

To assess if a possible increase in food intake were due to impaired leptin secretion from adipose tissue, circulating leptin could be measured from plasma of these animals. Another possibility underlying an increase in food intake could be impaired communication between leptin and POMC neurons. To answer this, a comparison of the number of POMC neurons between the *C2cd4b* null and their WT littermates could be performed.

4.3.2. Impaired glycaemic profile in *C2cd4b* null mice *versus* WT

Female *C2cd4b* null mice maintained on regular chow diet showed impaired glucose tolerance when assessed by IPGTTs but not OGTTs. The former result demonstrates an important role for *C2cd4b* in glucose metabolism, which appears to be due to altered circulating insulin. However, since OGTTs did not reveal any effect on glucose tolerance, this rules out a role of *C2cd4b* in regulating the secretion of gut hormones. Interestingly, the impaired glucose tolerance phenotype was sex- and age-dependent. Glucose intolerance was observed in animals on RC only in females, starting from 12 weeks of age and becoming stronger at 20 and 22 weeks of age. Our data also confirmed that the glucose intolerance is not due to insulin intolerance but is as result of decreased plasma insulin levels in the *C2cd4b* null female mice compared to their WT littermates.

The gender-specific glucose tolerance impairment observed in *C2cd4b* females may be the consequence of alterations in the reproductive cycle. It is known that glucose homeostasis is significantly influenced by sex steroids such as oestrogen and progesterone (Trout *et al.*, 2007; Radavelli-Bagatini *et al.*, 2011) whose production is stimulated by LH and FSH, hormones produced from the pituitary gland. Since *C2cd4b* is also highly expressed in the pituitary gland, we measured the secretion of FSH and LH in the plasma of ovariectomised animals. Interestingly, our data demonstrated a significant reduction in FSH levels in *C2cd4b* null female mice, which might contribute to the sexual dimorphism in glucose tolerance observed in these animals.

When maintained on HFD, *C2cd4b* null females showed impaired glucose intolerance from 8 weeks of age, after only two weeks of HFD maintenance. Compared to the animals maintained on RC, the animals maintained on HFD showed glucose intolerance phenotypes at an earlier stage (8 weeks instead of 12 weeks of age). Also, this phenotype was stronger in the animals maintained on HFD compare to animals maintained on RC. In addition to IPGTTs, *C2cd4b* null females on HFD show impaired glucose tolerance measured by OGTTs. These observed phenotypes suggest that a lack of *C2cd4b* increases the susceptibility to high-fat and -sugar intake.

Furthermore, when maintained on HFD, although plasma insulin in *C2cd4b* null females was comparable with their WT littermates, the glycaemia after 15 min of glucose injections was significantly higher in these animals. We showed that the observed phenotypes in animals maintained on HFD were not the result of insulin intolerance. These results together indicate impairment in β-cell function in *C2cd4b* null female mice when maintained on HFD.

Unexpectedly, when maintained on HFD, *C2cd4b* null males also showed glucose intolerance during IPGTTs and significant increase in fasting glycaemia. Since male *C2cd4b* null animals showed a significant increase in body weight and, therefore, significantly more glucose was injected into these animals, we tested the IPGTTs based on the lean body weight. IPGTTs based on lean body weight in males showed no differences in glycaemia between *C2cd4b* null and their WT littermates. This suggests that the observed glucose intolerance was rather due to the increased amount of injected glucose rather than impairment in glucose homeostasis. However, the underlying result behind the significant increase in fasting glycaemia is unknown and would imply a change in glucose handling. Since *C2cd4b* is also expressed in α-cells further investigation in glucagon levels in these animals might provide an answer to this question. Another tissue which affects fasting glycaemia is liver, therefore, analysing the function of this organ in these animals could shed light on altered fasting glycaemia.

Interestingly, the higher fasting glycaemia in males may also be due to sexual differences in metabolic homeostasis between males and females. It has been shown, in human subjects, while it is more prevalent in females to show glucose

impairment, in males, it is more prevalent to have higher fasting glycaemia (Williams *et al.*, 2003; Sicree *et al.*, 2008). The reason behind these differences is unknown.

4.3.3. Unchanged secretory dynamics in β-cells from isolated islets from *C2cd4b*$^{-/-}$ *versus* WT mice

To address whether decreased plasma insulin levels in female *C2cd4b* null versus WT mice was because of lower insulin secretion, we assessed glucose-stimulated insulin secretion from isolated islets of these animals. The results revealed no differences in insulin secretion from isolated islets between null and WT animals. These results suggest that the reduced *in vivo* insulin secretion could be a result of interactions of other regulators with islets. Further investigations to measure other circulating factors, and compare them between the *C2cd4b* male and female null and WT mice, are essential to understand the underlying cause of decreased plasma insulin in these animals.

We also studied β-cell Ca^{2+} dynamics using isolated islets from *C2cd4b* null females, stimulated with glucose or KCl. No significant changes in Ca^{2+} dynamics or intercellular connectivity was observed between the null and WT littermates, consistent with unaltered GSIS.

Since β-cell mass was also unchanged in *C2cd4b* null animals (although we noted a trend towards an increase in α: β cell ratio) other explanations must be sought for the lowering in circulating insulin in female *C2cd4b*$^{-/-}$ mice. One possibility is the altered action of FSH and, therefore, altered levels of cycling E2 (Mauvais-Jarvis, 2015), or altered autonomic tone. Since we have already shown lower FSH levels in female *C2cd4b* null mice compared to WT, further investigations to measure other circulating factors (such as E2 and leptin) are essential to understand the underlying cause of decreased plasma insulin in females. Other possibilities include alterations in endogenous regulators such as incretins, locally released neurotransmitters, and other islet-derived hormones (such as glucagon, somatostatin etc.).

Our data revealed no differences between genotypes during OGTTs, when animals were maintained on RC, making an altered incretin effect less likely. However, since *C2CD4A* and *C2CD4B* are expressed in the stomach and intestine, and impaired glucose tolerance was observed in *C2cd4b*$^{-/-}$ females when maintained on HFD, an accurate measurement of circulating incretin hormones needs to be performed to

address the possible role of C2CD4A and C2CD4B in the processing and secretion of glucose-dependent insulinotropic peptide (GIP), GLP-1 and other entero-endocrine derived hormones.

4.3.4. Unchanged proinsulin levels in *C2cd4b*$^{-/-}$ mice

GWAS have previously revealed a significant increase in fasting proinsulin levels associated with variants at the *C2CD4A/C2CD4B/VPS13C* locus (Strawbridge *et al.*, 2011a). Since higher proinsulin levels are associated with β-cell dysfunction (Strawbridge *et al.*, 2011a), we measured insulin and proinsulin levels after six h of fasting in *C2cd4b* animals. No changes were observed between the null and WT mice on either diet. This could suggest that murine and human *C2CD4B* might play different roles in glucose homeostasis. It could also suggest that the increased proinsulin levels observed in humans is as a result of impairment in *C2CD4A* rather than *C2CD4B*. For this reason, it is crucial to study the role *C2CD4A* in insulin secretion. In addition, one possible reason behind the lack of phenotype in mice could be the sample number used. In females 8-9 animals/group have been used which is a sufficient number of samples to detect a 1.2-fold difference in the mean between two groups. However, in males 4-7 samples/genotype was used which might not have enough power to detect changes in the insulin/proinsulin levels.

Chapter 5: Role of *C2CD4A* in glucose homeostasis and insulin secretion

5.1. Introduction

C2CD4A is expressed in a range of human tissues including pituitary gland, pancreas, kidney, stomach and liver (Figure 1. 13). Interestingly, although detectable in mouse islets, its expression is 10-fold lower than *C2cd4b.* In a human pancreatic cell line, EndoC βH1, *C2CD4A* is more abundantly expressed compared to *C2CD4B* (https://shinyapps.jax.org/endoc-islet-multi-omics/) (Kycia *et al.*, 2018). Thus, the latter study showed that the expression levels of *C2CD4A* and *C2CD4B* in human islets were between 20 and 25 read-depth, while in EndoC βH1 cells the reads were ~3 for *C2CD4A*, and <0.5 for *C2CD4B* (Kycia *et al.*, 2018). Keeping in mind these differences in the expression patterns of this gene, it is essential to use an appropriate model to study its role in pancreatic β-cells.

While the function of C2CD4A and, hence, the actions of nearby T2D associated variants have not been elucidated in human β-cells, one of the main characteristics of this protein is the presence of a C2 domain at its C-terminus (Mehta *et al.*, 2016). It is not clear, however, if this C2 domain has the ability to bind to intracellular Ca^{2+}. In Chapter 3, we demonstrated that an increase in intracellular [Ca^{2+}] levels leads to increased C2CD4A translocation to the plasma membrane, suggesting it responds to the increased intracellular Ca^{2+} levels resulting from glucose stimulation. However, the role of C2CD4A in insulin secretion in human β-cells remained to be addressed. In Chapter 3, we also showed that C2CD4A is localised to the plasma membrane, cytoplasm and the nucleus. In contrast to our findings, it was shown by Kuo *et al.,* that murine C2CD4A is localised exclusively to the nucleus (Mehta *et al.*, 2016). Therefore, one could suggest that human and murine C2CD4A play different roles in insulin secretion and glucose homeostasis.

It has recently been shown that a mouse model lacking *C2cd4a* specifically in β-cells is glucose intolerant, and displays reduced plasma insulin levels. Glucose and arginine-stimulated insulin secretion from isolated islets of these animals are also significantly perturbed (Holst *et al.*, 2016). Furthermore, it has been shown by the IMPC that global null *C2cd4a* mice have a significant decrease in neutrophil cell numbers and a significant increase in platelet volume and lymphocyte cell number (https://www.mousephenotype.org/data/genes/MGI:3645763). These phenotypes

are consistent with the high expression level of this gene in hematopoietic cells (Warton *et al.*, 2004). However, no glucose tolerance impairment phenotypes were reported by the IMPC studies. It needs to be emphasised that the phenotyping experiments performed by IMPC compared null animals to the results from the database from WT animals and they did not directly compare *C2cd4a* null to their WT littermates (see Chapter 4.1, Introduction)

Therefore, to understand the possible roles of *C2CD4A* in the regulation of insulin secretion and glucose homeostasis in mouse and human β-cells, in this chapter we study global null *C2cd4a* (generated by IMPC) and knockout EndoC βH1 cells as our models.

5.2. Results

5.2.1. Increased GSIS upon over-expression of *C2CD4A*

To assess if *C2CD4A* and *C2CD4B* play roles in insulin secretion, we studied the effect of over-expression of these genes on GSIS in the rat INS1 (832/13) cell line. To address this, *C2CD4A* or *C2CD4B* were co-transfected in cells with human growth hormone (hGH), and hGH secretion was measured upon stimulating these cells with either 17 mM glucose or 20 mM KCl. We used this method instead of direct insulin secretion measurement in order to specifically measure secretion in the cells that have been transfected with our constructs (see also Chapter 3). hGH measurement is an indirect way to measure insulin secretion since it co-localises in the same secretory granules as insulin. Cells were co-transfected with hGH and a construct with no insert as a control. The results indicated that upon over-expression of *C2CD4A* insulin secretion was significantly increased upon stimulation with 17 mM glucose or 20 mM KCl (Figure 5. 1, A: 14.8 ± 0.4 *vs.* 27.9 ± 1.53 control *vs.* C2CD4A stimulated with 17 mM glucose, $p<0.001$, and 10.7 ± 0.5 *vs.* 18.1 ± 1.4 control *vs.* C2CD4A stimulated with 20 mM KCl, $p=0.004$; n=3 independent experiments; data were assessed for significance using a 2-way ANOVA test with Bonferroni's multiple comparison test).

Strikingly, insulin secretion at a non-stimulating glucose concentration (3 mM) was also affected by over-expression of *C2CD4A* (3.48 ± 0.7 *vs.* 9.37 ± 2.1 control *vs.* C2CD4A in 3 mM glucose, $p=0.02$; n=3 independent experiments; data were assessed for significance using a 2-way ANOVA test, with Bonferroni's multiple

comparison test). To assess if the change observed in 3 mM glucose condition was a result of different total hGH content or the total number of cells in different pools of cells, total cellular insulin content was also measured and compared separately (Figure 5. 1, B). There were no apparent changes in total insulin content between the different pools of cells that could result in changes in secretion in 3 mM glucose condition. However, when insulin secretion in 17 mM glucose or 20 mM KCl was normalised to basal insulin secretion, 3 mM glucose, we observed a significant decrease in the fold-change in secretion levels upon over-expression of either *C2CD4A* or *C2CD4B* in 17 mM glucose (Figure 5. 1, C). We also observed a significant reduction in secretion upon over-expression of *C2CD4A* in 20 mM KCl condition. The latter results are in the same direction as the studies from the Kycia *et al.* (Kycia *et al.*, 2018), who showed an association between the risk allele rs7163757 and increased *C2CD4B* mRNA levels analysing pancreatic islet samples from human donors.

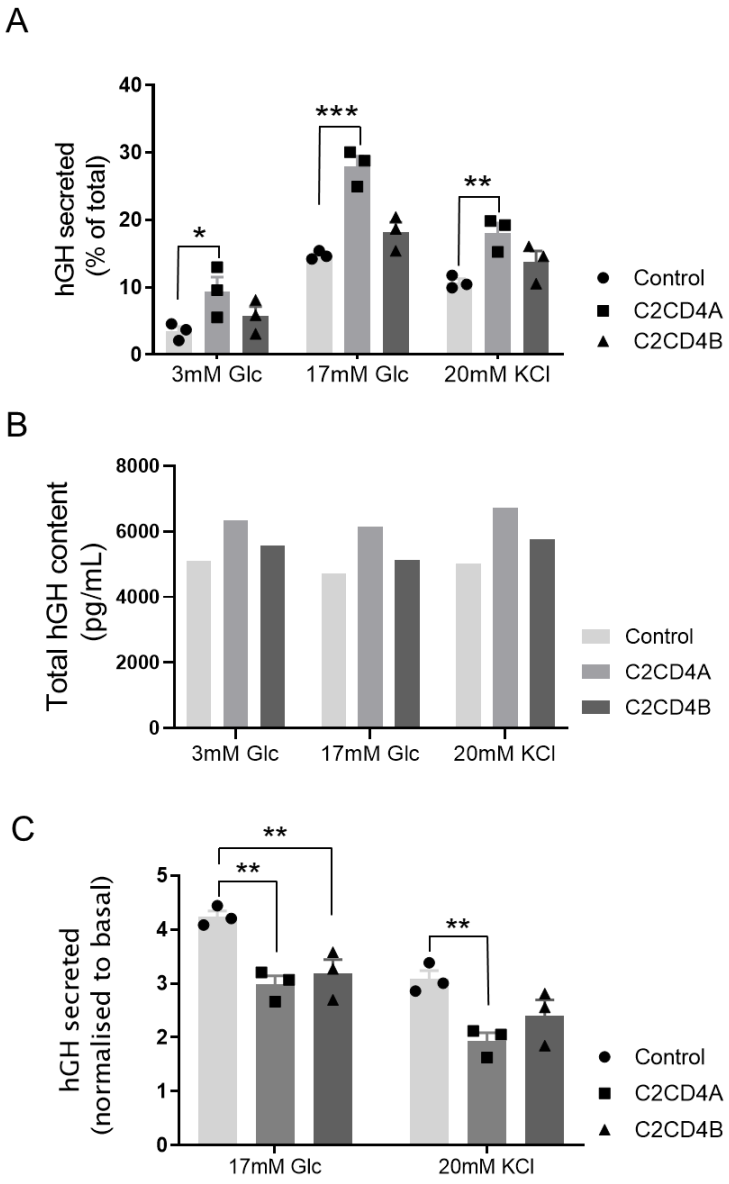

Figure 5.1. GSIS upon over-expression of *C2CD4A* and *C2CD4B*. A. GSIS and KCl-stimulated insulin secretion (KSIS) from cells over-expressing either *C2CD4A* or *C2CD4B*. FLAG-tagged-*C2CD4A* or -*C2CD4B* constructs were co-transfected with hGH into INS1 (832/13) cells. As a control, a FLAG-tagged construct p3xFLAG-CMV-14 (Addgene) lacking an inserted gene was co-transfected with hGH construct. Upon over-expression of *C2CD4A*, a significant increase in insulin secretion was observed at both 3 and 17 mM glucose and at 20 mM KCl conditions. B. Total hGH content in cells was measured in the same pool of cells to assess consistency between total hGH contents within the different pools of cells. C. Fold-change in hGH secretion at 17 mM glucose and 20 mM KCl compared to basal secretion levels at 3 mM glucose. * $p<0.05$, ** $p<0.01$, *** $p<0.001$, data were assessed for significance using a 2-way ANOVA with Bonferroni's multiple comparison tests. Values represent mean ± SEM.

5.2.2. CRISPR/Cas9-mediated deletion of *C2CD4A* in human EndoC βH1 cells causes reduced insulin secretion

Given the high expression levels of *C2CD4A* and almost undetectable *C2CD4B* mRNA levels in human EndoC βH1 cells (Kycia *et al.*, 2018) (https://shinyapps.jax.org/endoc-islet-multi-omics/), we used a lentiviral-mediated CRISPR/Cas9 system (lentiCRISPR V2 construct from Addgene modified in Prof Gadue's laboratory, see Chapter 2, Material and Methods) to delete *C2CD4A*. EndoC βH1 cells are human β-cell lines which derived from human foetal pancreatic buds (Ravassard *et al.*, 2011). Although some gene expression and secretion dynamics in these cells differs from human β-cells, they are now being used extensively to study human β-cell biology (Tsonkova *et al.*, 2018).

In order to induce truncation/frameshifts in *hC2CD4A* which results in perturbation in protein function, a guide RNA targeting the first 100 bp of the coding region of h*C2CD4A* was designed. To deliver the gRNA and Cas9 to the cells, cells were infected with lentivirus carrying the gRNA, a Cas9 sequence and a puromycin resistance gene. After infecting the cells with this construct, those which received the gRNA/Cas9/puromycin constructs were selected using puromycin (Figure 5. 2). We selected two independent pools of cells containing the latter constructs (containing gRNA1) for further analysis, and named them as gRNA1-a and gRNA1-b (explained in more details in Material and Methods, Chapter 2.6).

The efficiency of *C2CD4A* deletion was assessed by DNA sequencing (Figure 5. 2). Comparing the sequencing results from gRNA1-a and gRNA1-b cells with the negative control in each one revealed several mismatches in the sequence where Cas9 was predicted to cut the DNA, while in the negative control no mismatches to *C2CD4A* sequence were observed (Figure 5. 3).

Since there were no antibodies available to assess the reduction at the protein level, mRNA levels were measured to assess deletion efficiency of Cas9 and to measure the total *C2CD4A* mRNA levels. This revealed a significant efficiency in cutting the expected region in *C2CD4A* by Cas9 in both pools with gRNA (relative expressions: 47.1% ± 4.6 and 43.6% ± 2 at gRNA1 pool-a and pool-b respectively, $p<0.001$, data were assessed for significance using an Ordinary one-way ANOVA, Tukey's multiple comparison test). Total mRNA levels were also reduced in the transfected cells

comparing to control cells (*C2CD4A* total mRNA relative expression: 78.2% ± 13.8 and 94.1% ± 24 in gRNA pool-a and pool-b respectively, p=ns) (Figure 5. 4).

To measure C2CD4A at the protein level we attempted to produce a custom-made polyclonal antibody with Eurogentec. However, the antibody did not work in Western (immuno)blotting to recognise C2CD4A protein (results shown in Appendix 2). Considering that we never detected a change in total mRNA levels, and the fact that there is no antibody to prove the change at protein levels, no strong conclusions could be drawn from this experiment. This is indeed the significant limitation of this method.

Insulin secretion was measured in these cells *in vitro* upon incubation for 30 min under basal conditions (0.5 mM glucose; LG), or stimulating conditions at 15 mM glucose (HG), 20 mM KCl, or with 0.5 or 15 mM glucose plus 0.5 mM isobutyl methyl xanthine (IBMX; LG-IBMX, HG-IBMX), and finally with 0.5 or 15 mM glucose plus, the GLP-1 receptor agonist, 0.2 µM Exendin-4 (LG-Ex-4, HG-Ex-4). No change in insulin secretion was observed in HG versus LG, while stimulation with KCl and HG-IBMX, resulted in impaired insulin secretion in both pools of CRISPR-edited cells compared to control cells (Figure 5. 4: stimulated with KCl: 50.7% ± 2.8 and 60.1% ± 4.6 relative insulin secretion in pool-A and pool-B respectively *vs.* control, p=0.01 and 0.03 respectively; stimulated with HG-IBMX: 39.5 ± 3.6 and 34.9 ± 2 % relative insulin secretion in gRNA1-a and gRNA1-b respectively, *vs.* control; p=0.060 and 0.016 respectively; data were assessed for significance using a 2-way ANOVA, Bonferroni's multiple comparison test).

Since we observed effects of *C2CD4A* or *C2CD4B* over-expression on insulin secretion in unstimulated conditions (0.5 mM glucose) (Figure 5. 4, A), we next normalised insulin secretion values to basal glucose levels for each condition to remove the possible effect of different number of cells in each pool (Figure 5. 4, B). The results showed no differences in insulin secretion in knockout cells compared to the control when data was normalised to 0.5 mM glucose. We next compared the total insulin content of each pool of cells to determine if there is a significant difference between the total number of cells in the pools containing knockout cells compared to the control. Our results revealed no significant differences in total insulin content between the knockout pools and the control (Figure 5. 5, C).

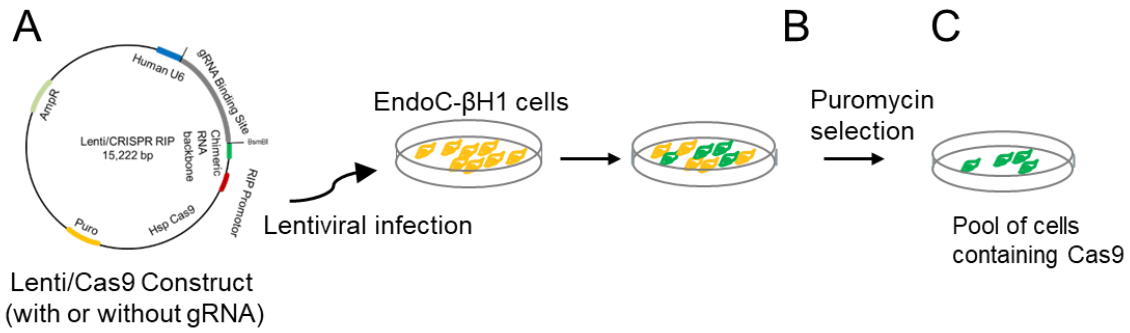

Figure 5.2. A lenti/Cas9 system was used to knockout *C2CD4A* in EndoC βH1 cells. A. A construct containing a Cas9, puromycin coding gene and a gRNA binding site was used to deliver a gRNA into EndoC βH1. B. Cells which received the construct were purified using puromycin treatment for one week. C. Pools of cells containing the Cas9 and a gRNA were selected for further investigations.

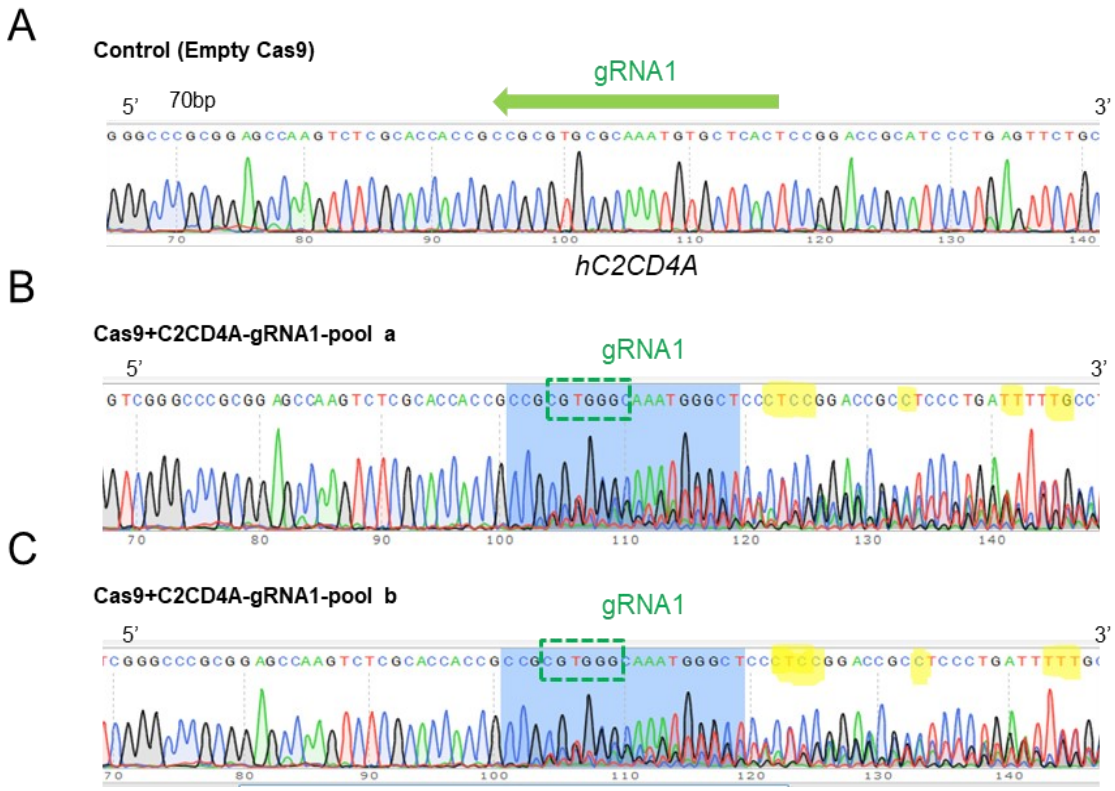

Figure 5.3. DNA sequencing after CRISPR/Cas9 mediated *C2CD4A* deletion from EndoC-βH1 cells. A lentiviral-based CRISPR/Cas9 system was used to target *C2CD4A* in EndoC- βH1 cells. A guide RNA (complementary sequence show by the green arrow) was designed at the first 100 bps of the coding region of human *C2CD4A*. An empty plasmid without any gRNA was used as a negative control (A), see Material and Methods. A. Sequencing map from the pools of cells infected with the control plasmid (no gRNA). B-C. Sequencing map from two independent pools of cells infected with Lenti/Cas9 construct containing gRNA1. The green hashed box indicates the possible site where Cas9 make cuts. Bases highlighted in yellow indicate single nucleotide mismatches compared to the control plasmid.

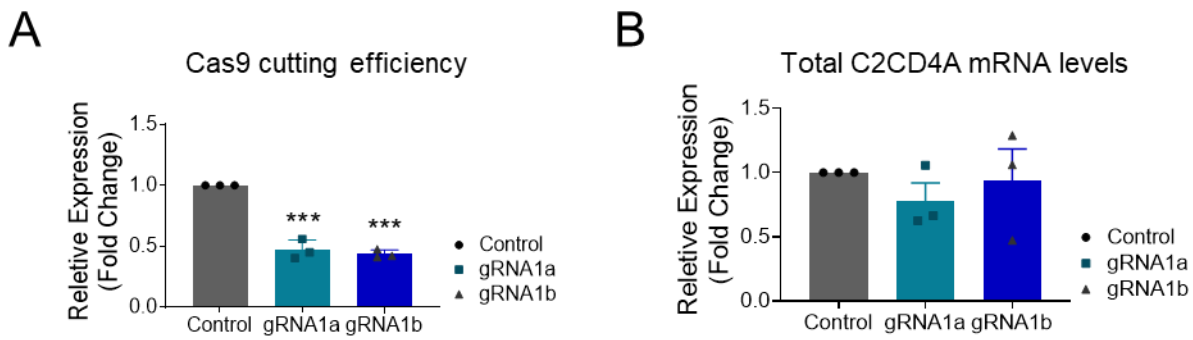

Figure 5.4. Characterisation of the CRISPR β-cell lines. A. q-RT-PCR experiments were performed by designing the forward primer where Cas9 is expected to demonstrate nuclease activity and cut the DNA in the *C2CD4A* coding region. Using this method we can estimate the percentage of cells which have mutations at this region. B. Measuring total mRNA in the CRISPR cell lines. * $p<0.05$, ** $p<0.01$, *** $p<0.001$, data were assessed for significance using a 2-way ANOVA with Bonferroni's multiple comparison tests. Values represent mean ± SEM.

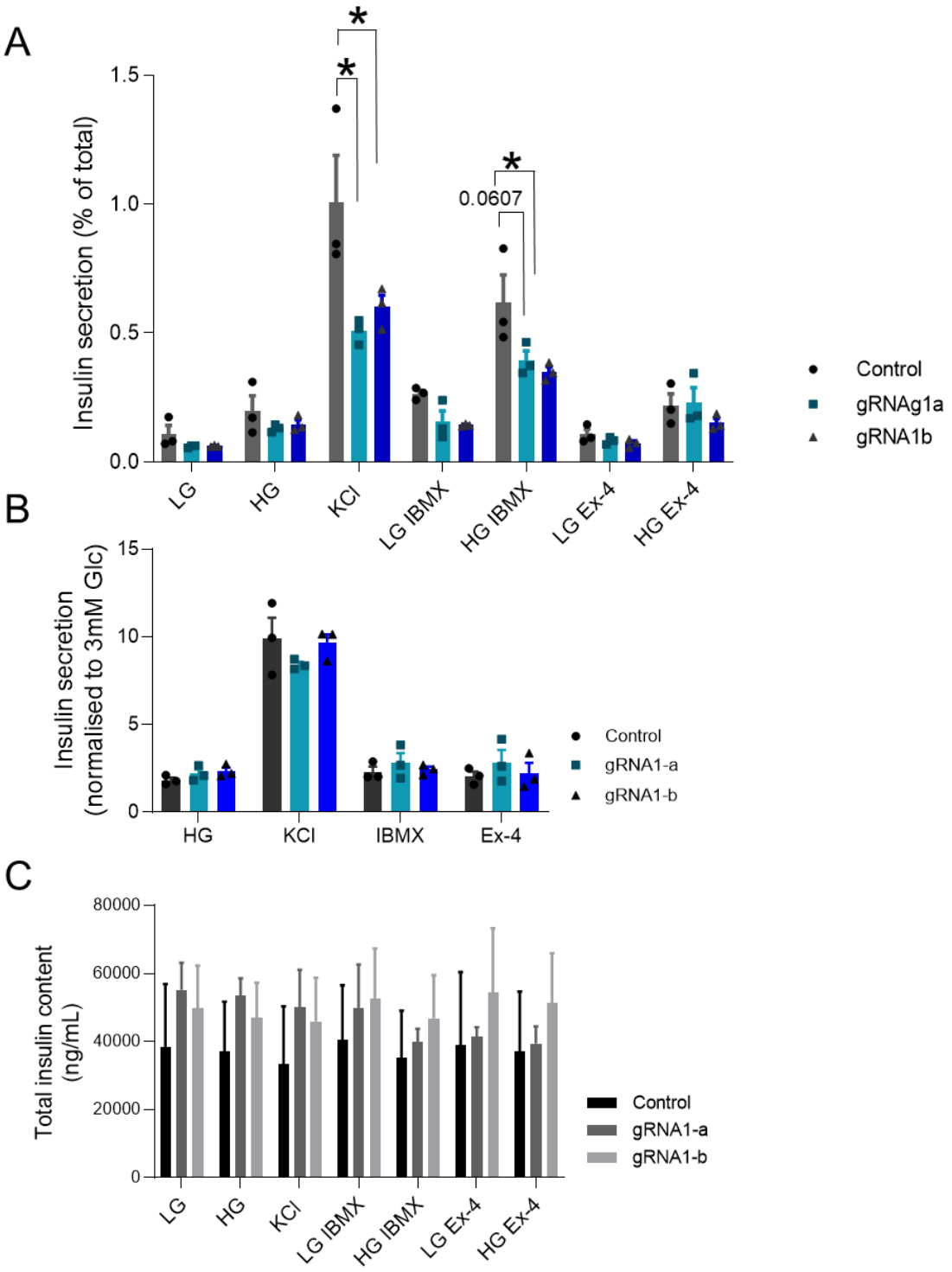

Figure 5.5. Effect of *C2CD4A* knockout on *in vitro* insulin secretion. A. *In vitro* insulin secretion assays, after stimulating the cells with 0.5 mM glucose (LG), 15 mM glucose (HG), 20 mM KCl, 0.5 and 15 mM glucose plus 0.5 mM IBMX (LG-IBMX, HG-IBMX), 0.5 and 15 mM glucose plus 0.2 µM Exendin-4 (LG-Ex4, HG-Ex4). B. *In vitro* insulin secretion (A) normalised to insulin secretions in low glucose conditions. C. Comparison on total insulin secretion in different pools of EndoC βH1. *p<0.05, data were assessed for significance using a 2-way ANOVA with Bonferroni's multiple comparison test. Values represent mean ± SEM.

5.2.3. Generation of *C2cd4a* null mice

C2cd4a null mice (C2cd4a-Del1724-EM1-B6N) were generated by the IMPC, using the CRISPR/Cas9 system, to delete 1724 bp of exon 2, the only expressing exon in mouse *C2cd4a* (Figure 5. 6, A-B). Inter-crossing of heterozygous animals resulted in wild type (WT, *C2cd4a*$^{+/+}$), heterozygous (*C2cd4a*$^{+/-}$) and null (*C2cd4a*$^{-/-}$) littermates. Note that accurate quantification of *C2cd4a* mRNA in islets of these animals was challenging due to the low levels of mRNA even in WT islets (Kone *et al.*, 2014)(Benner *et al.*, 2014). The WT and null animals were used for further characterisations (Figure 5. 6, B). The heterozygous breeders produced a significantly lower number of pups per litter and/or hardly bred (five breeding cages gave birth to six litters in six months; the litter sizes were between 3-9). However, it was not clear if there was a fertility issue in *C2cd4a*$^{+/-}$ mice. Both male and female *C2cd4a* null mice maintained on a regular chow diet (RC) gained weight at the same rate as their WT littermates.

5.2.4. Glucose tolerance do not alter in *C2cd4a*$^{-/-}$ *vs.* control mice

To investigate the possible effects of *C2cd4a* deletion *in vivo* on glucose homeostasis, intraperitoneal glucose tolerance tests (IPGTTs) were performed on male and female *C2cd4a* mice on regular chow diet (RC) at 12, 16, 20 and 22 weeks of age. After overnight fast, a single dose of 1g of glucose per kg of body weight was injected and glycaemia monitored over a 2-h period. Only males at 16 weeks of age showed a mild glucose intolerance as measured at 15 min after glucose injection (Figure 5. 7). No differences were apparent at this age on male mice when AUC values were compared (Figure 5. 7)

5.2.5. No abnormalities in plasma insulin levels in *C2cd4a*$^{-/-}$ mice

We next determined whether the deletion of *C2cd4a* affects insulin release upon stimulation with glucose *in vivo* in male mice. Animals at 21 weeks of age were fasted overnight and injected with a single dose of 3 g glucose per kg body weight. Blood samples were collected, and glycaemia was monitored at 5 and 15 min. after glucose injections. No significant differences were observed in plasma insulin levels or glycaemia between the null and WT animals (Figure 5. 8).

5.2.6. Deletion of *C2cd4a* does not affect GSIS or KSIS from isolated islets

We also measured insulin secretion from the isolated islets from *C2cd4a* null male mice. Isolated islets from *C2cd4a*$^{-/-}$ mice were stimulated with 17 mM glucose or 20 mM KCl. The results did not show any changes in the insulin secretion levels between *C2cd4a*$^{-/-}$ mice and their WT littermates (Figure 5. 9).

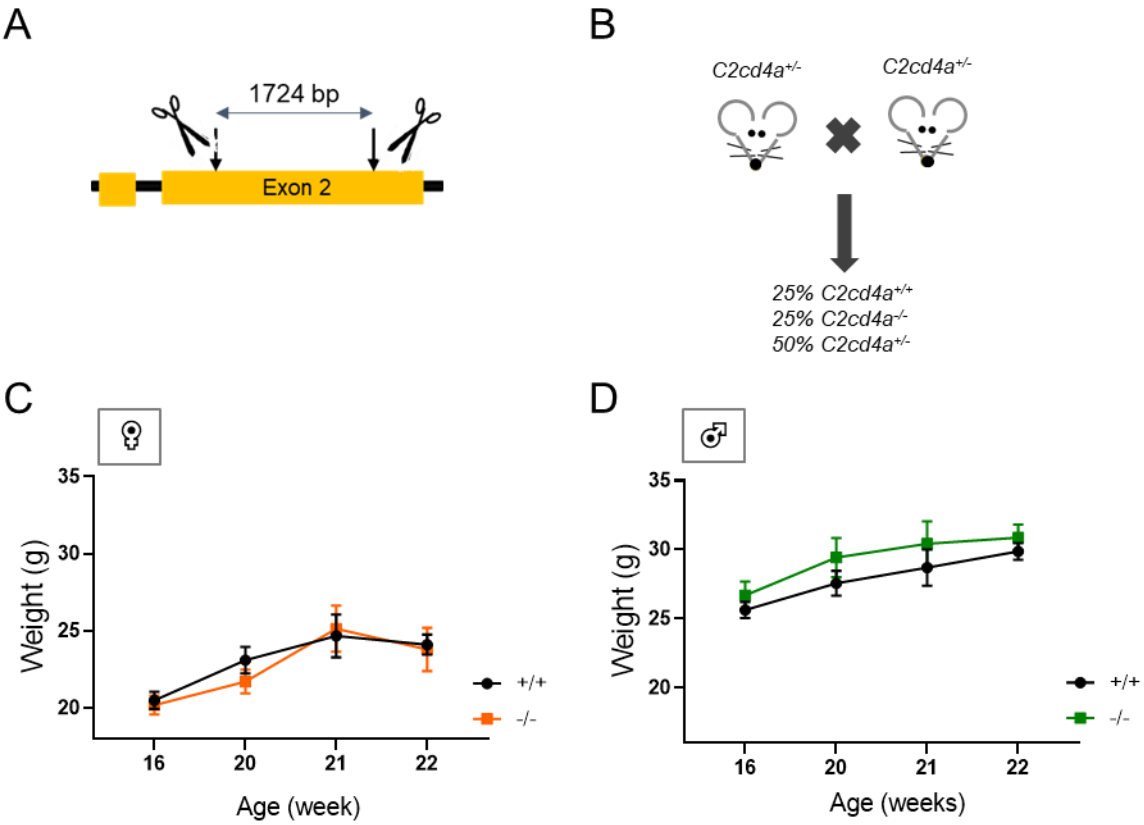

Figure 5.6. Generation of the *C2cd4a* null mice. A. *C2cd4a* mouse strain was generated at IMPC using CRISPR/Cas9 systems to target 1724 bps from exon 2 of *C2cd4a* gene. B. Inter-crossing the heterozygous mice resulted in the generation of wild type (WT, *C2cd4a*$^{+/+}$), heterozygous (*C2cd4a*$^{+/-}$) and null (*C2cd4a*$^{-/-}$) littermates. C-D. Body weight of *C2cd4a* females (C) and males (D) at 16, 20. 21 and 22 weeks of age ($F^{+/+}$ n=4-11, $F^{-/-}$ n=4-9, $M^{+/+}$ n=2-8, $M^{-/-}$ n=3-6 animals per stage). Mixed-effect analysis, Tukey's multiple comparison test. Values represent mean ± SEM.

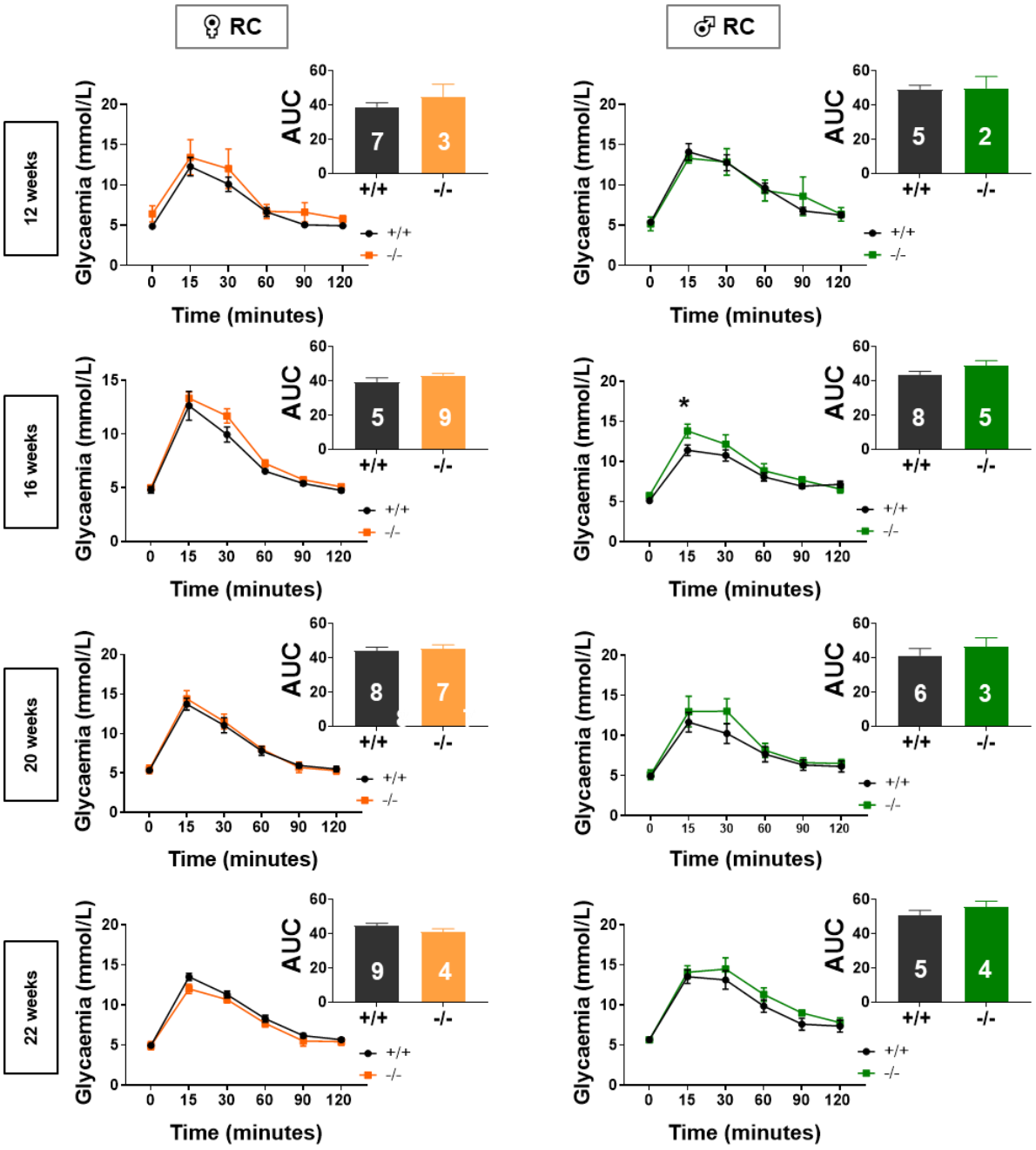

Figure 5.7. Effect of global deletion of *C2cd4a* on intraperitoneal glucose tolerance in animals maintained on regular chow diet (RC). Intraperitoneal glucose tolerance tests (IPGTTs) were performed on *C2cd4b* male and female mice maintained on RC at 12, 16, 20 and 22 weeks of age. *p<0.05, data were assessed using a 2-way ANOVA with Bonferroni's multiple comparison test. Inset: area under the curve (AUC) analysis, assessed for significance using an unpaired Student's t-test (same number of samples used for glycaemia and AUC graphs). Numbers in bar graphs represent the number of animals used. Values represent means ± SEM.

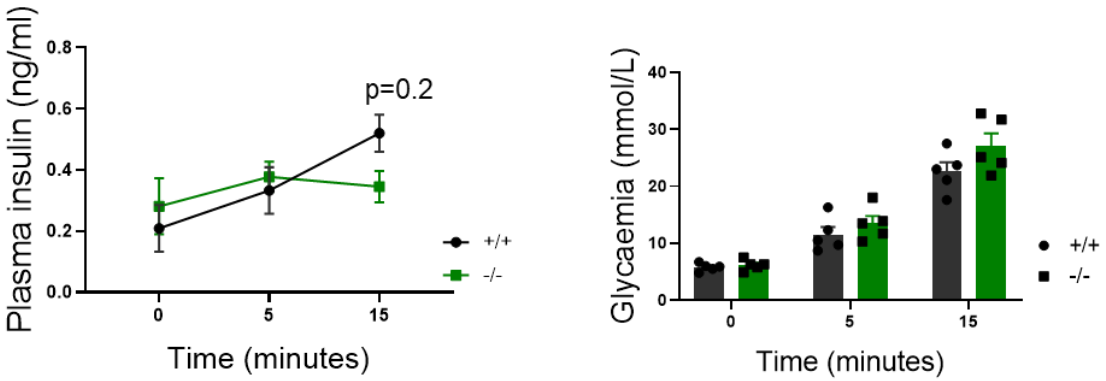

Figure 5.8. Effect of deletion of *C2cd4a* on glucose-stimulated insulin release *in vivo*. Intraperitoneal glucose tolerance tests were performed on *C2cd4a* null male animals maintained on RC at 21 weeks of age. Blood samples were collected, and glycaemia measured at 5 and 15 min. after injection of glucose at 3 g/kg body weight. n=5/genotype. *p<0.05, **p<0.01, ***p<0.001, data were assed for significance using a 2-way ANOVA with Bonferroni's multiple comparison test. Values represent means ± SEM.

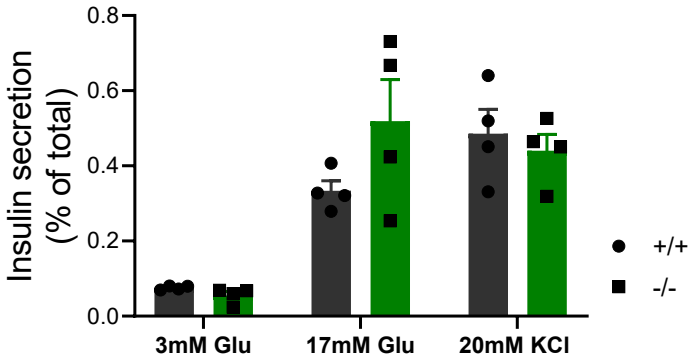

Figure 5.9. Effect of deletion of *C2cd4a* on GSIS from isolated islets. *In vitro* insulin levels in *C2cd4a* null *male* and WT mice maintained on RC. Measurements of insulin secretion were performed after stimulating isolated islets with 17 mM glucose or 20mM KCl (n= 4/genotype). * p<0.05, data were assessed for significance using a 2-way ANOVA with Bonferroni's multiple comparison test. Values represent mean ± SEM.

5.3. Discussion

This chapter explores the role of human *C2CD4A* in insulin secretion in β-cells. Furthermore, I aimed to study the effect of global deletion of *C2cd4a* on glucose homeostasis *in vivo*. Specifically, we showed that over expression and deletion of human *C2CD4A* affects insulin secretion in β-cells.

A previous attempt demonstrated the effect of deletion of *C2cd4a* selectively in the β-cells of mice (Kuo *et al.*, 2019). These animals showed glucose intolerance and a decrease in glucose-stimulated insulin secretion from the pancreatic islets. However, the effect of deletion of *C2cd4a* globally *in vivo* has not been demonstrated. Keeping in mind the relatively broad tissue specificity of this gene (Introduction, Figure 1. 13 and 1. 14), we hypothesised that understanding how global deletion of this gene might affect glucose homeostasis can give us a more robust answer about the role of this gene in glucose homeostasis.

5.3.1. *C2CD4A* may regulate insulin secretion

The present study shows that over-expression of *C2CD4A* in INS1 (832/13) cell line increases insulin secretion stimulated by 17 mM glucose or 20 mM KCl. Unexpectedly, our results also show a significant increase in unstimulated conditions (3 mM glucose). For this reason, and to assess if the changes observed in the unstimulated condition is due to a significant increase in the cell numbers, total insulin content was assessed. The data indicated a comparable total insulin content between each group of cells. However, when the data were examined in terms of the fold stimulation of secretion in respect to either 17 mM glucose or 20 mM KCl, the secretion was significantly *decreased* upon over-expression of either *C2CD4A* or *C2CD4B* at 17 mM glucose. Also, at 20 mM KCl a significant decrease in fold-change of secretion was observed upon over-expression of *C2CD4A* compared to the control (empty vector) condition. The differences observed when the data were analysed using this alternative approach could be the result of measuring different concepts (when directly measuring secretion or solely measuring fold-change secretion). When we only compared the secretion stimulation between unstimulated and stimulated conditions (Figure 5. 1, A), we in fact, measured the 'maximal secretion' capacity, i.e. how much the cells can secret maximally. However, when the data were normalised to the basal secretion levels, and therefore, the fold-change was measured (Figure 5. 1, A), the data better reflect the health, vitality and

responsiveness of β-cells to the stimuli. It is believed that the basal insulin secretion levels, in addition to the capacity to respond to stimuli, is crucial to maintain normal glucose homeostasis (Corkey, 2012). Thus, multiple studies have reported a strong correlation between basal insulin levels, obesity and diabetes in humans (reviewed by Corkey 2012 (Corkey, 2012)).

Interestingly, when *C2CD4A* was knocked-out in EndoC βH1 cells, an effect on insulin secretion in the unstimulated condition was similarly observed, but in the opposite direction. In *C2CD4A* CRISPR lines, in the 3 mM glucose condition, insulin secretion was decreased in knockout cells compared to control cells. This consistent change in insulin secretion in the unstimulated glucose condition could suggest that *C2CD4A* has a role in insulin vesicle numbers or processing of insulin before secretion. More experiments quantifying insulin vesicles in these conditions could examine this hypothesis. Another possibility underlying this unexpected phenotype could be that *C2CD4A* over-expression and knockout have an effect on the cell cycle. This could explain the cause of variation of cell numbers between over-expressed/knock out cells compared to controls. This possibility could be addressed by measuring the cell numbers by quantifying proteins or mRNA content between these conditions.

Our *in vitro* insulin secretion experiments on *C2CD4A* knockout cells in human β-cells show a reduction in glucose and IBMX- and KCl-stimulated insulin secretion. These results suggest that *C2CD4A* plays a role in the control of insulin secretion in human β-cells. However, further experiments need to be carried out to prove that this insulin secretion impairment is the direct result of deletion of *C2CD4A* and not an artefact of its possible role in the cell cycle. Further characterisation of these cell lines is needed to assess whether off-target genes were affected.

To validate the results from *C2CD4A* deletion in human β-cells, the effect of down-regulation of this gene in human islets on insulin secretion should also be assessed. For this, small hairpin RNAs (shRNA) could be used. In the lab we have designed shRNAs to down-regulate both human *C2CD4A* and *C2CD4B* expression, since both of these genes are expressed in human islets. The efficiency of these shRNAs has been assessed previously by Dr Zenobia Mehta. Using these shRNAs to down-regulate our genes of interest in human islets and study the effect on insulin secretion with similar stimuli used in our CRISPR cells, might potentially give us a confirmation of the phenotype we observed, but also show the possible role of *C2CD4B* in insulin

secretion in human pancreatic islets. Also, this method should give us the possibility to down-regulate both of these genes at the same time. Studying the effect of down-regulation of both of these genes will give us much better insight about their roles in insulin secretion since a compensatory mechanism may be expected if targeting only one of these genes due to high similarity between their structures. Using RNA-seq in mouse islets from the *C2cd4b* null mice, we have also previously observed that the expression of *C2cd4a* is significantly increased compared to WT islets. Another advantage of using shRNA to down-regulate these genes is that it gives us the ability to assess the efficiency of this process solely by measuring mRNA levels. This is possible since shRNAs directly target mRNA. This method is highly preferred since no working antibody is available to detect human C2CD4A at the protein level.

Our data suggest that human C2CD4A plays a role in insulin secretion. However, more studies need to be carried out to first confirm this in different models and secondly to shed light on the mechanism of action.

5.3.2. Murine *C2cd4a* does not regulate insulin secretion in *C2cd4a* null mice

Characterisation of the global *C2cd4a* null mice showed that there is no significant glucose intolerance phenotype in these animals. Furthermore, *C2cd4a* null animals show no deficiency in plasma insulin levels nor in GSIS from isolated islets. These findings are predictable, considering the very low-level of expression of *C2cd4a* in mouse islets. However, our findings are in contrast to the insulin secretion impairment seen in the mouse model deleted for *C2cd4a* specifically in β-cells (Kuo *et al.*, 2019). The latter study showed glucose intolerance in *C2cd4a* null males at 12 weeks of age. In addition to glucose intolerance, decreased plasma insulin levels and decreased GSIS from isolated islets from *C2cd4a* null mice were observed.

The differing phenotypes between these knockout animal models could be the result of several factors. First, the difference in the tissues where *C2cd4a* was deleted. While we used a global null *C2cd4a,* Kuo *et al.* (Kuo *et al.*, 2019), used a RIP-Cre line and deleted *C2cd4a* selectively in β-cells as well as subset of hypothalamic nucleus (Wicksteed *et al.*, 2010). It is possible that, in the global *C2cd4a* null mice, *C2cd4b* compensates for the effect of the deletion of *C2cd4a.* This possibility can be examined by comparing the *C2cd4b* expression levels between the two mouse strains. In RNA-seq data we observed that *C2cd4a* expression is significantly

increased in response to deletion of *C2cd4b* in the islets of these animals. However, whether *C2cd4b* is upregulated in response to the deletion of *C2cd4a*, needs to be further investigated.

Second, differences in the background of the mice is another possibility. However, the background of the mice studied in Kuo *et al*. article is not indicated.

Kuo *et al.* also (Kuo *et al.*, 2019) showed that the deletion of *C2cd4a* in clonal mouse β-cells (MIN6 cells) results in reduced insulin secretion upon stimulation with high glucose and arginine. However, their study did not show if this effect is only apparent when arginine is added or if insulin secretion in cells stimulated with high glucose alone was also affected by the deletion of *C2cd4a*. Further studies are needed to investigate the role of *C2cd4a* in control of insulin secretion in murine β-cell lines.

Our findings suggest that *in vivo* global deletion of *C2cd4a* does not, if any, have a major effect on glucose homeostasis or insulin secretion in mice. Further studies are needed to understand the reason behind the absence of an apparent glycaemic phenotype in our hands and to understand the differences between our study compared to that of Kuo *el al* (Boesgaard *et al.*, 2010).

The lack of phenotype observed in *C2cd4a* null mice does not exclude a role of this gene in humans. This could be as a result of fundamental differences between human and mouse physiology. In addition, mouse *C2cd4a* in islets is expressed at very low levels compared to human in which both *C2CD4A* and *C2CD4B* are expressed at high levels. This could suggest that *C2cd4a* in mouse does not play a significant role in this tissue.

Chapter 6: Final Discussion

The primary goal of GWAS is to understand the biology of human disease and, ultimately, to prevent and/or provide more efficient treatments (Visscher *et al.*, 2017). Nearly 250 *loci* have been discovered in association with T2D (Mahajan *et al.*, 2018a). However, associations detected by GWAS do not yield a specific gene target or mechanism of action. Therefore, further functional studies are essential to find the key target genes associated with human diseases.

An achievement towards this goal has been the establishment of the IMPC to uncover mammalian gene function by conducting genome and phenome-wide phenotyping on knockout mouse lines (Cacheiro *et al.*, 2019). The extensive phenotyping conducted by the IMPC provides the potential to allow the identification of new models for human disease by direct comparison of the observed phenotypes between these two species. Although the IMPC performs extensive phenotyping in the mouse models generated by them, to specifically address the function of a gene in a human trait, further detailed characterisation of the strains needs to be carried out by laboratories specialised in the relevant studies.

Although global knockout mouse models for both *C2CD4A* and *C2CD4B* were made by the IMPC, no significant glucose impairment phenotypes were observed in these animals. Taking into account the SNPs discovered by GWAS (Grarup *et al.*, 2011; Yamauchi *et al.*, 2010b, 2010a; Cui *et al.*, 2011; Strawbridge *et al.*, 2011b; Wood *et al.*, 2017; Mahajan *et al.*, 2014) at this locus that strongly point at the possible function of these genes in glucose homeostasis, we used these strains for further glycaemic trait characterisation in depth. Table 1 indicates the SNPs and associated glycaemic traits from different GWAS studies at this locus, in different ethnic groups.

Since no comprehensive studies up to now had addressed the role *C2CD4A* and *C2CD4B* in β-cells or in the tissues relevant to glucose homeostasis, the aim of this project was to focus on this matter. We used *in vitro, in vivo* and *ex vivo* models to study the possible roles of these genes in glucose homeostasis and insulin secretion.

Since these two genes were only discovered in 2004 by Warton *et al*. (Warton *et al.*, 2004), and not much has been done to further elucidate their functions, to pursue our investigation we faced very limited available materials such as antibodies or mouse *Cre* lines to be able to conditionally deactivate these genes. Furthermore, a

lack of a comprehensive structural analysis of these proteins has made it more challenging to predict their possible roles in different tissues.

In order to explore the possible mechanism of action(s) of these genes in β-cells, we used over-expressed tagged proteins initially. This has given us the possibility to predict a novel role for these gene products since we observed distinct localisation patterns compared to what had been shown previously in the literature. We observed localisation at the plasma membrane in addition to the nucleus and cytoplasm. This interesting observation suggests that human C2CD4A could possibly play a role in signal transduction. Furthermore, these data could highlight the role of the putative C2 domains in the former protein, since these domains are predicted to bind to Ca^{2+} and phospholipids. We also showed the translocation of C2CD4A to the plasma membrane in response to elevated intracellular Ca^{2+}, similar to several classical proteins containing C2 domains such as e-Syt1 (Idevall-hagren *et al.*, 2015)·(Corbalán-García & Gómez-Fernández, 2010). This argues against a previous report (Omori *et al.*, 2016) suggesting that the C2 domain of C2CD4A has lost the ability to bind to Ca^{2+}. These data suggest that *C2CD4A* may have a role in the transduction of signals arising from elevated Ca^{2+} levels at the plasma membrane in the control of insulin secretion.

Considering the possible roles of these genes in signal transduction in insulin secretion, PTPRN (PTP IA-2) and PTPRN2 (IA-2β or phogrin) might be strong candidates interacting with C2CD4A and C2CD4B. PTPRN2 and PTPRN are involved in the accumulation of secretory vesicles at the plasma membrane in the hippocampus, pituitary gland and pancreatic islets (Marullo, El-Sayed Moustafa & Prokopenko, 2014; Kubosaki *et al.*, 2006; Saeki *et al.*, 2002). C2CD4A and C2CD4B are also expressed in the latter tissues. Interestingly, the knockout of PTPRN family members in mouse leads to a highly similar phenotype to *C2cd4b* knockout (Kubosaki *et al.*, 2006)·(Saeki *et al.*, 2002).

Showing the possible role of these genes in Ca^{2+} signal transduction and in vesicle formation, raises the possibility that these proteins might also play similar role(s) in different endocrine tissues where these are expressed. Indeed, these genes are expressed in several organs with endocrine function such as, the pituitary gland, adipose tissue, gonads and hypothalamus. This might suggest the impairment in C2CD4A and C2CD4B could also affect the secretory dynamics from these tissues.

Therefore, understanding the possible roles of these genes in the secretory dynamic in β-cells may open the possibility to understand their role in other tissues.

Importantly, we characterised the global null *C2cd4b* and *C2cd4a* mouse strains made by the IMPC. We observed glucose tolerance impairment in *C2cd4b* null females, indicating a role for this gene in glucose homeostasis. The glucose impairment was a result of reduction of circulating insulin rather than insulin resistance. However, direct insulin secretion in islets from these animals was not affected by deletion of *C2cd4b*, suggesting the involvement of other circulating factors such as leptin or FSH as the underlying cause of this phenotype.

Since the phenotypes observed in *C2cd4b* null mice were sex- and age- dependent, and given the high expression of this gene in the pituitary gland, we also measured FSH secretion in gonadectomised animals. Interestingly, we demonstrated that *C2cd4b* deletion in female mice causes FSH deficiency which could be argued as the core underlying reason behind the sexual dimorphism in glucose tolerance.

T2D is more prevalent in humans with higher BMI and lower physical activity (Anon, n.d.). To simulate these conditions partially in mice, we maintained *C2cd4b* animals on a high-fat and -sucrose diet from six weeks of age. The *C2cd4b* null males maintained on HFD presented with significantly higher weight gain compared to their WT littermates, a phenotype which was also linked to mutations at the *C2CD4A/C2CD4B/VPS13C* locus (Boesgaard *et al.*, 2010). Although in humans HFD mediated weight gain is observed in both genders, in mouse it is specific to males. This difference could be due to differences in the metabolism between mouse and human or could be as a result of differences between the function of these genes between the two species. We have not observed differences between the expression of *C2cd4b* in islets between male and female mice (data not shown). Also, no gender-specific differences in the expression of *C2CD4A* and *C2CD4B* has been demonstrated in humans in different tissues including pancreas (GTEx database, data not shown). However, since it has been shown in human islets that palmitate induces an elevation in the expression of *C2CD4A* (Cnop *et al.*, 2014), it would be very interesting measure to the expression of these genes in animals maintained on HFD compared to RC, as well as between human donors with different BMI.

Although the *C2cd4b* null mice showed glucose tolerance phenotype and elevated plasma insulin, *C2cd4a* null mice were comparable to WT littermates in glycaemic

traits. We did not find glucose intolerance or any deficiency in plasma insulin levels nor any reduction in GSIS/KSIS from the isolated islets from these animals compared to WTs. These results demonstrated opposite phenotypes compared to what was shown by Kuo *et al* (Boesgaard *et al.*, 2010). One could suggest that the differences observed between these two lines are as a result of compensatory mechanism caused by an increase in *C2cd4b* in the global *C2cd4a null* animals. However, we showed in human β-cells (EndoC βH1), that deletion of *C2CD4A* decreases KCl- and glucose and IBMX- induced insulin secretion (although no differences were observed when the data were normalised as fold-change). More studies need to be carried out to confirm the role of these genes in insulin secretion in human β-cells. For instance, deletion or down-regulation of *C2CD4A* (and also *C2CD4B*) in human islets and/or in EndoC βH3 cells (Benazra *et al.*, 2015), which express both these genes, can to be performed.

The relatively mild phenotype of the *C2cd4b* strain and lack of glycaemic phenotype in the *C2cd4a* line, could also be due to compensatory mechanisms caused by an increase in expression of *C2cd4a* or *C2cd4b* in these animals, respectively. This possibility is highly probably since we have already observed an increase in *C2cd4a* mRNA levels upon deletion of *C2cd4b* is the islets of *C2cd4b* null mice using RNA-seq (Table 7). This phenomenon could be due to the fact that these genes have a high sequence similarity and some functional redundancy. This similarity is more striking at the C2 domains of these genes (Figure 1. 12). The similarities between the two genes specifically in the C2 domains could suggest they could (partially) compensate each other's role in the absence of the other. Furthermore, this could potentially suggest that these genes, perhaps indirectly, control the expression of one another. Further experiments could examine these possibilities and give us a better perspective on the functions and the regulatory dynamics of these genes.

To have a more comprehensive understanding of the role of these genes, a double knockout line could be generated to eliminate the possible compensatory mechanisms between *C2CD4A* and *C2CD4B*. The latter genes are expressed in diverse tissues also in tissues having roles in glucose and metabolic homeostasis. Therefore, it is essential to generate/use tissue-specific mouse models to shed light of the role of these genes in specific tissues. To gain full advantage from a highly β-cell specific mouse model, from the commonly used transgenic mouse models, it is preferable to use Ins-*Cre* mouse line compared to RIP-*Cre* line which was used in

Kuo *et al*. study (Kuo *et al.*, 2019) . Among other factors, ectopic expression of RIP in the hypothalamus as well as the glucose intolerance phenotype observed in these mice in the absence of genes targeted by *loxP* sites (Brouwers *et al.*, 2014), are the disadvantages using the latter mouse model.

In summary, in this study we suggest a novel role for *C2CD4A* and *C2CD4B* in β-cells compared to previous studies. We provide evidence that human *C2CD4A* plays a role in insulin secretion in β-cells. More importantly, we showed that *C2cd4b* plays a role *in vivo* in glucose homeostasis and controls circulating insulin levels in response to increased glycaemia. More studies as mentioned in discussion chapters could be carried out to understand the mechanism of action of these genes in the control of insulin secretion from β-cells.

Importantly, the expression dynamics of these genes are poorly understood. Although a super enhancer region has been discovered at the intronic region between *C2CD4A* and *C2CD4B* (Miguel-Escalada *et al.*, 2018), how β-cell-enriched transcription factors regulate the expression of these genes remains to be addressed. Furthermore, the effect of the causal SNP at this locus on the expression of *C2CD4A* and *C2CD4B* is not well characterised. Previous eQTL studies (Mehta *et al.*, 2016)[,](Kycia *et al.*, 2018) aimed to address the effect of the SNPs at the *C2CD4A/C2CD4B* locus on mRNA expression. However, the results of these studies are not consistent and are in the opposite direction in the two studies. More robust studies, perhaps using a significantly larger sample size, are needed to investigate the direct effect of the causal SNPs in this locus and the regulation of the expression of these two genes in humans. Understanding how the SNPs mediate their effect in this locus could give us a better insight into the function of these genes. Revealing their unique functions specifically in β-cells in the control of insulin secretion in mice and implicating these findings in humans, may highlight these genes as potential targets to improve the treatments for T2D.

Appendix1: List of Antibodies

Antibody	Company	Ref	Dilution used
Mouse anti-FLAG	Sigma	F1804-200UG	1:1000
Guinea-Pig anti-insulin ready to use	Dako	IR002	not diluted
Mouse anti-glucagon	Sigma	G2654-100UL	1:1000
Rabbit anti-TGN46	Abcam	Ab16059	1:500
Rat anti-LAMP1	Santa Cruz	Sc-19992	1:200
Alexa Fluor 488 goat anti-guinea-pig	Invitrogen	A-11073	1:1000
Alexa Fluor 532 goat anti-rabbit	Invitrogen	A11009	1:1000
Alexa Fluor 488 goat anti-mouse	Invitrogen	A11029	1:1000

Appendix 2: Western (immuno)blots to test C2CD4A antibodies

Two antibodies against human *C2CD4A* were designed (Eurogentec). Proteins extracted from MIN6 cells, EndoC βH1 cells, and MIN6 cells transfected with *C2CD4A* construct were used as negative and positive controls to test hC2CD4A antibodies. Several bands were detected for each load of protein. However, no band (39.75 kDa) which was highly marked in EndoC βH1 cells/MIN6:*C2CD4A* and absent in MIN6 cells was detected. 25 µg of protein was loaded in each well. Dilutions were 1:50 (and 1:500, not shown).

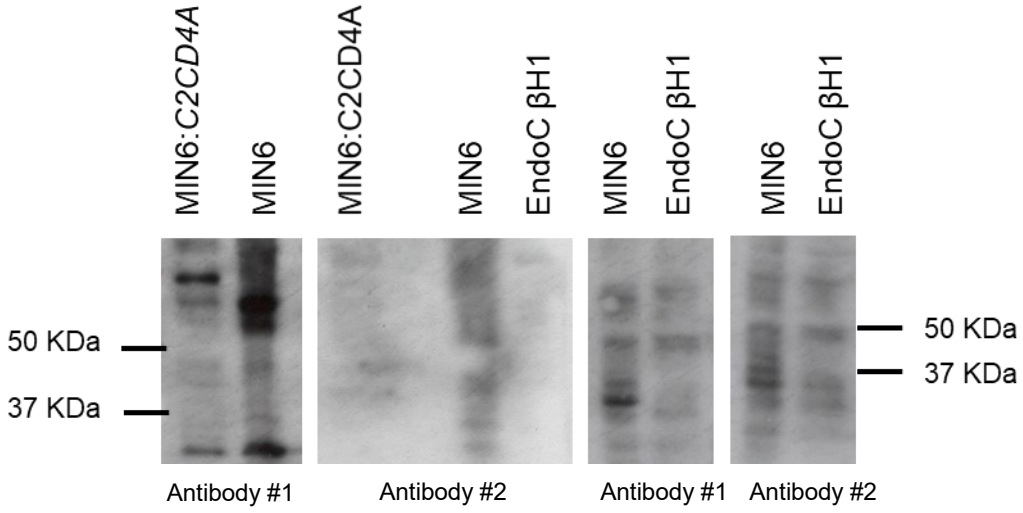

Appendix 3: List of Publications

Original (peer reviewed) articles:

Salem V., Delgadillo Silva L., Suba K., Georgiadou E., **Mousavy Gharavy S.N.,** *Akhtar* N., Martin-Alonso A., Gaboriau D., Rothery S., Stylianides T., Carrat G., Pullen T., Sinhj S. Hodson D., Leclerc I., Shapiro A.M.J., Marchetti p., Linford B., Distaso W., Ninov N., and Rutter G. A., Leader β cells coordinate Ca^{2+} dynamics across pancreatic islets 3 in vivo. ***Nature Metabolism* 1**, pages 615–629 (2019)

Janjuha S., Singh S. P., Tsakmaki A., **Mousavy Gharavy S.N.**, Murawala P., Konantz J., Hodson D.J., Rutter G. A., Bewick G. A., Ninov N., Age-related islet inflammation marks the proliferative decline of pancreatic beta-cells in zebrafish. ***e-life*,** 2018. doi: 10.7554/eLife.32965.

External oral presentations:

The Francis Crick Institute, Cell Biology & Signalling Interest Group, external speaker, Nov. 2019.
Title: Roles for the type 2 diabetes-associated genes *C2CD4A* and *C2CD4B* in the control of insulin secretion.

Published abstracts:

Mousavy, N., Li, X., Martinez-Sanchez-A., and Rutter, G.A. Putative roles of the Type 2-diabetes associated genes *C2CD4A* and *C2CD4B* in the control of insulin secretion *Diabet Med*, 34 (S1), 79 (2017) (Poster presentation, Diabetes UK Annual Conference, 2017, Manchester, U.K.)

Mousavy Gharavy, SN., Li, X, Martinez-Sanchez,A., and Rutter G.A. Roles for the type 2 diabetes-associated genes C2CD4A and C2CD4B in the control of insulin secretion. *Diabetic Med* μ35:40-41 (2018) For Diabetes UK APC, March 2018 (Poster/oral)

Salem, V., Delgadillo Silva, L-F., Suba, K., Akhtar, N., **Mousavy, N.**, Martin-Alonso, A., Georgiadou, E., Gaboriau, D.C.A., Rotheray, S., Stylianides, T., Hodson, D.J., Marchetti, P., Briant, L., Ninov, N. and Rutter, G.A. Glucose regulates pancreatic beta cell Ca^{2+} dynamics and connectivity *in vivo*. *Diabetologia* 61 (Supp1), S18. EASD Annual Conference Berlin, 2018

Mousavy, N., Martinez-Sanchez, A. and Rutter, G.A. Roles for the type 2 diabetes-associated genes *C2CD4A* and *C2CD4B* in the control of insulin secretion. *Diabetologia*, 61 (Supp1), S198. (2018) EASD Annual Conference Berlin, 2018

Mousavy-Gharavy, S.N., Hu, M., Gadue, P., Leclerc, I., Martinez-Sanchez, A., and Rutter, G.A. Roles for the type 2 diabetes-associated genes C2CD4A and C2CD4B in the control of glucose homeostasis and insulin secretion *Diabet Med*. 36 (Supp 1), p43 (P30) 2019

References

Abdel-halim, S.M., Guenifi, A., Khan, A., Larsson, O., et al. (1996) *Impaired Coupling of Glucose Signal to the Exocytotic Machinery in Diabetic GK Rats A Defect Ameliorated by cAMP*. 45 (July).

Ahrén, B. (2000) Autonomic regulation of islet hormone secretion -- Implications for health and disease. *Diabetologia*. [Online] 43 (4), 393–410. Available from: doi:10.1007/s001250051322.

Anders, S., McCarthy, D.J., Chen, Y., Okoniewski, M., et al. (2013) Count-based differential expression analysis of RNA sequencing data using R and Bioconductor. *Nature Protocols*. [Online] 8, 1765. Available from: https://doi.org/10.1038/nprot.2013.099.

Anon (n.d.) *International Diabetes Federation*. [Online]. Available from: https://www.idf.org/.

Atkinson, M.A. (2012) The pathogenesis and natural history of type 1 diabetes. *Cold Spring Harbor Perspectives in Biology*. [Online] 4 (12). Available from: doi:10.1101/cshperspect.a007641.

Bader, E., Migliorini, A., Gegg, M., Moruzzi, N., et al. (2016) Identification of proliferative and mature β-cells in the islets of Langerhans. *Nature*. [Online] 535, 430. Available from: https://doi.org/10.1038/nature18624.

Baggio, L.L. & Drucker, D.J. (2007) Biology of Incretins: GLP-1 and GIP. *Gastroenterology*. [Online] 132 (6), 2131–2157. Available from: doi:10.1053/j.gastro.2007.03.054.

Barg, S., Eliasson, L., Renström, E. & Rorsman, P. (2002) A Subset of 50 Secretory Granules in Close Contact With l-Type Ca²⁺ Channels Accounts for First-Phase Insulin Secretion in Mouse β-Cells. *Diabetes*. [Online] 51 (suppl 1), S74 LP-S82. Available from: doi:10.2337/diabetes.51.2007.S74.

Barg, S. & Rorsman, P. (2004) Insulin Secretion: Figure 1. *The Journal of General Physiology*. [Online] 124 (6), 623–625. Available from: doi:10.1085/jgp.200409206.

Barrangou, R., Fremaux, C., Deveau, H., Richards, M., et al. (2007) CRISPR Provides Acquired Resistance Against Viruses in Prokaryotes. *Science*. [Online] 315 (5819), 1709 LP – 1712. Available from: doi:10.1126/science.1138140.

Beery, A.K. & Zucker, I. (2011) Sex bias in neuroscience and biomedical research. *Neuroscience & Biobehavioral Reviews*. [Online] 35 (3), 565–572. Available from: doi:https://doi.org/10.1016/j.neubiorev.2010.07.002.

Benazra, M., Lecomte, M.J., Colace, C., Müller, A., et al. (2015) A human beta cell line with drug inducible excision of immortalizing transgenes. *Molecular Metabolism*. [Online] 4 (12), 916–925. Available from: doi:10.1016/j.molmet.2015.09.008.

Benner, C., van der Meulen, T., Cacéres, E., Tigyi, K., et al. (2014) The transcriptional landscape of mouse beta cells compared to human beta cells reveals notable species differences in long non-coding RNA and protein-coding gene expression. *BMC Genomics*. [Online] 15 (1). Available from: doi:10.1186/1471-2164-15-620.

Besterman, H.S., Cook, G.C., Sarson, D.L., Christofides, N.D., et al. (1979) Gut hormones in tropical malabsorption. *British medical journal*. [Online] 2 (6200), 1252–1255. Available from: doi:10.1136/bmj.2.6200.1252.

Beswick, R.W., Ambrose, H.E. & Wagner, S.D. (2006) Nocodazole, a microtubule depolymerising agent, induces apoptosis of chronic lymphocytic leukaemia cells associated with changes in Bcl-2 phosphorylation and expression. *Leukemia Research*. [Online] 30 (4), 427–436. Available from: doi:https://doi.org/10.1016/j.leukres.2005.08.009.

Blodgett, D.M., Nowosielska, A., Afik, S., Pechhold, S., et al. (2015) Novel observations from next-generation RNA sequencing of highly purified human adult and fetal islet cell subsets. *Diabetes*. [Online] 64 (9), 3172–3181. Available from: doi:10.2337/db15-0039.

Bocian-Sobkowska, J., Zabel, M., Wozniak, W. & Surdyk-Zasada, J. (1999) Polyhormonal aspect of the endocrine cells of the human fetal pancreas. *Histochemistry and Cell Biology*. [Online] 112 (2), 147–153. Available from: doi:10.1007/s004180050401.

Boesgaard, T.W., Grarup, N., Jørgensen, T., Borch-Johnsen, K., et al. (2010) Variants at DGKB/TMEM195, ADRA2A, GLIS3 and C2CD4B loci are associated with reduced glucose-stimulated beta cell function in middle-aged Danish people. *Diabetologia*. [Online] 53 (8), 1647–1655. Available from: doi:10.1007/s00125-010-1753-5.

Brickner, J.H. & Fuller, R.S. (1997) SOI1 encodes a novel, conserved protein that promotes TGN- endosomal cycling of Kex2p and other membrane proteins by modulating the function of two TGN localization signals. *Journal of Cell Biology*. [Online] 139 (1), 23–36. Available from: doi:10.1083/jcb.139.1.23.

Brissova, M., Fowler, M.J., Nicholson, W.E., Chu, A., et al. (2005) Assessment of human pancreatic islet architecture and composition by laser scanning confocal microscopy. *Journal of Histochemistry and Cytochemistry*. [Online] 53 (9), 1087–1097. Available from: doi:10.1369/jhc.5C6684.2005.

Brouwers, B., De Faudeur, G., Osipovich, A.B., Goyvaerts, L., et al. (2014) Impaired islet function in commonly used transgenic mouse lines due to human growth hormone minigene expression. *Cell Metabolism*. [Online] 20 (6), 979–990. Available from: doi:10.1016/j.cmet.2014.11.004.

Bruns, D. & Jahn, R. (2002) Molecular determinants of exocytosis. *Pflügers Archiv*. [Online] 443 (3), 333–338. Available from: doi:10.1007/s00424-001-0742-4.

Burlison, J.S., Long, Q., Fujitani, Y., Wright, C.V.E., et al. (2008) Pdx-1 and

Ptf1a concurrently determine fate specification of pancreatic multipotent progenitor cells. *Developmental Biology*. [Online] 316 (1), 74–86. Available from: doi:10.1016/j.ydbio.2008.01.011.

Burton, P.R., Clayton, D.G., Cardon, L.R., Craddock, N., et al. (2007) Genome-wide association study of 14,000 cases of seven common diseases and 3,000 shared controls. *Nature*. [Online] 447 (7145), 661–678. Available from: doi:10.1038/nature05911.

Busby, M.A., Stewart, C., Miller, C.A., Grzeda, K.R., et al. (2013) Scotty: a web tool for designing RNA-Seq experiments to measure differential gene expression. *Bioinformatics*. [Online] 29 (5), 656–657. Available from: doi:10.1093/bioinformatics/btt015.

Cacheiro, P., Haendel, M.A., Smedley, D., the International Mouse Phenotyping Consortium and the Monarch Initiative, et al. (2019) New models for human disease from the International Mouse Phenotyping Consortium. *Mammalian Genome*. [Online] 30 (5), 143–150. Available from: doi:10.1007/s00335-019-09804-5.

Catterall, W.A. (2000) Structure and Regulation of Voltage-Gated Ca 2+ Channels. *Annual Review of Cell and Developmental Biology*. [Online] 16 (1), 521–555. Available from: doi:10.1146/annurev.cellbio.16.1.521.

Cells, P.I., Thorens, B. & Sarkar, H.K. (1988) *Cloning and Functional Expression in Bacteria of a Novel G lucose Transporter Present in Liver ,*. 55, 281–290.

Chan, O. & Sherwin, R.S. (2012) Hypothalamic Regulation of Glucose-Stimulated Insulin Secretion. *Diabetes*. [Online] 61 (3), 564 LP – 565. Available from: doi:10.2337/db11-1846.

Chance, R.E., Ellis, R.M. & Bromer, W.W. (1968) Porcine proinsulin: Characterization and amino acid sequence. *Science*. [Online] 161 (3837), 165–167. Available from: doi:10.1126/science.161.3837.165.

Cheng, P.-C. (2006) The Contrast Formation in Optical Microscopy. In: James B Pawley (ed.). *Handbook Of Biological Confocal Microscopy*. [Online]. Boston, MA, Springer US. pp. 162–206. Available from: doi:10.1007/978-0-387-45524-2_8.

Cho, Y.M., Merchant, C.E. & Kieffer, T.J. (2012) Targeting the glucagon receptor family for diabetes and obesity therapy. *Pharmacology and Therapeutics*. [Online] 135 (3), 247–278. Available from: doi:10.1016/j.pharmthera.2012.05.009.

Claussnitzer, M., Dankel, S.N., Klocke, B., Grallert, H., et al. (2014) Leveraging Cross-Species Transcription Factor Binding Site Patterns: From Diabetes Risk Loci to Disease Mechanisms. *Cell*. [Online] 156 (1), 343–358. Available from: doi:https://doi.org/10.1016/j.cell.2013.10.058.

Cnop, M., Abdulkarim, B., Bottu, G., Cunha, D.A., et al. (2014) RNA Sequencing Identifies Dysregulation of the Human Pancreatic Islet

Transcriptome by the Saturated Fatty Acid Palmitate. *Diabetes*. [Online] 63 (6), 1978 LP – 1993. Available from: doi:10.2337/db13-1383.

Corbalán-García, S. & Gómez-Fernández, J.C. (2010) The C2 domains of classical and novel PKCs as versatile decoders of membrane signals. *BioFactors*. [Online] 36 (1), 1–7. Available from: doi:10.1002/biof.68.

Corkey, B.E. (2012) Banting Lecture 2011. *Diabetes*. [Online] 61 (1), 4 LP – 13. Available from: doi:10.2337/db11-1483.

Cowley, M.A., Smart, J.L., Rubinstein, M., Cerdán, M.G., et al. (2001) Leptin activates anorexigenic POMC neurons through a neural network in the arcuate nucleus. *Nature*. [Online] 411 (6836), 480–484. Available from: doi:10.1038/35078085.

Crespin, S.R., Greenough III, W.B. & Steinberg, D. (1969) Stimulation of insulin secretion by infusion of free fatty acids. *The Journal of Clinical Investigation*. [Online] 48 (10), 1934–1943. Available from: doi:10.1172/JCI106160.

Cui, B., Zhu, X., Xu, M., Guo, T., et al. (2011) A Genome-Wide association study confirms previously reported loci for type 2 diabetes in Han Chinese. *PLoS ONE*. [Online] 6 (7). Available from: doi:10.1371/journal.pone.0022353.

Curry, D.L., Bennet, L.L. & Grodsky, G.M. (1968) Dynamics of Insulin Secretion by the Perfused Rat Pancreas. *Endocrinology*. [Online] 83 (3), 572–584. Available from: doi:10.1210/endo-83-3-572.

Dalvi, P.S., Nazarians-Armavil, A., Purser, M.J. & Belsham, D.D. (2012) Glucagon-Like Peptide-1 Receptor Agonist, Exendin-4, Regulates Feeding-Associated Neuropeptides in Hypothalamic Neurons in Vivo and in Vitro. *Endocrinology*. [Online] 153 (5), 2208–2222. Available from: doi:10.1210/en.2011-1795.

Dhanvantari, S., Seidah, N.G. & Brubaker, P.L. (1996) Role of prohormone convertases in the tissue-specific processing of proglucagon. *Molecular Endocrinology*. [Online] 10 (4), 342–355. Available from: doi:10.1210/mend.10.4.8721980.

Dolenšek, J., Rupnik, M.S., Stožer, A. & Dolen, J. (2015) *Structural similarities and differences between the human and the mouse pancreas Structural similarities and differences between the human and the mouse pancreas*. [Online] 2014. Available from: doi:10.1080/19382014.2015.1024405.

Dong, P.D.S., Provost, E., Leach, S.D. & Stainier, D.Y.R. (2008) Graded levels of Ptf1a differentially regulate endocrine and exocrine fates in the developing pancreas. *Genes and Development*. [Online] 22 (11), 1445–1450. Available from: doi:10.1101/gad.1663208.

Dorrell, C., Schug, J., Canaday, P.S., Russ, H.A., et al. (2016) Human islets contain four distinct subtypes of β cells. *Nature Communications*. [Online] 7 (1), 11756. Available from: doi:10.1038/ncomms11756.

Drucker, D.J., Philippe, J., Mojsov, S., Chick, W.L., et al. (1987) Glucagon-like peptide I stimulates insulin gene expression and increases cyclic AMP levels in a rat islet cell line. *Proceedings of the National Academy of Sciences*. [Online] 84 (10), 3434 LP – 3438. Available from: doi:10.1073/pnas.84.10.3434.

Dupuis, J., Langenberg, C., Prokopenko, I., Saxena, R., et al. (2010) New genetic loci implicated in fasting glucose homeostasis and their impact on type 2 diabetes risk. *Nature Genetics*. [Online] 42 (2), 105–116. Available from: doi:10.1038/ng.520.

Dwivedi, O.P., Lehtovirta, M., Hastoy, B., Chandra, V., et al. (2019) Loss of ZnT8 function protects against diabetes by enhanced insulin secretion. *Nature Genetics*. [Online] 51 (11), 1596–1606. Available from: doi:10.1038/s41588-019-0513-9.

Eizirik, D.L., Sammeth, M., Bouckenooghe, T., Bottu, G., et al. (2012) The Human Pancreatic Islet Transcriptome: Expression of Candidate Genes for Type 1 Diabetes and the Impact of Pro-Inflammatory Cytokines. *PLOS Genetics*. [Online] 8 (3), e1002552. Available from: https://doi.org/10.1371/journal.pgen.1002552.

Eliasson, L., Abdulkader, F., Braun, M., Galvanovskis, J., et al. (2008) Novel aspects of the molecular mechanisms controlling insulin secretion. *Journal of Physiology*. [Online] 586 (14), 3313–3324. Available from: doi:10.1113/jphysiol.2008.155317.

Færch, K., Pacini, G., Nolan, J.J., Hansen, T., et al. (2013) Impact of Glucose Tolerance Status, Sex, and Body Size on Glucose Absorption Patterns During OGTTs. *Diabetes Care*. [Online] 36 (11), 3691 LP – 3697. Available from: doi:10.2337/dc13-0592.

Fajans, S.S., Bell, G.I. & Polonsky, K.S. (2001) Molecular Mechanisms and Clinical Pathophysiology of Maturity-Onset Diabetes of the Young. *New England Journal of Medicine*. [Online] 345 (13), 971–980. Available from: doi:10.1056/NEJMra002168.

Ferdaoussi, M., Bergeron, V., Zarrouki, B., Kolic, J., et al. (2012) G protein-coupled receptor (GPR)40-dependent potentiation of insulin secretion in mouse islets is mediated by protein kinase D1. *Diabetologia*. [Online] 55 (10), 2682–2692. Available from: doi:10.1007/s00125-012-2650-x.

Flanagan, S.E., Dũng, V.C., Houghton, J.A.L., De Franco, E., et al. (2017) An ABCC8 Nonsense Mutation Causing Neonatal Diabetes Through Altered Transcript Expression. *Journal of clinical research in pediatric endocrinology*. [Online] 9 (3), 260–264. Available from: doi:10.4274/jcrpe.4624.

Flannick, J., Thorleifsson, G., Beer, N.L., Jacobs, S.B.R., et al. (2014) Loss-of-function mutations in SLC30A8 protect against type 2 diabetes. *Nature Genetics*. [Online] 46 (4), 357–363. Available from: doi:10.1038/ng.2915.

Fogarty, M.P., Cannon, M.E., Vadlamudi, S., Gaulton, K.J., et al. (2014)

Identification of a regulatory variant that binds FOXA1 and FOXA2 at the CDC123/CAMK1D type 2 diabetes GWAS locus. *PLoS genetics*. [Online] 10 (9), e1004633–e1004633. Available from: doi:10.1371/journal.pgen.1004633.

Fogarty, M.P., Panhuis, T.M., Vadlamudi, S., Buchkovich, M.L., et al. (2013) Allele-Specific Transcriptional Activity at Type 2 Diabetes–Associated Single Nucleotide Polymorphisms in Regions of Pancreatic Islet Open Chromatin at the JAZF1 Locus. *Diabetes*. [Online] 62 (5), 1756 LP – 1762. Available from: doi:10.2337/db12-0972.

Frayling, T.M., Evans, J.C., Bulman, M.P., Pearson, E., et al. (2001) beta-cell genes and diabetes: molecular and clinical characterization of mutations in transcription factors. *Diabetes*. [Online] 50 (suppl 1), S94. Available from: doi:10.2337/diabetes.50.2007.S94.

Fredriksson, S., Gullberg, M., Jarvius, J., Olsson, C., et al. (2002) Protein detection using proximity-dependent DNA ligation assays. *Nature Biotechnology*. [Online] 20 (5), 473–477. Available from: doi:10.1038/nbt0502-473.

Frias, J.P., Macaraeg, G.B., Ofrecio, J., Yu, J.G., et al. (2001) Decreased Susceptibility to Fatty Acid–Induced Peripheral Tissue Insulin Resistance in Women. *Diabetes*. [Online] 50 (6), 1344 LP – 1350. Available from: doi:10.2337/diabetes.50.6.1344.

Fukui, K., Yang, Q., Cao, Y., Takahashi, N., et al. (2005) The HNF-1 target Collectrin controls insulin exocytosis by SNARE complex formation. *Cell Metabolism*. [Online] 2 (6), 373–384. Available from: doi:10.1016/j.cmet.2005.11.003.

Gautam, D., de Azua, I.R., Li, J.H., Guettier, J.-M., et al. (2010) Beneficial Metabolic Effects Caused by Persistent Activation of β-Cell M3 Muscarinic Acetylcholine Receptors in Transgenic Mice. *Endocrinology*. [Online] 151 (11), 5185–5194. Available from: doi:10.1210/en.2010-0519.

Gilbert, S.F. (2014) *Developmental Biology*. 10th edition. Andrew D. Sinauer.

Gilontj, P. (1992) *Influence of Membrane Potential Changes on Cytoplasmic Ca2 ' Concentration in an Electrically Excitable Cell , the Insulin-secreting Pancreatic B-cell **.

Giordano, E., Bosco, D., Cirulli, V. & Meda, P. (1991) Repeated glucose stimulation reveals distinct and lasting secretion patterns of individual rat pancreatic B cells. *The Journal of Clinical Investigation*. [Online] 87 (6), 2178–2185. Available from: doi:10.1172/JCI115251.

Gittes, G.K. (2009) Developmental biology of the pancreas : A comprehensive review. *Developmental Biology*. [Online] 326 (1), 4–35. Available from: doi:10.1016/j.ydbio.2008.10.024.

Gittes, G.K. & Rutter, W.J. (1992) Onset of cell-specific gene expression in the developing mouse pancreas. *Proceedings of the National Academy of*

Sciences of the United States of America. [Online] 89 (3), 1128–1132. Available from: doi:10.1073/pnas.89.3.1128.

Gloyn, A.L., Pearson, E.R., Antcliff, J.F., Proks, P., et al. (2004) Activating mutations in the gene encoding the ATP-sensitive potassium-channel subunit Kir6.2 and permanent neonatal diabetes. *New England Journal of Medicine*. [Online] 350 (18), 1838–1849. Available from: doi:10.1056/NEJMoa032922.

Goodge, K.A. & Hutton, J.C. (2000) Translational regulation of proinsulin biosynthesis and proinsulin conversion in the pancreatic β-cell. *Seminars in Cell and Developmental Biology*. [Online] 11 (4), 235–242. Available from: doi:10.1006/scdb.2000.0172.

Gookin, S., Min, M., Phadke, H., Chung, M., et al. (2017) A map of protein dynamics during cell-cycle progression and cell-cycle exit. *PLOS Biology*. [Online] 15 (9), e2003268. Available from: https://doi.org/10.1371/journal.pbio.2003268.

Grant, S.F.A., Thorleifsson, G., Reynisdottir, I., Benediktsson, R., et al. (2006) Variant of transcription factor 7-like 2 (TCF7L2) gene confers risk of type 2 diabetes. *Nature Genetics*. [Online] 38 (3), 320–323. Available from: doi:10.1038/ng1732.

Grarup, N., Overvad, M., Sparsø, T., Witte, D.R., et al. (2011) The diabetogenic VPS13C/C2CD4A/C2CD4B rs7172432 variant impairs glucose-stimulated insulin response in 5,722 non-diabetic Danish individuals. *Diabetologia*. [Online] 54 (4), 789–794. Available from: doi:10.1007/s00125-010-2031-2.

Gromada, J., Bokvist, K., Ding, W.-G., Holst, J.J., et al. (1998) Glucagon-Like Peptide 1(7-36) Amide Stimulates Exocytosis in Human Pancreatic β-Cells by Both Proximal and Distal Regulatory Steps in Stimulus-Secretion Coupling. *Diabetes*. [Online] 47 (1), 57 LP – 65. Available from: doi:10.2337/diab.47.1.57.

Grotz, A.K., Gloyn, A.L. & Thomsen, S.K. (2017) Prioritising Causal Genes at Type 2 Diabetes Risk Loci. *Current Diabetes Reports*. [Online] 17 (9), 1–9. Available from: doi:10.1007/s11892-017-0907-y.

Gu, G., Dubauskaite, J. & Melton, D.A. (2002) Direct evidence for the pancreatic lineage: NGN3+ cells are islet progenitors and are distinct from duct progenitors. *Development*. 129 (10), 2447–2457.

Gutierrez, G.D., Gromada, J. & Sussel, L. (2017) Heterogeneity of the Pancreatic Beta Cell. *Frontiers in Genetics*. [Online] 8, 22. Available from: doi:10.3389/fgene.2017.00022.

Hagège, H., Klous, P., Braem, C., Splinter, E., et al. (2007) Quantitative analysis of chromosome conformation capture assays (3C-qPCR). *Nature Protocols*. [Online] 2, 1722. Available from: https://doi.org/10.1038/nprot.2007.243.

Hay, C.W. & Docherty, K. (2006) Comparative Analysis of Insulin Gene

Promoters. *Diabetes*. [Online] 55 (12), 3201 LP – 3213. Available from: doi:10.2337/db06-0788.

Heart, E., Corkey, R.F., Wikstrom, J.D., Shirihai, O.S., et al. (2006) Glucose-dependent increase in mitochondrial membrane potential, but not cytoplasmic calcium, correlates with insulin secretion in single islet cells. *American Journal of Physiology-Endocrinology and Metabolism*. [Online] 290 (1), E143–E148. Available from: doi:10.1152/ajpendo.00216.2005.

Hebrok, M., Kim, S.K. & Melton, D.A. (1998) Notochord repression of endodermal sonic hedgehog permits pancreas development. *Genes and Development*. [Online] 12 (11), 1705–1713. Available from: doi:10.1101/gad.12.11.1705.

Henquin, J.-C., Nenquin, M., Stiernet, P. & Ahren, B. (2006) In Vivo and In Vitro Glucose-Induced Biphasic Insulin Secretion in the Mouse. *Diabetes*. [Online] 55 (2), 441 LP – 451. Available from: doi:10.2337/diabetes.55.02.06.db05-1051.

Henquin, J.C. (2009) Regulation of insulin secretion: A matter of phase control and amplitude modulation. *Diabetologia*. [Online] 52 (5), 739–751. Available from: doi:10.1007/s00125-009-1314-y.

Henquin, J.C. (2000) Triggering and amplifying pathways of regulation of insulin secretion by glucose. *Diabetes*. [Online]. 49 (11) pp.1751–1760. Available from: doi:10.2337/diabetes.49.11.1751.

Henquin, J.C. & Nenquin, M. (1988) The muscarinic receptor subtype in mouse pancreatic B-cells. *FEBS Letters*. [Online] 236 (1), 89–92. Available from: doi:10.1016/0014-5793(88)80290-4.

Herrmann, C., Göke, R., Richter, G., Fehmann, H.-C., et al. (1995) Glucagon-Like Peptide-1 and Glucose-Dependent Insulin-Releasing Polypeptide Plasma Levels in Response to Nutrients. *Digestion*. [Online] 56 (2), 117–126. Available from: doi:10.1159/000201231.

Hodel, A. & Edwardson, J.M. (2000) Targeting of the zymogen-granule protein syncollin in AR42J and AtT-20 cells. *The Biochemical journal*. [Online] 350 Pt 3 (Pt 3), 637–643. Available from: https://www.ncbi.nlm.nih.gov/pubmed/10970774.

Hodson, D.J., Mitchell, R.K., Marselli, L., Pullen, T.J., et al. (2014) ADCY5 Couples Glucose to Insulin Secretion in Human Islets. *Diabetes*. [Online] 63 (9), 3009 LP – 3021. Available from: doi:10.2337/db13-1607.

Hohmeier, H.E., Mulder, H., Chen, G., Henkel-rieger, R., et al. (2000a) *Isolation of INS-1–Derived Cell Lines With Robust ATP-Sensitive K + Channel-Dependent and -Independent Glucose-Stimulated Insulin Secretion*. 49 (March).

Hohmeier, H.E., Mulder, H., Chen, G., Henkel-Rieger, R., et al. (2000b) Isolation of INS-1-derived cell lines with robust ATP-sensitive K+ channel-dependent and -independent glucose-stimulated insulin secretion.

Diabetes. [Online] 49 (3), 424–430. Available from: doi:10.2337/diabetes.49.3.424.

Holst, J.J., Gribble, F., Horowitz, M. & Rayner, C.K. (2016) Roles of the gut in glucose homeostasis. *Diabetes Care*. [Online] 39 (6), 884–892. Available from: doi:10.2337/dc16-0351.

Huyghe, J.R., Jackson, A.U., Fogarty, M.P., Buchkovich, M.L., et al. (2013) Exome array analysis identifies new loci and low-frequency variants influencing insulin processing and secretion. *Nature Genetics*. [Online] 45 (2), 197–201. Available from: doi:10.1038/ng.2507.

Idevall-hagren, O., Lü, A., Xie, B. & Camilli, P. De (2015) *Triggered Ca 2 + influx is required for extended membrane tethering*. 34 (17), 2291–2305.

Infirmary, R. (1977) *Diabetologia*. 486, 481–486.

Ingelsson, E., Langenberg, C., Hivert, M., Prokopenko, I., et al. (2010) *Detailed Physiologic Characterization Reveals Diverse Mechanisms for Novel Genetic Loci Regulating Glucose and Insulin Metabolism in Humans*. [Online] 59 (May). Available from: doi:10.2337/DB09-1568.E.I.

Ingvorsen, C., Karp, N.A. & Lelliott, C.J. (2017) The role of sex and body weight on the metabolic effects of high-fat diet in C57BL/6N mice. *Nutrition and Diabetes*. [Online] 7 (4), e261-7. Available from: doi:10.1038/nutd.2017.6.

Islam, Md. Shahidul, C.A.F. and W.S.S. (n.d.) *Calcium Signaling*. Springer Dordrecht Heidelberg New York London.

Jennings, R., Berry, A., Preston, R., Roberts, N., et al. (2013) Development of the Human Pancreas From Foregut to Endocrine Commitment. *Diabetes*. [Online] 62. Available from: doi:10.2337/db12-1479.

Jijakli, H. & Malaisse, W.J. (1997) *Cationic Events Stimulated by D-Glucose in Depolarized Islet Cells*. 9 (3), 283–290.

Johnson, J.D., Bernal-Mizrachi, E., Alejandro, E.U., Han, Z., et al. (2006) Insulin protects islets from apoptosis via Pdx1 and specific changes in the human islet proteome. *Proceedings of the National Academy of Sciences*. [Online] 103 (51), 19575 LP – 19580. Available from: doi:10.1073/pnas.0604208103.

Johnston, N.R., Mitchell, R.K., Haythorne, E., Pessoa, M.P., et al. (2016a) Beta Cell Hubs Dictate Pancreatic Islet Responses to Glucose. *Cell Metabolism*. [Online] 24 (3), 389–401. Available from: doi:10.1016/j.cmet.2016.06.020.

Johnston, N.R., Mitchell, R.K., Haythorne, E., Pessoa, M.P., et al. (2016b) Beta Cell Hubs Dictate Pancreatic Islet Responses to Glucose. *Cell Metabolism*. [Online] 24 (3), 389–401. Available from: doi:10.1016/j.cmet.2016.06.020.

Jørgensen, M.C., Ahnfelt-Rønne, J., Hald, J., Madsen, O.D., et al. (2007) An Illustrated Review of Early Pancreas Development in the Mouse. *Endocrine Reviews*. [Online] 28 (6), 685–705. Available from: doi:10.1210/er.2007-0016.

Kallman, F. & Grobstein, C. (1964) Fine Structure of Differentiating Mouse Pancreatic Exocrine Cells in Transfilter Culture. *The Journal of cell biology*. [Online] 20, 399–413. Available from: doi:10.1083/jcb.20.3.399.

Karastergiou, K., Smith, S.R., Greenberg, A.S. & Fried, S.K. (2012) *Sex differences in human adipose tissues – the biology of pear shape Kalypso Karastergiou, MD, PhD and Susan K. Fried, PhD*. 617–638.

Kone, M., Pullen, T.J., Sun, G., Ibberson, M., et al. (2014) LKB1 and AMPK differentially regulate pancreatic β-cell identity. *FASEB Journal*. [Online] 28 (11), 4972–4985. Available from: doi:10.1096/fj.14-257667.

Koole, C., Pabreja, K., Savage, E.E., Wootten, D., et al. (2013) Recent advances in understanding GLP-1R (glucagon-like peptide-1 receptor) function. *Biochemical Society Transactions*. [Online] 41 (1), 172–179. Available from: doi:10.1042/BST20120236.

Kubosaki, A., Nakamura, S., Clark, A., Morris, J.F., et al. (2006) Disruption of the transmembrane dense core vesicle proteins IA-2 and IA-2β causes female infertility. *Endocrinology*. [Online] 147 (2), 811–815. Available from: doi:10.1210/en.2005-0638.

Kuo, T., Kraakman, M.J., Damle, M., Gill, R., et al. (2019) Identification of C2CD4A as a human diabetes susceptibility gene with a role in {beta} cell insulin secretion. *Proceedings of the National Academy of Sciences of the United States of America*. [Online] 1–10. Available from: doi:10.1073/pnas.1904311116.

Kycia, I., Wolford, B.N., Huyghe, J.R., Fuchsberger, C., et al. (2018) A Common Type 2 Diabetes Risk Variant Potentiates Activity of an Evolutionarily Conserved Islet Stretch Enhancer and Increases C2CD4A and C2CD4B Expression. *American Journal of Human Genetics*. [Online] 102 (4), 620–635. Available from: doi:10.1016/j.ajhg.2018.02.020.

Lammert, E., Cleaver, O. & Melton, D. (2001) Induction of pancreatic differentiation by signals from blood vessels. *Science*. [Online] 294 (5542), 564–567. Available from: doi:10.1126/science.1064344.

Li, J., Klughammer, J., Farlik, M., Penz, T., et al. (2016) Single-cell transcriptomes reveal characteristic features of human pancreatic islet cell types. *EMBO reports*. [Online] 17 (2), 178–187. Available from: doi:10.15252/embr.201540946.

Lin, H. V, Ren, H., Samuel, V.T., Lee, H.-Y., et al. (2011) Diabetes in mice with selective impairment of insulin action in Glut4-expressing tissues. *Diabetes*. [Online] 60 (3), 700–709. Available from: doi:10.2337/db10-1056.

Ling, Z., Chen, M.-C., Smismans, A., Pavlovic, D., et al. (1998) Intercellular Differences in Interleukin 1β-Induced Suppression of Insulin Synthesis and Stimulation of Noninsulin Protein Synthesis by Rat Pancreatic β-Cells*. *Endocrinology*. [Online] 139 (4), 1540–1545. Available from: doi:10.1210/endo.139.4.5894.

Lomedico, P., Rosenthal, N., Efstratiadis, A., Gilbert, W., et al. (1979) The structure and evolution of the two nonallelic rat preproinsulin genes. *Cell*. [Online] 18 (2), 545–558. Available from: doi:10.1016/0092-8674(79)90071-0.

Love, M.I., Huber, W. & Anders, S. (2014) Moderated estimation of fold change and dispersion for RNA-seq data with DESeq2. *Genome Biology*. [Online] 15 (12), 550. Available from: doi:10.1186/s13059-014-0550-8.

Lynn, F.C., Pamir, N., Ng, E.H.C., McIntosh, C.H.S., et al. (2001) Defective Glucose-Dependent Insulinotropic Polypeptide Receptor Expression in Diabetic Fatty Zucker Rats. *Diabetes*. [Online] 50 (5), 1004 LP – 1011. Available from: doi:10.2337/diabetes.50.5.1004.

Maechler, P. & Wollheim, C.B. (2000) *Topical Review Mitochondrial signals in glucose-stimulated insulin secretion in the beta cell*. (April), 49–56.

Mahajan, A., Go, M.J., Zhang, W., Below, J.E., et al. (2014) Genome-wide trans-ancestry meta-analysis provides insight into the genetic architecture of type 2 diabetes susceptibility. *Nature Genetics*. [Online] 46 (3), 234–244. Available from: doi:10.1038/ng.2897.

Mahajan, A., Taliun, D., Thurner, M., Robertson, N.R., et al. (2018a) Fine-mapping of an expanded set of type 2 diabetes loci to single-variant resolution using high-density imputation and islet-specific epigenome maps. *Nature Genetics*. [Online] 245506. Available from: doi:10.1101/245506.

Mahajan, A., Wessel, J., Willems, S.M., Zhao, W., et al. (2018b) Refining the accuracy of validated target identification through coding variant fine-mapping in type 2 diabetes article. *Nature Genetics*. [Online] 50 (4), 559–571. Available from: doi:10.1038/s41588-018-0084-1.

Mali, P., Esvelt, K.M. & Church, G.M. (2013) Cas9 as a versatile tool for engineering biology. *Nature Methods*. [Online] 10, 957. Available from: https://doi.org/10.1038/nmeth.2649.

Martinez-Sanchez, A., Pullen, T.J., Chabosseau, P., Zhang, Q., et al. (2016) Disallowance of Acot7 in β-cells is required for normal glucose tolerance and insulin secretion. *Diabetes*. [Online] 65 (5), 1268–1282. Available from: doi:10.2337/db15-1240.

Marullo, L., El-Sayed Moustafa, J.S. & Prokopenko, I. (2014) Insights into the genetic susceptibility to type 2 diabetes from genome-wide association studies of glycaemic traits. *Current diabetes reports*. [Online] 14 (11), 1–30. Available from: doi:10.1007/s11892-014-0551-8.

Mauvais-Jarvis, F. (2017) Epidemiology of Gender Differences in Diabetes and Obesity. In: Franck Mauvais-Jarvis (ed.). *Sex and Gender Factors Affecting Metabolic Homeostasis, Diabetes and Obesity*. [Online]. Cham, Springer International Publishing. pp. 3–8. Available from: doi:10.1007/978-3-319-70178-3_1.

Mauvais-Jarvis, F. (2015) Sex differences in metabolic homeostasis, diabetes, and obesity. *Biology of Sex Differences*. [Online] 6 (1), 1–9. Available from: doi:10.1186/s13293-015-0033-y.

Mauvais-Jarvis, F., Clegg, D.J. & Hevener, A.L. (2013) The Role of Estrogens in Control of Energy Balance and Glucose Homeostasis. *Endocrine Reviews*. [Online] 34 (3), 309–338. Available from: doi:10.1210/er.2012-1055.

Le May, C., Chu, K., Hu, M., Ortega, C.S., et al. (2006) Estrogens protect pancreatic β-cells from apoptosis and prevent insulin-deficient diabetes mellitus in mice. *Proceedings of the National Academy of Sciences*. [Online] 103 (24), 9232 LP – 9237. Available from: doi:10.1073/pnas.0602956103.

McCulloch, L.J., van de Bunt, M., Braun, M., Frayn, K.N., et al. (2011) GLUT2 (SLC2A2) is not the principal glucose transporter in human pancreatic beta cells: Implications for understanding genetic association signals at this locus. *Molecular Genetics and Metabolism*. [Online] 104 (4), 648–653. Available from: doi:https://doi.org/10.1016/j.ymgme.2011.08.026.

McEwen, B.S. & Reagan, L.P. (2004) Glucose transporter expression in the central nervous system: Relationship to synaptic function. *European Journal of Pharmacology*. [Online] 490 (1–3), 13–24. Available from: doi:10.1016/j.ejphar.2004.02.041.

Medici, F., Hawa, M., Ianari, A., Pyke, D.A., et al. (1999) Concordance rate for Type II diabetes mellitus in monozygotic twins: actuarial analysis. *Diabetologia*. [Online] 42 (2), 146–150. Available from: doi:10.1007/s001250051132.

Mehta, Z.B., Fine, N., Pullen, T.J., Cane, M.C., et al. (2016) Changes in the expression of the type 2 diabetes-associated gene *VPS13C* in the β-cell are associated with glucose intolerance in humans and mice. *American Journal of Physiology - Endocrinology And Metabolism*. [Online] 311 (2), E488–E507. Available from: doi:10.1152/ajpendo.00074.2016.

Meredith, M., Rabaglia, M.E. & Metz, S.A. (1995) *Evidence of a Role for GTP in the Potentiation of Ca2 " -induced Insulin Secretion by Glucose in Intact Rat Islets*. 96 (August), 811–821.

Merino, P.L.H. (2004) Developmental biology of the pancreas. *Cell biochemistry and biophysics*. 40 (3 Suppl), 127–142.

Miguel-Escalada, I., Bonàs-Guarch, S., Cebola, I., Joan, P.-C., et al. (2018) Human pancreatic islet 3D chromatin architecture provides insights into the genetics of type 2 diabetes. *Nature Genetics*. [Online] 51 (July), 400291. Available from: doi:10.1101/400291.

Miguel-Escalada, I., Bonàs-Guarch, S., Cebola, I., Ponsa-Cobas, J., et al. (2019) Human pancreatic islet three-dimensional chromatin architecture provides insights into the genetics of type 2 diabetes. *Nature Genetics*. [Online] 51 (7), 1137–1148. Available from: doi:10.1038/s41588-019-0457-0.

Millership, S.J., Da Silva Xavier, G., Choudhury, A.I., Bertazzo, S., et al. (2018) Neuronatin regulates pancreatic β cell insulin content and secretion. *Journal of Clinical Investigation*. [Online] 128 (8), 3369–3381. Available from: doi:10.1172/JCI120115.

Mitchell, K.J., Lai, F.A. & Rutter, G.A. (2003) Ryanodine receptor type I and nicotinic acid adenine dinucleotide phosphate receptors mediate Ca2+ release from insulin-containing vesicles in living pancreatic β-cells (MIN6). *Journal of Biological Chemistry*. [Online] 278 (13), 11057–11064. Available from: doi:10.1074/jbc.M210257200.

Miyazaki, J.-I., Araki, K., Yamato, E., Ikegami, H., et al. (1990) Establishment of a Pancreatic β Cell Line That Retains Glucose-Inducible Insulin Secretion: Special Reference to Expression of Glucose Transporter Isoforms*. *Endocrinology*. [Online] 127 (1), 126–132. Available from: doi:10.1210/endo-127-1-126.

Montgomery, M.K., Hallahan, N.L., Brown, S.H., Liu, M., et al. (2013) Mouse strain-dependent variation in obesity and glucose homeostasis in response to high-fat feeding. *Diabetologia*. [Online] 56 (5), 1129–1139. Available from: doi:10.1007/s00125-013-2846-8.

Morton, G.J., Cummings, D.E., Baskin, D.G., Barsh, G.S., et al. (2006) Central nervous system control of food intake and body weight. *Nature*. [Online] 443 (7109), 289–295. Available from: doi:10.1038/nature05026.

Mueckler, M. & Thorens, B. (2013) Molecular Aspects of Medicine The SLC2 (GLUT) family of membrane transporters q. *Molecular Aspects of Medicine*. [Online] 34 (2–3), 121–138. Available from: doi:10.1016/j.mam.2012.07.001.

Muraro, M.J., Dharmadhikari, G., Grün, D., Groen, N., et al. (2016) A Single-Cell Transcriptome Atlas of the Human Pancreas. *Cell Systems*. [Online] 3 (4), 385-394.e3. Available from: doi:10.1016/j.cels.2016.09.002.

Nagy, T.R., Gower, B.A., Trowbridge, C.A., Dezenberg, C., et al. (1997) Effects of Gender, Ethnicity, Body Composition, and Fat Distribution on Serum Leptin Concentrations in Children1. *The Journal of Clinical Endocrinology & Metabolism*. [Online] 82 (7), 2148–2152. Available from: doi:10.1210/jcem.82.7.4077.

Nalefski, E.A. & Falke, J.J. (1996) The C2 domain calcium-binding motif: Structural and functional diversity. *Protein Science*. [Online] 5 (12), 2375–2390. Available from: doi:10.1002/pro.5560051201.

Naylor, R., Knight Johnson, A., Del Gaudio, D.;, Adam, M.P., et al. (2018) *Maturity-Onset Diabetes of the Young Overview*. 1–20.

Nelson, M.R., Tipney, H., Painter, J.L., Shen, J., et al. (2015) The support of human genetic evidence for approved drug indications. *Nature Genetics*. [Online] 47 (8), 856–860. Available from: doi:10.1038/ng.3314.

Ng, M.C.Y., Park, K.S., Oh, B., Tam, C.H.T., et al. (2008) IImplication of Genetic

Variants Near TCF7L2, SLC30A8, HHEX, CDKAL1, CDKN2A/B, IGF2BP2, and FTO in Type 2 Diabetes and Obesity in 6,719 Asians. *Diabetes*. [Online] 57 (8), 2226 LP – 2233. Available from: doi:10.2337/db07-1583.

Ng, M.C.Y., Shriner, D., Chen, B.H., Li, J., et al. (2014) Meta-analysis of genome-wide association studies in African Americans provides insights into the genetic architecture of type 2 diabetes. *PLoS genetics*. [Online] 10 (8), e1004517–e1004517. Available from: doi:10.1371/journal.pgen.1004517.

Nishizawa, H., Shimomura, I., Kishida, K., Maeda, N., et al. (2002) Androgens Decrease Plasma Adiponectin, an Insulin-Sensitizing Adipocyte-Derived Protein. *Diabetes*. [Online] 51 (9), 2734 LP – 2741. Available from: doi:10.2337/diabetes.51.9.2734.

Nolan, C.J., Madiraju, M.S.R., Delghingaro-Augusto, V., Peyot, M.-L., et al. (2006) Fatty Acid Signaling in the β-Cell and Insulin Secretion. *Diabetes*. [Online] 55 (Supplement 2), S16 LP-S23. Available from: doi:10.2337/db06-S003.

Olofsson, C.S., Göpel, S.O., Barg, S., Galvanovskis, J., et al. (2002) Fast insulin secretion reflects exocytosis of docked granules in mouse pancreatic B-cells. *Pflugers Archiv European Journal of Physiology*. [Online] 444 (1–2), 43–51. Available from: doi:10.1007/s00424-002-0781-5.

Omori, H., Ogaki, S., Sakano, D., Sato, M., et al. (2016) Changes in expression of C2cd4c in pancreatic endocrine cells during pancreatic development. *FEBS Letters*. [Online] 590, 2584–2593. Available from: doi:10.1002/1873-3468.12271.

Osundiji, M.A., Lam, D.D., Shaw, J., Yueh, C.-Y., et al. (2012) Brain Glucose Sensors Play a Significant Role in the Regulation of Pancreatic Glucose-Stimulated Insulin Secretion. *Diabetes*. [Online] 61 (2), 321 LP – 328. Available from: doi:10.2337/db11-1050.

Panten, U., Christians, J., Poser, W. & Hasselblatt, A. (1973) *Effect of Carbohydrates upon Fluorescence of Reduced Pyridine Nucleotides from Perifused Isolated Pancreatic Islets*. 482, 477–482.

Paranjape, S.A., Chan, O., Zhu, W., Horblitt, A.M., et al. (2011) Chronic reduction of insulin receptors in the ventromedial hypothalamus produces glucose intolerance and islet dysfunction in the absence of weight gain. *American Journal of Physiology-Endocrinology and Metabolism*. [Online] 301 (5), E978–E983. Available from: doi:10.1152/ajpendo.00304.2011.

Parillo, M. & Riccardi, G. (2004) Diet composition and the risk of type 2 diabetes: epidemiological and clinical evidence. *British Journal of Nutrition*. [Online] 92 (1), 7–19. Available from: doi:DOI: 10.1079/BJN20041117.

Parker, M.W. (2003) Protein structure from x-ray diffraction. *Journal of biological physics*. [Online] 29 (4), 341–362. Available from: doi:10.1023/A:1027310719146.

Parker, S.C.J., Stitzel, M.L., Taylor, D.L., Orozco, J.M., et al. (2013) Chromatin stretch enhancer states drive cell-specific gene regulation and harbor human disease risk variants. *Proceedings of the National Academy of Sciences*. [Online] 110 (44), 17921–17926. Available from: doi:10.1073/pnas.1317023110.

Pascoe, L., Tura, A., Patel, S.K., Ibrahim, I.M., et al. (2007) Common Variants of the Novel Type 2 Diabetes Genes CDKAL1 and HHEX/IDE Are Associated With Decreased Pancreatic β-Cell Function. *Diabetes*. [Online] 56 (12), 3101 LP – 3104. Available from: doi:10.2337/db07-0634.

Pasquali, L., Gaulton, K.J., Rodríguez-Seguí, S.A., Mularoni, L., et al. (2014) Pancreatic islet enhancer clusters enriched in type 2 diabetes risk-associated variants. *Nature genetics*. [Online] 46 (2), 136–143. Available from: doi:10.1038/ng.2870.

Patro, R., Duggal, G., Love, M.I., Irizarry, R.A., et al. (2017) Salmon provides fast and bias-aware quantification of transcript expression. *Nature Methods*. [Online] 14, 417. Available from: https://doi.org/10.1038/nmeth.4197.

Peifer, M. & Polakis, P. (2000) Wnt Signaling in Oncogenesis and Embryogenesis--a Look Outside the Nucleus. *Science*. [Online] 287 (5458), 1606 LP – 1609. Available from: doi:10.1126/science.287.5458.1606.

Perley, M.J. & Kipnis, D.M. (1967) Plasma Insulin Responses to Oral and Intravenous Glucose: Studies in Normal and Diabetic Subjects. *The Journal of Clinical Investigation*. [Online] 46 (12), 1954–1962. Available from: doi:10.1172/JCI105685.

Perseghin, G., Scifo, P., Pagliato, E., Battezzati, A., et al. (2001) Gender Factors Affect Fatty Acids-Induced Insulin Resistance in Nonobese Humans: Effects of Oral Steroidal Contraception1. *The Journal of Clinical Endocrinology & Metabolism*. [Online] 86 (7), 3188–3196. Available from: doi:10.1210/jcem.86.7.7666.

Pickrell, J.K. (2014) Joint Analysis of Functional Genomic Data and Genome-wide Association Studies of 18 Human Traits. *The American Journal of Human Genetics*. [Online] 94 (4), 559–573. Available from: doi:10.1016/J.AJHG.2014.03.004 [Accessed: 8 August 2019].

Pihoker, C., Gilliam, L.K., Ellard, S., Dabelea, D., et al. (2013) Prevalence, Characteristics and Clinical Diagnosis of Maturity Onset Diabetes of the Young Due to Mutations in HNF1A, HNF4A, and Glucokinase: Results From the SEARCH for Diabetes in Youth. *The Journal of Clinical Endocrinology & Metabolism*. [Online] 98 (10), 4055–4062. Available from: doi:10.1210/jc.2013-1279.

Pillay, K. & Govender, P. (2013) Amylin uncovered: A review on the polypeptide responsible for type II diabetes. *BioMed Research International*. [Online] 2013. Available from: doi:10.1155/2013/826706.

Pinheiro, P.S., Houy, S. & Sørensen, J.B. (2016) C2-domain containing calcium

sensors in neuroendocrine secretion. *Journal of Neurochemistry*. [Online] 139 (6), 943–958. Available from: doi:10.1111/jnc.13865.

Prado, C.L., Pugh-Bernard, A.E., Elghazi, L., Sosa-Pineda, B., et al. (2004) Ghrelin cells replace insulin-producing β cells in two mouse models of pancreas development. *Proceedings of the National Academy of Sciences of the United States of America*. [Online] 101 (9), 2924 LP – 2929. Available from: doi:10.1073/pnas.0308604100.

Prentkisg, M., Vischers, S., Glennons, M.C., Regazzis, R., et al. (1992) *Malonyl-CoA and Long Chain Acyl-CoA Esters as Metabolic Coupling Factors in Nutrient-induced Insulin Secretion **. 267 (9), 5802–5810.

Prokopenko, I., Poon, W., Mägi, R., Prasad B, R., et al. (2014) A Central Role for GRB10 in Regulation of Islet Function in Man. *PLoS Genetics*. [Online] 10 (4), 1–13. Available from: doi:10.1371/journal.pgen.1004235.

Quang, D.X., Erdos, M.R., Parker, S.C.J. & Collins, F.S. (2015) Motif signatures in stretch enhancers are enriched for disease-associated genetic variants. *Epigenetics & Chromatin*. [Online] 8 (1), 23. Available from: doi:10.1186/s13072-015-0015-7.

Quianzon, C.C. & Cheikh, I. (2012) History of insulin. *Journal of Community Hospital Internal Medicine Perspectives*. [Online] 2 (2), 18701. Available from: doi:10.3402/jchimp.v2i2.18701.

Radavelli-Bagatini, S., Blair, A.R., Proietto, J., Spritzer, P.M., et al. (2011) The New Zealand obese mouse model of obesity insulin resistance and poor breeding performance: Evaluation of ovarian structure and function. *Journal of Endocrinology*. [Online] 209 (3), 307–315. Available from: doi:10.1530/JOE-11-0022.

Ran, F.A., Hsu, P.D., Wright, J., Agarwala, V., et al. (2013) Genome engineering using the CRISPR-Cas9 system. *Nature Protocols*. [Online] 8, 2281. Available from: https://doi.org/10.1038/nprot.2013.143.

Rathmann, W. & Giani, G. (2004) Global Prevalence of Diabetes: Estimates for the Year 2000 and Projections for 2030. *Diabetes Care*. [Online] 27 (10), 2568 LP – 2569. Available from: doi:10.2337/diacare.27.10.2568.

Ravassard, P., Hazhouz, Y., Pechberty, S., Bricout-neveu, E., et al. (2011) Technical advance A genetically engineered human pancreatic β cell line exhibiting glucose-inducible insulin secretion. *The Journal of clinical investigation*. [Online] 121 (9), 3589–3597. Available from: doi:10.1172/JCI58447DS1.

Redondo, M.J., Jeffrey, J., Fain, P.R., Eisenbarth, G.S., et al. (2008) Concordance for Islet Autoimmunity among Monozygotic Twins. *New England Journal of Medicine*. [Online] 359 (26), 2849–2850. Available from: doi:10.1056/NEJMc0805398.

Reno, C.M., Puente, E.C., Sheng, Z., Daphna-Iken, D., et al. (2017) Brain GLUT4 Knockout Mice Have Impaired Glucose Tolerance, Decreased

Insulin Sensitivity, and Impaired Hypoglycemic Counterregulation. *Diabetes*. [Online] 66 (3), 587–597. Available from: doi:10.2337/db16-0917.

Ribas, V., Nguyen, M.T.A., Henstridge, D.C., Nguyen, A.-K., et al. (2010) Impaired oxidative metabolism and inflammation are associated with insulin resistance in ERalpha-deficient mice. *American journal of physiology. Endocrinology and metabolism*. [Online] 298 (2), E304–E319. Available from: doi:10.1152/ajpendo.00504.2009.

Richards JS and Pangas SA (2010) Review series The ovary : basic biology and clinical implications. *J Clin Invest*. [Online] 120 (4), 963–972. Available from: doi:10.1172/JCI41350.critical.

Richards, P., Parker, H.E., Adriaenssens, A.E., Hodgson, J.M., et al. (2014) Identification and Characterization of GLP-1 Receptor–Expressing Cells Using a New Transgenic Mouse Model. *Diabetes*. [Online] 63 (4), 1224 LP – 1233. Available from: doi:10.2337/db13-1440.

Roger, B., Papin, J., Vacher, P., Raoux, M., et al. (2010) Adenylyl cyclase 8 is central to glucagon-like peptide 1 signalling and effects of chronically elevated glucose in rat and human pancreatic beta cells. *Diabetologia*. [Online] 54, 390–402. Available from: doi:10.1007/s00125-010-1955-x.

Rorsman, P. & Braun, M. (2013) Regulation of Insulin Secretion in Human Pancreatic Islets. *Annual Review of Physiology*. [Online] 75 (1), 155–179. Available from: doi:10.1146/annurev-physiol-030212-183754.

Rorsman, P. & Braun, M. (n.d.) *Regulation of Insulin Secretion in Human Pancreatic Islets*. [Online] Available from: doi:10.1146/annurev-physiol-030212-183754.

Rorsman, P., Braun, M. & Zhang, Q. (2012) Regulation of calcium in pancreatic α- and β-cells in health and disease. *Cell Calcium*. [Online] 51 (3–4), 300–308. Available from: doi:10.1016/j.ceca.2011.11.006.

Rorsman, P., Eliasson, L., Kanno, T., Zhang, Q., et al. (2011) Electrophysiology of pancreatic b -cells in intact mouse islets of Langerhans. *Progress in Biophysics and Molecular Biology*. [Online] 107 (2), 224–235. Available from: doi:10.1016/j.pbiomolbio.2011.06.009.

Rorsman, P. & Renström, E. (2003) Insulin granule dynamics in pancreatic beta cells. *Diabetologia*. [Online] 46 (8), 1029–1045. Available from: doi:10.1007/s00125-003-1153-1.

Rosen, E.D. & Spiegelman, B.M. (2006) Adipocytes as regulators of energy balance and glucose homeostasis. *Nature*. [Online] 444 (7121), 847–853. Available from: doi:10.1038/nature05483.

Rosenbaum, M., Nicolson, M., Hirsch, J., Heymsfield, S.B., et al. (1996) Effects of gender, body composition, and menopause on plasma concentrations of leptin. *The Journal of Clinical Endocrinology & Metabolism*. [Online] 81 (9), 3424–3427. Available from: doi:10.1210/jcem.81.9.8784109.

Ross, S.A., Brown, J.C. & Dupré, J. (1977) Hypersecretion of Gastric Inhibitory Polypeptide Following Oral Glucose in Diabetes Mellitus. *Diabetes*. [Online] 26 (6), 525 LP – 529. Available from: doi:10.2337/diab.26.6.525.

Rutter, G.A. (2014) Dorothy Hodgkin Lecture 2014 Understanding genes identified by genome-wide association studies for Type 2 diabetes. *Diabetic Medicine*. [Online] 31 (12), 1480–1487. Available from: doi:10.1111/dme.12579.

Rutter, G.A. (2001) *Nutrient – secretion coupling in the pancreatic islet b -cell : recent advances*. 22, 247–284.

Rutter, G.A. & Chimienti, F. (2015) SLC30A8 mutations in type 2 diabetes. *Diabetologia*. [Online] 58 (1), 31–36. Available from: doi:10.1007/s00125-014-3405-7.

Saeki, K., Zhu, M., Kubosaki, A., Xie, J., et al. (2002) Targeted disruption of the protein tyrosine phosphatase-like molecule IA-2 results in alterations in glucose tolerance tests and insulin secretion. *Diabetes*. [Online] 51 (6), 1842–1850. Available from: doi:10.2337/diabetes.51.6.1842.

Safayhi, H., Haase, H., Kramer, U., Bihlmayer, A., et al. (2014) L-Type Calcium Channels in Insulin-Secreting Cells: Biochemical Characterization and Phosphorylation in RINm5F Cells. *Molecular Endocrinology*. [Online] 11 (5), 619–629. Available from: doi:10.1210/mend.11.5.9922.

Salem, V., Silva, L.D., Suba, K., Georgiadou, E., et al. (2019) Leader β-cells coordinate Ca2+ dynamics across pancreatic islets in vivo. *Nature Metabolism*. [Online] 1 (6), 615–629. Available from: doi:10.1038/s42255-019-0075-2.

Sansbury, F.H., Flanagan, S.E., Houghton, J.A.L., Shuixian Shen, F.L., et al. (2012) SLC2A2 mutations can cause neonatal diabetes, suggesting GLUT2 may have a role in human insulin secretion. *Diabetologia*. [Online] 55 (9), 2381–2385. Available from: doi:10.1007/s00125-012-2595-0.

Savic, D., Ye, H., Aneas, I., Park, S.-Y., et al. (2011) Alterations in TCF7L2 expression define its role as a key regulator of glucose metabolism. *Genome research*. [Online] 21 (9), 1417–1425. Available from: doi:10.1101/gr.123745.111.

Saxena, R., Hivert, M.F., Langenberg, C., Tanaka, T., et al. (2010) Genetic variation in GIPR influences the glucose and insulin responses to an oral glucose challenge. *Nature Genetics*. [Online] 42 (2), 142–148. Available from: doi:10.1038/ng.521.

Schaffer, A.E., Taylor, B.L., Benthuysen, J.R., Liu, J., et al. (2013) Nkx6.1 Controls a Gene Regulatory Network Required for Establishing and Maintaining Pancreatic Beta Cell Identity. *PLOS Genetics*. [Online] 9 (1), 1–15. Available from: doi:10.1371/journal.pgen.1003274.

Schaub, M.A., Boyle, A.P., Kundaje, A., Batzoglou, S., et al. (2012) Linking disease associations with regulatory information in the human genome.

Genome Research. [Online] 22 (9), 1748–1759. Available from: doi:10.1101/gr.136127.111.

Schnell, A.H., Swenne, I. & Borg, L.A.H. (1988) Lysosomes and pancreatic islet function - A quantitative estimation of crinophagy in the mouse pancreatic B-cell. *Cell and Tissue Research*. [Online] 252 (1), 9–15. Available from: doi:10.1007/BF00213820.

Van Schravendijk, C.F., Kiekens, R. & Pipeleers, D.G. (1992) Pancreatic beta cell heterogeneity in glucose-induced insulin secretion. *Journal of Biological Chemistry* . [Online] 267 (30), 21344–21348. Available from: http://www.jbc.org/content/267/30/21344.abstract.

Schuit, F.C. (1997) *Is GLUT2 required for glucose sensing ?* 104–111.

Schulla, V., Renstro, E., Feil, R., Feil, S., et al. (2003) Impaired insulin secretion and glucose tolerance in b cell-selective Ca. *EMBO Journal*. 22 (15).

Schwartz, M.W., Woods, S.C., Porte, D., Seeley, R.J., et al. (2000) Central nervous system control of food intake. *Nature*. [Online] 404 (6778), 661–671. Available from: doi:10.1038/35007534.

Schwartz, M.W., Woods, S.C., Seeley, R.J., Barsh, G.S., et al. (2003) Is the Energy Homeostasis System Inherently Biased Toward Weight Gain? *Diabetes*. [Online] 52 (2), 232 LP – 238. Available from: doi:10.2337/diabetes.52.2.232.

Seeley, R.J. & Woods, S.C. (2003) Monitoring of stored and available fuel by the CNS: implications for obesity. *Nature Reviews Neuroscience*. [Online] 4 (11), 901–909. Available from: doi:10.1038/nrn1245.

Sharma, A. & Stein, R. (1994) Glucose-induced transcription of the insulin gene is mediated by factors required for beta-cell-type-specific expression. *Molecular and Cellular Biology*. [Online] 14 (2), 871 LP – 879. Available from: doi:10.1128/MCB.14.2.871.

Shih, H.P., Wang, A. & Sander, M. (2013) Pancreas Organogenesis : From Lineage Determination to Morphogenesis. *Cell Dev. Biol.* [Online] Available from: doi:10.1146/annurev-cellbio-101512-122405.

Shin, O.-H., Rizo, J. & Südhof, T.C. (2002) Synaptotagmin function in dense core vesicle exocytosis studied in cracked PC12 cells. *Nature Neuroscience*. [Online] 5 (7), 649–656. Available from: doi:10.1038/nn869.

Shu, L., Matveyenko, A. V, Kerr-Conte, J., Cho, J.-H., et al. (2009) Decreased TCF7L2 protein levels in type 2 diabetes mellitus correlate with downregulation of GIP- and GLP-1 receptors and impaired beta-cell function. *Human Molecular Genetics*. [Online] 18 (13), 2388–2399. Available from: doi:10.1093/hmg/ddp178.

Sicree, R.A., Zimmet, P.Z., Dunstan, D.W., Cameron, A.J., et al. (2008) Differences in height explain gender differences in the response to the oral glucose tolerance test - The AusDiab study. *Diabetic Medicine*. [Online] 25

(3), 296–302. Available from: doi:10.1111/j.1464-5491.2007.02362.x.

da Silva Xavier, G., Mondragon, A., Sun, G., Chen, L., et al. (2012) Abnormal glucose tolerance and insulin secretion in pancreas-specific Tcf7l2-null mice. *Diabetologia*. [Online] 55 (10), 2667–2676. Available from: doi:10.1007/s00125-012-2600-7.

Slack, J.M.W. (1995) Developmental biology of the pancreas. *Development*. 1580, 1569–1580.

Sladek, R., Rocheleau, G., Rung, J., Dina, C., et al. (2007) A genome-wide association study identifies novel risk loci for type 2 diabetes. *Nature*. [Online] 445, 881. Available from: https://doi.org/10.1038/nature05616.

Srimanunthiphol, J., Beddow, R. & Arakaki, R. (2000) A review of the United Kingdom Prospective Diabetes Study (UKPDS) and a discussion of the implications for patient care. *Hawaii Medical Journal*. 59 (7), 295–298, 313.

Steiner, D.F. & Oyer, P.E. (1967) the Biosynthesis of Insulin and a Probable Precursor of Insulin By a Human Islet Cell Adenoma. *Proceedings of the National Academy of Sciences*. [Online] 57 (2), 473–480. Available from: doi:10.1073/pnas.57.2.473.

Steinthorsdottir, V., Thorleifsson, G., Reynisdottir, I., Benediktsson, R., et al. (2007) A variant in CDKAL1 influences insulin response and risk of type 2 diabetes. *Nature Genetics*. [Online] 39 (6), 770–775. Available from: doi:10.1038/ng2043.

Straub, S.G., James, R.F.L., Dunne, M.J. & Sharp, G.W.G. (1998) *Glucose Activates Both K*. 47 (May).

Strawbridge, R.J., Dupuis, J., Prokopenko, I., Barker, A., et al. (2011a) Genome-wide association identifies nine common variants associated with fasting proinsulin levels and provides new insights into the pathophysiology of type 2 diabetes. *Diabetes*. [Online] 60 (10), 2624–2634. Available from: doi:10.2337/db11-0415.

Strawbridge, R.J., Dupuis, J., Prokopenko, I., Barker, A., et al. (2011b) Genome-wide association identifies nine common variants associated with fasting proinsulin levels and provides new insights into the pathophysiology of type 2 diabetes. *Diabetes*. [Online] 60 (10), 2624–2634. Available from: doi:10.2337/db11-0415.

Sussel, L., Kalamaras, J., Hartigan-O'Connor, D.J., Meneses, J.J., et al. (1998) Mice lacking the homeodomain transcription factor Nkx2.2 have diabetes due to arrested differentiation of pancreatic beta cells. *Development*. [Online] 125 (12), 2213 LP – 2221. Available from: http://dev.biologists.org/content/125/12/2213.abstract.

Tattersall, R.B. & Mansell, P.I. (1991) Maturity Onset-type Diabetes of the Young (MODY): One Condition or Many? *Diabetic Medicine*. [Online] 8 (5), 402–410. Available from: doi:10.1111/j.1464-5491.1991.tb01623.x.

Theodorakis, M.J., Carlson, O., Michopoulos, S., Doyle, M.E., et al. (2006) Human duodenal enteroendocrine cells: source of both incretin peptides, GLP-1 and GIP. *American Journal of Physiology-Endocrinology and Metabolism*. [Online] 290 (3), E550–E559. Available from: doi:10.1152/ajpendo.00326.2004.

Thomas, C.C. & Philipson, L.H. (2015) Update on Diabetes Classification. *Medical Clinics of North America*. [Online] 99 (1), 1–16. Available from: doi:10.1016/j.mcna.2014.08.015.

Thorens, B. (2011) Brain glucose sensing and neural regulation of insulin and glucagon secretion. *Diabetes, Obesity and Metabolism*. [Online] 13 (SUPPL. 1), 82–88. Available from: doi:10.1111/j.1463-1326.2011.01453.x.

Thorens, B. (2015) *GLUT2 , glucose sensing and glucose homeostasis*. [Online] 221–232. Available from: doi:10.1007/s00125-014-3451-1.

Trout, K.K., Rickels, M.R., Schutta, M.H., Petrova, M., et al. (2007) Menstrual Cycle Effects on Insulin Sensitivity in Women with Type 1 Diabetes: A Pilot Study. *Diabetes Technology & Therapeutics*. [Online] 9 (2), 176–182. Available from: doi:10.1089/dia.2006.0004.

Tsonkova, V.G., Sand, F.W., Wolf, X.A., Grunnet, L.G., et al. (2018) The EndoC-βH1 cell line is a valid model of human beta cells and applicable for screenings to identify novel drug target candidates. *Molecular metabolism*. [Online] 8, 144–157. Available from: doi:10.1016/j.molmet.2017.12.007.

Unoki, H., Takahashi, A., Kawaguchi, T., Hara, K., et al. (2008) SNPs in KCNQ1 are associated with susceptibility to type 2 diabetes in East Asian and European populations. *Nature Genetics*. [Online] 40, 1098. Available from: https://doi.org/10.1038/ng.208.

Varadi, A., Johnson-Cadwell, L.I., Cirulli, V., Yoon, Y., et al. (2004) Cytoplasmic dynein regulates the subcellular distribution of mitochondria by controlling the recruitment of the fission factor dynamin-related protein-1. *Journal of Cell Science*. [Online] 117 (19), 4389 LP – 4400. Available from: doi:10.1242/jcs.01299.

Varshney, A., Scott, L.J., Welch, R.P., Erdos, M.R., et al. (2017) Genetic regulatory signatures underlying islet gene expression and type 2 diabetes. *Proceedings of the National Academy of Sciences*. [Online] 114 (9), 2301–2306. Available from: doi:10.1073/pnas.1621192114.

Villasenor, A., Chong, D.C. & Cleaver, O. (2008) Biphasic Ngn3 expression in the developing pancreas. *Developmental Dynamics*. [Online] 237 (11), 3270–3279. Available from: doi:10.1002/dvdy.21740.

Vilsbøll, T., Krarup, T., Deacon, C.F., Madsbad, S., et al. (2001) Reduced Postprandial Concentrations of Intact Biologically Active Glucagon-Like Peptide 1 in Type 2 Diabetic Patients. *Diabetes*. [Online] 50 (3), 609 LP – 613. Available from: doi:10.2337/diabetes.50.3.609.

Visscher, P.M., Wray, N.R., Zhang, Q., Sklar, P., et al. (2017) 10 Years of

GWAS Discovery: Biology, Function, and Translation. *American journal of human genetics*. [Online] 101 (1), 5–22. Available from: doi:10.1016/j.ajhg.2017.06.005.

Wang, Y.J., Golson, M.L., Schug, J., Traum, D., et al. (2016) Single-Cell Mass Cytometry Analysis of the Human Endocrine Pancreas. *Cell Metabolism*. [Online] 24 (4), 616–626. Available from: doi:https://doi.org/10.1016/j.cmet.2016.09.007.

Warton, K., Foster, N.C., Gold, W.A. & Stanley, K.K. (2004) A novel gene family induced by acute inflammation in endothelial cells. *Gene*. [Online] 342 (1), 85–95. Available from: doi:10.1016/j.gene.2004.07.027.

Watson, H.J., Yilmaz, Z., Thornton, L.M., Hübel, C., et al. (2019) Genome-wide association study identifies eight risk loci and implicates metabo-psychiatric origins for anorexia nervosa. *Nature Genetics*. [Online] 51 (8), 1207–1214. Available from: doi:10.1038/s41588-019-0439-2.

Whirledge, S. & Cidlowski, J.A. (2010) Glucocorticoids, stress, and fertility. *Minerva Endocrinologica*. 35 (2), 109–125.

Wicksteed, B., Brissova, M., Yan, W., Opland, D.M., et al. (2010) Conditional gene targeting in mouse pancreatic ß-Cells: analysis of ectopic Cre transgene expression in the brain. *Diabetes*. [Online] 59 (12), 3090–3098. Available from: doi:10.2337/db10-0624.

Williams, J.A. (2010) Regulation of acinar cell function in the pancreas. *Current Opinion in Gastroenterology*. [Online] 26 (5), 478–483. Available from: doi:10.1097/MOG.0b013e32833d11c6.

Williams, J.W., Zimmet, P.Z., Shaw, J.E., De Courten, M.P., et al. (2003) Gender differences in the prevalence of impaired fasting glycaemia and impaired glucose tolerance in Mauritius. Does sex matter? *Diabetic Medicine*. [Online] 20 (11), 915–920. Available from: doi:10.1046/j.1464-5491.2003.01059.x.

Wiser, O., Trus, M., Hernandez, A., Renstrom, E., et al. (2002) The voltage sensitive Lc-type Ca2+ channel is functionally coupled to the exocytotic machinery. *Proceedings of the National Academy of Sciences*. [Online] 96 (1), 248–253. Available from: doi:10.1073/pnas.96.1.248.

Wollheim, C.B. & Maechler, P. (2002) β-cell mitochondria and insulin secretion: Messenger role of nucleotides and metabolites. *Diabetes*. 51 (SUPPL.), 37–42.

Wong, W.P.S., Tiano, J.P., Liu, S., Hewitt, S.C., et al. (2010) Extranuclear estrogen receptor-α stimulates NeuroD1 binding to the insulin promoter and favors insulin synthesis. *Proceedings of the National Academy of Sciences*. [Online] 107 (29), 13057 LP – 13062. Available from: doi:10.1073/pnas.0914501107.

Wood, A.R., Jonsson, A., Jackson, A.U., Wang, N., et al. (2017) A genome-wide association study of IVGTT-based measures of first-phase insulin

secretion refines the underlying physiology of type 2 diabetes variants. *Diabetes*. [Online] 66 (8), 2296–2309. Available from: doi:10.2337/db16-1452.

Woods, S.C. & Seeley, R.J. (2006) Hap1 and GABA: Thinking about food intake. *Cell Metabolism*. [Online] 3 (6), 388–390. Available from: doi:10.1016/j.cmet.2006.05.007.

Wu, Y., Li, H., Loos, R.J.F., Yu, Z., et al. (2008) Common variants in CDKAL1, CDKN2A/B, IGF2BP2, SLC30A8, and HHEX/IDE genes are associated with type 2 diabetes and impaired fasting glucose in a Chinese Han population. *Diabetes*. [Online] 57 (10), 2834–2842. Available from: doi:10.2337/db08-0047.

Yamauchi, T., Hara, K., Maeda, S., Yasuda, K., et al. (2010a) A genome-wide association study in the Japanese population identifies susceptibility loci for type 2 diabetes at UBE2E2 and C2CD4A-C2CD4B. *Nature Genetics*. [Online] 42 (10), 864–868. Available from: doi:10.1038/ng.660.

Yamauchi, T., Hara, K., Maeda, S., Yasuda, K., et al. (2010b) A genome-wide association study in the Japanese population identifies susceptibility loci for type 2 diabetes at UBE2E2 and C2CD4A-C2CD4B. *Nature Genetics*. [Online] 42 (10), 864–868. Available from: doi:10.1038/ng.660.

Zeggini, E., Scott, L.J., Saxena, R., Voight, B.F., et al. (2008) Meta-analysis of genome-wide association data and large-scale replication identifies additional susceptibility loci for type 2 diabetes. *Nature Genetics*. [Online] 40 (5), 638–645. Available from: doi:10.1038/ng.120.

Zeggini, E., Weedon, M.N., Lindgren, C.M., Frayling, T.M., et al. (2007) Replication of Genome-Wide Association Signals in UK Samples Reveals Risk Loci for Type 2 Diabetes. *Science*. [Online] 316 (5829), 1336 LP – 1341. Available from: doi:10.1126/science.1142364.

Zhang, W., Cline, M.A. & Gilbert, E.R. (2014) Hypothalamus-adipose tissue crosstalk: neuropeptide Y and the regulation of energy metabolism. *Nutrition & Metabolism*. [Online] 11 (1), 27. Available from: doi:10.1186/1743-7075-11-27.